2002

Biogenesis and Traffic of the Potassium Channel

Natalie de Souza

BIOGENESIS AND TRAFFIC OF THE POTASSIUM CHANNEL

A thesis presented to the faculty of
The Rockefeller University
in partial fulfillment of the requirements for
the degree of Doctor of Philosophy

by

Natalie de Souza

April 11, 2002

" Denn alles Fleisch, es ist wie Gras."

ACKNOWLEDGEMENT

My warmest thanks to Sandy, for his unwavering patience and support, and his positive and exuberant attitude to science. Also to every member of the Simon Lab over the years, but especially to Doris Peter and Mark Goulian, who taught me many things, at many different levels, about the doing of science.

I thank the Dean, Sid Strickland and the faculty on my thesis committee, George Cross, Fred Cross and Tom Sakmar, not only for their time, but for their vital support over the past year. I thank Tom Sakmar, especially, for his tremendous kindness and guidance. Many thanks also to Tim McGraw, for agreeing to join the committee as external member.

So many friends have contributed to the emotional scaffold on which my well-being rests, and I thank them all, collectively. I thank especially my dear friend Carien Niessen for her input, scientific and otherwise.

I thank my family; my parents Trudy and Noel, and my spectacular brothers Adrian and Gregory, for the deep core of love and irreverence that we have built to sustain us.

Most of all, I thank my dearest friend Jan Schmoranzer, partner in PhD thesis submission and in all else.

Table of Contents

List of Figures

List of Tables

Abbreviations

AgTx	Agitoxin
BFA	Brefeldin-A
CDG	Congenital disorders of glycosylation
CFTR	Cystic Fibrosis Transmembrane Regulator
conA	concanavalinA
CRT	Calreticulin
CST	Castanospermine
CTR	C-terminal truncated Shaker
DMEM	Dulbecco's Modified Eagle Medium
DSP	Dithiobis(succinimidylpropionate)
ECF	Enhanced Chemifluorescence
EndoH	Endoglycosidase H
ERGIC	Endoplasmic Reticulum-Golgi-Intermediate Compartment
FBS	Fetal Bovine Serum
FITC	Fluorescein Isothiocyanate
FSH/LH	Follicle stimulating hormone/Luteinizing hormone
GlcNAc	N-acetylglucosamine
GFP	Green Fluorescent Protein
Glu	Glucose
RP-HPLC	Reversed phase high performance liquid chromatography
IP	Immunoprecipitation
MAGUK	Membrane associated guanylate kinase
Man	Mannose
MTSEA	(2-aminoethyl)methanethiosulfonate hydrobromide
NEM	N-ethyl maleimide
NFDM	Non-fat dry milk
NGS	Normal Goat Serum
NHS	N-hydroxysulfosuccinimide
NMJ	neuromuscular junction

NSF	N-ethyl maleimide Sensitive Factor
NQ	N259Q+N263Q mutant Shaker channel
PBS	Phosphate Buffered Saline
RM	Rough Microsome
RRL	Rabbit Reticulocyte Lysate
SDS-PAGE	sodium dodecyl sulfate-polyacrylamide gel electrophoresis
SNARE	Soluble NSF Attachment Protein Receptor
SRP	Signal Recognition Particle
SRP-R	SRP Receptor
TBS	Tris Buffered Saline
TM	Transmembrane domain
TP	N-Ac-NYT tripeptide
TRAM	Translocon associated membrane protein

ABSTRACT

The excitability of nerve and muscle cells depends on the number and the types of ion channels expressed at the plasma membrane. This work examines aspects of biogenesis and traffic of the Shaker voltage-gated potassium channel. Shaker is an oligomeric, polytopic membrane protein and, as such, its biogenesis begins at the endoplasmic reticulum (ER). I have studied (i) targeting of Shaker to the ER and stable integration into the lipid bilayer, (ii) N-linked glycosylation, assembly and folding of Shaker in the ER, and (iii) export of Shaker from the ER and subsequent traffic to the cell surface.

Targeting to the endoplasmic reticulum, integration into the lipid bilayer and assembly into tetramers occurs efficiently for Shaker translated *in vitro*. The first transmembrane domain (TM1) is most likely the earliest ER targeting signal on the growing Shaker polypeptide. TM1 that has adequately emerged from the ribosome is sufficient to initiate targeting to the ER in the absence of additional transmembrane domains. Further, efficient integration of Shaker into the bilayer is promoted by a glycoprotein fraction of ER microsomes, in which the active component was the translocon associated membrane protein (TRAM). Shaker is N-glycosylated on two consensus sites in the first extracellular loop. The importance of glycosylation at this location for Shaker biogenesis has not been previously studied. Elimination of the two consensus sites for N-linked glycosylation yields a channel that targets to the ER, integrates and tetramerizes normally, but is transported at a reduced rate to the surface of the cell. This is due at least in part to a retardation of the unglycosylated channel at an early (i.e. pre-Golgi) step in its secretory traffic. Lastly, we attempted to develop assays

to determine the efficiency at which the Shaker channel acquires its final, folded, conduction-competent state in the endoplasmic reticulum.

1. INTRODUCTION

1.1. General introduction to the ion channels

A century ago, Julius Bernstein (1902) postulated the existence of a selective potassium permeability in the resting membrane of the cell. He proposed that the membrane is an insulating medium that separates solutions of different ionic concentration on the inside and the outside of the cell. The selective potassium permeability, it was theorized, sets the resting membrane potential of cells close to the equilibrium potential for potassium. Further, the phenomenon of excitability in nerve and muscle cells was proposed to be the result of "membrane breakdown", in which permeability to other ions transiently increases. This theory has been largely borne out, in its broadest terms, by research over the past hundred years. I begin this dissertation with a simplified, and necessarily very abridged, description of the work that has culminated in our present understanding of the potassium channels and their role in physiology.

1.1.1. History

1.1.1.1. Ion flux is central to cell excitability

The idea that ion fluxes play a role in the excitability of nerve and muscle was based on work in the late nineteenth century. Ringer (1881 – 1887) showed that the heart of a frog, *ex vivo*, continues to beat for a substantial period only if bathed in a solution with a fixed proportion of sodium, potassium and chloride. Nernst (1888) studied the diffusion of electrolytes in solution, and his mathematical descriptions of the electrical

potentials that result are fundamental to the understanding of biological potentials generated by ion flux across cell membranes. More importantly, from a historical point of view, his work supported the possibility of an ionic basis for biological potentials. Contemporary with these scientists, Hermann (1872) hypothesized that excitability is a phenomenon of "electrical self-stimulation". He proposed, in other words, that local excitation of the membrane results in electrical currents that stimulate nearby unexcited regions of the membrane, thus propagating the excitation along the length of the cell. It is worth noting that this theory was formulated at a time when the centrality of the membrane in excitability was far from established, and when electrical events were considered by many to be merely an epiphenomenon of putative chemical processes fundamental to the propagation of the nervous impulse.

1.1.1.2. The classical period : description of the action potential

It was to be several decades before these ideas were experimentally tackled. The years between 1935 and 1952, in one sense arguably the darkest period of human history, were nevertheless a glorious time for biophysics. This period (sometimes referred to as the classical period of biophysics) was propelled by the work of Curtis and Cole, and Hodgkin, Huxley and Katz. Working in large part on the giant axon of the squid, these scientists studied both the passive electrical properties of the axonal membrane as well as the changes that occur during the propagation of an action potential. It was these studies that experimentally established excitability as indeed based upon ion permeability changes, and that laid the foundation for work that continues until today.

Cole and Curtis, in 1923, began to study the passive electrical properties of cells. Using a Wheatstone bridge on a wide variety of cell types, they established that cells

have a high conductance cytosol surrounded by a high resistance membrane(Cole, 1968). The experimental demonstration of these properties was necessary for Bernstein's theory. On studies of both the squid axon (Cole and Curtis, 1939)as well as of the giant alga Nitella (Cole, 1938), Cole and Curtis showed that the conductance of the membrane increases dramatically (40–50 fold) during an action potential, thus further confirming the "membrane breakdown" hypothesis of excitability. When axonal voltage changes during an action potential were directly measured with an intracellular micropipette (Curtis and Cole, 1940; Hodgkin and Huxley, 1939), it was found that the cell does indeed transiently depolarize[1] during this process. However, instead of a depolarization to electrical neutrality (0 mV), as would be expected to result from a membrane that "breaks down" and becomes briefly permeable to all ions, the depolarization was seen to overshoot zero and to become positive by 10–20 mV. This was the first indication that the action potential is the result of a transient increase in sodium permeability of the cell membrane. The influx of sodium ions (down their concentration gradient) that would result from such a permeability increase would carry the overall membrane potential closer to the reversal potential for sodium (~ + 60 mV in physiological solutions). Experiments in which the action potential was observed in the (partial) absence of sodium ions later proved this idea to be correct, since the membrane potential overshoot was smaller and the propagated action potential was substantially reduced (Hodgkin and Katz, 1949). Increased influx of radioactive tracer sodium ions during the action potential further confirmed this idea (Keynes, 1951).

The development of the voltage clamp (Marmont, 1949; Cole, 1949; Hodgkin et al., 1949; Marmont, 1949) made possible the detailed study of the currents that flow

[1]In depolarization, the membrane potential becomes more positive than at rest.

across the cell membrane during a propagated action potential. Simply stated, the voltage clamp allows the potential across a cell membrane to be fixed at some desired value. This is achieved with the following combination. An intracellular electrode measures the potential across the cell membrane, a feedback amplifier amplifies the difference between this measured voltage and the voltage at which the cell is to be clamped, and another intracellular electrode injects current to maintain the cell at the clamped voltage. Thus the current required to clamp the cell at the desired voltage is known, and this is a measure of the current that flows across the membrane, at that voltage. Hodgkin and Huxley used this technique to define two major components of the current that flows across the cell membrane during a propagated action potential (Hodgkin and Huxley, 1952b; Hodgkin and Huxley, 1952c). Depolarization of the cell produces a rapid, initial inward current, followed by a more prolonged outward current. The reversal potential of these currents suggested that they were carried by sodium and potassium ions respectively, and this was proven in experiments that specifically replaced these ions in the external solution. Studies of ion fluxes at different voltages showed that the sodium and potassium currents were voltage-dependent. This led to the concepts of activation and inactivation of ionic currents as a function of voltage, as well as to the development of an empirical model (the Hodgkin-Huxley model) that describes these processes as a function of voltage and time (Hodgkin and Huxley, 1952a). Based on their kinetic measurements, the potassium channel was modeled as an oligomer of four identical subunits.

The classical period of biophysics culminated in the description of the propagated action potential. A local depolarization results in a voltage-sensitive inward sodium

current. This influx of sodium ions further depolarizes the cell and brings nearby unexcited regions above the firing threshold, resulting in a regenerative spread of the excitation along the length of the axon. The sodium currents rapidly inactivate, which is a voltage-dependent process. At approximately the same time, depolarization gives rise to voltage-sensitive potassium currents, and the resulting outward flow of potassium ions repolarizes the membrane.

1.1.1.3. Ion flux occurs through distinct channels

Until the 1960s, the concept of the ion channel as a specific pore-like molecule through which ions flow across the membrane was only one of several possible models to explain permeation. Other mechanisms considered at this time include direct movement through the membrane bilayer or transport via carriers (Hille, 1984). The mechanistic nature of the ion permeation "passageway" notwithstanding, it was not clear whether different ions flowed through molecularly distinct passages, or whether selective permeability of the membrane was regulated in some other way. Several lines of experiment were important in establishing the notion that distinct pore molecules function to effect the flux of a particular type of ion across the cell membrane. First, certain pharmacological agents were seen to block certain ion currents but not others. Specifically, puffer fish tetrodotoxin (TTX) (Narahashi et al., 1964) and marine dinoflagellate saxitoxin (STX)(Narahashi et al., 1967) block the sodium current during an action potential, but leave the potassium current unaffected, whereas the reverse is true of the tetraethylammonium ion (TEA^+)(Hagiwara and Saito, 1959). This supported the idea that specific pore molecules were indeed involved in the movement of specific ions across the membrane. Second, the development of a technique for studying proteins

reconstituted into a planar lipid bilayer (Mueller et al., 1962)led to the demonstration that these formed aqueous pores that opened in a discrete all-or-nothing manner (Ehrenstein et al., 1970). Third, the development of the patch clamp and gigaseal methods (Neher and Sakmann, 1976; Hamill et al., 1981) further advanced the study of individual channels. Briefly, it was discovered that a micropipette pressed against the cell membrane could be induced, by gentle suction, to form a seal of extremely high electrical resistance and mechanical stability with the underlying membrane. This enabled the study of few (or even single) ion channels within the small area of the underlying "patched" membrane. The unitary steps recorded by patch clamping constituted further support for the unique molecular nature of ion channels.

Once it had been accepted that ions flow across the membrane through discrete channels, it did not take long until these molecules were defined as being proteinaceous in nature. The tools of protein chemistry, in the 1970s, and then of molecular genetics, in the next decade, were used to firmly establish this fact. The first channel to be cloned was the nicotinic acetylcholine receptor (nAChR)(Noda et al., 1983). The approach used, later also successful for the sodium channel, the GABA receptor and the glycine receptor, involved purifying the protein from a rich source (in the case of AchR the Torpedo electric organ) (Weill et al., 1974), chemically identifying protein sequences (Raftery et al., 1980), and then preparing probes for the identification of the corresponding mRNA. This depended on the availability of high affinity ligands that could be used for purification of the channel. At the time, the known potassium channel ligands TEA^+ and 4 – aminopyridine (4-AP) lacked the affinity and the specificity to be useful purification reagents. The first potassium channel to be cloned was the Shaker channel, the fruits of a

coalescence of Drosophila behavioral genetics, electrophysiology and molecular cloning approaches. The Shaker channel has been the subject of intense study since that time, and is also the focus of this work.

1.1.1.4. The potassium channels : the Shaker locus in Drosophila

Several behavioral mutants in *Drosophila melanogaster* were important for the identification of ion channels involved in excitability. The Drosophila nervous system is similar to that of other arthropods (Tanouye et al., 1986). Propagated action potentials are regenerative sodium spikes, and potassium channels are critical for repolarization of the excited cell membrane. Putative excitability mutant flies showed uncontrolled leg-shaking under ether anesthaesia, as compared to wild type Drosophila, which are immobile when etherized (Trout and Kaplan, 1973; Kaplan and Trout, III, 1969). Of the loci linked to the leg-shaking phenotype, Shaker was initially the most intensively studied. The other loci were ether-a-go-go (eag) and hyperkinetic (hk) (Kaplan and Trout, III, 1969; Wu et al., 1983), both later also found to encode potassium channel components.

Evidence began to accumulate that the Shaker locus indeed encoded a potassium channel. The larvae of mutant flies were seen to have abnormally large and asynchronous neurotransmitter release at the neuromuscular junction (Jan et al., 1977). This was determined to be the result of a prolonged calcium influx at the nerve terminal, which in turn was shown to be due to abnormally slow potassium-based repolarization after the action potential (Jan et al., 1977). Alternative possible explanations, such as slowed repolarization due to inactivation defects in sodium channels, or increased calcium influx due to inactivation defects in calcium channels, were ruled out. Further,

the potassium channel blocker 4-AP was shown to mimic the mutant phenotype, at the wild type larval neuromuscular junction (NMJ) (Ganetzky and Wu, 1983). Intracellular recordings of the axonal action potentials in the cervical giant fibres of *Sh* flies also indicated a delay in action potential repolarization (Tanouye and Ferrus, 1985). Again, this could be mimicked in the wild type fly by blocking potassium channel activity.

Voltage clamp experiments on the pupal flight muscle (Salkoff and Wyman, 1981a; Salkoff and Wyman, 1981b) showed that the normal development of specific potassium currents was inhibited. In these experiments, wild type and *Sh* mutant pupal flight muscle was voltage clamped at different times post-pupation. As will be discussed in more detail in the following section, different types of potassium currents (but not the underlying channels) had been identified and characterized by this time, based on their activation and inactivation kinetics, and their voltage-dependent properties. The developing wild type pupal flight muscle shows a well-defined temporal sequence of potassium current appearance (Tanouye et al., 1986). In a normal fly, transient I_A currents are at their maximal levels after 72 hours of pupal development at 25 °C. The delayed rectifier (I_K) appears more slowly, reaching a peak at ~90 hours, at which time calcium channels (I_{Ca}) begin to appear as well. For certain *Sh* mutant pupae (Sh^{KS133}), no I_A currents were seen at 72 hours post-pupal development, but the I_K and I_{Ca} currents developed normally. Similar results were obtained in voltage clamp experiments on adult and larval muscle (Salkoff and Wyman, 1983; Wu et al., 1983). Importantly, other mutant alleles (*Sh5*) did exhibit a transient A-type channel, but with altered (speeded-up) kinetics of inactivation, further supporting the idea that Shaker does indeed encode a structural component of the transient potassium channel (Wu and Haugland, 1985). In

summary, different mutant alleles of Shaker were seen to differ somewhat in the degree to which they resulted in a perturbed potassium current. However, the net effect tended in all cases to result in a defect or a delay in the repolarization of an excitable cell. This correlates well with the hyperexcitability phenotype of the mutant flies.

1.1.1.5. The Shaker gene encodes a transient potassium channel

The implication of the Shaker locus in encoding a structural component of a potassium channel resulted in a concerted effort to clone the Shaker gene. This was accomplished by chromosome walking. In 1987, several groups had obtained fragments of the gene, which were then used to identify complete cDNA clones (Tempel et al., 1987; Papazian et al., 1987; Kamb et al., 1987) that were verified as encoding transient A-type channels by heterologous expression in Xenopus oocytes. Several aspects of the Shaker gene were of immediate interest. First, the sequence and the predicted protein structure showed unmistakable resemblance to the voltage-gated sodium and calcium channels, except that the latter channels (i.e. Na^{+} and Ca^{++}) contain four repeats of the motif that appears singly in Shaker. Not only did this give an early indication that the Shaker channel is tetrameric, but it suggested the existence of a family of evolutionarily related voltage-gated ion channels, within which the potassium channel is a comparably ancient relative. Second, the Shaker gene was seen to undergo alternative splicing to generate cDNAs that encoded four kinetically distinct ion channels (Tempel et al., 1987; Papazian et al., 1987; Pongs et al., 1988; Schwarz et al., 1988; Kamb et al., 1988). All splice forms (named ShA, ShB, ShC and ShD) have the same central regions (encoded by eight common exons), but differ at their N- and C- termini. Localization of message and

protein in Drosophila indicated that the splice forms are expressed in a tissue-specific manner (Schwarz et al., 1990).

1.1.1.6. Cloning of genes that encode other potassium channels

The availability of the Shaker sequence made it possible to subsequently clone several related genes both from Drosophila and from mammals (Butler et al., 1989; Wei et al., 1990; Tempel et al., 1988; Douglass et al., 1990; Christie et al., 1989). The additional genes that encode voltage-gated potassium channels from Drosophila have been named Shal, Shab and Shaw. Heterologous expression in Xenopus oocytes (Wei et al., 1990) showed that the channels encoded by Shaker, Shal, Shab and Shaw produce currents that inactivate progressively more slowly. Thus the Shab and Shaw channels are delayed rectifier-type channels, as opposed to the transient Shaker and Shal. Homology to the Drosophila genes has been used to define gene families in the several mammalian voltage-gated potassium channels that have since been cloned. The Shaker-type mammalian channels are the Kv1, the Shal-type are Kv2, the Shab-type are Kv3 and the Shaw type are Kv4 (Chandy and Gutman, 1995). Each of these familes has multiple members (for instance Kv1.1 – Kv1.7, in the Shaker-type channels). As will be discussed in more detail later, this classification based on sequence homology does not always translate into neatly defined electrophysiological categories.

1.1.2. The potassium channels

1.1.2.1. Classification based on gating properties

Current gating characteristics were initially used to define different potassium channel types. Very broadly speaking, the potassium channels can be classified into the

delayed rectifiers (K), the transient, rapidly inactivating channels (K_A), the inward rectifiers (Kir) and the calcium-activated potassium channels K(Ca) (Hille, 1984).

K : The term "delayed rectifier" was first used to describe the voltage-gated potassium channels of axons, since they show delayed opening in response to depolarization during the action potential. The name is somewhat misleading, since many other potassium channels also show delayed activation in response to voltage. Nevertheless, the name is apparently retained for historical reasons. The delayed rectifiers are expressed in excitable cells, where they open in response to depolarization and help to keep action potentials short. The Drosophila Shab and Shaw are delayed rectifier potassium channels.

K_A : The transient K_A channels are characterized by rapid, voltage-dependent activation followed by rapid inactivation. Moreover, hyperpolarization[2] is required to remove the channel inactivation. So, K_A channels can be opened by depolarization after a period of hyperpolarization. Drosophila Shaker encodes a K_A type channel. Curiously, only one of the known Shaker-like mammalian channels (Kv1.4) encodes a transient K_A channel (Chandy and Gutman, 1995). In other words, although the other Kv1 (Kv1.1 – Kv 1.3, Kv1.5) and Kv2 (Kv2.1 & Kv2.2) channels are homologous to the transient Shaker and Shal in Drosophila, their inactivation is nevertheless that of delayed rectifiers.

At steady state, the K_A channels conduct in the –65 to –40 mV range, and are thought to function at sub-threshold voltages in the interspike interval of excitable cells, where they help to regulate action potential frequency. Specifically, since outward potassium flux tends to repolarize the cell, and carry it away from the firing threshold, K_A channels tend to act as a damper in the interspike interval.

Kir : The inward rectifier channels are characterized by steep voltage-dependent opening. The difference, in this case, from K and K_A is that the inward rectifiers tend to open upon hyperpolarization. This feature, as well as regulation by a large number of intracellular signals and modifiers, constitute the biophysical signature of the inward rectifiers, and result in physiological roles that range from maintenance of the cell resting potential to control of potassium secretion and homeostasis.

K_{Ca} : The calcium-gated potassium channels K_{Ca} open in response to raised intracellular calcium. These channels are expressed in almost every excitable cell. They have some voltage-dependence both as a result of the voltage-dependence of calcium entry, as well as (in some sub-types) due to an intrinsic property. The kinetics of this channel are thus a complex mixture of the kinetics of calcium entry, buffering, diffusion, extrusion and sequestration, combined with the binding kinetics of the calcium to K_{Ca} and voltage-dependent changes in the channel itself.

1.1.2.2. Classification based on structure

The potassium channels may also be classified according to structural motifs (Miller, 2000)(Figure1.1). There are three broad classes of potassium channel structural motif, with some variations and combinations that will doubtless become only more plentiful as research continues. The first is the voltage-gated, six-transmembrane (TM) domain class (Kv), to which the Shaker channel belongs. The N- and C- termini of these channels are in the cytosol. The highly conserved region between TMs 5 and 6 is often called the P-loop and is thought to form part of the lining of the pore (Heginbotham et al., 1994). Another highly conserved region is the predicted voltage sensor in TM4, in which

[2] In hyperpolarization, the membrane potential becomes more negative than at rest.

several positively charged residues (K/R) occur at every three or four amino acids (Papazian et al., 1995). For the Shaker channel, epitope-tagging combined with immunofluorescence microscopy has been used to verify the predicted topology of the channel expressed in Xenopus oocytes (Shih and Goldin, 1997). In a different approach, glycosylation of a reporter construct placed at different locations in mammalian Kv1.3 (a Shaker-type channel expressed in lymphocytes) was used to verify topology of the *in vitro* translated protein (Tu et al., 2000).

The second class of channels consists of the two-transmembrane domain inward rectifiers (Kir) (Ho et al., 1993). Here too, both the N- and the C-termini are in the cytosol, but the core domain consists only of two, rather than of six, TM domains. The P-loop is present in between these two TM domains. Tandem '2P' channels that are either hybrids of a Kv module and a Kir module, or that consist of two Kir modules, as well as a calcium-gated voltage channel with an extra TM domain near the N-terminus have been reported (Miller, 2000). The third class of channels are the cardiac I(ks) channels, which are formed by coassembly of KvLQT1 and the single transmembrane domain protein minK (Sanguinetti et al., 1996; Barhanin et al., 1996). Both stoichiometry and structure of these channels are controversial.

1.1.2.3. Voltage-gated potassium channels are tetramers

Based on the fact that the structural motif of the voltage-gated potassium channels (Kv) is clearly homologous to each of the four internal repeats of the voltage-gated sodium and calcium channels, Kv channels were long predicted to function as tetramers. Upon co-expression (in Xenopus oocytes) of voltage-gated channels that could be clearly distinguished based on their rates of inactivation or their sensitivity to TEA or peptide

toxins, the currents seen could not be adequately described by a simple summation of each of the component currents (Isacoff et al., 1990; Ruppersberg et al., 1990; Christie et al., 1990). The intermediate currents suggested that the channel did indeed form multimers. The tetrameric nature of the Shaker channel was first proven in experiments where wild type and (D431N) mutant Shaker channels were co-expressed in Xenopus oocytes (MacKinnon, 1991). These channels differ significantly in their sensitivity to block by the scorpion peptide toxin charybdotoxin[3], with the mutant being relatively insensitive. Hybrid channels were generated by injecting various ratios of WT:mutant mRNA, and the kinetics of charybdotoxin block of these channels were analysed. The analysis yielded a channel subunit stoichiometry of four. This was later confirmed by biochemical cross-linking experiments in oocytes, mammalian tissue culture cells and insect cells (Schulteis et al., 1996).

1.1.3. Diversity of potassium currents

The potassium channels are the most diverse group of ion channels. More than 30 distinct potassium currents have been characterized based on their biophysical properties alone and, when differences in pharmacology are included in the picture, this diversity grows to an even higher number. Variability is seen between organisms for the same channel class and cell type, as well as between cell types for the same channel class in a given organism. This almost dizzying diversity is likely to derive from a few fundamental sources. These are (i) the presence of several potassium channel genes, (ii)

[3] It was later discovered that the high affinity toxin in the preparation was not charybdotoxin but a contaminating peptide, but since this does not alter the interpretation of the experiment, the paper is here taken at face value.

alternative splicing, (iii) heterotetramerization, (iv) post-translational modifications and regulation and (v) auxiliary subunits.

1.1.3.1. Potassium channel genes and the regulation of gene expression.

The cloning of Shaker led the way to the discovery not only of related genes in Drosophila (Shal, Shab, Shaw), but also to the cloning of ~ 30 vertebrate voltage-gated potassium channels, primarily in mammals (Wei et al., 1990). The list of these genes is constantly growing, and it is clear that the potassium channels constitute a large gene family. The situation is made considerably more complex by the discovery that potassium channels show both developmental and tissue-specific regulation of gene expression.

Tissue-specific gene expression : Vertebrate voltage-gated potassium channels are all expressed in the brain, but in addition show variable expression in other tissues (Table 1). In Drosophila, Shaker is expressed in muscle and photoreceptor cells, as well as in neurons (Solc et al., 1987; Hardie, 1991). The molecular mechanisms that result in tissue and cell-type specific expression of potassium channels are not well understood. There is some understanding of enhancer and silencer elements that control tissue specific expression in the voltage-gated sodium channels (Maue et al., 1990). In contrast to the situation for potassium channels, the sodium channels expressed in nerve and muscle cells appear to be encoded by different genes (Trimmer et al., 1989).

Table 1 : Tissue Distribution of Voltage-Gated K^+ Channel Genes (Chandy & Gutman, 1995)

	Expression in tissue													
Gene	**Brain**	**Atr**	**Vent**	**Kid**	**Retina**	**Lung**	**Liver**	**Skm**	**Islet**	**Thy**	**Spl**	**Lym**	**GH3**	**Aorta**
Kv1.1	+	+	-		+		-	+	+					-
Kv1.2	+	+	+				-	-	+					-
Kv1.3	+	-	-	-		+	-	-	+	+	+	+		
Kv1.4	+	+	+	-			-	+	+				+	-
Kv1.5	+	+	+	+		+	-	+	+				+	
Kv1.6	+	-	-	-		-	-	-	+					

Developmental regulation of gene expression : There are several examples of developmental regulation of voltage-gated potassium channels, the molecular bases for which are largely unclear. During development of the rat heart, ventricular Kv1.5 message is downregulated, but atrial expression does not change (Matsubara et al., 1991). In developing spinal cord neurons, Kv1.1 and Kv2.2 transcriptional upregulation results in a significant reduction in action potential duration (Gurantz et al., 1996). Further, overexpression of these genes interferes with normal neuronal development (Jones and Ribera, 1994) indicating that developmental control of potassium channel expression levels can indeed be physiologically important.

Control by hormones/external stimuli : Potassium channel expression is affected by a variety of intracellular molecules and external stimuli (Table 2) (Levitan and Takimoto, 1998). For instance, glucocorticoid hormone treatment results in the up-regulation of Kv1.5 message and protein, with a consequent increase in potassium current, in the GH3 pituitary cell line as well as in primary anterior pituitary cells (Takimoto et al., 1993; Attardi et al., 1993; Levitan et al., 1991). Cyclic AMP treatment, on the other hand, decreases Kv1.5 transcript levels in GH3 cells (Mori et al., 1993), but increases it in cardiac myocytes. The 5' UTR of Kv1.5 is known to contain a cAMP response element (CRE) and a potential glucocorticoid response element (GRE) that may be involved in these transcriptional responses (Mori et al., 1995). Sequences in the 3' UTR of the Kv1.4 gene have been shown to affect Kv1.4 channel expression in Xenopus oocytes, most probably by affecting translation efficiency (Wymore et al., 1996). Based on the fact that these 3'UTR sequences are absent in one of the two Kv1.4 transcripts expressed in mouse

brain and heart, these sequences are predicted to affect endogenous translation levels as well, but this has not been experimentally tested.

Table 2 : Regulation of K^+ Channel Gene Expression (Levitan and Takimoto, 1998)

Stimulus	Genes	Tissues and Cells
Glucocorticoids (stress)	Kv1.5 ↑	GH_3 cells, Anterior pituitary Ventricles, Skeletal muscle
Thyrotropin-releasing hormone	Kv1.5 ↓ Kv2.1 ↓	GH_3 cells
Membrane depolarization	Kv1.5 ↓	GH_3 cells
Morphine	Kv1.5 ↓ Kv1.6 ↓ Kv1.5 ↑ Kv1.6 ↑	Striatal neurons Spinal cord neurons
Myelination	Kv1.1 ↑ Kv1.2 ↑	Schwann cells
Thyroid hormones	Kv4.2 ↑ Kv4.3 ↑ Kv1.4 ↓ Kv4.2 ↑	Ventricles Neonatal ventricular myocytes
Myocardial infarction	Kv2.1 ↓ Kv4.2 ↓	Ventricles
Renovascular hypertension	Kv4.2 ↓ Kv4.3 ↓	Ventricles
Atrial fibrillation	Kv1.5 ↓	Atria
IGF-I	Kv1.5 ↑	Neonatal ventricular myocytes
Chronic hypoxia	Kv1.2 ↓ Kv1.5 ↓	Pulmonary arterial smooth muscle cells

1.1.3.2. Alternative splicing

The Shaker gene has multiple exons covering 120 kB of DNA, and can be alternatively spliced to produce at least five different transcripts that encode kinetically distinct channels (Pongs et al., 1988; Schwarz et al., 1988). The voltage-gated mammalian Shaker-like channels, on the other hand, have uninterrupted, intron-less coding regions (Chandy and Gutman, 1995). The only exception to this is Kv1.7, which has an intron in the loop linking its first two TM domains. The variable splicing of a small intron in the 5' UTR of Kv1.1 has been proposed to affect translation initiation of this channel, since it contains three potential initiation codons that could delay arrival of scanning ribosomes at the true start site (Tempel et al., 1988; Chandy and Gutman, 1995).

1.1.3.3. Heteromultimerization

As in the case of the ShA and ShB Shaker splice forms (Isacoff et al., 1990), co-expression of two different Shaker-like mammalian channels (Kv1.1 and Kv1.4) in Xenopus oocytes yielded currents that could not be described as the algebraic sum of those produced by individual mRNAs (Ruppersberg et al., 1990; Christie et al., 1990). This was interpreted to mean that hetero-oligomers were formed. Moreover, Drosophila Shaker and the homologous rat Kv1.1 were also seen to form heteromultimers in Xenopus oocytes (Isacoff et al., 1990).

In contrast, fly Shaker and ether-a-go-go channels do not oligomerize (Tang et al., 1998). Likewise, it has been shown both by electrophysiology (Salkoff et al., 1992; Covarrubias et al., 1991) and by co-immunoprecipitation experiments (Shen and Pfaffinger, 1995) that channels from different sub-families of the voltage-gated potassium channels do not hetero-oligomerize. Sequences that are important for sub-family-specific channel assembly have been identified in the amino termini of several channels (Tu et al., 1995; Shen and Pfaffinger, 1995; Babila et al., 1994).

Importantly, heterooligomers of voltage-gated potassium channels have been shown to exist in vivo. Kv1.2 and Kv1.4 have distinct but overlapping expression patterns in rat brain. They can be co-purified and co-immunoprecipitated with subunit-specific antibodies (Sheng et al., 1993). Similar results were obtained for Kv1.1 and Kv1.2 in mouse brain (Wang et al., 1993). Since then, several studies have confirmed the existence of heteromeric channels in vivo. It is worthwhile to point out, however, that despite the apparent promiscuous assembly (within sub-families) of heterogously expressed channels, specific Kv1 heteromers predominate in the brain, and some possible combinations are not detected.

1.1.3.4. Post-translation modification and/or modulation

Voltage-gated potassium channel activity may be modulated by a wide variety of post-translational mechanisms. These include covalent modifications such as glycosylation and phosphorylation, potential allosteric effects of lipids, nucleotides, other ions, or G proteins, and even direct effects of the mechanical or biophysical environment. Since glycosylation is dealt with in detail in the following section, it will not be described here. Two of the several modulators of channel function are summarized in the following.

Phosphorylation : Shaker and its homologues have a conserved potential tyrosine kinase site in the amino-terminus. However, deleting this region had no effect on Kv1.3 channel function (Aiyar et al., 1993), so the physiological relevance is unclear. In contrast, there is evidence for the significance of the PKC site(s) present in the cytosolic loop between TM domains 4 and 5 of all voltage-gated potassium channels. Several channels, specifically Kv1.3, Kv3.1, Kv1.4, Kv 4.2 and Shaker, are phosphorylated by PKC (Chandy and Gutman, 1995). Mutation of the Shaker PKC sites has been reported to produce a non-functional channel (Isacoff et al, 1992).

Effect of nucleotides : The ATP-gated potassium channels are expressed in heart and skeletal muscle, pancreatic beta cells, kidney and brain (Babenko et al., 1998; Ashcroft et al., 1988). These channels function in the pancreatic islets to control the secretion of insulin. Beta cells secrete insulin in response to depolarizing calcium action potentials when there is glucose in the bloodstream and high ATP levels in the cells. The K(ATP) channels are kept closed by intracellular ATP. When serum glucose levels and consequently cellular ATP levels fall, the K(ATP) channels tend to open and to

hyperpolarize the cell, thus preventing calcium spikes and the consequent secretion of insulin. The function of the K(ATP) channels at the other locations is not known.

1.1.3.5. Auxiliary subunits : the cytosolic Kvβ subunit

The association of potassium channels with auxiliary subunits can affect the biophysical, pharmacological or cell biological properties of the channel. The best-studied example is the cytosolic Kvβ subunit of the voltage-gated potassium channels (Trimmer, 1998). Kvβwas first cloned using sequence from a protein that co-purified with the α-dendrodotoxin binding complex of bovine brain (Scott et al., 1994). Since then, at least four mammalian genes encoding beta subunits have been identified (Trimmer, 1998). The hyperkinetic (Hk) gene was found to encode the Kvβ homologue in Drosophila (Chouinard et al., 1995).

Kvβ subunits are peripheral membrane proteins that themselves form tetramers, and are stably associated with the channel in the stoichiometry α4β4. They are members of the NAD(P)H-dependent oxidoreductase superfamily. The catalytic NADPH-binding site has been retained, and the protein is seen to possess the characteristic oxido-reductase fold (Gulbis et al., 1999). Kvβ1, 2 and 3 interact with members of the Kvα1 Shaker-like sub-family both in heterologous expression systems as well as (for Kvβ1 and 2) in the brain (Rhodes et al., 1995; Rhodes et al., 1996). However, the Kvβ2 isoform is significantly more abundant in the mammalian brain and has been shown to predominantly colocalize with the alpha subunits in native channels (Rhodes et al., 1997). Kvβ1 and 2 have also been shown to interact with heterogously expressed Kvα4 (Nakahira et al., 1996; Perez-Garcia et al., 1999), however, only Kvβ2 is found in

association with endogenous brain Kvα4 channels. The beta subunits vary in the nature of their modulatory effects on potassium channels.

Kvβ1 and Kvβ3. In co-expression studies on Xenopus occytes, Kvβ1 and Kvβ3 result in an acceleration of the macroscopic inactivation rates of several channels (Aldrich, 1994). The mechanism of this effect is thought to be similar to that seen in the rapidly inactivating alpha subunits (for instance, Shaker). In Shaker, the distal N-terminal region of the alpha subunit (residues 5 – 44; the "ball") is linked to the channel by the rest of the flexible N –terminus (the "chain") and is thought to rapidly plug the pore on the cytosolic face of the channel upon depolarization, resulting in fast (N-type) inactivation and a transient potassium current (Zagotta et al., 1990; Hoshi et al., 1990). Kvβ1 subunits have an amino-terminal domain with structural and possible functional similarity to the inactivating "ball" of the alpha subunits (Heinemann et al., 1994; Rettig et al., 1994) and are therefore proposed to effect rapid inactivation in a similar manner.

Kvβ2. The Kvβ2 isoform lacks the inactivation domain, despite high overall amino acid identity with Kvβ1, and has no effect on channel inactivation kinetics. Rather, it increases the cell surface expression levels of several channel alpha subunits, including Kvα1.1, Kvα1.2, Kvα1.4 and Kvα4.3 (Yang et al., 2001). This has been shown by electrophysiological measurements on channels expressed in Xenopus oocytes (Accili et al., 1997; Accili et al., 1998), by radioligand binding studies on channels in transfected tissue culture cells (Shi et al., 1996) and by immunofluorescence staining of transfected primary neurons with antibodies directed towards extracellular epitopes (Manganas and Trimmer, 2000). A combination of voltage clamp and single channel patch clamp studies on Kv1.2α expressed in Xenopus oocytes showed that, whereas macroscopic current

amplitude was increased six-fold by Kvβ2 co-expression, there was no effect on single channel properties (Accili et al., 1997). This argues strongly for an effect of Kvβ2 on functional surface channel number. This effect is not seen for all voltage-gated potassium channels, however. In fact, Kvβ2 co-expression reduces the surface levels of Kv1.5α (Accili et al., 1997). The mechanism by which Kvβ2 promotes increased surface channel expression is not known.

Drosophila Hk. The only study, to date, of native beta subunit modulation of potassium channels has been carried out in Drosophila (Wang and Wu, 1996). As mentioned earlier, the Drosophila beta subunit is encoded by the Hyperkinetic gene. The relevance of this protein for Shaker physiology is manifest in the leg-shaking phenotype, very similar to that of *Sh* mutants, exhibited by *Hk* mutant flies (Chouinard et al., 1995). Voltage clamp analysis of the Drosophila larval body wall muscle showed diverse effects of *Hk* mutations. The mutations specifically affected the I_A current while leaving I_K and I_{Ca} unchanged, thus confirming the specific interaction of the beta subunit with the Shaker channel in Drosophila. The kinetics of I_A current inactivation as well as recovery from inactivation were accelerated in flies with mutant Hk alleles. Interestingly, the I_A current amplitude was also reduced (by about 60 %) in *Hk* fly muscle, possibly due to an effect on channel surface levels similar to that seen in homologous mammalian systems. The hyperexcitability of mutant Hk neurons (Stern and Ganetzky, 1989) as well as the leg-shaking phenotype of mutant flies (Kaplan and Trout, III, 1969) corresponds well to the fact that the encoded beta subunit modulates I_A.

There are other auxiliary subunit proteins that are known to affect potassium channel activity and surface expression, and therefore to contribute to channel diversity.

As already mentioned, the sulfonylurea receptor (SUR) subunit of the K(ATP) channel confers upon an inward rectifying potassium channel (Kir6.2) the property of gating by intracellular ATP Further, a yeast two-hybrid screen was used to identify a putative chaperone protein KChap (Wible et al., 1998), which interacts with voltage-gated Kvα1 and Kvα2 subunits and increases current amplitude three-fold when co-expressed with these channels in Xenopus oocytes. Since single channel properties were not affected by KChap, it was proposed to increase the cell surface levels of functional channel.

To briefly summarize what has been discussed so far : the voltage-gated potassium channels constitute one of several classes of potassium-conducting pores, and are expressed in all organisms examined so far. The first channel of this class to be cloned was the Shaker channel of *Drosophila melanogaster*, which encodes the transient, rapidly-inactivating I_A current of Drosophila neurons and muscle. Based on homology to Shaker, several other families of voltage-gated channels were identified in Drosophila. Homology to these channels has been used in the classification of most subsequently identified vertebrate voltage-gated channels. Potassium currents are extraordinarily diverse, probably due to the converging influence of several aspects of potassium channel structure, expression, regulation, and cell biology.

1.1.4. Frontiers of potassium channel biology

1.1.4.1. High resolution structure

The determination of high-resolution structure of potassium channels by X ray crystallography has only been accomplished recently. Native channels are expressed in relatively low abundance. Moreover, they are multi-spanning membrane proteins and, as

such, pose difficulties in generating crystals that diffract at atomic resolution. The early era of structure-function analysis, in the decade or so that followed cloning of the channels, was largely indirect. Structure was inferred from the pharmacological and biophysical effects of specific channel mutations, as well as from the accessibility of certain channel residues to externally applied modifying reagents. Nevertheless, a great deal was learned about potassium channel structure in this way. Very simply summarized, these approaches helped define the amino acids that line the conduction pore, that make up the voltage sensor, that constitute the binding sites of several pharmacological agents and toxins, and that contribute to selectivity of the channel for potassium over other cations. However, confirmation of this plethora of indirect information required a high-resolution structure. The discovery and cloning of a simple, two-TM domain bacterial potassium channel (KcsA) with very similar properties and extremely high homology to the TM5-P loop-TM6 pore region of eukaryotic channels (Schrempf et al., 1995) eventually culminated in a high-resolution structure of the potassium channel pore (Doyle et al., 1998).

KcsA. The channel is a highly asymmetric structure proposed to resemble an "inverted teepee" (if the outside of the cell is defined as "up") with four transmembane helices, one from each subunit, acting as the "poles" of the teepee. The helices are tilted (~25°) relative to the membrane. The pore is narrowest close to the extracellular aspect of the channel, with a width of ~3Å. This region corresponds to the signature sequence or P-loop of the potassium channel, and is what constitutes the selectivity filter. It is lined by polar residues, the carbonyl oxygen atoms of which are proposed to function as "surrogate water" to compensate for dehydration of a potassium ion as it enters the filter,

thus providing evidence for predictions made early on (Hille, 1975). A ring of aromatic residues is positioned around the selectivity filter, and is proposed to function as a spring-like "cuff", which holds the filter open at precisely the dimensions to accommodate a potassium ion. The pore widens to ~10Å deeper into the channel, thus forming an aqueous cavity within the membrane, a strategy that would tend to counter the electrostatic destabilization that results from moving a charged ion across the phospholipid bilayer.

Kvβ2 . The cytosolic Kvβ2 subunit of mammalian voltage-gated channels has been crystallized and the structure solved (Gulbis et al., 1999). The beta subunit is tetrameric under native conditions and, as predicted from its sequence, is structurally similar to other members of the aldo-keto reductase enzyme family. Based on the fact that the cofactor NADP+ is seen tightly bound in the active site of Kvβ2, and that the active site residues are appropriately positioned to effect catalysis, the beta subunit of mammalian voltage-gated channels is proposed to be a competent aldo-keto reductase, and to putatively function in linking channel activity to the redox state of the cell.

T1 domain. Lastly, the structure of a cytosolic amino-terminal domain (the T1 assembly domain) of the Kv1.1 channel from Aplysia californica has been solved (Kreusch et al., 1998; Gulbis et al., 2000). The T1 tetramer is oriented coaxial with the transmembrane portion of the channel, and has been proposed to form a "hanging gondola" structure in the cytosol. At its membrane-proximal face, this structure is separated by ~20Å from the rest of the channel, and it is through these 20Å openings, lined by negatively charged residues, that potassium ions are proposed to approach the conduction pore. At its membrane-distal face, the T1 tetramer is seen to engage the beta subunit. However, it has

been proposed that the structure of the isolated cytosolic domain may not be identical to that in the native channel (Kobertz and Miller, 1999).

For all its power, X-ray crystallography is a technique that necessarily provides static structures, such that information about the molecular bases of dynamic behavior is largely inferential. Still, some predictions can be made. In the structure of KcsA, the poles of the inverted tepee are bundled together at the intracellular face of the channel, creating an occlusion that is predicted to be the closed gate of the channel (Doyle et al., 1998; Miller, 2000). Presumably, preparations of channels that can be manipulated into specific states (open or inactivated, for instance) will provide direct structural evidence for such predictions. Likewise, crystallization of the more complex eukaryotic channels could provide direct insight into structural transitions during voltage sensing. Clearly however, the power of crystallographic structure determination is limited to probing those states of the channel that can be stably and predictably maintained.

1.1.4.2. Regulation of gene expression

This aspect of potassium channel biology was summarized in the previous section and will not be dealt with in detail here. Potassium channel genes are indeed regulated at the transcriptional level, and the potential importance of such regulation is clear at the levels of development, cell and organismal physiology. For the potassium channels, as for all protein superfamilies, deciphering the molecular bases of gene expression is a pre-requisite for a synthetic comprehension of the complex role that they play in the biology of living creatures.

1.1.4.3. Cell biology

The voltage-gated potassium channels function, according to all existing knowledge, at the plasma membrane of the cell. Both the localization of channels to the cell surface and the distribution of channels once at the cell surface are not uniform, but vary with channel- and cell-type and, as such, are possibly the result of regulated processes in vivo. The generation of accurately localized and distributed channels may be broken down, cell biologically speaking, into (i) biogenesis of the channel, which includes translation of the protein, targeting to the endoplasmic reticulum, integration into the ER membrane, post-translational modification, folding and assembly; (ii) transport of the channel through the secretory pathway and the endocytic recycling pathway; and (iii) localization or immobilization of the channel at specific cell surface domains. Perturbations in one or other of these processes has been implicated, for several ion channels, in human pathology (Jurkat-Rott and Lehmann-Horn, 2001; Bockenhauer, 2001). The "channelopathies" are manifest ubiquitously through human physiology, affecting kidney and pulmonary epithelia (ENaC in Liddle's syndrome, CFTR in cystic fibrosis) (Snyder et al., 1995; Qu et al., 1997), cardiac function (HERG in long QT syndrome) (Zhou et al., 1998) and the nervous system (Kv1 in episodic ataxia) (Adelman et al., 1995; Manganas et al., 2001) .

1.2. Ion channel cell biology

The experiments presented in this thesis deal principally with aspects of Shaker channel cell biology. The following therefore also serves as a more specific introduction to the work.

1.2.1. Biogenesis of oligomeric membrane proteins in the ER

1.2.1.1. Targeting to the endoplasmic reticulum

The synthesis of channel proteins bound for the cell surface begins, as for most other integral membrane proteins, in the cytosol. The ribosome-nascent chain complexes are rapidly targeted to the ER, in a process that is initially thought to be very similar to the targeting of secreted proteins. Nascent chain competition experiments showed that a membrane protein, but not a cytosolic protein, was able to compete for binding sites at the ER membrane with a signal sequence-bearing secreted protein (Lingappa et al., 1978). This suggested that translocation and integration utilize a common initial pathway for movement across or into the ER membrane. Further, proteins such as immunoglobulins are generated in either secreted or membrane-integrated forms, again suggesting a common pathway for biogenesis (McCune et al., 1980). Indeed, yeast secretion mutants that are unable to translocate proteins into the ER lumen are also defective in protein integration (Stirling et al., 1992). Very simplistically stated, the process occurs as follows (Fig. 1.2) (Walter and Johnson, 1994) (Matlack et al., 1998). The cytosolic ribonucleoprotein signal recognition particle (SRP) recognizes a hydrophobic targeting sequence on the membrane protein as it emerges from the ribosome, and temporarily arrests translation. The arrest is relieved upon engagement of SRP with the SRP receptor (SRP-R) at the ER membrane. Translation then resumes, the targeted ribosome associates with the protein conducting pore (sec61 or 'translocon') and the membrane protein is inserted into the translocon and integrated, in a poorly understood process, into the ER membrane. With a few noteworthy exceptions (e.g. the nicotinic acetylcholine receptor) (Karlin and Akabas, 1995; Anderson and Blobel, 1981),

integral membrane proteins lack the N-terminal hydrophobic signal sequence necessary for targeting of secreted proteins to the ER. Instead, the transmembrane (TM) domains are thought to function in this capacity. This was initially based on experiments on the 7-TM protein opsin, which lacks an amino-terminal signal sequence (Schechter et al., 1979). Several transmembrane domains (including TM1) of opsin were shown to target a reporter protein to the ER in an SRP-dependent manner, but there was no targeting information in the protein amino terminus (Friedlander and Blobel, 1985).

Targeting of the voltage-gated channels has been studied for Kv1.1 and Kv1.3. *In vitro* translation of truncated Kv1.1 constructs in the presence of dog microsomes suggested that, indeed, TM1 was required for targeting to the ER (Shen et al., 1993). Surprisingly, both TM1 and TM2 were required for targeting Kv1.3 (Tu et al., 2000). The prokaryotic potassium channel KcsA, which is highly homologous to eukaryotic channels in the pore region, is targeted to the bacterial inner membrane by an SRP-dependent mechanism (van Dalen et al., 2002). Initial ER targeting of the Shaker channel is assumed to require TM1, but this has not been studied. We have addressed this question in our work.

1.2.1.2. Integration into the lipid bilayer

The minimum 'integration machinery' in the mammalian ER is thought to be the same as the minimum 'translocation machinery', namely the SRP receptor and the sec 61 trimer or translocon (sec 61 α, β and γ). Proteoliposomes reconstituted with only these four proteins were seen to integrate a test membrane protein (Heinrich et al., 2000; Gorlich and Rapoport, 1993). Since the efficiency of reconstituted systems is inevitably extremely low, however, it is difficult to predict how relevant the concept of the

'minimum machinery' is for either translocation or integration *in vivo*. Membrane protein nascent chains (i.e. translation intermediates that are still attached to the ribosome) of any desired length may be generated by translating mRNA that lacks a stop codon. This is a commonly used method to 'freeze' translation at specific points along the length of the protein being studied, with the aim of analyzing the protein and lipid environment of the growing nascent chain. As is the case for secreted proteins, nascent chains of single-pass and polytopic membrane proteins can be cross-linked to sec61 α, sec 61β and to a third ER protein named the translocon associated membrane protein (TRAM) (Gorlich et al., 1992; High et al., 1991; High et al., 1993; Mothes et al., 1997; Do et al., 1996; Knight and High, 1998; Laird and High, 1997).

Mechanistically, membrane protein integration is not completely understood. The schematic version of this process is that, at some point during translocation, the TM domain(s) of an integral membrane protein stop moving along the translocon axis perpendicular to the plane of the bilayer, but rather move laterally, perpendicular to the translocon axis and into the lipid bilayer. Several models have been proposed as to how exactly this process takes place. Specifically, the debate focuses on two issues. First, whether or not the ribosome remains tightly associated with the membrane during the synthesis of cytosolic loops of a polytopic membrane protein. Second, the degree to which N-terminal TM domains can stably integrate into the bilayer while the C-terminus of the protein is still being synthesized, and, in polytopic proteins, whether the integration occurs one TM domain at a time, or in groups of two or more.

Cross-linking of membrane protein nascent chains to lipid has been demonstrated (Heinrich et al., 2000; Mothes et al., 1997; Martoglio et al., 1995), supporting the idea of

individual TM domain integration prior to release from the ribosome. In contrast, nascent chains of the 12-TM domain P-glycoprotein were seen to remain urea-extractable unless released from the ribosome (Borel and Simon, 1996), arguing against co-translational integration of single TM domains. The argument for post-translational (or post-ribosome release) integration is that it would allow for co-operative folding of the TM domains, possibly within the translocon lumen, to form tertiary structure(s) that may be required for stable integration and for eventual protein function. However, the intriguing fact that "half molecules" of several membrane proteins, including transporters (Ste6) (Berkower et al., 1996) and channels (CFTR) (Chan et al., 2000), are able to assemble into functional proteins within the lipid bilayer is a strong indication that productive interactions between TM domains need not be limited to the pre-integration aqueous environment. Further, experiments that combine the lipid cross-linking and urea extraction approaches show that cross-linkability to lipid and extractability from the membrane are not necessarily mutually exclusive scenarios. In other words, nascent chains that could be cross-linked to lipid could also be extracted from the bilayer (Heinrich et al., 2000). The integration process may be more dynamic than has previously been appreciated, such that a TM domain on a nascent membrane protein may have reversible access to the bilayer before it is inextractably integrated. Indeed, the fact that membrane proteins destined for degradation are 'reverse translocated' via the translocon (i.e. sec61) makes this suggestion far from untenable (Kopito, 1997). Nevertheless, it is quite possible that different membrane proteins vary in the details of their integration process, and that this is reflected in the results obtained for different model proteins.

Integration of potassium channels has been studied for the Kv1.3 channel, which requires both TM1 and TM2 for stable integration. This is the case in the context of the complete channel, whereas individual TM domains can integrate in isolation (Tu et al., 2000). Surprisingly, the prokaryotic KcsA channel associated as efficiently with pure lipid vesicles as with microsomes derived from the bacterial inner membrane or with proteoliposomes containing the bacterial translocon secYEG (van Dalen et al., 2002). Integration of the KcsA channel into lipid vesicles was not explicitly examined. However, since tetramerization was very efficient in pure lipid membranes, a result speculatively attributed to the relief from 'molecular crowding' in microsomes, integration was assumed to have occurred normally. Since the targeting of KcsA is SRP-dependent, efficient channel formation in pure lipid is an intriguing, if somewhat inexplicable, result and will require more careful examination. Integration of the Shaker channel has not been studied. We have examined integration of truncated Shaker as well as of full-length channel in TRAM-depleted microsomes.

1.2.1.3. Oligomerization, folding and topogenesis

Oligomeric membrane proteins must assemble into their final quaternary structure (Fig. 1.2). The ion channels, in particular, present an intriguing case, since assembly necessarily results in the generation of an aqueous passage at the core of the fully assembled multi-subunit protein. This passage is lined, it is thought, by one face of amphipathic transmembrane helices contributed by each subunit of the channel (Unwin, 1989; Imoto et al., 1988; Leonard et al., 1988; Akabas and Karlin, 1995). With a few, sometimes controversial, exceptions (Musil and Goodenough, 1993), assembly of oligomeric membrane proteins occurs in the ER (Hurtley and Helenius, 1989). This is

true for the Shaker channel (Nagaya and Papazian, 1997a; Schulteis et al., 1998) as well as for mammalian and squid voltage-gated potassium channels (Babila et al., 1994; Shen et al., 1993; Deal et al., 1994). Association between potassium channel α and β subunits also occurs in the ER (Nagaya and Papazian, 1997a).

An N-terminal region (the tetramerization or T1 domain) of voltage-gated potassium channels (Figure 1.1) may be involved in the tetramerization process. It is generally well accepted that the T1 domain is responsible for the specificity of heteromultimerization, whereby only channels from the same sub-family assemble into tetramers (Shen and Pfaffinger, 1995; Deutsch, 2002). This is likely to be crucial for maintenance of the cellular potassium current repertoire. The role of T1 in assembly *per se* has been more complicated to define. Deletion of the Shaker T1 domain (Schulteis et al., 1998) or specific mutations of conserved T1 residues (Liu et al., 2001; Minor et al., 2000; Cushman et al., 2000) have been shown to result in unassembled, non-functional channels. In contrast, T1-less versions of Kv1.3 (Tu et al., 1995; Tu et al., 1996), Kv1.1 (Babila et al., 1994) and Shaker (Kobertz and Miller, 1999) are functional cell-surface channels, but may be formed at a reduced rate and efficiency. Further analysis shows that mutations that disrupt Kv T1-T1 association, although they do not completely prevent assembly, produce elevated levels of channel monomer (Strang et al., 2001). Further, the resulting tetramers are more susceptible to denaturation, and there is an overall redistribution of the channel to a perinuclear location that possibly corresponds to the ER. In addition to its function in maintaining sub family-specific heteromultimerization, therefore, the T1 domain may aid channel assembly and probably increases the stability of the tetrameric state, but is not absolutely required. Consistent with its proposed

function in promoting potassium channel assembly, T1 forms a tetramer in solution, as seen in the Xray crystal structure (Pfaffinger and DeRubeis, 1995). Additionally, the transmembrane domains of Kv channels (Sheng et al., 1997), and the C-terminal domains of the inward rectifier channels (Tinker et al., 1996), have been implicated in assembly.

It is worth pointing out that, by virtue of its position at the N-terminus of the voltage-gated potassium channels (Kv), the T1 domain is ideally placed to promote rapid assembly. It could begin to fold, and perhaps even to assemble with neighboring channels, early in translation. Co-translational folding has been suggested to occur on nascent proteins (Kolb et al., 2000; Nicola et al., 1999; Chen and Helenius, 2000). Kv channel tetramerization occurs more rapidly than can be measured using standard biochemical or cell biological techniques (Deal et al., 1994; Shen et al., 1993). It has been suggested that assembly is a co-translational process and, indeed, nascent chains of the Kv1.3 channel may be cross-linked to each other via the T1 domain (Lu et al., 2001). This is somewhat surprising, since the dimensions of the ribosome relative to the translated protein should theoretically preclude association between two nascent channel subunits. Nevertheless it is quite possible that, here too, the cartoon version of the world does not apply, and that exit sites in adjacent translating ribosomes are closer together than has previously been imagined. Nascent chains of influenza haemagglutinin (HA) have also been shown to be competent for trimerization when still attached to the ribosome, although in this case, association was between the nascent chain, on one hand, and ribosome-released, integrated subunits, on the other (Chen and Helenius, 2000).

The ER is the cellular location at which all membrane proteins, including the ion channels, are thought to fold, although it is not clear that the final, ion-conducting

architecture of a channel is indeed attained in this organelle. Folding is often presented as a process distinct from translocation, integration and assembly, but it is likely that channel biogenesis is a continuum of events that are cooperative to one or other degree. There is not a great deal known about folding of potassium channels. Point mutations that neutralize positive charges in the Shaker voltage sensor (S4) have been shown to block maturation of the channel, suggesting that the protein is improperly folded (Papazian et al., 1995; Schulteis et al., 1998; Tiwari-Woodruff et al., 1997). Second-site mutations that reverse negative charges on adjacent transmembrane domains rescue maturation of the S4 mutants, implicating intra-subunit electrostatic interactions in folding of the protein. Oxidative inter-subunit cross-linking of cytosolic cysteines (N-terminal C96 and C-terminal C505) was seen to occur in wild type Shaker, but not in the folding mutants (Schulteis et al., 1998). Therefore, proximity of the N- and C-termini of adjacent subunits was proposed to be a hallmark of folded Shaker, and, since it occurred in non-tetramerizing "T1-less" channels, was proposed to occur independent of channel assembly.

1.2.2. N-linked glycosylation : role in protein folding and structure

1.2.2.1. Core glycosylation

N-linked glycosylation occurs at asparagine residues on secreted and transmembrane proteins in the context Asn-X-Ser/Thr, where X is any amino acid other than proline (Helenius and Aebi, 2001; Kornfeld and Kornfeld, 1985). Most (~ 90%) extracellular consensus sites are thought to indeed be glycosylated, although with variable efficiency. A 14-saccharide "core" unit ($Glc_3Man_9GlcNac_2$) (Figure1.3) is

assembled as a lipid-linked, dolichylpyrophospate precursor at the ER membrane, in a series of sequential reactions catalyzed by enzymes on both faces of the membrane. It is the first step of this assembly process (i.e. the transfer of GlcNac-1-P from UDP-GlcNac to dolichylphospate) that is blocked by the glycosylation inhibitor tunicamycin. The core oligosaccharide is coupled via an N-glycosidic linkage to the asparagine residue of the growing nascent polypeptide (Nilsson and von Heijne, 1993) by the action of the oligosaccharyl transferase in the ER lumen (Silberstein and Gilmore, 1996). The core glycan is identical for all proteins in a given organism. The great structural diversity of mature glycans results from modifications that occur later in the secretory pathway. Core glycosylation is, further, almost identical in all eukaryotes. The N-linked core moiety added in *S. cerevisae, C. elegans, D. melanogaster* and *S. pombe* is the same 14-saccharide unit as in mammals. The only organisms known to transfer unglucosylated oligosaccharides (i.e Man6-9GlcNac2) to nascent proteins are the trypanosomes (Parodi, 2000; Parodi, 1993).

1.2.2.2. Processing and maturation of the core glycans

In the ER, core glycosylation is rapidly followed by "trimming", in which the three glucose and some mannose residues are removed by ER-glucosidases I and II (GI/II), and by mannosidases I and II (MI/II) (Figure 1.4) (Helenius and Aebi, 2001; Dennis et al., 1999). A single glucose residue may be re-added by the action of the UDP-glucose:glycoprotein glucosyl transferase (GT), which is important for glycoprotein folding, as will be discussed later. Upon traffic to the cis-Golgi, the mannoses are further trimmed by Golgi mannosidases, followed by the addition of GlcNac by N-acetyl-glycosaminyl transferase I (T1) in the medial Golgi. The activity of T1, found in all

metazoan animals and plants but not in yeast or protozoa, is required for generation of the complex-type oligosaccharides. These are formed by further elaboration of the now "branched" sugar, by the action of additional GlcNAc transferases (TII-V), and the galactosyl- (Gal-T), fucosyl- (Fuc-T) and sialyl- (ST) transferases, in the trans-Golgi. Mature glycoproteins contain a mixture of complex and "high mannose" sugars, the latter having been incompletely processed in the Golgi. There is great diversity between complex glycans themselves, sometimes even between those at two glycosylation sites on the same protein. Glycan diversity is thought to be the result of the protein context, the tissue-specific gene expression of Golgi glycosylation enzymes, and the metabolic state of the cell. It results in the generation of several possible protein "glycoforms" with, in some cases, demonstrably different properties. In principle, this has a potentially enormous impact on the complexity of the protein repertoire in multicellular organisms. In vertebrates, proteins known to be involved in some aspect of oligosaccharide biosynthesis and processing constitute 0.5 1% of the translated genome (Dennis et al., 1999). It is perhaps not surprising, then, that the only gene in which humans and chimpanzees have, to date, been shown to differ, is CMP-sialic acid hydroxylase, which modifies N-acetyl neuraminic acid to create Neu5Gc (Varki, 2001). Chimpanzees have this gene, as do all other mammals examined so far, but humans do not. The significance of this observation, if any, remains to be determined.

1.2.2.3. Two broadly defined roles for glycosylation

The sequence of events that generates mature glyoproteins may be regarded as somewhat inefficient, since it involves building a large core sugar unit, then trimming it down, then building it up further, trimming again, and so on. This is likely to reflect the

fact that glycosylation plays two types of roles, broadly speaking, in biology. First, it plays a role in protein folding in the ER. Addition of the hydrophilic, soluble core sugar to nascent polypeptides promotes efficient folding either via direct effects on protein stability/ conformational flexibility or via interaction with glycosylation-dependent chaperones. It is worth noting that sugars are rarely required to maintain the folded state of the protein, once it has been achieved (Helenius and Aebi, 2001; Imperiali and O'Connor, 1999; Olden et al., 1982). Thus, the role of glycosylation in protein folding is a transient one, occurring early in the life of a protein, and generally played out by the time traffic to the Golgi apparatus has occurred.

Second, glycans have multiple effects on the structure and function of mature proteins. Because of the diversity of complex sugars, these effects may not be summarized as easily, and must be more generally described. A single complex glycan is thought to extend about 3 nm away from the protein surface, and is thus of the appropriate dimensions to function as a separate domain and to affect protein-protein interactions. Complex sugars are known to extend the serum half-life of several hormones (erythropoeitin, follicle stimulating hormone, luteinizing hormone) and coagulation factors (anti-thrombin, protein C, protein S, factor XI, VIII and IX)(Aebi and Hennet, 2001), to possibly regulate the specificity of protein-protein interactions at the T-cell immunological synapse(Dustin et al., 1997), to protect lysosomal membrane proteins from proteolysis (Kundra and Kornfeld, 1999), to mediate intracellular sorting of the lysosomal hydrolases (Hille-Rehfeld, 1995) and to effect the adhesion and extravasation of circulating leukocytes (Rudd et al., 2001).

It has been speculated that the distinct roles played, on the one hand by core glycosylation early in protein biogenesis, and on the other, by complex glycans in mature proteins, reflect the different evolutionary origins of the ER and the Golgi glycosylation machineries (Helenius and Aebi, 2001). N-linked glycosylation has most likely evolved from enzymes involved in synthesis of the N-glycan-containing archaebacterial cell wall (Bugg and Brandish, 1994). Archaeal genomes have oligosaccharyl transferase homologues, and glycans are transferred from dolichylphosphate/pyrophosphate precursors to the same Asn-X-Ser/Thr consensus sequence as in eukaryotic cells (Lechner and Wieland, 1989). Golgi enzymes, in contrast, show highest sequence homology to cytosolic enzymes involved in sugar nucleotide metabolism (Wiggins and Munro, 1998; Helenius and Aebi, 2001), and may thus have evolved quite differently.

1.2.2.4. Complex sugars are essential

In keeping with the diverse and plentiful roles of complex sugars, deficiencies in glycosylation enzymes often have diverse and plentiful effects. As one might expect, the more upstream the enzyme that is deficient, the more severe the disorder that results. For example, mice lacking GlcNac-T1 die *in utero* with defects in multiple organs, whereas animals without α2,6-sialyl transferase are defective in B cell activation, but are nevertheless viable and fertile. Likewise, the congenital disorders of glycosylation (CDG) in humans present with varying severity, depending on the enzyme affected and the nature of the mutation (Table 3) (Aebi and Hennet, 2001). Phosphomannomutase is

Table 3 : Congenital disorders of glycosylation (Aebi and Hennet, 2001).

Name	Gene (yeast)	Activity
CDG-Ia	*PMM2*	Phosphomannomutase (Man-6-P → Man-1-P)
CDG-Ib	*PMI*	Phosphomannose isomerase (Fru-6-P → Man-6-P)
CDG-Ic	*ALG6*	α1-3 Glycosyltransferase
CDG-Id	*ALG3*	α1-3 Mannosyltransferase
CDG-Ie	*DPM1*	Dolichyl-phosphate-mannose synthase (GDP-Man → Dol-P-Man)
CDG-If	*LEC35*	Unknown
CDG-IIa	*MGAT2*	β1-2 N-acetylglycosaminyltransferase
CDG-IIb	*GLS1*	α1-2 Glucosidase
LADII/CDG-IIc	*GDP-Fuc transporter*	Import of GDP-Fuc into Golgi and export of GMP
Ehlers-Danlos syndrom (progeroid form)	*XGPT*	Xylose β1-4 galactosyltransferase
Galactosemia I	*GALT*	Gal-1-P uridyltransferase (Gal-1-P + UDP-Glc ↔ UDP-Gal + Glc-1-P)
Galactosemia I	*GALE*	Galactose epimerase (UDP-Gal ↔ UDP-Glc)
Galactosemia II	*GALK*	Galactokinase (Gal → Gal-1-P)

required for synthesis of an indispensable precursor of the oligosaccharide core, and is the most frequently deficient enzyme in CDG (CDG-Ia). The effects range from early death due to cardiac or liver failure to frequent stroke-like episodes and severe coagulopathy. Deficiency in the Golgi GDP-fucose transporter results in hypo-fucosylation, problems of leukocyte adhesion and consequent immunodeficiency (CDG-IIc). Female CDG patients often do not go through puberty, which has been linked to the serum instability of unglycosylated FSH/LH. At the other end of the spectrum, people with reduced xylose β1,4-galactosyl transferase activity have glycan-deficient proteoglycans, leading to fragile skin and a progeroid appearance.

1.2.2.5. Direct effects of N-linked glycosylation on protein folding

The development and maintenance of the multicellular organism clearly requires complex oligosaccharides. At the cellular level, it is the early effects of glycosylation on protein folding that are more obviously disrupted upon inhibition of this process. Global inhibition results in misfolded and aggregated proteins and is toxic for the cell, but the importance of core glycans for folding of specific proteins varies. In some cases, folding and subsequent export from the ER are absolutely dependent on glycosylation; for instance in the nicotinic acetylcholine receptor (Gehle et al., 1997; Ramanathan and Hall, 1999), rhodopsin (Kaushal et al., 1994), CD4 (Tifft et al., 1992) or the high affinity IgE receptor (Albrecht et al., 2000). In other proteins, for example the V1a vasopressin receptor (Hawtin et al., 2001) and the human choriogonadotropin receptor (Davis et al., 1997), traffic has been reported to be independent of glycosylation. The oligosaccharide moiety may have a direct effect on the folding process. Calorimetric and spectroscopic studies comparing glycosylated and unglycosylated forms of the same protein indicate that sugar groups tend to improve solubility and increase folding rate, the latter perhaps by limiting the conformational options of the polypeptide close to the glycosylation site. Chitobiose (GlcNAc-β1,4-GlcNAc), for instance, has been shown to induce a β-turn in a test substrate (Wormald and Dwek, 1999). The hydrophilic sugar groups would also presumably direct the adjacent polypeptide chain to the surface of the folding protein. Alternatively, core glycans affect protein folding by mediating interactions with the lectin-based quality control machinery of the ER.

1.2.2.6. Chaperone-mediated effects of glycosylation on protein folding

Calnexin (CNX) and calreticulin (CRT) are ER resident lectins that bind specifically to monoglucosylated core glycans (Cannon and Helenius, 1999; Hammond et al., 1994; Hebert et al., 1995). The two chaperones show some difference in the spectrum of cellular proteins with which they interact (Peterson et al., 1995), but this is thought to be largely the result of the difference in their disposition in the ER lumen, since CNX is membrane bound and CRT soluble (Wada et al., 1995). Specifically, if CRT was fused to the transmembrane domain of CNX, it associated with a set of nascent polypeptides very similar to those bound by CNX. There have been several reports of protein-based CNX/CRT interactions with de-glycosylated substrates *in vitro*, but they will not be discussed here (Ware et al., 1995). Monoglucosylated glycans are generated in the ER initially by the sequential action of membrane-bound ER glucosidase I (GI) and lumenal ER glucosidase II (GII) (Figure 1.4) (Helenius and Aebi, 2001). Further GII activity cleaves off the last glucose residue, resulting in release of the substrate protein from CNX or CRT. Re-glucosylation is effected by a remarkable ER lumenal enzyme, the glucosyl transferase (GT), which preferentially re-attaches a single glucose to incompletely folded proteins (Parodi, 2000). This results in re-binding of CNX/CRT, thus retaining the substrate protein in the ER, possibly to allow folding to proceed to completion. The binding specificity of the chaperones, as well as the importance of de-glucosylation/ re-glucosylation cycles and consequently of chaperone unbinding/re-binding cycles, in productive protein folding, were initially studied using VSVG (vesicular stomatitis virus glycoprotein) and influenza HA (Ellgaard et al., 1999; Hammond et al., 1994; Hammond and Helenius, 1994a). The list of glycoproteins subsequently found to interact with these chaperones, however, is extensive (Tatu and Helenius, 1999; van Leeuwen and Kearse,

1996; Vassilakos et al., 1996; Gelman et al., 1995) and the folding of several proteins requires this interaction to proceed efficiently (Vassilakos et al., 1996; Bass et al., 1998; Hebert et al., 1995).

How exactly GT functions as a 'folding sensor' is incompletely understood. In vitro experiments have shown that purified GT prefers to glucosylate partially folded RNaseB over either completely folded or completely unfolded protein (Trombetta and Helenius, 2000). The prediction is that GT recognizes global features of partially unfolded proteins, such as hydrophobic patches. Indeed, GT interacts much more readily with hydrophobic than with hydrophilic peptides, although no functional significance of this interaction has been shown (Sousa and Parodi, 1995). Lastly, GT recognizes partially deglycosylated substrate proteins that still retain the innermost GlcNAc of the core oligosaccharide, but not completely deglycosyalted proteins. This has been interpreted to suggest a specific recognition by GT of this GlcNAc in the context of unfolded polypeptide, since the sugar is largely buried in folded proteins, and so not available for interaction with external macromolecules (Sousa and Parodi, 1995). Overall, the observation is that productive folding of a glycoprotein makes it a poor substrate for re-glucosylation by GT, as a result of which it exits the CNX/CRT cycle, and is exported from the ER.

Proteins that are unable to fold are eventually eliminated, in a process called ER-associated degradation (ERAD). Briefly, ERAD has been shown to occur in the proteasome, and requires ubiquitination of the substrate protein and retrograde translocation out of the ER, although not necessarily in that order (Kopito, 1997). Sequestration of proteolysis away from other folding intermediates in the ER lumen is a

satisfying mechanism for the selective removal of unfolded proteins. Retrograde translocation of both lumenal and membrane proteins is thought to occur through the same channel used for forward translocation i.e. sec61 (Wiertz et al., 1996), although there are some substrates that are degraded by a sec61-independent pathway (Walter et al., 2001). The current ERAD model is supported by genetic interaction between sec61 and ubiquitin-conjugation enzymes (Sommer and Jentsch, 1993), by the retro-translocation-defective phenotype of some sec61 mutants (Wilkinson et al., 2000), and by the accumulation of de-glycosylated, ubiquitinated substrate proteins upon inhibition of the proteasome (Gelman et al., 2002; Yu et al., 1997). Inhibition of ER mannosidase I activity, which removes a single α1,2-linked mannose from the core sugar, has been shown to block ERAD of several substrate proteins (Su et al., 1993; Liu et al., 1999). However, properly folded proteins are not degraded as a result of mannose trimming, so it is not itself sufficient to promote degradation. Since it is a relatively slow process, mannose trimming has been proposed to serve as a "timer" in the ER, such that older (i.e. less recently synthesized) proteins are segregated away from the CNX/CRT cycle and, if still unfolded, are targeted for degradation (Jakob et al., 1998).

CNX itself binds to the thiol:protein oxido-reductase Erp57, and thus can indirectly promote disulfide bond formation in the nascent glycoprotein (Oliver et al., 1997). Deglucosylation-mediated functional Erp57 interactions have been shown to occur for both secreted and membrane proteins (Oliver et al., 1999; Molinari and Helenius, 1999). If a protein is glycosylated within its first 50 amino acids, interaction with CNX/CRT is thought to occur co-translationally (Molinari and Helenius, 2000). Moreover, this is thought to "shunt" the glycoprotein into interactions with

CNX/CRT/Erp57 rather than with the ER lumenal ATPase Bip, and its associated oxido-reductase PDI (protein disulfide isomerase). Inhibiting glycosylation has been shown to result in increased interaction with Bip/PDI, suggesting that there are several, possibly redundant pathways for the productive folding of proteins.

Perhaps reflecting this redundancy, the CNX/CRT cycle may not be absolutely required for protein folding in the ER. Both *S. pombe* and mammalian cells are viable if ER glucosidases I and II are inhibited, but Bip and other ER chaperones are seen to be up-regulated, in this case (D'Alessio et al., 1999). Under ER stress, however, *S. pombe* requires mono-glucosylated glycans to grow normally (Fanchiotti et al., 1998). *S. cerevisiae* has no GT (Fernandez et al., 1994), and its CNX differs quite considerably from the mammalian and *S. pombe* homologue (Parlati et al., 1995), yet budding yeast is able to fold glycoproteins normally. However, disruption of the *S. cerevisiae* CNX-like gene results in increased secretion of heterologously expressed mammalian α1-antitrypsin and of a ts mutant α-pheromone receptor (ste2-3p) that is normally ER-retained at the restrictive temperature (Parlati et al., 1995). Therefore, there may indeed be some participation of the CNX-like chaperone in quality control in *S. cerevisiae* ER. The infectivity of some viruses (HIV, for instance) absolutely requires mono-glucosylated glycans, presumably for the proper folding of surface glycoproteins (Gruters et al., 1987).

The impact of lectin-based quality control at the organismal level is also somewhat unclear. CRT-null mice are embryonic lethals with severe defects in development of the heart (Mesaeli et al., 1999). Since CNX *is* expressed in these mice, the effect may be due to involvement of CRT in a process unrelated to glycoprotein

folding (for instance, in intracellular calcium storage). Alternatively, the chaperones are not functionally redundant, and CRT-mediated glycoprotein folding is indeed essential for cardiac development. Mice that are homozygous null for the testis-specific protein calmegin, 54 % identical to CNX and with similar lectin properties, are sterile, although spermatogenesis proceeds normally. Sperm from these mice do not adhere to the ovum extracellular matrix in vitro, and it has been speculated that calmegin is required as a chaperone for sperm glycoprotein(s) that must interact with the egg for fertilization to occur (Ikawa et al., 1997). In humans, a fatal congenital disorder of glycosylation has been reported to result from deficiency in glucosidase I (De Praeter et al., 2000). However, it is not clear whether this is due to a global problem in glycoprotein folding, or due to the sluggish generation of complex sugars. That complex sugars form at all, in the absence of ER glucosidase trimming activity, is due to the presence of a Golgi endomannosidase that is able to cleave mannoses from untrimmed core oligosaccharides, albeit at a reduced rate (Moore and Spiro, 1992; Moore and Spiro, 1990).

1.2.2.7. N-linked glycosylation of potassium channels

The mammalian voltage-gated potassium channels of rat, mouse and human (except for Kv1.6, in each case), as well as the Kv1 channel of Aplysia, all have a single, conserved glycosylation site in the first extracellular loop (Chandy and Gutman, 1995). The Drosophila Shaker channel has two consensus sites at this position. It is worth pointing out that this conserved glycosylation site occurs in a region of the Shaker/Shaker-like channels (i.e. the TM1-TM2 loop) that is otherwise very divergent (Stuhmer et al., 1989), suggesting that sugars at this location are important. Rat brain Kv1.1, Kv1.2 and Kv1.4, but not Kv1.6, have been shown to bear complex

oligosaccharides (Shi and Trimmer, 1999). Shaker is glycosylated at both sites when expressed in mammalian, Xenopus and insect cells (Santacruz-Toloza et al., 1994a; Schulteis et al., 1998). It binds transiently to calnexin in a glycosylation-dependent manner (Nagaya et al., 1999), but no functional significance of this binding has been demonstrated. Shaker 'folding mutants' that fail to acquire mature Golgi glycosylation due to misfolding and prolonged residence in the ER, are not actively retained by calnexin since their association with the chaperone was seen to remain transient. It is not known whether Shaker is O-glycosylated, or whether it shows O-GlcNac modifications (Wells et al., 2001) on its cytosolic domains.

Expression of Kv1.1 in Lec8 or Lec2 mutant CHO cells, which produce hypo-sialidated proteins, was seen to induce a positive shift in the voltage-dependence of channel activation (Thornhill et al., 1996). This effect could be mimicked by sialidase treatment of channel expressed in control cells, further implicating sialic acids in channel physiology. Both voltage-gated sodium and potassium channels are thought to be unusually heavily sialidated. Sodium channel voltage-dependent gating is also reported to be sensitive to channel sialic acid content (Recio-Pinto et al., 1990), possibly via an electrostatic mechanism (Bennett et al., 1997). Further, the scorpion peptide agitoxin exhibits high affinity binding to Shaker expressed in mammalian cells, but does not bind at all to the Drosophila channel. Although alternative explanations are quite possible, differences in insect and mammalian complex glycosylation have been speculatively invoked as being suggestive of glycan-specific differences in channel pharmacology. Surprisingly, given the extremely conserved nature of TM1-TM2 loop glycosylation, no gross folding or expression defects were reported for mutant Shaker channels in which

both asparagines had been changed to glutamine (N259Q+N263Q) (Santacruz-Toloza et al., 1994a). This mutant could be expressed in heterologous systems and appeared to be electrophysiologically normal, although detailed biophysical analysis was not performed. In contrast, glycosylation is required for normal expression of the voltage-gated sodium channel in neuroblastoma cells (Waechter et al., 1983).

We further analysed the folding and traffic kinetics of the unglycosylated mutant Shaker channel. During the course of this work, two closely related reports were published. First, glycosylation was shown to increase the stability and surface expression of Shaker expressed in HEK293T cells (Khanna et al., 2001b), with degradation of the mutant proposed to occur in the cytosolic proteasome. Second, glycosylation was shown to increase the rate of surface delivery, but not the surface levels, of Aplysia Kv1 expressed in Xenopus oocytes (Liu et al., 2001).

1.2.3. Export from the endoplasmic reticulum (ER)

1.2.3.1. Organization of the early secretory pathway

In addition to the classical compartments of the early secretory pathway i.e. the ER and the *cis*-cisternae of the Golgi apparatus, new structural elements have recently been defined. The ER-Golgi-intermediate compartment (ERGIC) consists, at the ultrastructural level, of vesiculo-tubular elements that are often seen to be continuous with the fenestrated *cis*-most cisterna of the Golgi (Klumperman et al., 1998). The ERGIC is defined by marker proteins (such as ERGIC 53) and by temperature and pharmacological treatments that block either anterograde ERGIC-Golgi traffic, retrograde ERGIC-ER traffic, or both (Hauri et al., 2000). ERGIC proteins are thought to cycle

constantly between the ER, ERGIC and *cis*-Golgi (Schweizer et al., 1990; Klumperman et al., 1998; Saraste and Svensson, 1991). Whether the ERGIC is a stable compartment, or whether it is dynamically maintained by fusion and maturation of ER-derived vesicles, is still unresolved. If the Golgi serves as an example, this is likely to remain a hotly disputed topic for some time to come.

1.2.3.2. The COPII coat

Export from the ER requires the COPII coat (Barlowe et al., 1994), whereas both forward and retrograde traffic away from the ERGIC require COPI (coatomer) (Schekman and Orci, 1996). The COPII coat is a polymer of several cytosolic proteins that can together intrinsically effect the deformation of the lipid bilayer required for vesicle formation (Barlowe et al., 1994; Matsuoka et al., 1998). Sar1-GTP (a GTPase) binds directly to the lipid, and sequentially recruits the Sec23/24p and the Sec13/31p complexes (Aridor et al., 2001). The Sar1-GEF Sec12p is resident at the ER membrane, and thus localizes the COPII budding reaction to this site in the cell. Putative pre-assembly complexes of Sar1-GTP, Sec23/24 and cargo are relatively stable at the ER membrane, but addition of Sec13/31 to the complex greatly accelerates the Sar1-GAP activity of Sec23 (Antonny et al., 2001) resulting in GTP hydrolysis and coat disassembly. Thus, it is thought, complete COPII polymer assembly is intrinsically unstable. This would result in rapid shedding of the coat upon vesicle budding, such that the transport vesicle is rendered competent for fusion with its target membrane (Antonny and Schekman, 2001). The details of this process are still under investigation. For instance, the role of cargo molecules, if any, is not clearly understood.

At the ER, the COPII complex accumulates at specific ribosome-free sites, which have been termed the transitional elements (TE) or ER exit sites. These are mostly at the perinuclear ER, facing the ERGIC and the cis-Golgi, although some are also seen in the periphery of cells (Klumperman, 2000). At the ultrastructural level, the exit sites appear as ~350 nm protrusions of the ER membrane, often with several COPII-coated bud-like structures (Sesso et al., 1994; Barlowe et al., 1994). In time-lapse fluorescence microscopy on GFP-tagged VSVG ts045, transient accumulation at the exit sites is seen after release of the high temperature ER export block (Hammond and Helenius, 1994b).

1.2.3.3. Models for selective ER export

Essentially two different models have been proposed to describe the fundamental operating principle of ER export (Antonny and Schekman, 2001; Klumperman, 2000). As the process is studied for an increasing number of substrates, it appears that all proposed models may be valid in one or other case. First, the bulk flow model proposes that all proteins passively diffuse into export vesicles and that the ER resident proteins constitute a specific cadre that is actively retained or retrieved (Wieland et al., 1987). Alternatively, the active transport model proposes that cargo proteins are actively recruited into COPII-coated vesicles (Warren and Mellman, 1999). Support for the bulk flow model has been generated by quantitative immunoelectron microscopy on secreted amylase and chymotrypsinogen in exocrine pancreatic cells (Martinez-Menarguez et al., 1999). These proteins are seen to be at the same concentration at ER exit sites as in the rest of the organelle, although they are subsequently significantly concentrated in the ERGIC lumen. This was interpreted to be inconsistent with the active transport model. Since pancreatic enzymes are likely to be at a high concentration in the ER of dedicated

secretory cells, it is not clear how applicable these observations are to export of less abundant substrates.

Active recruitment into export vesicles could occur by several mechanisms. Membrane protein cargo could interact with COPII coat components directly via cytoplasmic domains, or such an interaction could be mediated by a 'transport receptor'. Lumenal cargo would necessarily require a transmembrane transport receptor. Cytosolic ER export sequences (i.e. a sequence that is necessary for export of the protein and that can effect export of a reporter) that directly interact with components of COPII have been identified in several 'frequent flyers' proteins that routinely shuttle between ER, ERGIC and *cis*-Golgi. These include ERGIC 53[4] (Kappeler et al., 1997), the yeast ER-Golgi SNAREs Bet1p and Bos1p (Springer and Schekman, 1998), sed5p (Peng et al., 1999), and members of the p24 family (Dominguez et al., 1998), all of which have themselves been implicated in ER – Golgi traffic. Sequences that promote ER export have also been identified in other proteins, for instance in VSVG (the DXE motif) (Nishimura and Balch, 1997; Sevier et al., 2000), in the dopamine receptor (the FxxxFxxxF motif) (Bermak et al., 2001) and in several potassium channels, as described below. However, none of these proteins are known to directly interact with COPII components.

A few putative transport receptors or adaptors have been identified. The yeast protein Shr3p mediates complex formation between amino acid permeases and COPII, suggesting that it may be an adaptor protein for traffic of the permeases out of the ER (Gilstring et al., 1999). ERGIC53 is a mannose-binding lectin that could be cross-linked to a soluble cathepsinZ-like molecule (Appenzeller et al., 1999), making it a potential

[4] The C-terminal FF motif of ERGIC53 does not effect export of a reporter, suggesting that it may be part of a larger export sequence.

glycoprotein transport receptor and the first putative adaptor for a lumenal cargo molecule. That this lectin is significant in the traffic of soluble glycoproteins is evident from the severely deficient coagulation factor V/VIII secretion seen in humans with truncated ERGIC53 (Nichols et al., 1999; Nichols et al., 1998; Neerman-Arbez et al., 1999)(Nichols et al, Cell 93, 61; Nichols et al, Blood 93, 2261; Neerman-Arbez et al, Blood 93, 2253).

Although it seems clear that active transport does occur for some proteins, it is not obvious whether a few central receptors and universal signals mediate this process, or whether there are dedicated factors and pathways for different classes of proteins. Indeed, a yeast GPI-linked protein (Gas1p) was shown to enter a distinct population of (presumably COPII-coated) vesicles compared to pro-α-factor, lending credence to the notion that different types of proteins may be sorted differently at the ER membrane (Muniz et al., 2001).

1.2.3.4. ER export signals in potassium channels

There has been a surge of interest in potassium channel export signals, in recent years, as a potential control mechanism for the cell surface channel profile (Griffith, 2001). This was perhaps initiated by the discovery that traffic of the K(ATP) channel subunits, the Kir6.2 inward rectifier and the sulfonylurea receptor (SUR1), is regulated by novel ER retention signals (Zerangue et al., 1999). Both Kir6.2 channels and SUR1 have C-terminal cytosolic RKR sequences that serve to retain the unassembled subunits in the ER (Zerangue et al., 1999), but also see (Makhina and Nichols, 1998). Assembly into the complete octamer (4:4) is thought to mask these sequences and allow traffic out of the ER, although additional regions of the subunits are also important (Hough et al.,

2000; Sharma et al., 1999). The factors that decode RKR at the cytosolic face of the ER are not known.

Individual members of several potassium channel families are seen to attain very different cell surface levels when expressed in heterologous systems such as Xenopus oocytes and COS cells. For instance, the Kir2.1, Kir2.2, Kir2.3 and Kir1.1 inward rectifier channels are present at easily measurable surface levels in oocytes, whereas Kir3.1 and Kir 6.1 are not. The variable nature of the cytosolic C-termini of these channels led to a search for ER export sequences in the C-terminal tails of high surface expressors. Indeed, the FCYENE motif in the cytosolic tail of the Kir2 channels has all the features of an export sequence, being both necessary for Kir2.1 export and sufficient to promote that of a reporter protein (Ma et al., 2001). The sequence is reminiscent of the diacidic ER exit sequence of VSVG (Nishimura and Balch, 1997). Similarly, several sequences in the cytosolic amino- and carboxyl termini of the Kir3 channels have been shown to promote cell surface expression, probably via an effect on ER export (Ma et al., 2002). In an interesting new development, additional sequences in the Kir3 channels have been implicated in the regulation of exit from a different intracellular location, possibly the endosomal recycling compartment (Ma et al., 2002). However, validation of the role that these sequences play in neuron or muscle channel traffic is still in its preliminary stages.

The voltage-gated potassium channels (Kv) also show differences in their propensity to traffic to the cell surface, either of COS cells or hippocampal neurons (Manganas and Trimmer, 2000). Kv1.4 is present robustly at the cell surface, Kv1.1 is largely in the ER, and Kv1.2 is intermediate in its distribution. Co-expression can change

the distribution of individual subunits, in a dose-dependent manner. ER export of the Kv channels has not been studied in detail. The VXXSL motif was shown to be important for the efficient cell surface expression of Kv1.4 (Li et al., 2000). However, mutating this sequence in the Shaker channel does not affect traffic (Khanna et al., 2001a), and replacement of the Kv1.1 C-terminus with that of Kv1.4 generated a chimaera that did not traffic (Zhu et al., 2001). We have generated C-terminal truncated versions of the Shaker channel to begin to define regions that may be important for export from the endoplasmic reticulum.

1.2.4. Immobilization of ion channels at the cell surface

In contrast to some membrane proteins, such as rhodopsin in photoreceptor cells (Poo and Cone, 1974), voltage-gated channels at the surface of neurons and muscle are not free to diffuse in the plasma membrane. In experiments on adult frog skeletal muscle, a combination of loose-patch clamp and UV photodestruction through the patch pipette was used to measure the diffusion of sodium and potassium channels at the cell surface (Weiss et al., 1986). When compared to the average diffusion of muscle glycoproteins, measured by FRAP (fluorescence recovery after photobleaching) of fluorescently labeled lectins bound to the cell surface, the sodium channels and a large fraction (75%) of the potassium channels, were seen to be immobile. Some degree of immobility is practically a requirement for the very specific sub-cellular distributions maintained for various channels. In muscle, voltage-gated sodium channels are distributed in patches on the sarcolemma, are excluded from transverse tubules, and are present in high concentrations at the end plate (Roberts et al., 1986). In myelinated axons, sodium channels are present at high concentration in the nodes, but not in the internodal regions (Hille, 1984). Even

different voltage-gated potassium channels show marked variations in cell surface distribution. For instance, the Shaker-like Kv1.4 channel is densely localized to the pre-synaptic swellings at nerve terminals, and also present along some axonal shafts (Cooper et al., 1998). In contrast, Kv1.1 and Kv1.2, which are members of the same sub-family as Kv1.4, are found in the juxtaparanodal regions of myelinated axons and in terminal fields of unmyelinated CNS axons (Wang et al., 1993; Rhodes et al., 1997; Rasband et al., 1998).

The PSD-95 family of the membrane-associated guanylate kinases (MAGUKs), are putative molecular effectors of potassium channel immobility and localization. PSD-95 was the earliest-identified member of this family, isolated in a yeast two-hybrid screen for proteins that associate with the voltage-gated potassium channel (Kim et al., 1995). It binds to the distal C-terminus of several potassium channels, including Shaker, via its amino terminal PDZ (PSD95/Dlg/ZO1) domains. Co-expression of PSD-95 with Shaker or Shaker-like potassium channels in transfected cells leads to clustering of the channels at the cell surface (Kim and Sheng, 1996). The degree of clustering depends on the intrinsic cell surface levels of the channel in question (Tiffany et al., 2000) and requires palmitoylation of PSD-95 at two N-terminal cysteines (El Husseini et al., 2000). Importantly, Drosophila with mutations in discs large (dlg), the homologue of PSD-95 (Woods and Bryant, 1991), have abnormal synapse structure (Lahey et al., 1994), and fail to cluster Shaker at the fly neuromuscular junction (Tejedor et al., 1997). Other cell surface receptors, adhesion molecules and signaling proteins have been shown to interact with the PSD-95 family of MAGUKs , making these proteins good candidates for scaffolds or organizers of multimolecular complexes at the cell surface.

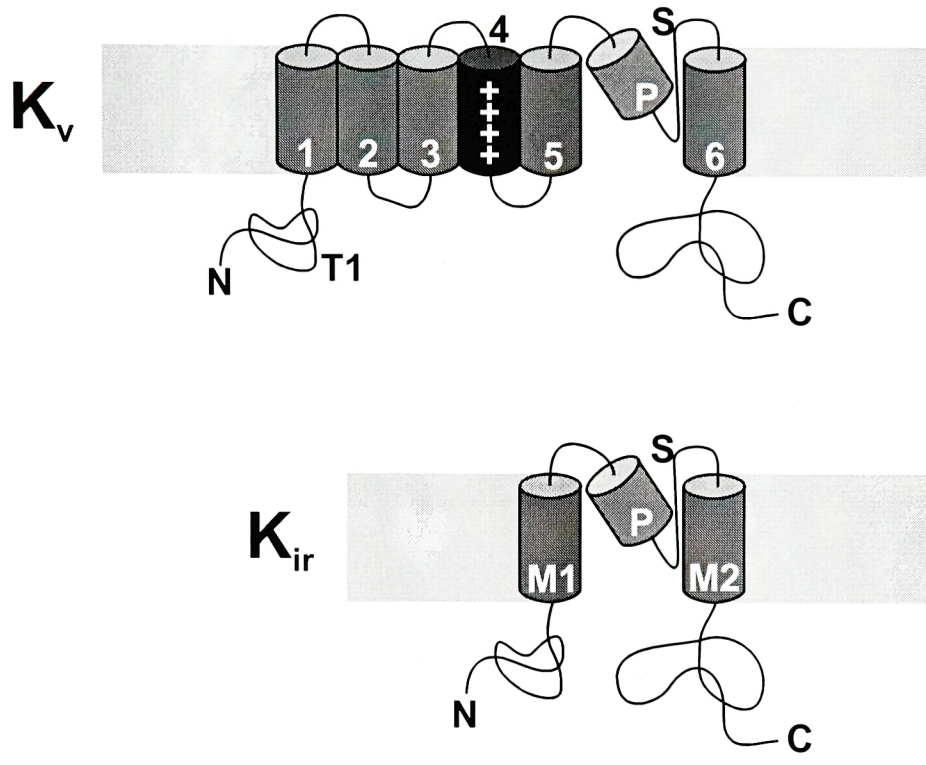

Figure 1.1 : Membrane topologies of the K_v and K_{ir} potassium channel subtypes.

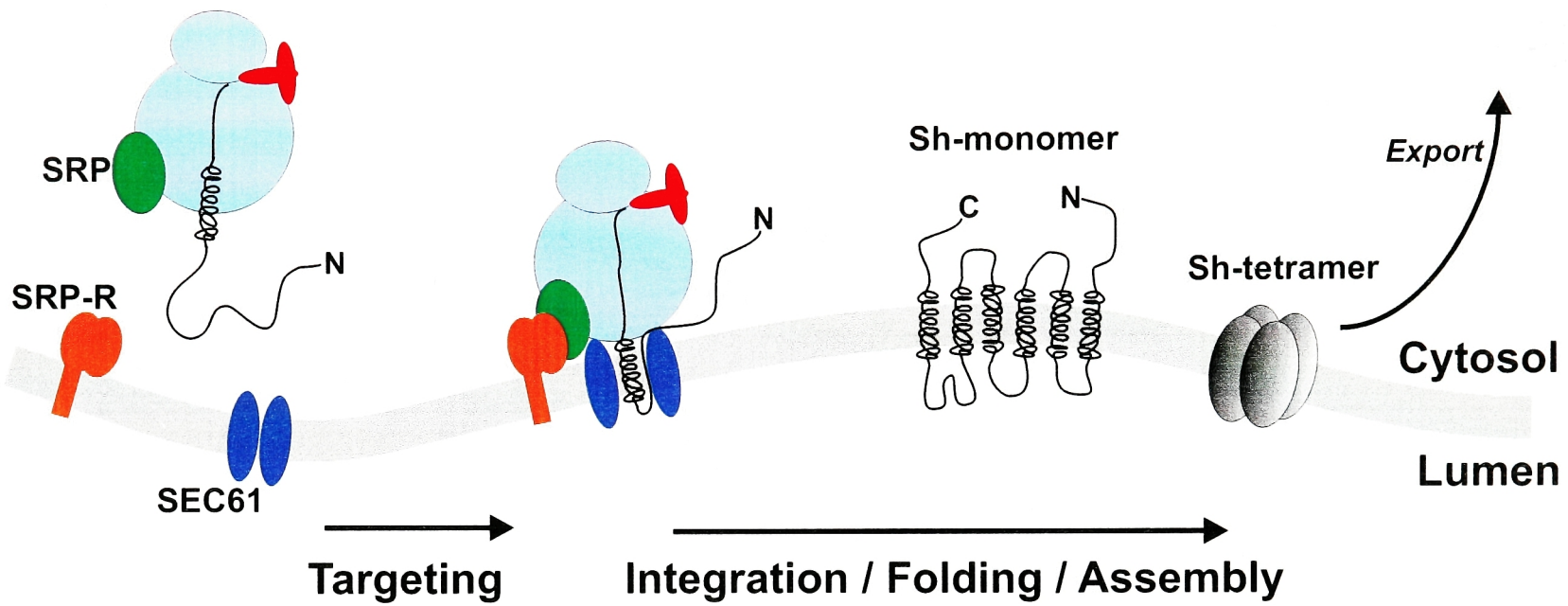

Figure 1.2 : Biogenesis of an oligomeric membrane protein.

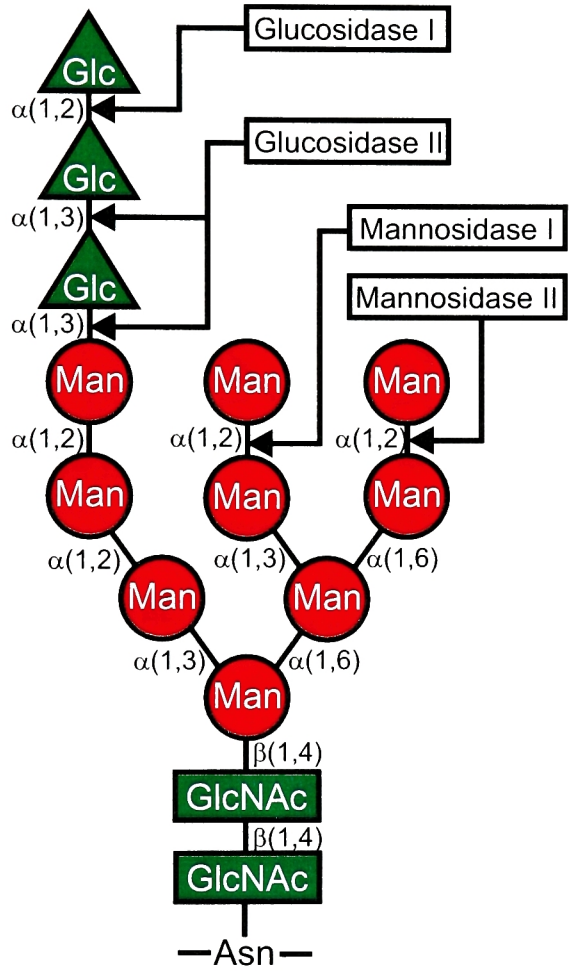

Figure 1.3 : The core N-linked glycan.

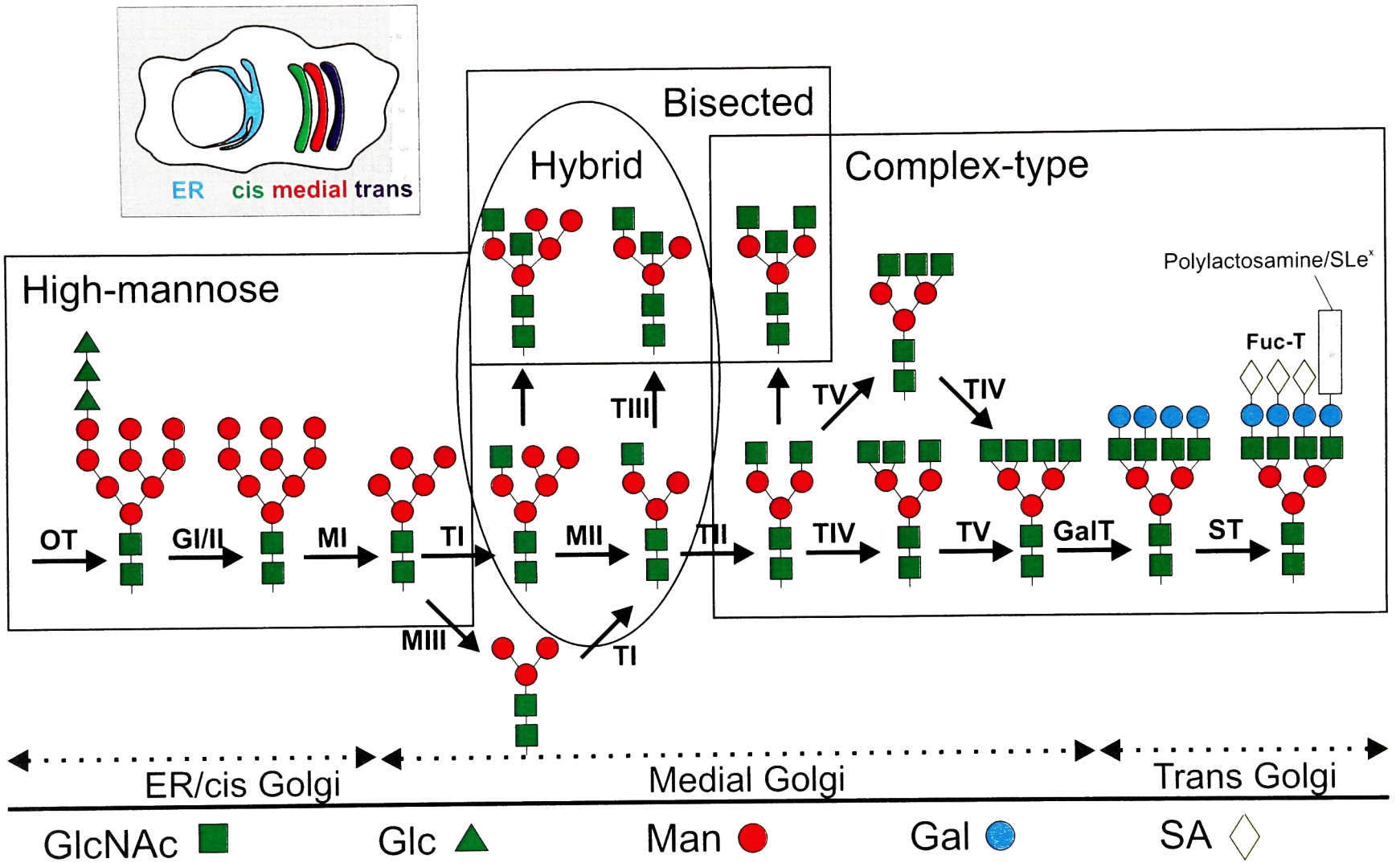

Figure 1.4: N-linked glycosylation (OT, oligosaccharyltransferase; G, glucosidase; M, mannosidase; T, N-acetyl glycosaminyltransferase; GalT, galactosyltransferase; Fuc-T, fucosyltransferase; ST, sialyltransferase)

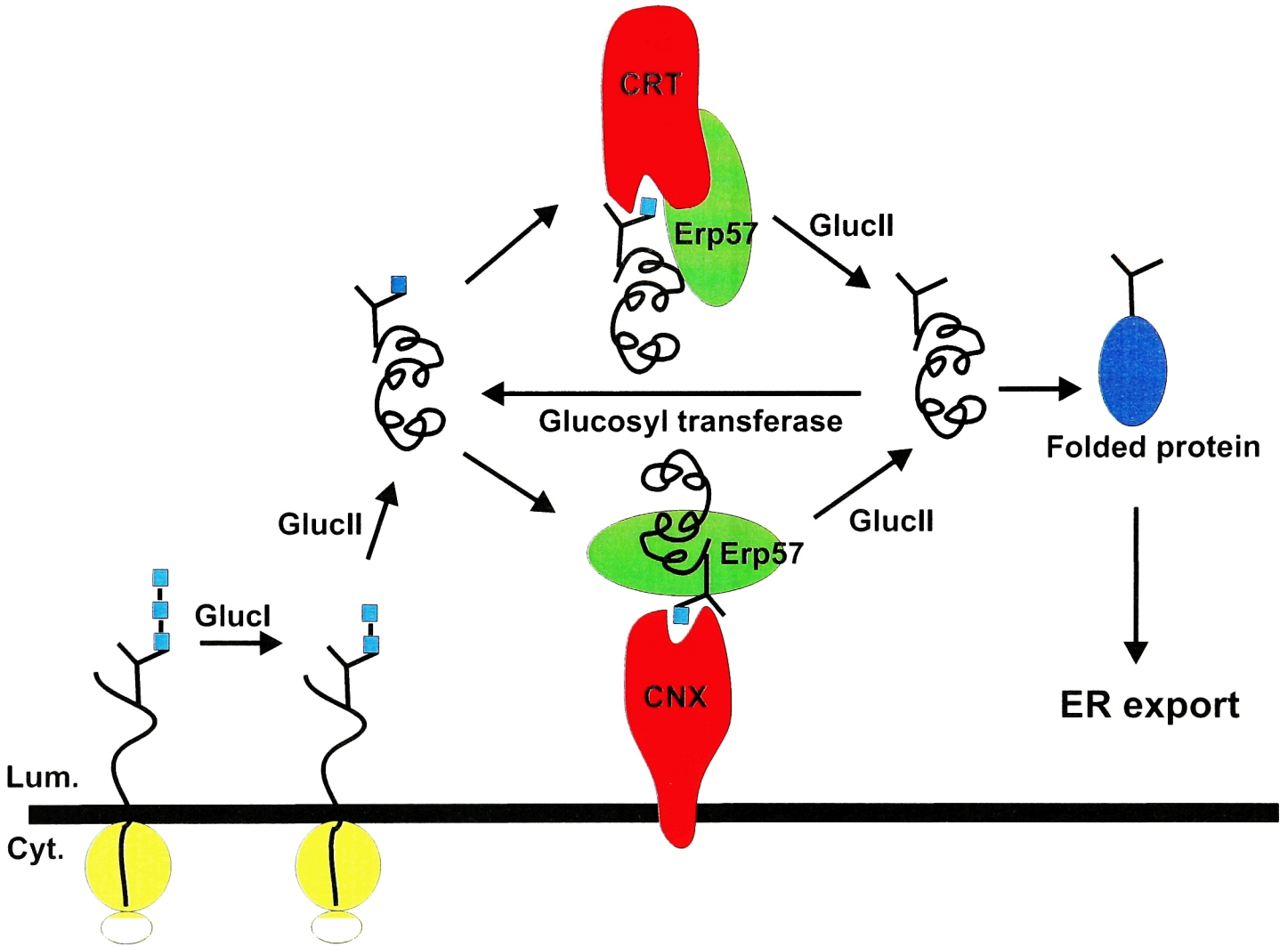

Figure 1.5 : The calnexin-calreticulin cycle (CNX, calnexin; CRT, calreticulin; GlucI/II, glucosidase I/II).

2. MATERIALS AND METHODS

2.1. MATERIALS

Unless otherwise stated, chemicals were purchased from Sigma Chemical Co (St. Louis, MO) or Roche (Indianapolis, IN).

2.1.1. Antibodies and antibody-conjugates

Mouse and rabbit α-HA (HA.11) antibodies were from Covance (Richmond, CA), rat α-HA (3F10) and mouse α-MYC (9E10) antibodies were from Roche, mouse monoclonal α-GFP (C163) and α-huTfr (H68.4) were from Zymed (So. San Francisco, CA) and polyclonal α-GFP was from Clontech (Palo Alto, CA). Antibodies to ER markers (α-calnexin, α-calreticulin, α-PDI) were from Stressgen Biotechnologies (Victoria BC, Canada), α-p58 and α-actin were from Sigma, α-GOS28 was a gift from J. Rothman (Memorial Sloan Kettering Cancer Center, NYC) and α-preprolactin was a gift from V. Lingappa (UCLA). Secondary antibodies and blocking goat serum used in immunofluorescence were from Jackson Immunoresearch Labs (West Grove, PA). Alkaline phosphatase-conjugated secondaries for Western blotting were from Sigma.

2.1.2. Molecular biology

Restriction enzymes were from New England Biolabs (Beverly, MA), DNA ligase was from Gibco (Rockville, MD), dNTPs were from AmershamPharmacia (Piscataway, NJ)

and Pfu DNA polymerase from Stratagene (La Jolla, CA). The PCR-Blunt kit (Invitrogen, Carlsbad, CA) was used for PCR cloning.

2.1.3. Conjugation reagents

Sulfo-NHS-LC-biotin, Sulfo-NHS-SS-biotin, NHS-biotin, biotin-PEO-maleimide, FITC-maleimide and rhodamine-maleimide were from Pierce (Rockford, IL). Methanethiosulfonate reagents (MTSET-biotin, MTSEA-biotin) were from Toronto Biochemicals (Ontario, Canada). Alexa 488- and Alexa 594-maleimides were from Molecular Probes (Eugene, OR). ^{3}H-N-ethyl-maleimide was from New England Nuclear (Boston, MA).

2.2. Methods

2.2.1. Constructs

Shaker cDNA was obtained from R. Aldrich (Stanford, CA) and N259Q+N263Q Shaker cDNA was obtained from D. Papazian (UCLA). Both constructs were expressed in mammalian cells from pcDNA3 (Invitrogen) and in Xenopus oocytes by injection of mRNA constructs transcribed off the pGEM-HE vector (Liman et al., 1992). All tagged constructs (Sh-HA, Sh-MYC, HA-Sh, Sh-FLAG, Sh-RKR-HA, Sh-DEKKMP-HA) were prepared by standard PCR techniques. T3ΔTM2 was prepared by overlap extension PCR. All PCR products were checked by sequencing (Rockefeller University PDTC). Constructs lacking stop codons, where necessary, were prepared by site-directed mutagenesis (Kunkel et al., 1991) and sub-cloned into eGFP-N1 and eGFP-C1 vectors (Clontech) for expression of GFP fusions. Agitoxin2D20C-T7 phage gene9 cDNA was

obtained from R. Mackinnon and sub-cloned into the pQE31 vector (Quiagen, Valencia, CA) for fusion to the His6 tag.

2.2.2. Cell culture and transient transfection

COS-1 and HeLa cells (ATCC, Manassas, VA) were maintained in Dulbecco's MEM (Cellgro, Herndon, VA) supplemented with 10 % FBS in a humidified incubator at 37°C and 5 % CO_2. For biochemical experiments, cells were transiently transfected using Fugene6 (Roche) or Lipofectamine 2000 (Invitrogen). For microinjection and imaging, cells were plated on acid-washed glass coverslips pre-coated for an hour at 37°C with 50 μg/ml bovine plasma fibronectin (Gibco).

2.2.3. Gel electrophoresis and analysis

Gel electrophoresis was carried out under standard denaturing and reducing conditions on 6%, 7%, 8%, 10% or 12% polyacryalmide gels. For non-denaturing gels, *in vitro* translations were solubilized in the desired detergent; 0.1–1% $C_{12}M$ (Calbiochem), 0.1-1% $C_{12}E_9$ (Calbiochem) or 0.1-2 % CHAPS for 1 hour at 4°C, the insoluble material removed by centrifugation (19000 x g, 5 min, 4°C) and the samples mixed directly with sample buffer without SDS. Non-denaturing gels were prepared by omitting SDS from the standard recipe. Agitoxin was run on 20% Tricine gels, to improve resolution (Schagger and von Jagow, 1987). Gels were visualized by autoradiography by exposing to a phosphor screen and scanning on a Molecular Dynamics Phosphorimager (Amersham). Quantification, where relevant, was done using ImageQuant software (Amersham). Typically, a band was quantified as follows. The band was demarcated

with a box that included all signal pixels, the intensity within the box determined, and the background signal from an adjacent box of identical size subtracted.

2.2.4. Preparation of cell lysates

Cells were mechanically dislodged into ice cold PBS, spun briefly to pellet, and resuspended in the desired volume of solubilization buffer (150 mM NaCl, 50 mM Tris pH 7.5, 1 mM EDTA) with 10mM iodoacetamide, 0.25 mM PMSF, protease inhibitor cocktail (Complete™, EDTA-free, Roche) and either 2% CHAPS, 1% Zwittergent 3-14 (Calbiochem, San Diego, CA), or 1% SDS. Solubilization was carried out either for 1 hour at 4 °C (CHAPS, Zwitt.) or for 5 minutes at 100°C (SDS). Lysates were cleared by centrifugation (19000 X g, 5 min, 4 °C) to remove insoluble material.

2.2.5. Western blotting

Samples were separated by SDS-PAGE and transferred to PVDF (AmershamPharmacia) or nitrocellulose (Osmonics Inc., Westborough, MA) at 100V for 1 hour. All subsequent manipulations were in Tris-buffered saline with 0.1 % Tween (TBS-T). Blots were blocked in 5 % nonfat dry milk (NFDM) and incubated in 1° antibody/1% NFDM either for 1 hr /RT or overnight /4°C. Standard antibody concentrations for Western blots were α-HA (1μg/ml), α-MYC (5 μg/ml), α-GFP (1μg/ml), α-actin (6 μg/ml), α-TfR (1μg/ml). All α-ER 1° antibodies were used at a 1:1000 dilution of the manufacturer's preparation. Blots were washed (5x) over 30 min., incubated with alkaline phosphatase-conjugated 2° antibody (1:20000) for 1 hour /RT, washed again as above and visualized by enhanced chemifluorescence (ECF) (AmershamPharmacia). For ECF, blots were incubated with the Vistra™ alkaline phosphatase substrate (5 sec – 5 min), dried, and scanned using the

450 nm laser line of a Molecular Dynamics Storm Phosphorimager (Amersham). For α-biotin blots, alkaline phosphatase-conjugated avidin-biotin complexes (ABC kit, Pierce) were added instead of antibodies, for 30 min/ RT.

2.2.6. Metabolic labeling , immunoprecipitation and EndoH digestion

Cells were incubated in cysteine/methionine/serum –free DMEM (Sigma) for 30 min at 37 °C, 24-26 hours post-transfection. Unless stated otherwise, labeling was carried out for 20 min at 37 °C with 0.25 mCi/ml EXPRE^{35}S^{35}Slabel (NEN) in cys/met/serum-free media, using 1.2 ml per 6 cm dish. The cells were chased at 37 °C in DMEM, 10 % FBS (or, where relevant, at 20°C in MEM, 5 % FBS) supplemented with 5 mM cysteine/methioine for various times, washed in cold PBS+ (PBS with 2 mM Ca^{++}, 1 mM Mg^{++}) and resuspended in solubilization buffer (150 mM NaCl, 50 mM Tris pH 7.5, 1 mM EDTA) with 2% CHAPS, 10mM iodoacetamide, 0.25 mM PMSF, and a protease inhibitor cocktail (Complete™, EDTA-free, Roche). Solubilization was carried out for 45 minutes at 4°C, and the insoluble material spun away at 19000 x g for 5 min, 4°C. Lysates were pre-incubated with protein A/G sepharose beads (Santa Cruz Biotechnology, Santa Cruz, CA) for 30 min. at 4°C to eliminate non-specific binding. Incubation with primary antibody was carried out overnight (10 μg/ml for HA.11; 1-3 μg/ml for 3F10) and with protein A/G beads for a further 2 hours, both at 4°C. Beads were washed with 3 ml of solubilization buffer with 1 % CHAPS, 1 % Triton and 0.25mM PMSF. The precipitated sample was eluted off the Protein A/G sepharose beads by heating to 100 °C for 5 minutes in 0.5% SDS, 0.1 M β-mercaptoethanol, and then recovered by centrifugation. Eluted samples were split into two equal aliquots, adjusted

to 75 mM sodium citrate pH 5.5 and incubated with or without Endoglycosidase H (0.05U/ml)(Roche) and with protease inhibitors for 12 hours at 30°C. Samples were boiled for 5 minutes in SDS-PAGE loading buffer, separated by SDS-PAGE, and visualized by autoradiography on a Molecular Dynamics Storm Phosphorimager (Amersham).

2.2.7. Surface biotinylation

Transiently transfected COS cells were rinsed in PBS+, 48 hours post-transfection, and labeled with freshly prepared 0.5 mg/ml Sulfo-NHS-LC-biotin (Pierce) in PBS+ for 1 hour at 4 °C. The reaction was quenched with Tris (50 mM), and the samples washed (X5) in cold Tris-buffered saline. Where applicable, the cells were labeled with 2.5mM freshly prepared MTSEA-biotin for 10 min at RT, and then quenched with cysteine (25 mM). The cells were lysed in solubilization buffer with 1 % SDS as described above. A fraction of the cleared lysate (usually 10%) was removed as the total sample (T) and the rest of the lysate incubated with Softlink™ avidin beads (Promega, Madison, WI) for 1 hour at RT. A fraction of the unbound sample equivalent to 10 % of starting material was removed (U), and the remaining re-bound to Softlink™ avidin beads. Beads from both precipitations were washed with 5 ml cold solubilization buffer supplemented with 1 % CHAPS, 1 % Triton, 0.1 % SDS, 0.25 mM PMSF and the samples were eluted by incubation at 100°C for 10 min (B & B2). Equal fractions of each sample (typically corresponding to 10 % of starting material) were subjected to Western blotting as described above. Quantification (only non-saturated blots) was done using ImageQuant software (Amersham).

2.2.8. Surface biotinylation of newly synthesized proteins

Transfected cells were pulse-labeled as described above, and chased for various times (0–3 hours). Brefeldin A, when added, was present at 5 μg/ml during the chase only. Castanospermine, when added, was present at 1 mM during the starvation, pulse and chase. At the end of the chase period, cells were rapidly cooled to 4°C, and then biotinylated as above. After washing in cold Tris-buffered saline (X5), the cells were scraped off, solubilized in 2% CHAPS, and the Shaker-HA immunoprecipitated. Immune complexes were eluted off the Protein A/G sepharose beads by incubation in elution buffer (50 mM glycine-HCl pH 2.5, 150 mM NaCl, 0.1 % Triton) at 4°C for 10 minutes (X2). Eluted samples were collected by centrifugation, neutralized with Tris, and then subjected to a second affinity precipitation with Softlink™ avidin beads (Promega) at 4°C, to determine the biotinylated fraction. The unbound sample and the first wash were recovered by TCA precipitation. Equal fractions of bound and unbound (the wash was not quantified as preliminary experiments indicated minimal sample in this fraction) were run on SDS-PAGE, and the gels scanned as above. Band intensities were quantified using ImageQuant software (Amersham) and the biotinylated fraction calculated as {B/(U+B)}*100.

2.2.9. Determination of channel half-time

Transfected cells were pulse-labeled as described above and chased for 0-24 hours at 37°C or 0-4 hours at 20 °C. At each time point, cells were solubilized as described above. Equal cpm (determined in triplicate) for each lysate were subjected to immunoprecipitation as described and separated by SDS-PAGE. The gels were

visualized by autoradiography using a Molecular Dynamics Storm Phosphorimager and the band intensities quantified using ImageQuant software (both Amersham).

2.2.10. Immunostaining

Cells plated on acid-washed, fibronectin-coated glass coverslips were fixed in methanol (10 min, -20°C), rinsed in PBS (10 min, x3), and blocked in 5 % normal goat serum (NGS) in PBS (30 min, RT). Coverslips were incubated in 1° antibody diluted in 1% NGS/PBS (1h, RT), rinsed as above, incubated in fluorescent 2° antibody (1h, 4°C, dark), rinsed as above, and imaged. 1° antibodies were used at the following working concentrations; mouse α-HA (1 μg/ml), rat α-HA (200 ng/ml), α-MYC (5μg/ml), α-GOS28 (1 μg/ml). All α-ER markers were diluted 1:200, and α-p58 was diluted 1:50 from the manufacturer's preparation. All 2° antibodies were used at 8 μg/ml.

2.2.11. Epifluorescence microscopy

Microscopy was done on an IX-70 inverted microscope (Olympus, Melville, NY) with a 40 X UplanApo (N.A. = 1.0) or a 60 X PlanApo (N.A. = 1.4) lens. FITC was imaged using an HQ485/10 excitation bandpass, a 505DCLP dichroic and an HQ515/30 emission bandpass filter (Chroma Technology Corp., Brattleboro, VT). TexasRed was imaged using a D560/40 excitation bandpass, a 595DCLP dichroic and a D630/60 emission bandpass filter (Chroma). The fluorescence illumination source was a 150-W xenon lamp (Optiquip, Highland Mills, NY). Images were acquired with a 12-bit Orca-ER cooled CCD (Hamamatsu, Bridgewater, NJ) controlled by our own software written in Labview 5.1 using the IMAQ Vision package (National Instruments, Austin, TX).

2.2.12. Microinjection and imaging of ER-Golgi traffic

Cells were microinjected using micropipettes pulled from borosilicate glass (1 mm outer diameter, 0.78 mm inner diameter) (Sutter, Novato, CA) on a P-87 puller (Sutter). The DNA was diluted to 30 μg/ml in nuclear injection buffer (140 mM KCl, 10 mM Hepes pH 7.4), centrifuged to remove insoluble material, back-loaded into the micropipette, and injected into cell nuclei under constant pressure. Cells were maintained in Hank's Balanced Salt Solution during the 10 minute injection period. Following this, the medium was exchanged for pre-warmed DMEM, 10 % FBS, and the cells were incubated at 37 °C for 2 hours to allow for expression. The medium was exchanged for pre-cooled (20 °C) MEM, 5 % FBS + 50 μg/ml cycloheximide, and the cells were maintained at 20°C for various times (0–4 hours). At the end of each traffic period, the cells were fixed in methanol and stained for Shaker (α-HA mouse monoclonal, anti-mouse TexasRed) and for the Golgi apparatus (α -GOS 28 rabbit polyclonal, anti-rabbit fluorescein). All imaging used a 40 X UplanApo lens (N.A. = 1.0).

2.2.13. Image analysis

All images for the quantitative experiment were acquired using identical parameters (i.e. exposure times and filters). Image analysis was done using Metamorph software (Universal Imaging, Downington, PA). For wild type as well as mutant channel, cells with a visible rim-stain were excluded from the analysis to minimize the confounding effect of surface channel on the data. Apart from this criterion, all cells with visually distinguishable signal over background were included in the analysis. The background was defined for each image as the average fluorescence signal from a region without cells. All images were background-subtracted in Metamorph. The area corresponding to

the Golgi signal was demarcated in the GOS28 fluorescence image and then transferred to the corresponding Shaker fluorescence image. Shaker fluorescence within this area was compared to total Shaker fluorescence, for each cell. Thresholding, region demarcation and analysis were done on a cell-by-cell basis.

2.2.14. *In vitro* transcription

mRNA was transcribed using T7, T3 or SP6 RNA polymerase (Ambion, Austin, TX) for 3 hours at 37°C, precipitated with lithium chloride, washed in 70 % ethanol and resuspended at 1μg/ml in RNase-free water. The template for transcription was either restriction-digested plasmid DNA or a Pfu-generated PCR fragment. Shaker truncations (the T2-T5 series) were all transcribed off PCR products, into which had been engineered 0-4 stop codons, as desired.

2.2.15. *In vitro* translation

Shaker mRNA (1 μg per 25 μl translation) was translated in Flexi™ rabbit reticulocyte lysate (RRL)(Promega) supplemented with amino acids lacking methionine, ^{35}S-methioine (NEN) and 60-100 mM KCl. All other mRNA was translated in regular RRL with amino acids as above. To improve the signal in translations of truncated Shaker (T2-T5), amino acids lacking both cysteine and methioine were used, supplemented with EXPRE^{35}S^{35}S label (NEN). Microsomes, when added, were at 1 eq (1 μl at 50A_{280} /ml) per 25 μl translation reaction. Tripeptide to competitively inhibit glycosylation (see section 2.2.24 below) when added, was at 0.3 mM, freshly diluted into the translation reaction from a 40 mM stock in DMSO. Translations were typically done at 30°C for 60 – 90 min, and then treated with 2 mM puromycin (5 min, 25°C+5 min, 37°C) unless

stated otherwise. Samples were prepared for separation on SDS-polyacrylamide gels by precipitation (2 volumes 3M ammonium sulphate, 20 min, 4°C) followed by centrifugation (19000 x g, 20min, 4°C) to recover the precipitated protein.

2.2.16. Sedimentation harvest of targeted proteins

In vitro translations were layered onto a 150 µl cushion of 1.0M buffered sucrose (140 mM KOAc, 2 mM $Mg[OAc]_2$, 20mM Hepes, pH 7.5) and centrifuged (20min, 163000 x g, 4°C). Material in the supernatant was recovered by ammonium sulfate precipitation. The pellet was directly resuspended in SDS sample buffer.

2.2.17. Floatation harvest of targeted proteins

In vitro translations were adjusted to 2.1M sucrose, placed (50 µl) in an ultracentrifuge tube, and overlayed with a step gradient of 1.9M (125 µl) and 0.25M (25 µl) buffered sucrose (140 mM potassium acetate, 2 mM magnesium acetate, 20 mM Hepes, pH 7.5, 0.2 mM PMSF). The gradients were centrifuged (2h, 217000 x g, 4°C). The top half (100 ul) was removed as the supernatant, and the lower half as the pellet. The protein was recovered from both fractions by ammonium sulfate precipitation.

2.2.18. Membrane integration assessed by alkali extraction

In vitro translations were harvested by sedimentation. The membrane pellets were resuspended in ice cold NaOH (100 mM, 30 min, 4°C) and centrifuged (30 min, 189000 x g, 4°C). The extracted material was recovered by TCA precipitation of the supernatant, and the unextracted material in the pellet was directly resuspended in SDS sample buffer.

2.2.19. Preparation of *in vitro* translated material for sucrose gradients

In vitro translations were harvested by sedimentation and the membrane pellets solubilized in 2% CHAPS, unless otherwise specified. Solubilization was carried out for 1 hour at 4°C, and the lysates cleared by centrifugation (19000 x g, 5 min, 4°C) to remove insoluble material.

2.2.20. Sucrose density gradient centrifugation

Continuous gradients of 5 – 20 % sucrose in solubilization buffer + 1 % CHAPS, 0.25mM PMSF were prepared using a Buchler Auto-Densi Flow II C (Haake Buchler Instruments, Saddle Brook, NJ), to a final volume of 11 ml per gradient. Cleared lysates from in vitro translations or pulse-labeled cells were loaded onto a pre-chilled gradient, and centrifuged for 20 hours at 36000 rpm (160000 x g) in an SW41 Ti rotor (Beckman Instruments, Palo Alto, CA) at 4°C. The gradients were fractionated and the fractions either TCA precipitated with 30 μg/ml BSA as a carrier or subjected to immunoprecipitation, as appropriate. Size markers (Boehringer Mannheim) were BSA, aldolase and catalase.

2.2.21. Lumenal depletion of ER microsomes by alkali extraction

Lumenal depletion was carried out according to (Nicchitta and Blobel, 1993). Microsomes were diluted 5-fold at high pH (50 mM Hepes, 50 mM CAPS pH 9.5), incubated 30 min/ice, overlayed on 100 μl 0.5M sucrose (50 mM TEA, pH 7.5) and centrifuged (20 min, 163000 x g, 4 °C). Microsomal pellets were resuspended (0.25M sucrose, 50 mM TEA pH 7.5) at the same volume as the starting material. All solutions contained freshly added DTT (1 mM) and PMSF (0.25 mM).

2.2.22. Lumenal depletion of ER microsomes by saponin treatment

Lumenal depletion was carried out according to (Bulleid and Freedman, 1990). Purified saponin was obtained from R Hegde (NIH). Microsomes were adjusted to 1 % saponin, layered onto a cushion of 0.5M sucrose (with 100 mM KOAc, 50 mM Hepes, pH 7.5), and centrifuged (20 min, 163000 x g, 4 °C). Membrane pellets were washed once (0.25M sucrose, 50 mM KOAc, 50 mM Hepes, pH 7.5), re-centrifuged as above, and then resuspended (0.25M sucrose, 50 mM KOAc, 50 mM Hepes, pH 7.5) at the starting volume. All solutions contained freshly added DTT (1 mM) and PMSF (0.25 mM).

2.2.23. Preparation of glycoprotein-depleted microsomes

All glycoprotein-depleted and TRAM-reconstituted microsomes were prepared by R. Hegde (NIH) (Hegde et al., 1998).

2.2.24. Preparation of competitor tripeptide

The N-acetylated-(Asn-Tyr-Thr)-NH2 tripeptide was prepared (Rockefeller University PDTC) according to (Kelleher et al., 1992) and stored at 40 mM in DMSO.

2.2.25. Agitoxin purification

The His6-AgTx2-D20C-gene 9 fusion was expressed in E.coli (XL1Blue or M15) from the pQE31 vector (Quiagen). Bacteria were harvested 4 hours post-induction with IPTG, and lysates prepared under native conditions were applied to a Ni-NTA agarose column (Quiagen). The protein was eluted with 250 mM imidazole, dialysed overnight (4°C) into 10 mM Tris-HCl, pH 7, adjusted to 1mM $CaCl_2$, 100 mM NaCl, and then incubated with TPCK-treated trypsin (5 mg/ml per A_{280} unit)(Worthington Biochem. Corp., Lakewood, NJ) for 2.5 hours at RT. The trypsin digest was treated with TLCK (40 μg/ml), filtered

(0.2 μm), applied to a Mono S FPLC column (AmershamPharmacia), equilibrated with 20 mM sodium phosphate, pH 8 and bound material eluted with a linear gradient of NaCl (0.75M/h) over 80 min. at a flow rate of 2ml/min. Peaks eluting later than 50 min were collected and further purified by HPLC (Waters, Milford, MA) on a reversed phase semi-preparative C8 column (10 μm particle size, 250 x 4.6 mm) (Vydac, Hesperia, CA). Under standard RP-HPLC conditions, the column was equilibrated in 0.1% TFA, and the sample separated using a gradient of 0.1% TFA/5% acetonitrile/10% isopropanol over 80 minutes, at a flow rate of 0.5 ml/min. Agitoxin dimer elutes at 75 minutes. The FPLC peak that demonstrated the characteristic retention time was collected, the material (75') dried down under vacuum and resuspended in 50 mM sodium phosphate, pH 7. The A_{235} was measured, the concentration determined using $\varepsilon = 8.88\ mM^{-1}cm^{-1}$, and the toxin stored in aliquots at -80°C.

2.2.26. Labeling of agitoxin

Agitoxin dimer was reduced with DTT (10 mM, 1hr, RT) and separated on HPLC under standard conditions. The monomer had a characteristic retention time of 45 minutes. The material was collected and immediately evaporated under vacuum, to just short of complete dryness. The monomeric toxin was reacted with freshly prepared N-ethyl maleimide, ^{3}H-N-ethyl maleimide or biotin-PEO-maleimide (0.5 mg/ml in 50 mM sodium phosphate, pH 7) for 2 hr/37°C and separated on RP-HPLC under standard conditions. Labeled material eluted at 46 - 47 minutes (NEM-conjugated toxin) or at 53 - 54 min (biotin-conjugated toxin). Peak and baseline (just before and after peak) fractions were collected, evaporated to dryness under vacuum, resuspended in water, the A_{235} measured, the material dried down again and resuspended in 50 mM sodium phospate,

pH 7. For tritiated agitoxin, serial dilutions of the labeled material were counted in a scintillation counter, and the specific activity determined.

2.2.27. Toxin binding assay

Sh-HA was translated in vitro under standard conditions, scaled up five to ten-fold. Targeted material was harvested by sedimentation and resuspended in toxin binding buffer (150 mM NaCl, 50 mM Tris, pH 7.5) with 0.5 % saponin. Bacterial membrane preparations -/+ the KcsA channel were obtained from A. Kuo and R. Mackinnon. The protein/membrane content was not determined. Equal volumes of the two preparations were bound to tritiated toxin in parallel with binding to in vitro-translated Shaker. ^{3}H-AgTx (24nM, 10-25 Ci/mmole) was bound to samples (1 h/RT) in duplicate, with cold toxin (2.4 μM) added to one aliquot. GF/C filters (Whatman) were pre-soaked in polyethylenemine in binding buffer. Binding reactions were applied to filters on a suction apparatus. Filters were washed (1x) with ice cold binding buffer, dried, and scintillation counted.

3. GLYCOSYLATION AFFECTS SHAKER CHANNEL TRAFFIC

The Shaker channel is glycosylated on two asparagines (N259 and N263) in the first extracellular loop. Elimination of glycosylation by mutation of these residues (N259Q+N263Q) generates a functional channel that is expressed at electrophysiologically measurable levels at the surface of Xenopus oocytes and HEK293T cells (Santacruz-Toloza et al., 1994a). In order to more closely examine possible effects of glycosylation on Shaker cell biology, we have carried out a study of the kinetics of traffic of the wild type (WT) and mutant (N259Q+N263Q, also referred to as NQ) channel through the secretory pathway.

3.1. Heterologous expression of Shaker in mammalian cells

We have used heterologous expression of wild type and NQ mutant channels in COS-1 and HeLa cells for our experiments. Both channels have been tagged at the carboxyl terminus with an HA epitope for convenient manipulation. Two-electrode voltage clamp measurements indicate that the epitope tag does not detectably disrupt structure, since the wild type tagged construct generated voltage-gated channels when expressed in Xenopus oocytes (data not shown). Cells transfected with the wild type Sh-HA channel showed two bands on an α-HA Western blot (Fig. 3.1A). The unglycosylated NQ mutant channel expressed as a single, slightly smaller band (Fig. 3.1A). Metabolic pulse labeling of transfected cells with ^{35}S cysteine+methionine followed by immunoprecipitation (IP) with an α-HA antibody is shown (Fig. 3.1B). Identical bands were seen using MYC-tagged Shaker and α-MYC antibodies for IP or Western (not shown). We determined the time course of Shaker expression in transiently

transfected COS (Fig 3.2A) and HeLa cells (Fig 3.2B). Unless otherwise mentioned, all subsequent steady-state experiments were done at 48 hours post-transfection. Radioactive label (^{35}Scysteine+methionine) incorporation was also monitored at various times post-transfection (12 –60 hr) (not shown). All subsequent kinetic studies that required metabolic pulse labeling were done at 24 hours post-transfection, which was the earliest time at which robust labeling was reproducibly detected.

Pulse-chase metabolic labeling of transfected COS cells, followed by Endoglycosidase H (EndoH) digestion and immunoprecipitation, was used to characterize the wild type and mutant channel expressed in COS cells (Fig. 3.3A). In the case of the wild type, a 3 hour chase resulted in the appearance of a higher molecular weight EndoH-resistant band and the concomitant disappearance of the lower molecular weight EndoH-sensitive band (lanes 1-4), which indicates traffic of this glycosylated protein from the ER to the Golgi. In contrast, the NQ mutant showed no shift in molecular weight after this chase period, and was endoH-resistant at all chase times, as one would expect of an unglycosylated protein (lanes 5-8). The channels displayed a very similar profile in HeLa cells (Fig. 3.3B). This is consistent with the electrophoretic mobility patterns that have been reported in Xenopus oocytes and HEK293T cells (Santacruz-Toloza et al., 1994a; Schulteis et al., 1998). Lower expression levels in HeLa cells resulted in more prominent background bands.

3.2. Shaker tetramerization

The oligomerization state of wild type and mutant channel expressed in COS cells was assayed by sucrose density gradient centrifugation (Fig. 3.3C). At least some of the mutant would be expected to form normal tetramers since its electrophysiological

behavior is normal (Santacruz-Toloza et al., 1994a). However, two-electrode voltage clamp would not report the presence of additional misfolded channels (such as aggregates of channels) either at the plasma membrane or at intracellular locations. Since tetramerization occurs in the ER, and since this is also the site of quality control, we were interested in comparing the channels in the ER-localized state. Transiently transfected cells were pulse-labeled for a brief enough period to allow no post-ER traffic (20 min), and solubilized in 2 % CHAPS or Zwittergent 3-14. Zwittergent, unlike CHAPS, is known to disrupt the quaternary structure of both Shaker and its mammalian counterpart Kv1.1 and render the channels monomeric (Nagaya and Papazian, 1997b; Shen et al., 1993; Santacruz-Toloza et al., 1994b; Nagaya and Papazian, 1997a; Santacruz-Toloza et al., 1994b). The lysates were run on a 5-20% sucrose gradient (Fig. 3.3C). There was no discernible difference between the wild type and mutant channels. Specifically, there was no indication of increased aggregation of the mutant channel. We conclude that glycosylation plays no significant role in the oligomerization of the Shaker channel, at least as assayed by density gradient centrifugation.

It is worth noting that, based on comparison to size markers, both the lighter and the heavier peaks of wild type Shaker migrate slightly smaller than expected. At ~75 kD, the glycosylated monomer would be expected to co-migrate with BSA (66kD), whereas the ~ 300 kD tetramer should be slightly larger than catalase (240kD). It is possible that the sedimentation properties of Shaker are slightly different from those of the marker proteins used. Importantly, detergents known to distinguish between the monomeric (as observed previously in Zwittergent) and the tetrameric (as observed previously in CHAPS) states of the Shaker channel result in peaks (Fig. 3.3C) that, relative to each

other, migrate in a manner consistent with tetramerization. A comparison of channel solubilization in CHAPS and in standard RIPA buffer indicated that CHAPS efficiently solubilized the Shaker channel (not shown).

3.3. Shaker traffic to the cell surface

We next compared the glycosylated and unglycosylated channels in terms of their rate of delivery to the cell surface. In order to exclusively label surface proteins, we made use of a membrane impermeant, 1° amine-directed biotinylating agent (Sulfo-NHS-LC-biotin). We first tested if this reagent was indeed membrane impermeant, under the conditions of our experiment (Fig. 3.4A). Upon surface biotinylation a fraction of both wild type (upper panel) and NQ mutant (middle panel) Shaker, but not of cytosolic actin (lower panel), could be precipitated by avidin beads. This precipitation depended upon biotinylation, and was therefore specific (compare lanes 3 and 6). Moreover, re-precipitation of the unbound fraction (lane 7) indicated that the precipitation was complete, since there was no further material recovered. Lastly, probing for the endogenous transferrin receptor (TfR) in biotinylated HeLa cells yielded a TfR surface fraction (~ 30 %) consistent with that reported by other methods (Fig. 3.4B) (Johnson et al., 1998). In contrast to the Sulfo-NHS-LC-biotinylating agent, an impermeant cysteine-directed reagent (MTSEA-biotin) was unable to biotinylate Shaker expressed in COS cells (Fig. 3.4C), in keeping with the predicted topology of the channel. Post-lysis treatment with MTSEA-biotin resulted in channel that bound completely to avidin beads, presumably as a result of biotinylation on intracellular cysteines (Fig. 3.4C, lanes 7-9).

The rate of surface delivery of wild type and mutant channel was quantified using 1° amine-directed surface biotinylation at various chase times after a pulse of radioactive cysteine/methionine. We employed a double precipitation protocol (Fig. 3.5A), in which the radiolabeled channel was first immunoprecipitated out of a CHAPS lysate (P1), then eluted from the protein A-sepharose at low pH, and finally re-precipitated with avidin to determine the biotinylated fraction (P2). We established conditions under which the precipitation reagents were not limiting, to ensure that both P1 and P2 were complete. This was tested by re-precipitation of the unbound material with the appropriate reagent, followed by α-HA Western blotting. Re-precipitation of the unbound material from P1 with α-HA and protein A/G beads (Fig. 3.5B, lane 2) or with beads alone (Fig. 3.5B, lane 3) yielded a very low signal (< 5%) compared to that in P1 (Fig. 3.5B, lane 1). Avidin re-precipitation of the unbound material from P2 also yielded a low to nonexistent signal (Fig. 3.5C, compare lanes 2 &3). These optimizations were also done on HeLa cells (not shown).

The unbound and bound fractions (P2) from a few time points of a representative pulse-chase experiment are shown (Fig. 3.6A). It is clear that the signal in the bound fraction increases at longer chase times for both the WT (upper panel) and the mutant (lower panel) channel, which is what would be expected as the channel traffics through the secretory pathway to the cell surface. Quantification of data from three independent experiments shows that the rate and extent of surface biotinylation was markedly higher in the wild type channel as compared to the mutant, at chase times of 1.5 – 3 hours (Fig. 3.6C). Surface fractions of the channel were compared at 0 and 3 hours of chase in HeLa cells (Fig. 3.6D) and a similar trend was seen. If brefeldin A (BFA), which blocks traffic

through the secretory pathway, was included during the chase period, the biotinylated fraction of wild type at 2 hours of chase was at background levels (Fig. 3.6B, lane 4; 3.7C). This strongly suggests that the experiment does indeed report on Shaker traffic through the secretory pathway to the cell surface. Moreover, when we assessed the avidin-bound fraction of radiolabeled actin, it was found to be vanishingly small at all chase times (< 0.5%, 3 hour chase; Fig. 3.6B, lane 6). This further confirms that the biotinylation is surface specific.

Representative data from an independent set of pulse chase/surface biotinylation experiments done for longer chase times is shown (Fig 3.7A). The WT ER-localized (*) and Golgi-localized (**) bands, as well as the mutant (<) have been indicated, to distinguish them from background bands seen in this experiment. Again, there was a difference in the initial rate of surface delivery of the two channels. However, at longer chase times (≥ 5 hours), the unglycosylated mutant Shaker attained surface levels indistinguishable from wild type (Fig. 3.7B). Combined data from all experiments at all time points is shown (Fig 3.7C, n varies for different time points), again emphasizing that the initial difference between WT and mutant channel is no longer apparent after ~ 5 hours of chase. This is consistent with the fact that the surface fractions of wild type and mutant channel at steady state, as measured by surface biotinylation at steady state, are not significantly different from each other (Fig. 3.7D).

3.4. Shaker traffic through the early secretory pathway

We set out to identify the step in Shaker traffic that is affected by glycosylation. The observation that the fraction of glycosylated channel at the surface increases more quickly than that of the non-glycosylated channel could be attributed to faster transport through the secretory pathway. Delivery to the cell surface may be crudely broken down, in traffic terms, into ER-Golgi and Golgi-plasma membrane traffic. Exit from the ER has been shown to be the rate-limiting step in transport of other membrane proteins through the secretory pathway, since it is the location at which folding and quality control occur (Helenius and Aebi, 2001; Lodish et al., 1983; Helenius and Aebi, 2001). Thus this was the transport step we examined.

3.4.1. Quantitative imaging of ER-to-Golgi traffic

Standard biochemical assays for ER-to-Golgi traffic rely upon changes in glycosylated moieties as the protein moves through the secretory pathway. Since this was not possible for the unglycosylated mutant channel, we used quantitative imaging to compare ER-to-Golgi traffic rates of wild type and mutant Shaker. The experiment is schematically depicted, and may be done either by imaging of GFP-tagged channel in live cells (Fig. 3.8B) or by imaging of HA-tagged channel with immunofluorescence staining in fixed cells (Fig. 3.8A). Briefly, intranuclear microinjection of cDNA was used to generate a synchronous population of cells expressing either wild type or mutant channel. Injection was limited to a period of (≤) ten minutes to maximize synchronicity. The cells were then incubated at 37 °C for 2 hours to allow for expression of the channel. This expression time was the shortest possible, balancing the requirement for a

reasonable signal against that for minimal traffic out of the ER. After this period, cells were treated with cycloheximide to inhibit further protein synthesis, and shifted to 20 °C to block any post-Golgi traffic. The cells were allowed to traffic at 20 °C for various times (between 0 and 4 hours). In the case of Sh-GFP imaging, the cells were allowed to traffic on a temperature-controlled microscope stage, and fluorescence images taken at appropriate intervals to monitor changes in the sub-cellular distribution of the channel over time. In the case of Sh-HA imaging, the cells were fixed at various traffic times, stained and then imaged. The Sh-HA channels were imaged by immunofluorescence staining using a monoclonal antibody against the carboxyl terminus HA tag. The Golgi apparatus was stained with affinity-purified polyclonal antibody to GOS 28, a Golgi SNARE with a fixed distribution throughout the cis-, medial- and trans-Golgi (Hay et al., 1998; Orci et al., 2000; Orci et al., 2000). The rate at which wild type and mutant channel moved from ER to Golgi was compared.

The value of intranuclear microinjection as the method of DNA introduction into the cell is that a synchronously expressing population of cells can be generated. Combined with the possibility to block protein synthesis after a certain expression period and to restrict post–Golgi traffic (with the 20 °C temperature block), this makes it possible to study a synchronously synthesized population of protein as it traffics through the early secretory pathway. Quantitative kinetic imaging is more often used to study traffic of GFP-tagged proteins in live cells, and this is the approach that we initially wished to use. Not only is the experiment simpler, as the cells do not have to be fixed or stained, but since traffic is monitored in a single cohort of cells over time, this approach limits the variation due to differences between cells.

3.4.2. Characterization of GFP-tagged Shaker

We generated Shaker constructs tagged with GFP either at the amino terminus (GFP-Sh-HA) or the carboxyl terminus (Sh-YFP) (Fig. 3.9A). Lysates from transfected COS cells were probed on α-GFP Western blots (Fig. 3.9A). As predicted, both constructs generated two bands, presumably corresponding to the immature (ER) and mature (Golgi) forms of the protein, each of which is ~30 kD heavier than the corresponding band for the untagged Shaker channel. Sh-YFP is specifically present in lysates from transfected cells (Fig. 3.9B) and can be labeled with a cell-impermeant amine-directed biotinylating agent, indicating that it is present on the cell surface (Fig. 3.9C, lane 3). Although Sh-YFP- transfected COS cells do appear to have surface GFP by fluorescence microscopy, diffuse cytosolic GFP is sometimes also seen (Fig. 3.9D, TF, upper panel), predominantly in cells with high expression levels. When Sh-YFP was expressed by microinjection of cDNA, which typically results in much lower expression levels than transfection (at early times post-injection), no cytosolic GFP fluorescence was seen (Fig. 3.9D, INJ, lower panel). Since our experiment required expression by microinjection, we continued characterizing Sh-YFP despite the presence of cytosolic YFP in transfected cells. Surprisingly, no YFP-containing lower molecular weight band was detected on an α-GFP Western (Fig. 3.9E).

GFP-Sh-HA expressed in COS cells was immunoprecipitated with α-HA, followed by Western blotting either with α-GFP or α-HA (Fig. 3.10A). A lower molecular weight (~46 kD) band was seen on the α-GFP (Fig. 3.11A, lane 2), but not the α-HA (Fig. 3.11A, lane 4), Western blot. Since the material had first been immunoprecipitated with an α-HA antibody, the source of this band was not initially

obvious. The GFP and HA tags are at two opposite ends of the > 75 kD Shaker protein, so they do not exist in cis other than on the full-length molecule. An explanation that accounts for all observations is that the 46 kD band represents an amino-terminal fragment of the protein, containing the GFP coding sequence (27 kD) as well as part of the Shaker amino terminus. Since Shaker tetramerization is promoted via amino-terminal domains, and since this can occur in solution (Pfaffinger and DeRubeis, 1995), it is possible that the 46 kD amino-terminal fragment was co-precipitated with full length channel in the α-HA IP. Indeed, fluorescence microscopy on GFP-Sh-HA-transfected (Fig. 3.10B, TF, left panel) or microinjected (Fig. 3.10B, INJ, middle panel) HeLa cells showed abundant cytosolic GFP, although fixation and immunofluorescence staining with α-HA indicated that the full-length channel was appropriately targeted to internal membranes (Fig. 3.10B, INJ, right panel). As a result, GFP-Sh-HA was not useful for imaging experiments. Consequently, experiments to conclusively establish the identity of the 46 kD band were not pursued further. Instead, we continued to characterize the Sh-YFP construct.

We performed pulse-chase experiments on transfected COS cells to compare the traffic of Sh-HA and Sh-YFP from the ER to the Golgi. Representative experiments are shown (Fig. 3.11A). Traffic of Sh-HA to the Golgi, as indicated by chase to the higher molecular weight form of the channel, is almost complete by 3 hours of chase. In contrast, traffic of Sh-YFP is very inefficient, over the same time period. The rate of appearance of the higher molecular weight Golgi band was quantified for multiple experiments (Fig. 3.11C). Sh-YFP transits more slowly from ER to Golgi than Sh-HA. Sh-YFP was therefore not considered optimal for an experiment in which traffic of

glycosylated and unglycosylated channel were to be compared. Specifically, we reasoned that an already depressed rate of ER export as a result of the C-terminal YFP could mask a putative difference between wild type and NQ mutant forms of this construct. GFP-Sh-HA trafficked from ER to Golgi with intermediate kinetics (not shown).

3.4.3. ER-to-Golgi traffic of WT and NQ mutant Shaker channel

The live cell experiment thus thwarted, we compared traffic of wild type and mutant forms of the Sh-HA channel, according to the alternative protocol (Fig. 3.8A). Although imaging of kinetics using fixed cells is more laborious and prone to error, we found that a large sample size and a rigid adherence to a short (< 10 min) injection period served to limit the spread of the data for a given protein in several independent experiments. A large sample size ($n \geq 40$ cells) and triple-blind experiments (at the injection, imaging and quantification stages) gave us confidence in the result. We used HeLa cells for these experiments, for two reasons. First, COS cells were found to be extremely sensitive to microinjection. A frustratingly small fraction survived this process and went on to show protein expression, in our hands. Second and more important, biochemical pulse-chase experiments at 20°C indicated that Sh-HA (WT) did not chase into the high molecular weight Golgi form within 3 hours, in COS cells (Fig 3.12A). This was also true at 6 hours of chase at 20°C (not shown). It is not clear whether this was due to a problem in traffic or due to inefficient activity of the Golgi glycosylation enzymes at the lower temperature. However, Sh-HA expressed in HeLa cells did chase into the high molecular weight Golgi form at 20°C, albeit at lower rates (predictably)

than observed at physiological temperature (Fig. 3.12B, lanes 4 –6). A short-lived background band (o) is present at ~93kD, inconveniently close to the immature (*) and mature (**) Sh-HA bands. Untransfected HeLa cells have been shown for comparison (Fig. 3.12B, lanes 1 – 3).

In preparation for the imaging of Shaker traffic from ER to Golgi, we were required to empirically determine two parameters. First, the optimum expression time post-injection was found to be 2 hours at 37 °C (not shown). This was the minimum time required for adequate Sh-HA fluorescence levels, upon immunostain. Second, a suitable chase time (at 20 °C) was determined. Preliminary experiments showed that the fluorescence pattern of wild type channel did not change a great deal after ~ 4 hours at 20°C, in the presence of cycloheximide. Thus, all subsequent experiments employed an expression period of 2 hours at 37°C (the "pulse") and a traffic period of 4 hours at 20°C (the "chase").

The images shown (Fig. 3.13A) represent the beginning and end-point of a complete kinetic imaging experiment for WT and NQ mutant Shaker channel. For both channels, the fluorescence pattern shifted from more diffuse and reticular to more localized and juxtanuclear, over time. Moreover, the juxtanuclear Shaker fluorescence at later times co-localized with Golgi fluorescence (shown in the lower row, in each case). We used antibodies against three different ER resident proteins PDI (not shown), calnexin (CNX, Fig. 3.14A, upper panel) and calreticulin (CRT. Fig. 3.14A, lower panel) to stain cells at early traffic times, in order to confirm that the reticular pattern did indeed colocalize with the ER. This indicates that, as is expected for a membrane protein, the channel moved from an ER to a Golgi location over time. Staining of uninjected cells

(Figure 3.13B) shows that there was no detectable bleedthrough from the Golgi fluorescence into the Shaker fluorescence signal. Moreover, if BFA was included during the 20°C chase period, WT channel remained largely reticular after 3 hours of traffic (Figure 3.13C). This is consistent with the conclusion that the change in fluorescence pattern is the consequence of transport out of the ER to the Golgi.

It is qualitatively evident from the images shown (Fig 3.13A), that the residual reticular non-Golgi stain after 4 hours of traffic was consistently higher in cells that expressed the unglycosylated mutant channel when compared to cells expressing the wild type. Immunofluorescence staining for a resident ER protein (CNX) after 3 hours of traffic at 20°C shows that this residual non-Golgi Shaker colocalized to some extent with the ER. This is shown for both wild type (Fig 3.14B, upper panel) and mutant (Fig 3.14B, lower panel) Shaker. The marked cell (Fig. 3.14B upper panel, indicated with arrow) is pointed out as an example of a cell that has undergone some traffic, yet nevertheless shows substantial Shaker fluorescence in the ER. Although there is punctate perinuclear Shaker fluorescence that does not significantly overlap with the ER stain, and almost certainly represents Golgi (red in merge, immediate upper-left of nucleus, also upper-right of nucleus but slightly further away from nuclear edge), there is a significant amount of Shaker that does co-localize with calnexin in this cell (along the right edge of the nucleus).

To quantify these data, we determined the fraction of Shaker fluorescence that co-localized with the Golgi at various traffic times after addition of cycloheximide and shift to 20 °C. For each cell, the signal in the Golgi fluorescence channel was used to delineate the boundary of the organelle, and the Shaker fluorescence intensity in this area was

quantified relative to the total Shaker fluorescence intensity in the same cell. Quantification of ≥40 cells for each time point is shown (Figure 3.15). The fraction of WT or NQ Shaker fluorescence in the Golgi area is shown over time. Although there is some increase in the Golgi fraction for the mutant channel, it is clear that the rate at which it moved from ER to Golgi is markedly slower than that of the wild type, at 20°C. Traffic of the WT channel was also incomplete, at the lower temperature. When this was monitored by pulse-chase of metabolically labeled HeLa cells, the mean estimated Golgi fraction (30% +/-7; n = 3) was roughly comparable to that measured by the imaging experiment, over a 3 hour chase period (Fig 3.12B). It should be emphasized that this is only an estimate, since a background band (see lanes 1-3, Fig 3.12B) close to the Shaker bands of interest made quantification difficult.

3.4.4. Imaging of ER-to-Golgi traffic : further controls and caveats

We attempted to create Sh-HA constructs that were retained in the ER by attaching ER retention sequences (DEKKMP or RKR) to the channel carboxyl terminus. This was for the purpose of testing the extent to which Shaker fluorescence that co-localizes with the Golgi does indeed represent protein that has trafficked to the Golgi. The constructs were expressed in COS cells and examined on α-HA Western blots (Fig. 3.16A) and by pulse-chase of metabolically labeled cells (Fig. 3.16B). Neither sequence functioned to retain Shaker in the ER, as evidenced by efficient chase to the Golgi form of the channel. Further, the DEKKMP-tagged channel was detected at very low levels. This approach was abandoned. Instead, we performed the identical image analysis on uninjected cells that had been stained for just ER and Golgi markers (Fig. 3.16C), and

determined the fraction of a protein in the ER that is reported, by our analysis method, to colocalize with the Golgi. This was found to be 5 % (+/- 2, n = 13) for the resident ER protein PDI. Since the fraction of Shaker fluorescence that co-localized with the Golgi at later traffic times was significantly higher, we conclude that we are measuring fluorescence from Shaker that has, indeed, trafficked to the Golgi and is not merely juxtaposed to it. Moreover, the mean fractional Golgi signal that was reported for uninjected cells that had been stained for Shaker and Golgi was also 5 % (+/- 1.5, n = 11). This latter signal is the overall background of the experiment, and would be a sum of cellular autofluorescence (which tends to be slightly higher in the perinuclear region than in the rest of the cell), any bleedthrough from the Golgi immunofluorescence channel, and non-specific fluorescence background. The fraction of an ER resident protein that is reported to co-localize with the Golgi, therefore, is at background levels. For the purpose of comparison, the identical analysis on cells stained for two different Golgi markers (p58 and GOS28), both of which maintain a uniform Golgi distribution, yields a co-localization of 85-90%. We conclude that unglycosylated mutant Shaker traffics more slowly from ER to Golgi than wild type, at 20 °C. We would predict that at least part of the observed difference in the surface delivery rate of the two channels stems from a difference in their ER-to-Golgi traffic.

As a caveat to this interpretation, the following must be considered. The method of image analysis we have employed makes the assumption that all non-Golgi fluorescence in the cell can be attributed to Shaker that has not as yet trafficked to the Golgi (i.e Shaker that is at a pre-Golgi location in the secretory pathway). This assumption is likely to be inaccurate. Specifically, there is most probably some Shaker

on the cell surface at all times measured, resulting both from delivery during the initial 2 hour expression period, when the cells are incubated at 37 °C, and from some "leakage" during the 0 – 4 hour traffic period at 20 °C. This would underestimate the Golgi fraction for both WT and mutant Shaker, at all times. However, biotinylation experiments suggest that wild type Shaker traffics faster than the mutant. Thus, the measured wild type Golgi fraction is likely to be a greater underestimation than the mutant fraction. If anything, therefore, the differences between the mutant and wild type transport rates are likely to be greater than those observed here. We engineered a FLAG epitope into the third extracellular loop of the channel in an attempt to directly measure the surface fraction at different traffic times. Although the FLAG epitope was clearly detected on a Western blot (not shown), immunoreactivity in both permeabilized and unpermeabilized cells was low to nonexistent, respectively. Attempted optimizations were unsuccessful, although these were not extensively done.

A fraction of injected cells (both WT and mutant) showed a clear "rim stain", suggesting that these cells had significant amounts of Sh-HA channel on the cell surface. Some selected fields are shown (Fig 3.17A), including rim stained, non-rim stained (marked with arrows) and non-expressing cells. As would be predicted, analysis of the rim stained cells reported an unusually low fraction of Shaker fluorescence in the Golgi, when compared to other cells at the same time point. For very flat cells, such as the HeLa used in our imaging experiments, a low level of surface protein need not manifest as a clear rim stain. It is therefore not possible to assume that the non-rim stained cells have no cell surface protein. However, we consider it likely that the levels, if any, are lower than in the rim-stained cells. We consistently removed all obviously rim-stained

cells, whether wild type or mutant-injected, from the analysis. This was done blind i.e. we did not know whether wild type or mutant cells were being looked at. Interestingly, the fraction (of all cells) that showed a rim stain was significantly higher for the wild type-injected, when compared to the mutant-injected cells, at all time points. Composite data for six independent experiments is shown (Fig. 3.17B). Since the fluorescence staining (α-HA) is against an intracellular epitope, the rim stain is by no means unequivocal evidence of surface channel. However, this observation is consistent with other previously described experiments that demonstrated more rapid transit of the glycosylated channel to the cell surface.

3.4.5. Stability of WT and NQ mutant Shaker

Since significant differences in stability of the WT and mutant channel could confound comparisons of surface or Golgi fractions, we compared the degradation of the two channels under the conditions in which our experiments were done. The stability of WT and mutant channel was compared over 24 hours at 37°C in COS cells (Fig. 3.18A, B), and was found to be very similar. Since our experiment to measure initial rates of surface delivery was terminated at 3 hours, it is reasonable to conclude that stability differences of the channels did not contribute to the perceived difference in surface delivery. There was no significant difference between stability of the WT and mutant channel over 4 hours at 20 °C in HeLa cells (Fig. 5.18C).

3.4.6. Do ER lectins contribute to the difference between channels ?

One of several possible explanations for the slowed ER-Golgi traffic of the unglycosylated N259Q+N263Q mutant is that, as a consequence of reduced (or

abolished) interaction with lectin-like ER chaperones, the mutant requires a longer initial lag time to fold to an export-competent conformation. Shaker is known to interact with the ER membrane chaperone calnexin in a glycosylation-dependent manner (Nagaya et al., 1999). As for most glycoproteins this interaction presumably occurs via calnexin binding to Shaker mono-glucosylated glycans, which initially arise due to trimming of the core $Glu_3Man_9GlcNAc_2$ sugar by ER-glucosidases I and II. Blocking the activity of the ER glucosidases with castanospermine (CST) prevents generation of the calnexin-binding moiety on the substrate glycoprotein, and consequently prevents interaction of the protein with the chaperone, in most cases. We tested the effect of CST on the delivery of wild type Shaker to the surface of transfected COS cells.

CST-treated proteins are predicted to have two extra glucose residues per glycosylated moiety in comparison to untreated proteins, and would consequently shift to a slightly slower mobility on SDS-PAGE. For a relatively large protein like Shaker, this shift is only just discernible (Fig. 3.19A, lanes 1-2). Shaker channel translated in vitro in the presence of CST does indeed co-immunoprecipitate less efficiently with calnexin than untreated channel (Fig. 3.19B). In vivo, treatment with CST was seen to reduce the rate of Shaker maturation (defined as appearance of a high molecular weight Golgi band), but did not affect the secretion of an unglycosylated protein (preprolactin). Representative pulse-chase experiments as well as composite data from several independent experiments are shown for Shaker (Fig. 3.19C) and secreted preprolactin (Fig. 3.19D). That CST-treated proteins mature at all is due to the existence of a Golgi endomannosidase. The retardation in Shaker maturation can be explained based on the fact that this enzyme, although able to cleave off core mannoses in the presence of the terminal glucose

residues, does so at a sluggish rate (Moore and Spiro, 1992; Moore and Spiro, 1990). Thus, CST had a predicted effect on Shaker association with calnexin *in vitro*, and on Shaker traffic *in vivo*. In preliminary experiments (n = 2), the rate of Shaker delivery to the cell surface was not significantly affected by treatment with castanospermine (Fig. 3.19E).

3.5. A method to monitor endocytosis

We attempted a comparison of the endocytic rates of the WT and the NQ mutant channel from the cell surface (Fig. 3.20A). In this experiment, a reversible biotinylation of surface proteins (the "pulse") was followed by incubation at 37°C for various lengths of time (the "chase"). At the end of each chase period, the cells were rapidly cooled to 4°C to stop all traffic and the surface biotin then stripped off with the cell-impermeant reducing agent glutathione. The remaining biotinylated fraction was determined. Depending on the degree of endocytosis during the chase, variable amounts of biotinylated protein would be expected to become resistant to stripping by extracellular glutathione. The remaining biotinylated fraction at each chase time, therefore, presumably represents the intracellular fraction at that time. We tested this approach on the transferrin receptor (TfR), the recycling of which has been extensively characterized. In another mammalian cell line (HEp2), the TfR is endocytosed constitutively with a half time of ~4 minutes, and is recycled back to the surface with a half time of ~7 minutes (Ghosh et al., 1994). The steady-state surface fraction of the TfR is estimated at ~ 30 % of total, in mammalian cells (Johnson et al., 1998). Indeed, 30.5 % (+/-3; n = 3) of the unstripped sample is seen to bind avidin beads (Fig 3.20B, lane 3), but this is reduced to 3% (+/-2; n = 3) when the cells are stripped with glutathione (Fig. 3.20B, lane 6). If the

cells are allowed to traffic for 5 minutes at 37°C prior to stripping, the biotinylated fraction increases again to 18 % (+/-4; n = 2) (Fig 3.20B, lane 9). At longer chase times, the biotinylated fraction again drops (not shown). So, to a first approximation, the biotinylation approach adequately reports the endocytosis of the TfR. However, we have been unable to consistently monitor endocytosis of the Shaker channel. This is most likely the result of an insufficient starting signal.

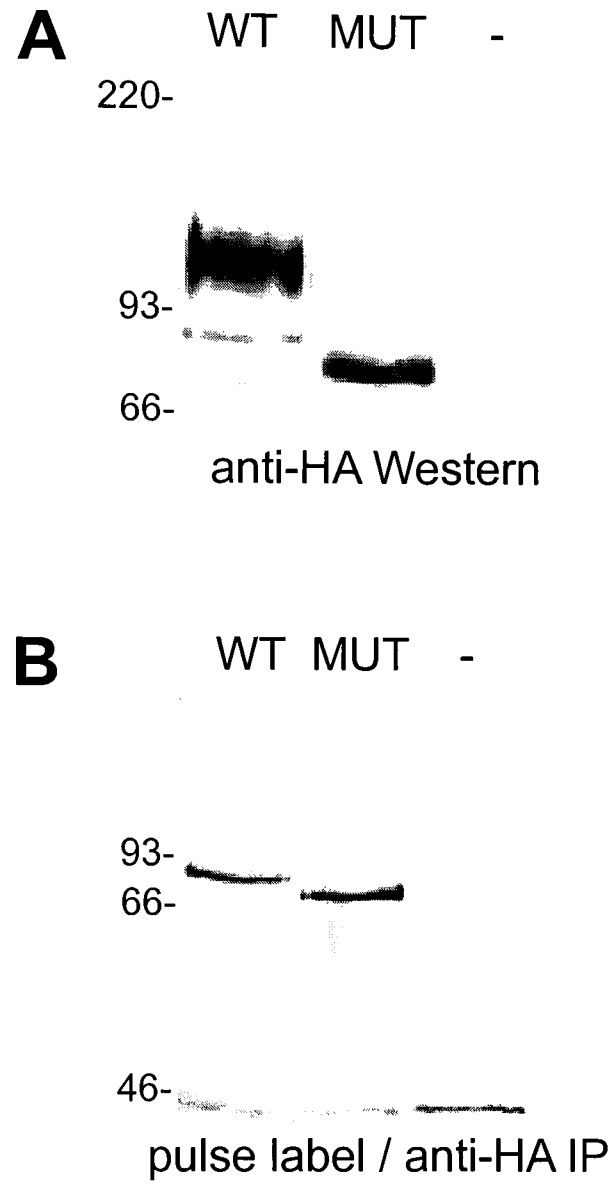

Figure 3.1 : Shaker expression in COS cells. (A) COS cells transfected as indicated were solubilized (2% CHAPS) and the lysates probed on an anti-HA Western blot. **(B)** COS cells transfected as indicated were pulse-labeled with ^{35}Scysteine+methioinine, solubilized as above and the lysates subjected to anti-HA IP.

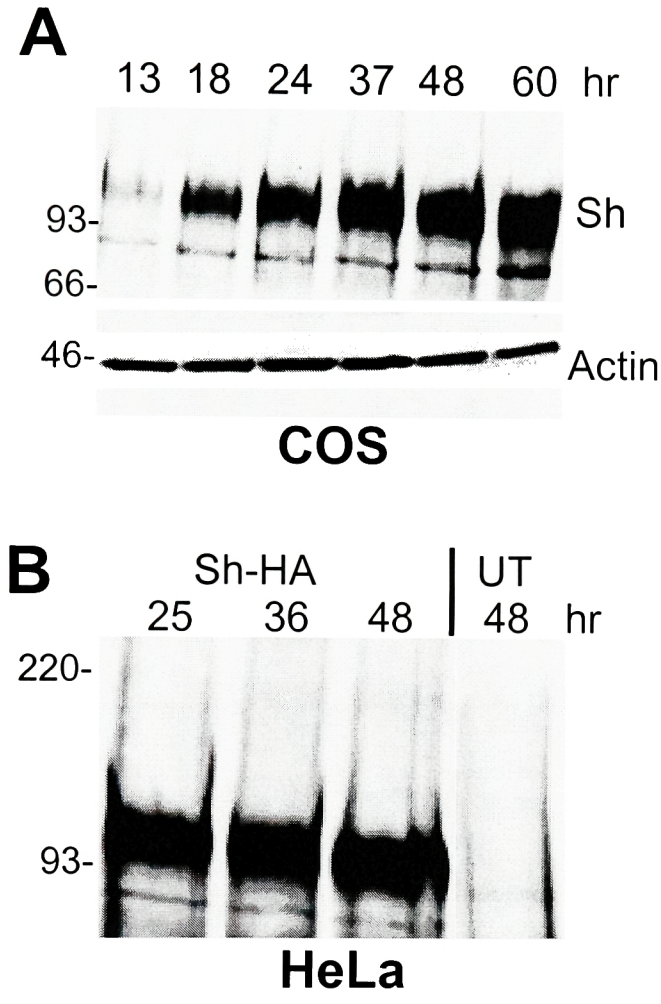

Figure 3.2 : Time course of Shaker-HA expression. Transfected COS **(A)** or HeLa **(B)** cells were lysed (2% CHAPS) at the indicated times post-transfection, and the lysates probed on an anti-HA Western blot.

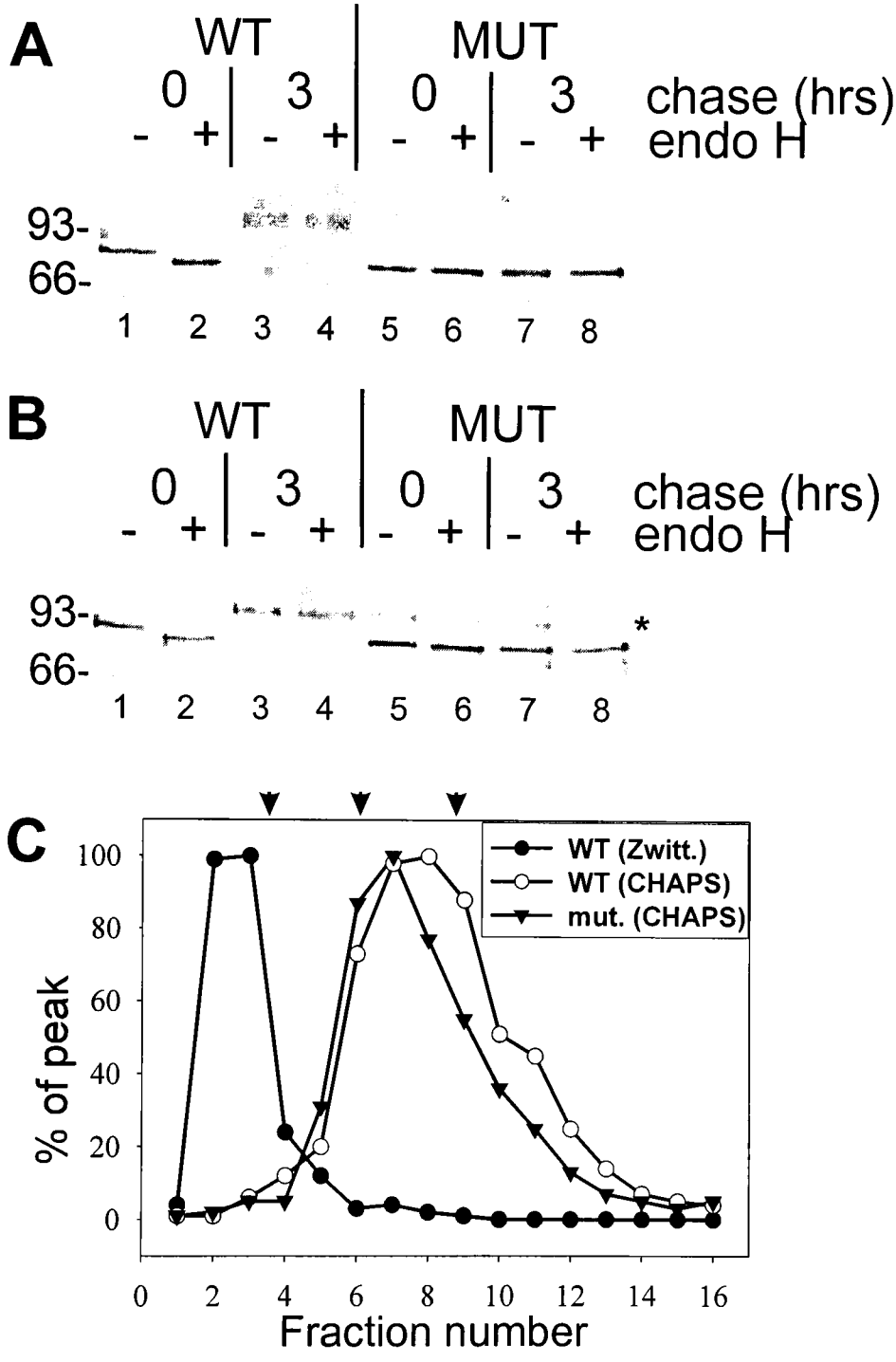

Figure 3.3 : Shaker assembly and traffic in mammalian cells. COS **(A)** or HeLa **(B)** cells transfected as indicated were pulse-labeled with ^{35}Scysteine+methioinine, chased (0-3h, 37°C), lysed (2 % CHAPS) and the lysates subjected to anti-HA IP and endoH digestion. **(C)** WT or N259Q+N263Q mutant Shaker-transfected COS cells were pulse-labeled as above, lysed (2% CHAPS or 1% Zwittergent) and the lysates centrifuged through a 5 – 20 % sucrose gradient. Sucrose density increases with increasing fraction number. The arrowheads above the plot indicate the peak migration of, from left to right, BSA (66 kD), aldolase (160 kD), and catalase (240 kD).

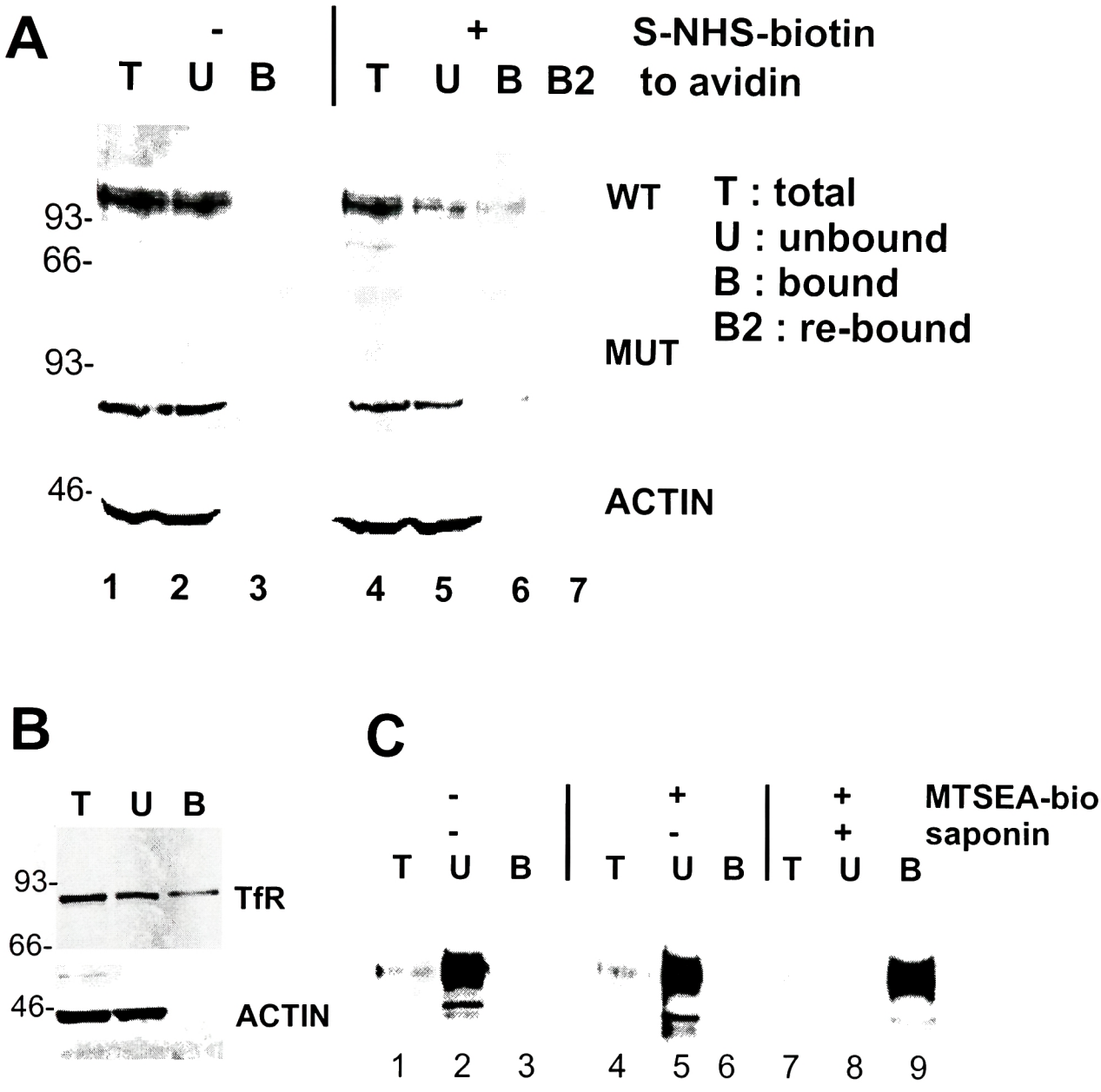

Figure 3.4 : Surface biotinylation of Shaker channel in COS cells. **(A)** WT- or NQ mutant-transfected COS cells were surface biotinylated and the cell lysates bound to avidin beads. To ensure that the avidin precipitation was complete, unbound material was re-incubated with avidin beads. Equal fractions of the total (T), unbound (U), bound (B) and re-bound (B2) samples were probed for wild type Shaker-HA (upper panel), mutant Shaker-HA (middle panel) or actin (lower panel) on Western blots. **(B)** HeLa cells were surface biotinylated and processed as above, and probed for the transferrin receptor (TfR, upper panel) or actin (lower panel). **(C)** Sh-HA-transfected COS cells were surface biotinylated with external (lanes 4-6) or internal (lanes 7-9) MTSEA-biotin and processed as above.

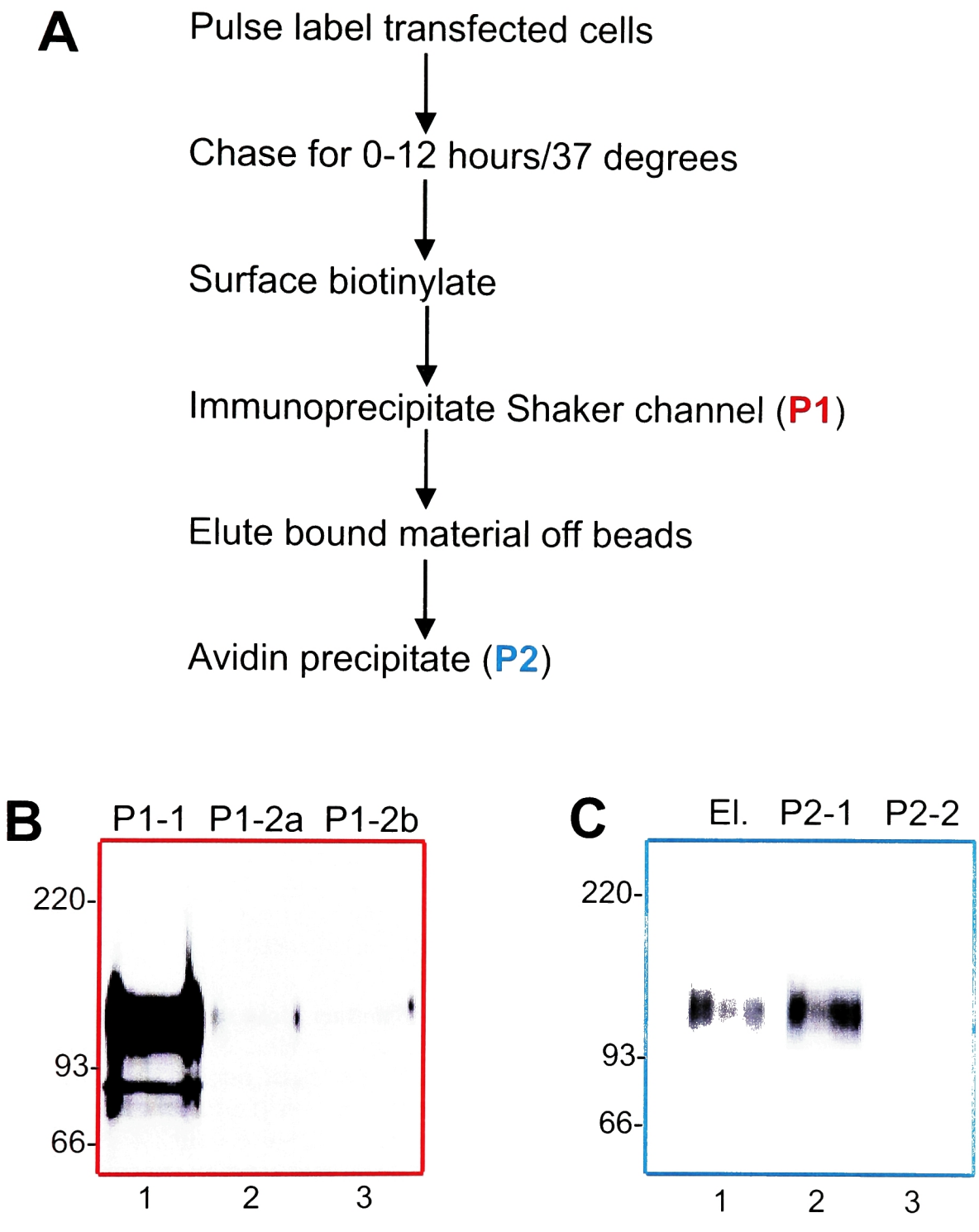

Figure 3.5 : Surface biotinylation of newly synthesized Shaker - controls. **(A)** Summary of experimental steps. **(B)** To ensure that IPs were complete, the unbound material from P1 was re-precipitated with either anti-HA antibody (lane 2) or with protein A beads alone (lane 3) and probed on an anti-HA Western blot. **(C)** To ensure that avidin precipitations were complete, unbound material from P2 was re-precipitated with avidin beads and probed on an anti-HA Western blot.

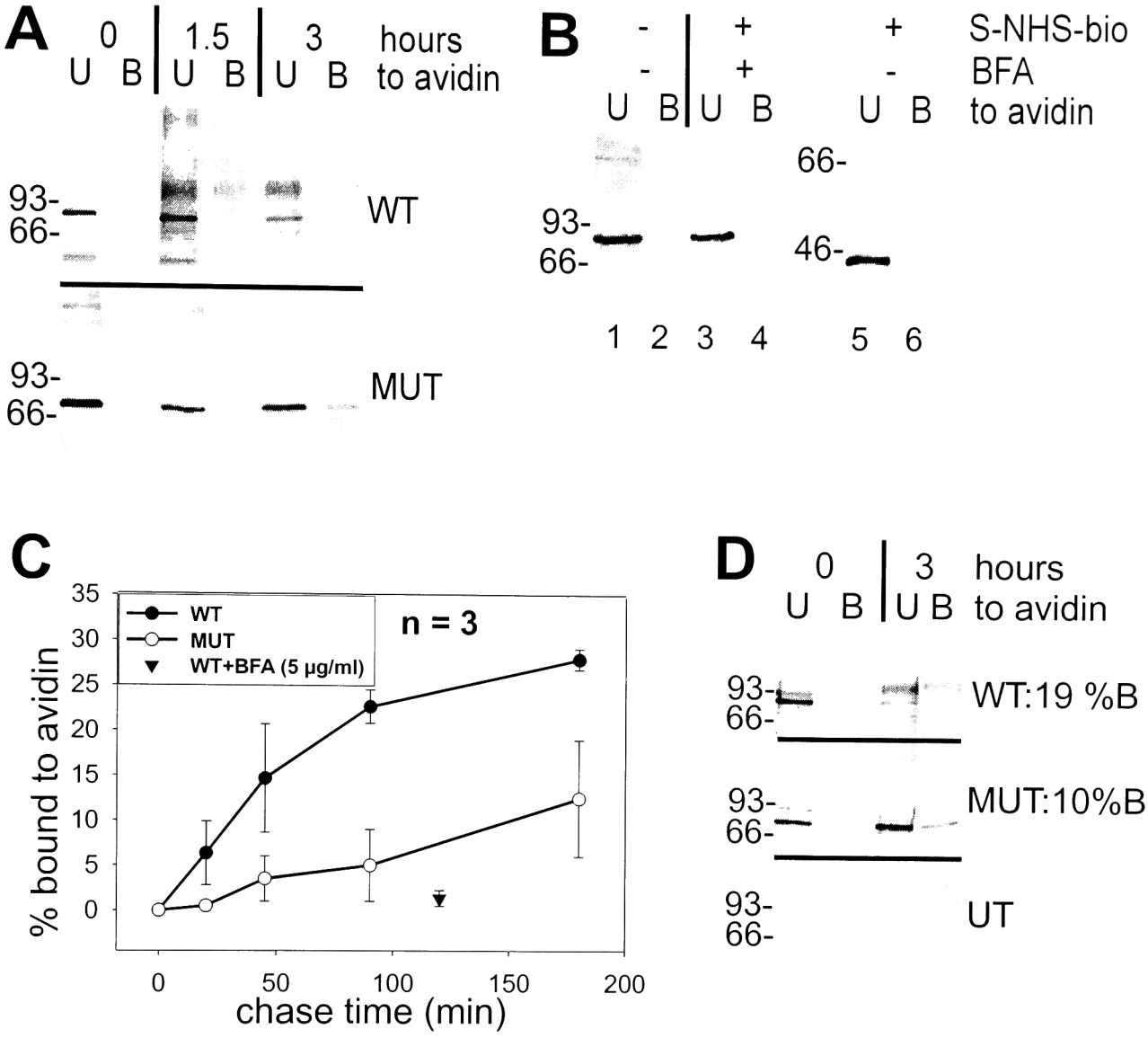

Figure 3.6 : Surface biotinylation of newly synthesized Shaker.
(A) Transfected COS cells were pulse-labeled with ^{35}Scysteine+methioinine, chased (0-3h), and surface biotinylated. The channel was IP'd, eluted off the protein-A beads at low pH and then affinity precipitated with avidin beads. The TCA precipitated unbound material **U** and the avidin-bound material **B** from the avidin precipitation were separated by SDS-PAGE. Selected time points from a representative experiment have been shown for WT (upper panel) and mutant (lower panel) Shaker. For clarity, the relevant bands have been indicated as follows (WT immature: *, WT mature: **, mutant: <). **(B)** The above protocol was carried out in the absence of biotinylating agent (lanes 1-2), on WT channel chased in BFA (lanes 3-4), or with α-actin IP in place of α-HA (lanes 5-6). **(C)** The biotinylated fraction of Shaker (B/{U+B})*100 was plotted over time. Data represent the mean +/- SEM (n = 3). The biotinylated fraction at time zero was subtracted as background, for each experiment. **(D)** The above protocol was carried out on HeLa cells transfected with WT (upper panel) or mutant (middle panel) Shaker, or on untransfected cells (lower panel).

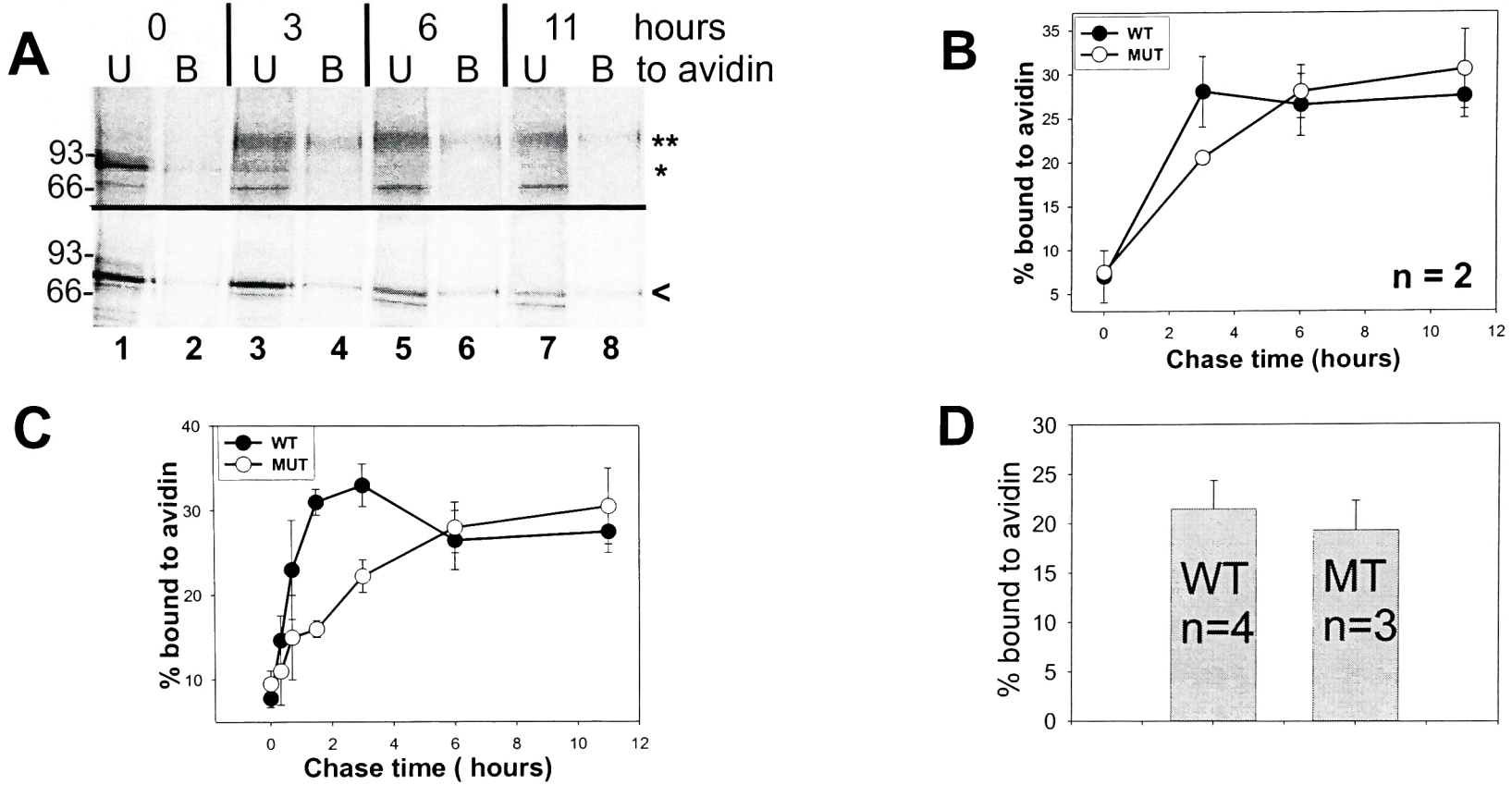

Figure 3.7 : Steady state surface levels of Shaker in COS cells. (A) Transfected COS cells were pulse-labeled with ^{35}Scysteine+methioinine, chased (0-11h), and surface biotinylated. The channel was IP'd, eluted off the protein-A beads at low pH and then affinity precipitated with avidin beads. The TCA precipitated unbound material **U** and the avidin-bound material **B** from the avidin precipitation were separated by SDS-PAGE. Selected time points from a representative experiment have been shown for wild type (upper panel) and mutant (lower panel) Shaker. For clarity, the relevant bands have been indicated as follows (WT immature: *, WT mature: **, mutant: <). **(B)** The biotinylated fraction (B/{U+B})*100 was plotted over time (n = 2). **(C)** The biotinylated fraction (B/{U+B})*100 at early and late chase times was plotted (n = 5, at 0h and 3h; n = 3 at 0.5-1.5h; n = 2 at 6h and 11h). **(D)** Transfected COS cells were surface biotinylated and cell lysates bound to avidin beads. Equivalent amounts of the total **T**, unbound **U** and bound **B** material were probed on α-HA Western blots, and the biotinylated fraction (B/T)*100 quantified and plotted. All data represents the mean +/- SEM.

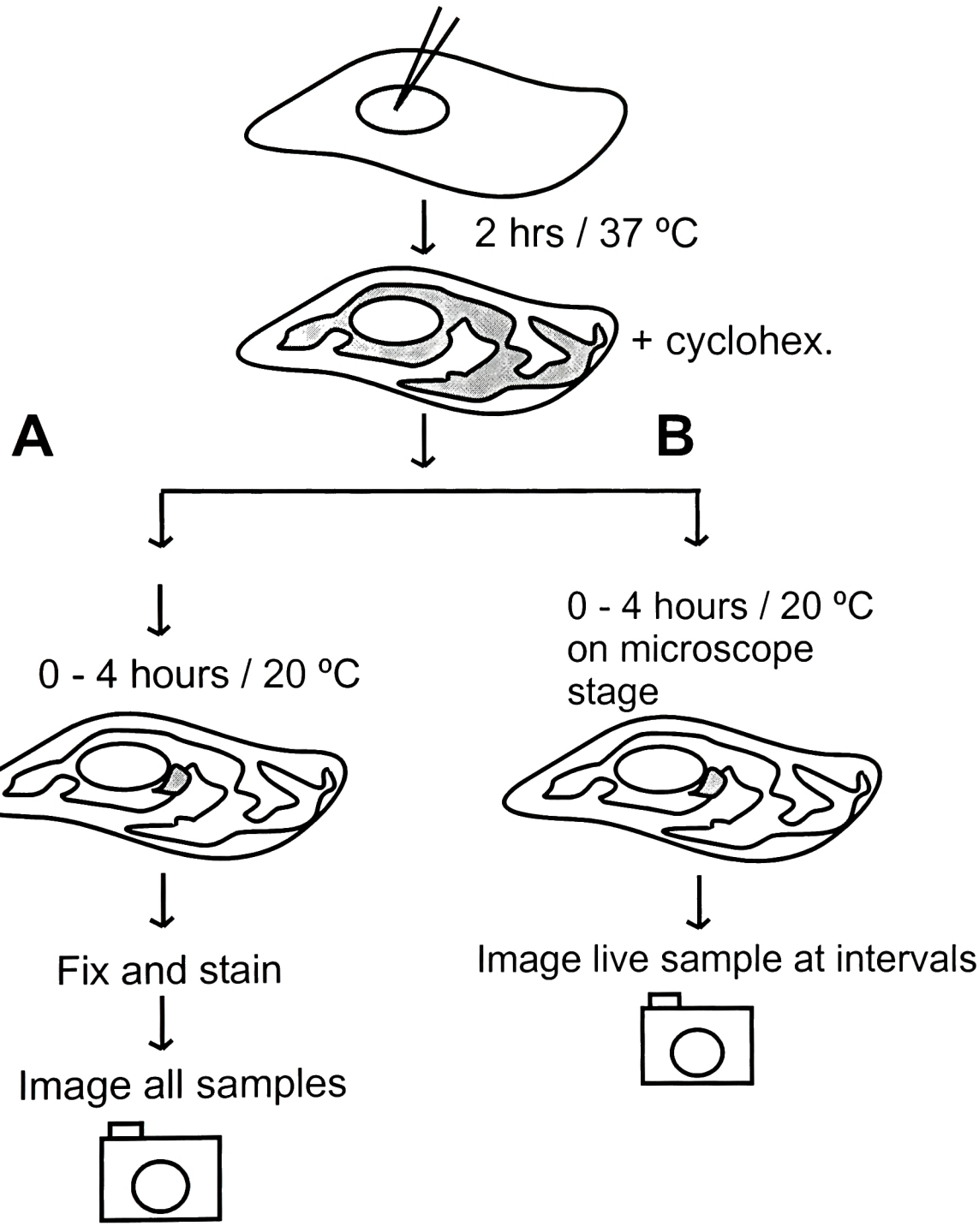

Figure 3.8 : Imaging Shaker traffic from ER to Golgi. Schematic of an experiment for monitoring traffic of **(A)** HA-tagged Shaker in fixed cells or **(B)** GFP-tagged Shaker in live cells.

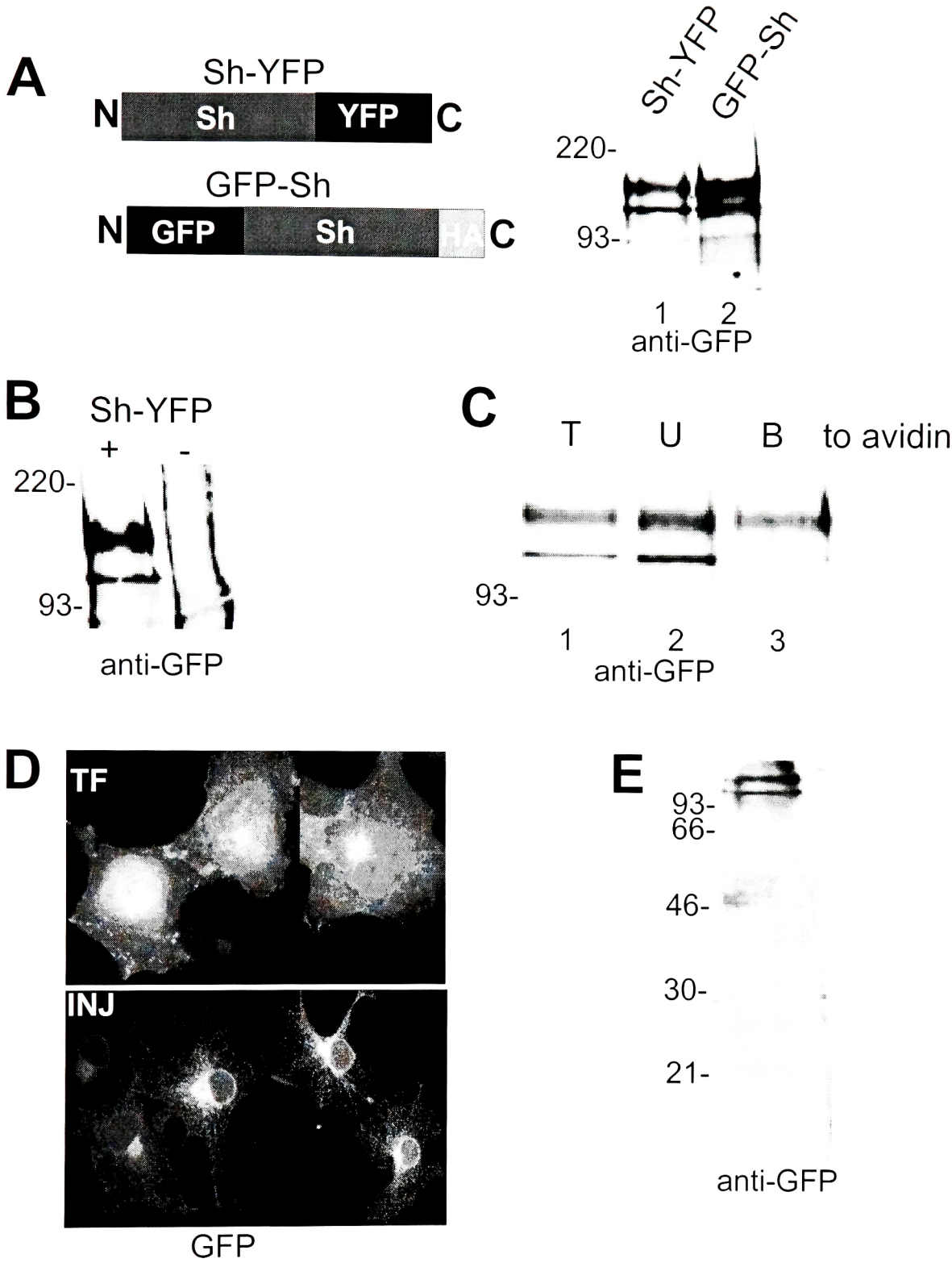

Figure 3.9 : Sh-YFP expressed in COS cells. **(A)**, **(B)** and **(E)** Lysates of transfected COS cells were probed on α-GFP Western blots. **(C)** Sh-YFP-transfected COS cells were surface biotinylated at steady state and the cell lysates bound to avidin beads. Equal fractions of total **T**, unbound **U** and bound **B** were probed on an α-GFP Western blot. **(D)** COS cells transfected (upper panel) or microinjected (lower panel) with the Sh-YFP construct were imaged for GFP by epifluorescence microscopy.

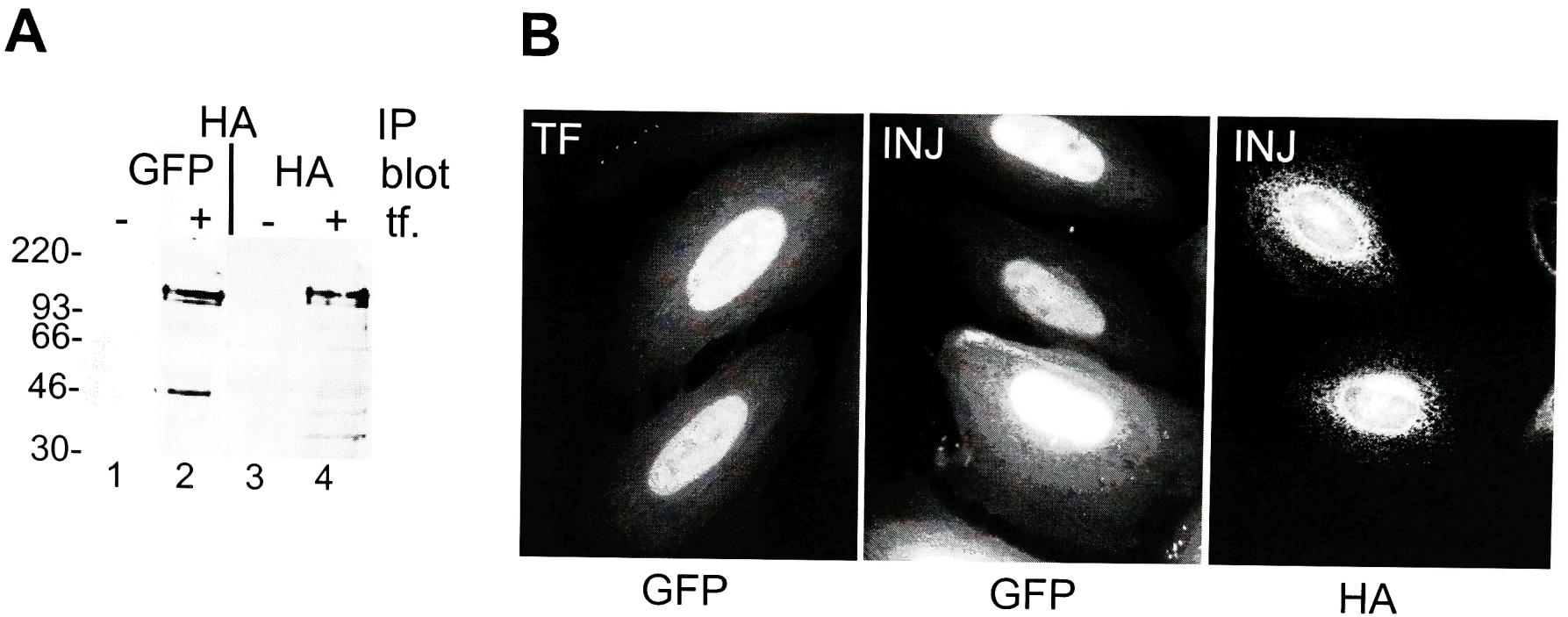

Figure 3.10 : GFP-Sh-HA expressed in mammalian cells. **(A)** Lysates of transfected COS cells were subjected to α-HA IP and probed on an α-GFP (lanes 1-2) or an α-HA (lanes 3-4) Western blot. **(B)** HeLa cells transfected (TF, left panel) or microinjected (INJ, middle and right panel) with the GFP-Sh-HA construct were imaged for GFP, or fixed and immunostained with α-HA (right panel).

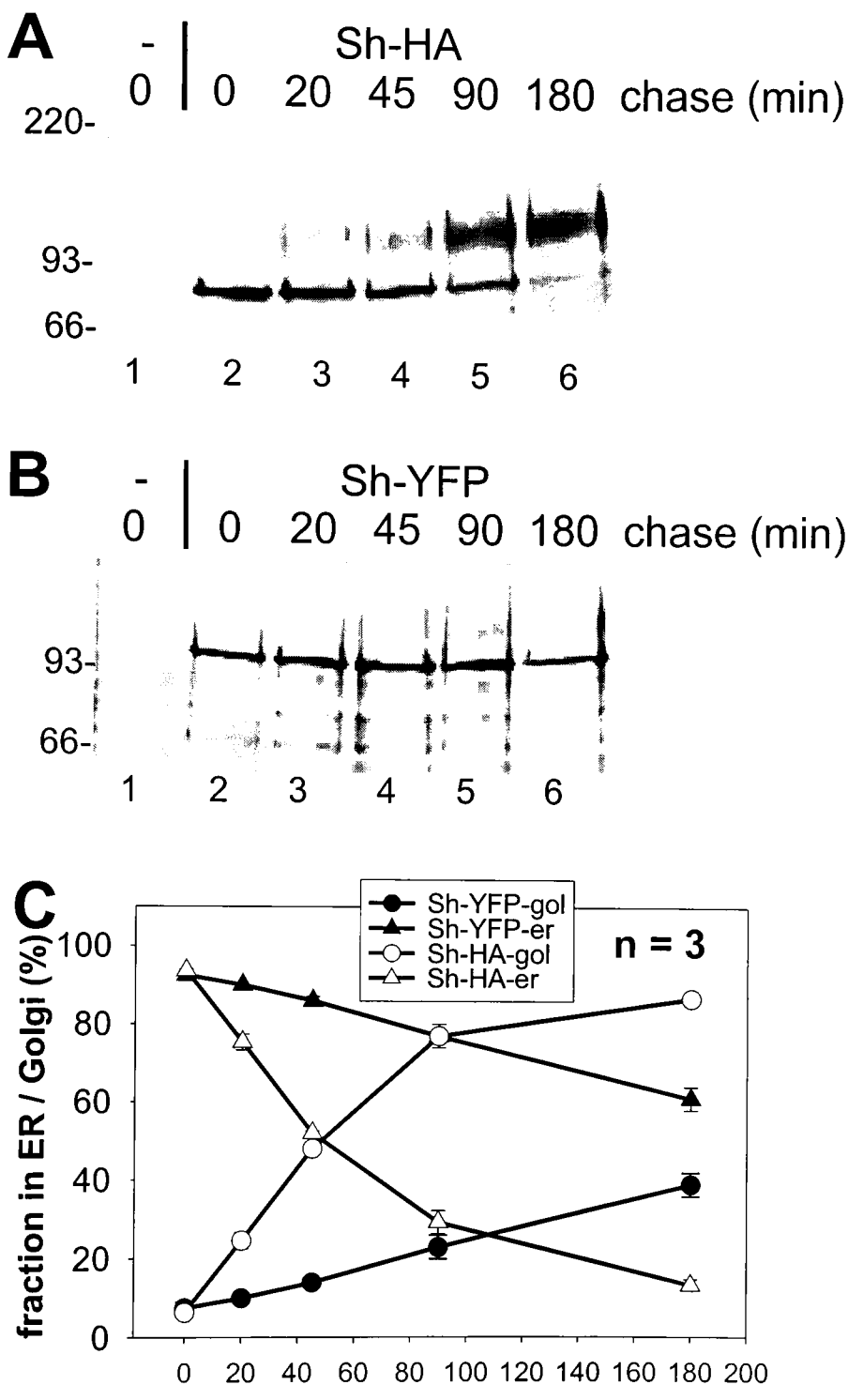

Figure 3.11 : ER-Golgi traffic of Sh-YFP. COS cells transfected with Sh-HA **(A)** or Sh-YFP **(B)** were pulse-labeled with ^{35}Scysteine+methioinine, chased for the indicated times, and the lysates subjected to α-HA or α-GFP IP. **(C)** The mean immature (ER) or mature (Golgi) fractions +/- SEM (n = 3) are plotted over time, for both constructs.

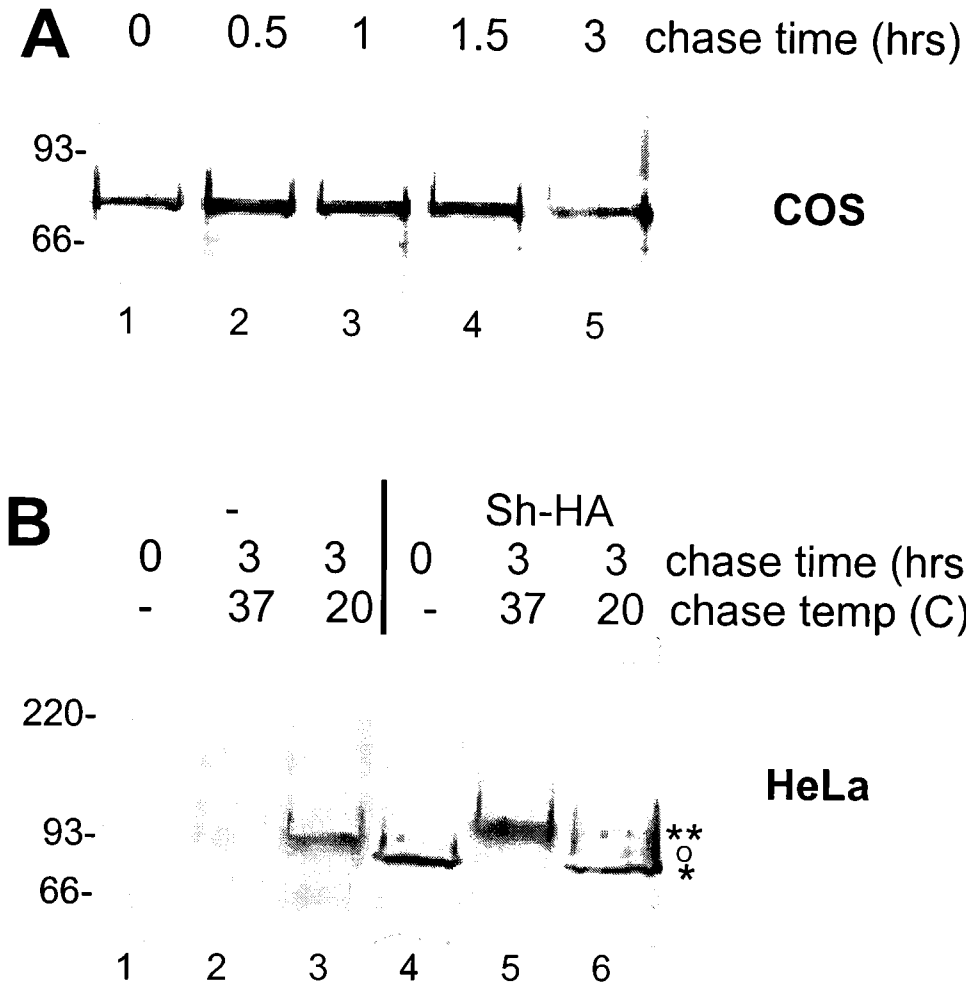

Figure 3.12 : ER-Golgi traffic at low temperature in mammalian cells. Sh-HA-transfected COS **(A)** or HeLa **(B)** cells were pulse-labeled with ^{35}Scysteine+methioinine, chased for the indicated times at 20°C, and the lysates subjected to α-HA IP. Untransfected HeLa cells have been show (lanes 1-3) to indicate the position of a background band. Immature Sh-HA (*), mature Sh-HA (**) and the background band (o) are indicated.

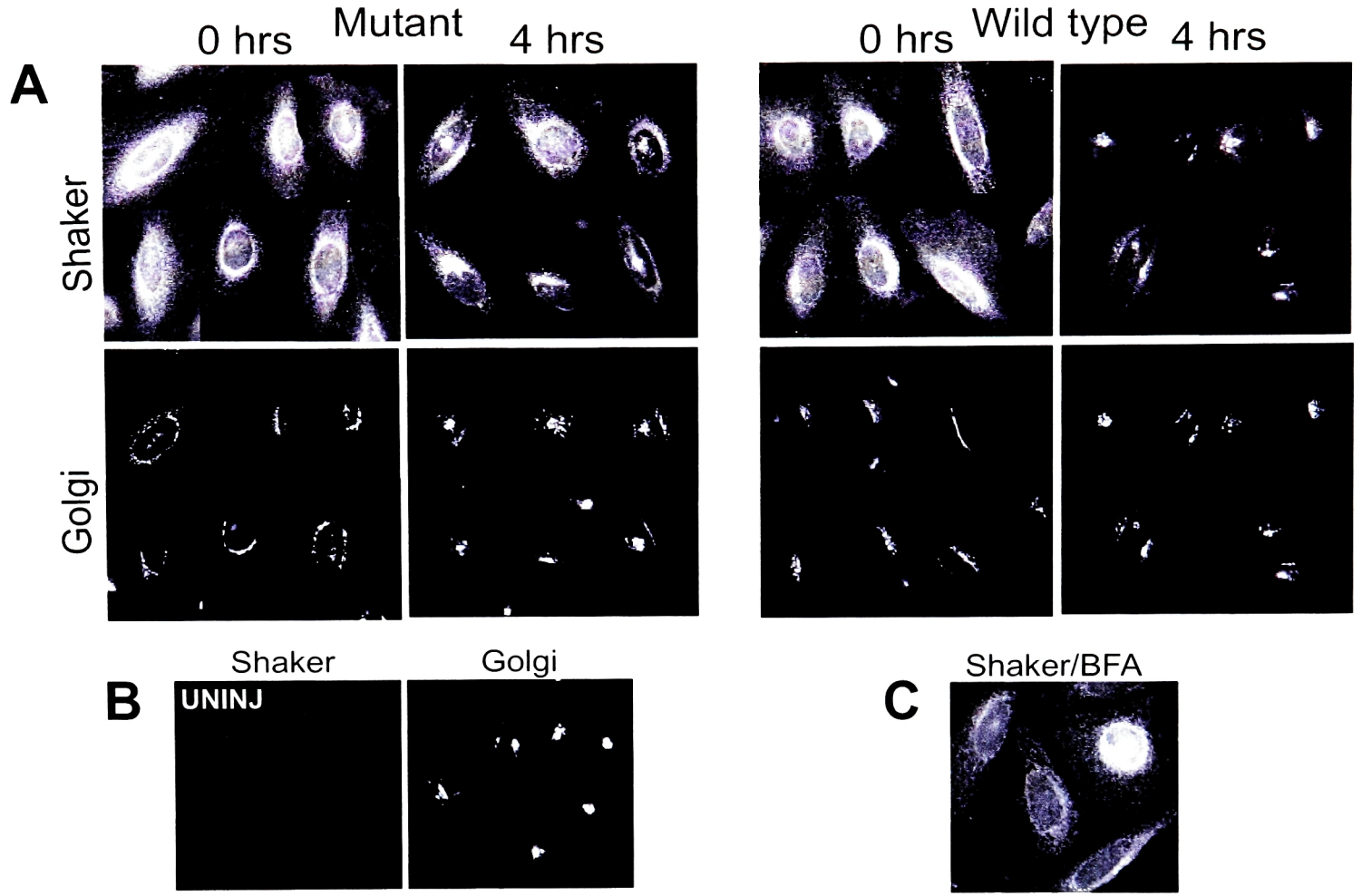

Figure 3.13 : Imaging Shaker traffic from ER to Golgi. **(A)** WT or N259Q+N263Q mutant Shaker cDNA was microinjected into HeLa nuclei and allowed to express (37°C, 2h). The cells were chased (20°C, 0–4h) in cycloheximide, fixed and stained for Shaker (anti-HA) and Golgi (anti-GOS 28), imaged by epifluorescence, and the fraction of Shaker fluorescence co-localizing with the Golgi determined for each cell. The 0h and 4h time points are shown. Each panel is a composite, display properties are identical for all images. The upper row represents Shaker and the lower row represents the corresponding Golgi image, in each case. **(B)** Uninjected cells were stained for Shaker and Golgi. **(C)** WT-injected cells chased (20°C, 3h) in the presence of BFA were stained for Shaker.

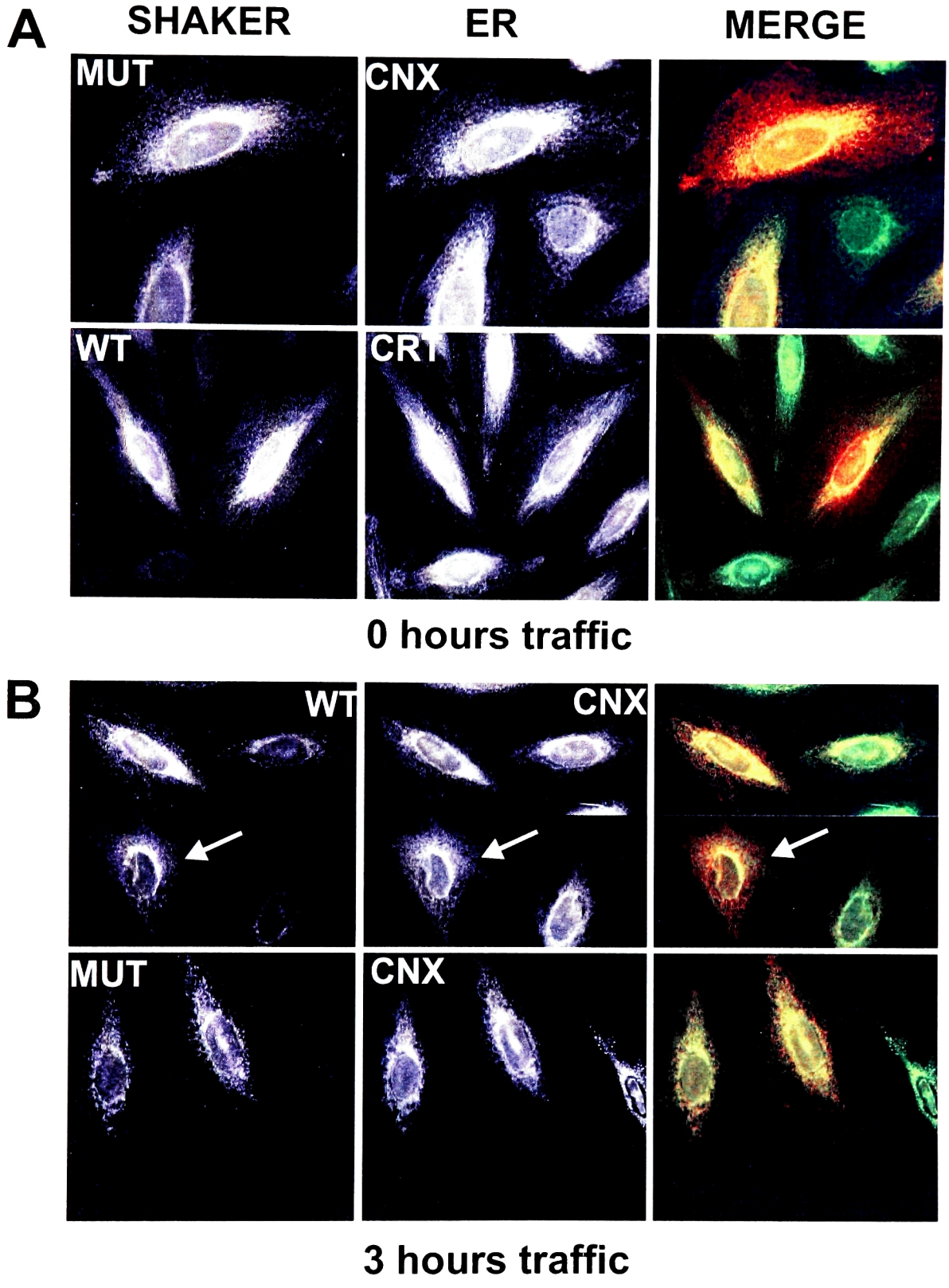

Figure 3.14 : Co-localization of Shaker with the ER at early and late traffic times. HeLa cells were intranuclearly microinjected as indicated, incubated at 37°C to allow for expression, chased for 0h **(A)** or 3h **(B)** at 20°C, fixed and stained for Shaker (α-HA, red) or ER (α-CNX or α-CRT, green).

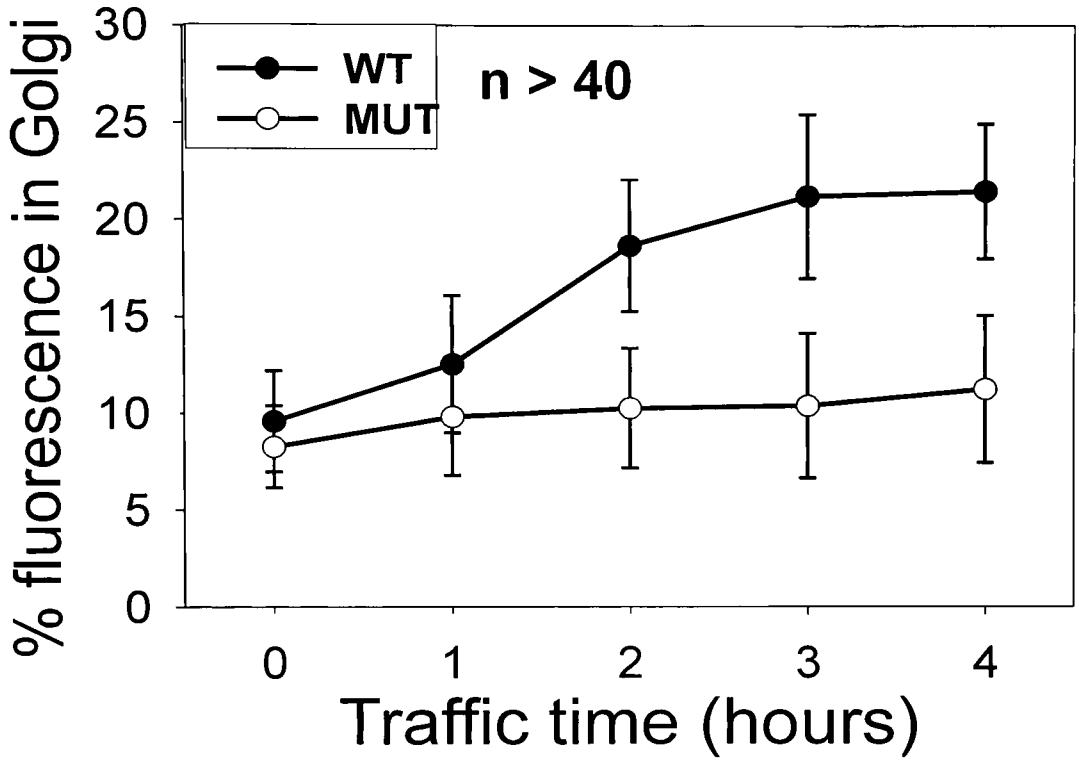

Figure 3.15 : ER-Golgi traffic of WT and N259Q+N263Q mutant Shaker. The fraction of WT or mutant Shaker fluorescence co-localizing with the Golgi after 0-4h of chase at 20°C was determined in several independent experiments (n > 40 cells; in most cases, n = ~ 60 cells) and plotted as the mean +/- S.D.

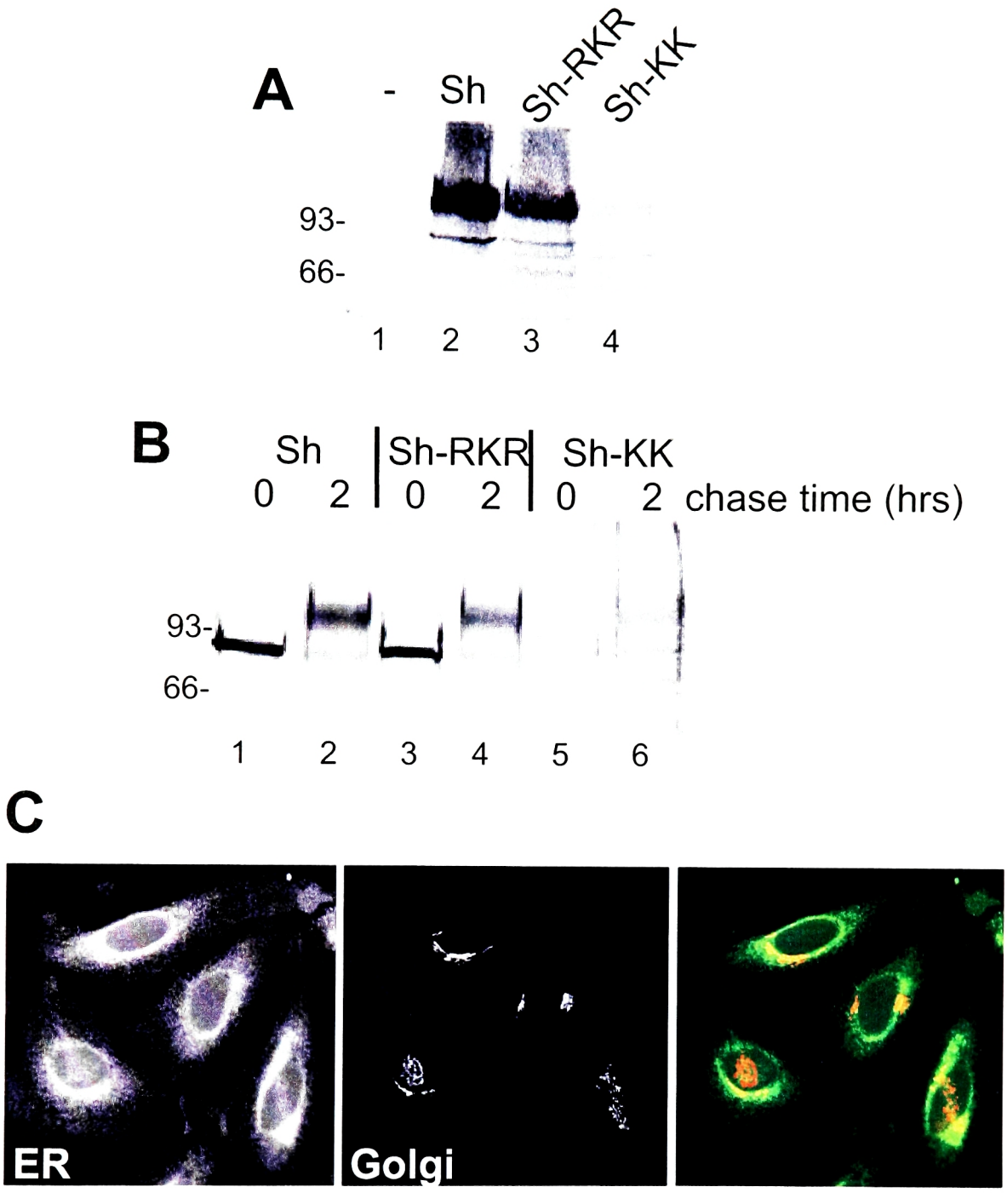

Figure 3.16 : Controls for quantitative imaging experiment. COS cells transfected as indicated were lysed and probed on α-HA Western blots **(A)**, or pulse-labeled with ^{35}Scysteine+methioinine, chased for 0-2h (37°C) and the lysates subjected to α-HA IP **(B)**. **(C)** Uninjected HeLa cells were stained for ER (α-PDI, green) and Golgi (α-p58, red) and the fraction of ER fluorescence that co-localized with the Golgi was determined.

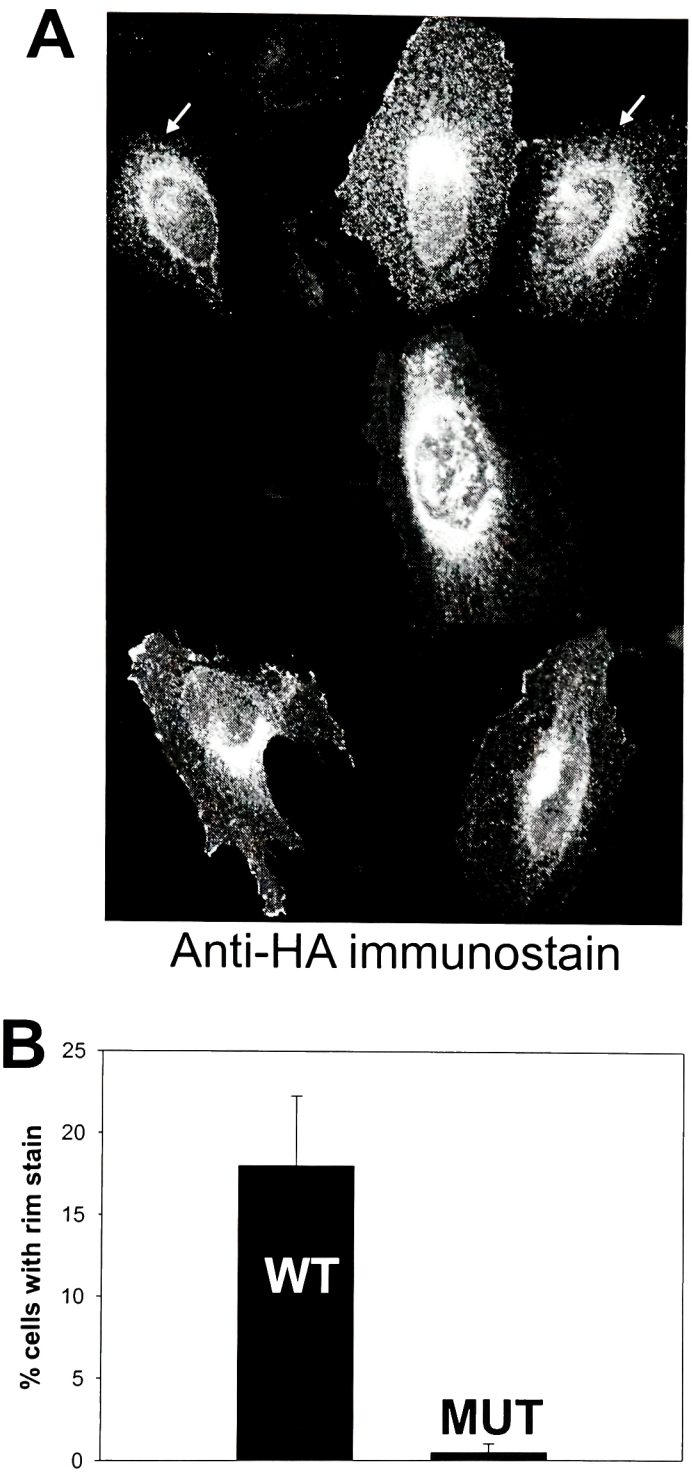

Figure 3.17 : "Rim-stained" cells. **(A)** Representative α-HA immunostains of WT injected HeLa cells are shown. Non-rim-stained cells are marked with arrows. **(B)** The fraction of WT or mutant-injected cells that shows a visible rim stain is plotted. The mean +/- SEM of three independent experiments is shown, with a total of 200 - 250 cells counted, for each construct.

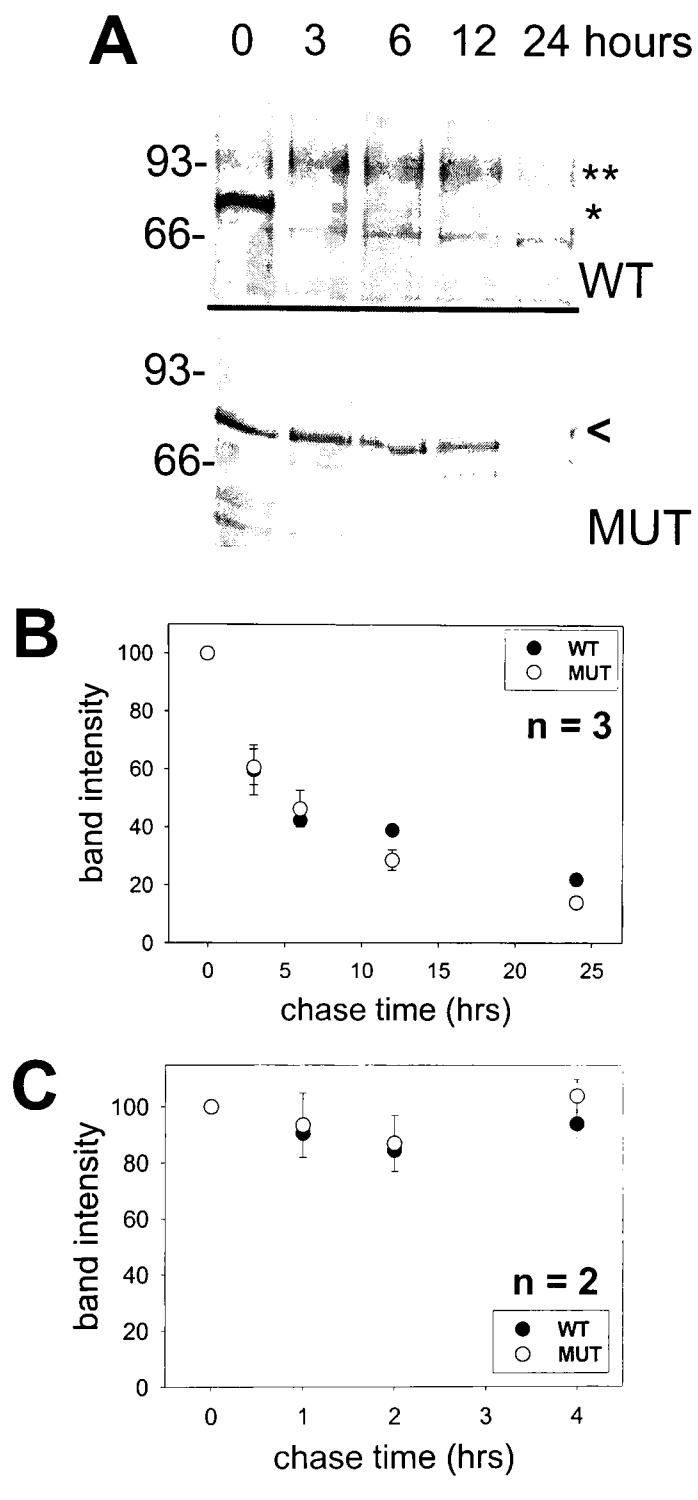

Figure 3.18 : Stability of the Shaker channel. **(A)** COS cells transfected with WT (upper panel) or NQ mutant (lower panel) Shaker were pulse-labeled with ^{35}Scysteine+methioinine, chased (0-24h) and equal cpm of each lysate subjected to α-HA IP. For clarity, the WT immature (*), WT mature (**), and mutant (<) bands have been indicated. **(B)** Mean signal intensities +/- SEM were quantified and plotted over time (n = 3). The band intensity at 0 hours is taken as 100 %, for each experiment. **(C)** Shaker channel stability in HeLa cells was determined (0-4h chase, 20°C) and plotted as above (n = 2).

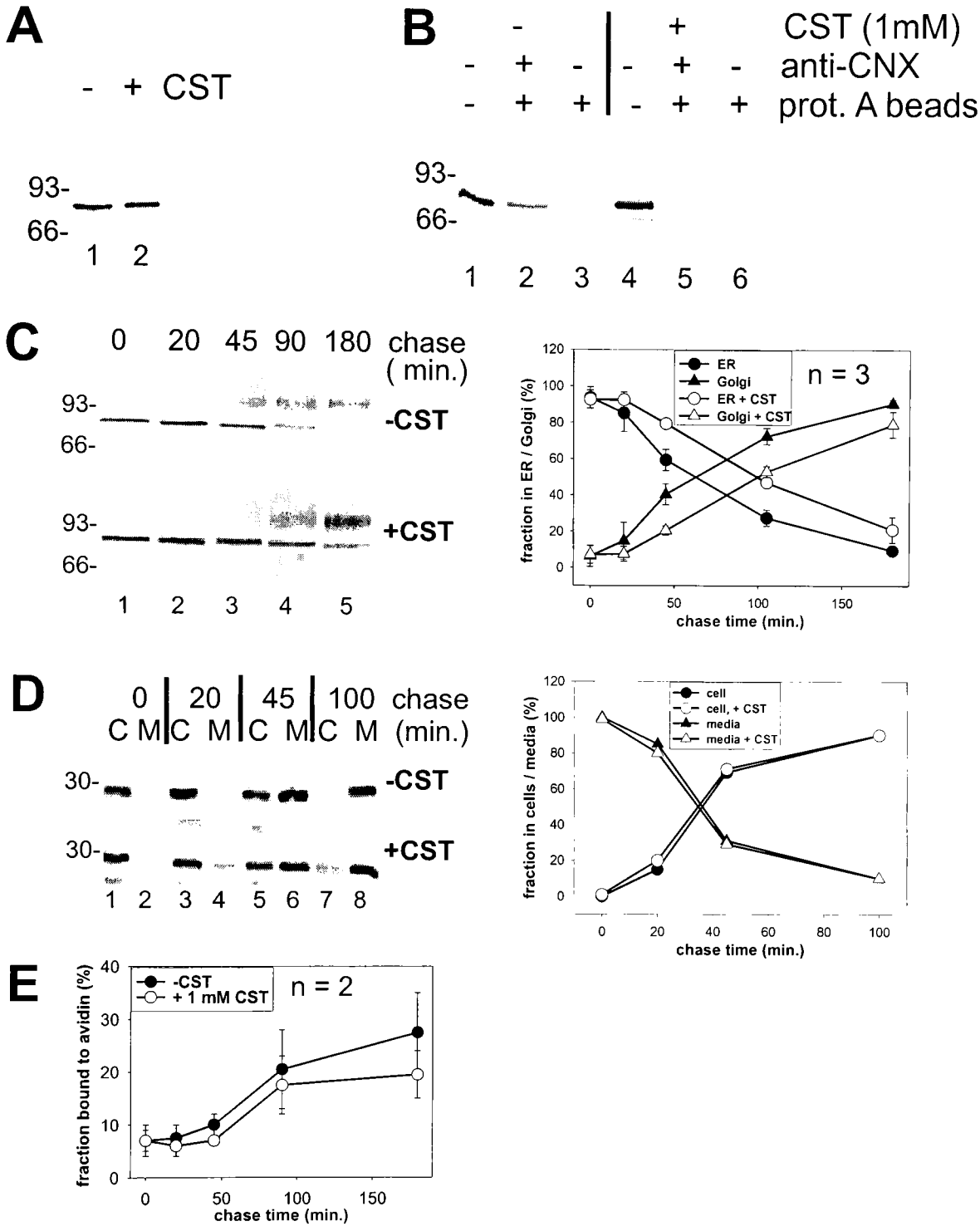

Figure 3.19 : Shaker traffic in castanospermine (CST)-treated cells. **(A)** Immature Shaker in COS cells -/+ CST (lanes 1-2). **(B)** α-calnexin co-IP of Shaker translated *in vitro* either without (lanes 1-3) or with (lanes 4-6) CST. Shaker **(C)** or pre-prolactin **(D)** transfected COS cells were pulse-labeled with ^{35}Scysteine+methioinine, and chased (0-3h) either in the absence (upper panel) or presence (lower panel) of CST. The fraction of total protein in the immature/mature form (Sh) or in the cell-associated/secreted form (ppl) is plotted over time. **(E)** Surface biotinylation of newly synthesized WT Shaker in COS cells pulse-chased -/+ CST. The mean biotinylated fraction +/- SEM has been plotted over time (n = 2).

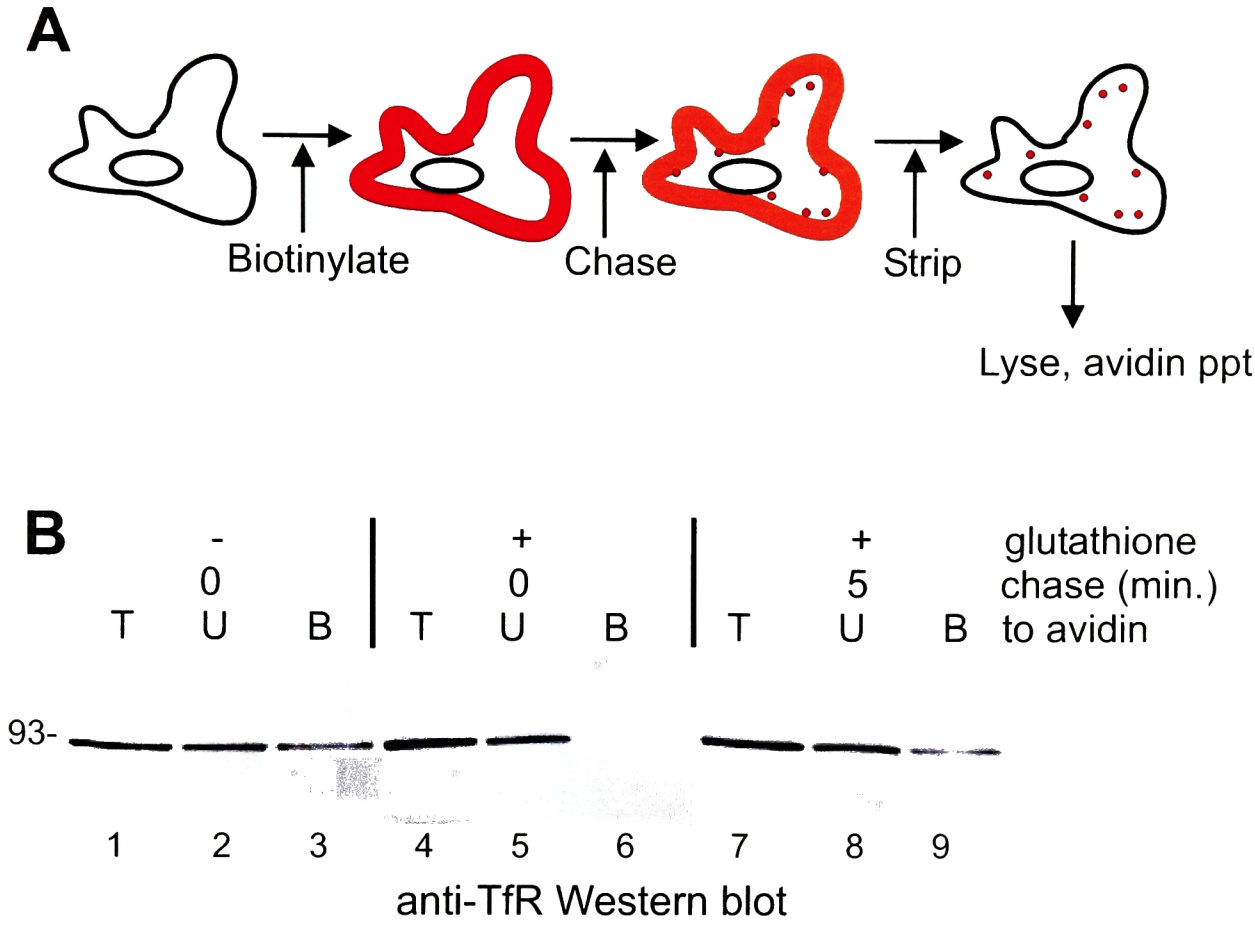

Figure 3.20 : A method to monitor endocytosis. **(A)** Schematic of the approach. **(B)** Reversibly surface-biotinylated HeLa cells were allowed to traffic (0-5 min, 37°C) and then left unstripped (lanes 1-3) or glutathione-stripped (lanes 4-9). Cell lysates were precipitated with avidin beads, and equivalent fractions of total **T**, unbound **U** and bound **B** were probed on an α-transferrin receptor Western blot.

4. TARGETING OF THE SHAKER CHANNEL TO THE ER

In vitro transcription, translation and translocation constitute a commonly used system to study the requirements for targeting of proteins to the endoplasmic reticulum (ER). The use of translocation-competent ER microsomes and well-characterized assays for protein modification by lumenally disposed ER enzymes allows the study of reactions that take place exclusively at/in this organelle. However, there are drawbacks inherent to the *in vitro* system, most notably the low efficiency at which all but the simplest reactions occur, when compared to the situation in the living cell.

The Shaker channel is a multi-spanning membrane protein with six transmembrane (TM) domains and no predicted N-terminal hydrophobic signal sequence. The ~220 amino acid N-terminal domain is topologically intracellular. Based on analogy to opsin, another membrane protein without a cleaved amino-terminal signal sequence, it is predicted that the earliest ER targeting information in Shaker is transmembrane domain 1 (TM1). However, this has not been investigated. In this chapter, the following topics are covered.

1) Characterization of the rabbit reticulocyte lysate/canine pancreatic microsome system for *in vitro* translation and translocation of the Shaker potassium channel.

2) Determination of the sequence requirements for targeting of Shaker to the ER.

3) Examination of Shaker truncated constructs in mammalian cells.

4.1. Characterization of Shaker translation/translocation

Shaker channel translated in rabbit reticulocyte lysate (RRL) yielded a major band at ~ 70 kD (Fig 4.1A, lane 1), approximately in keeping with the predicted size of this 656 amino acid protein. Epitope-tagged channels (Shaker-HA & Shaker-MYC) showed the identical band, and could be immunoprecipitated with the corresponding antibodies (Fig 4.1B). A prominent 30kD band was also seen (not shown here); the origin of this is unknown and will be discussed later (chapter 7). Optimal Shaker translation was seen with the addition of 60–100 mM K^+ and no Mg^{++} to commercially available rabbit reticulocyte Flexi™ lysate (Promega). Addition of DTT (1- 2 mM) also stimulated translation, but was not added in most cases so as to maintain the normal oxidizing environment of the ER. A viral 5' untranslated CITE (cap-independent translation enhancer) sequence has been previously reported to increase translation efficiency of the Kv1.1 channel *in vitro* (Shen et al., 1993) but had no effect on the translation of Shaker (not shown).

When Shaker was translated in the presence of canine microsomal membranes, a slightly higher molecular weight band appeared (Fig 4.1A, lane 2). This is predicted to result from N-linked glycosylation of the channel at the two consensus sites in its first extracellular loop. Translation of the channel in the presence of microsomes treated with the N-Ac-Asn-Tyr-Thr-NH_2 tripeptide, which contains a consensus sequence for N-linked glycosylation and therefore functions as a competitive inhibitor of this process, abolished this higher molecular weight band (Fig 4.1A, lane 3). Thus, this slower moving band is the glycosylated channel. As expected, the N259Q+N263Q (NQ) mutant channel, where both consensus glycosylation sites have been eliminated, does not show

the corresponding changes in mobility on SDS-PAGE when translated in the presence or absence of microsomes (not shown) and/or competitor tripeptide (Fig 4.1C). Shaker translation was assessed at different incubation times (Fig 4.2A) and temperatures (Fig 4.2B). All subsequent translations were done at 30°C for 60 – 90 minutes.

4.1.1. Targeting of Shaker to ER microsomes

Targeting of an *in vitro*-translated protein to the ER membrane is typically assayed by separating the translation reaction into membrane and cytosol fractions, and then assessing the fractionation profile of the protein. The separation may be achieved in one of two ways. Centrifugation through a 1.0M sucrose cushion results in pelleting of the ribosome-studded rough ER microsomes, while cytosolic proteins remain in the supernatant. When this was done on *in vitro*-translated Shaker, most of the channel was seen to be associated with the pelleted fraction when translated in the presence (Fig 4.3A, upper panel, lanes 3-4) but not in the absence (Fig 4.3A, upper panel, lanes 1-2) of microsomes. Further, for Shaker translated in the presence of microsomes, unglycosylated form of the protein was selectively enriched in the supernatant (i.e. untargeted) fraction. Parallel sedimentation of β-lactamase, an unglycosylated, signal peptide-containing protein that is completely translocated into the ER lumen, confirms the validity of the approach (Fig. 4.3A, lower panel). Again, pelleting occured only in the presence (lanes 3-4), but not in the absence (lanes 1-2) of microsomes, and the non-signal peptide cleaved form (<, Fig. 4.3A) of the protein was selectively enriched in the untargeted fraction. Occasional small incongruities in size are due to the fact that the samples were run on different gels.

A potential problem with membrane harvesting by sedimentation is that aggregates or polysome–associated proteins may also sediment under these centrifugation conditions. This may be avoided by instead harvesting the membranes via flotation through high-concentration sucrose. The translation reaction is adjusted to 2.1M sucrose, overlayed with 1.9 M sucrose, and then centrifuged. The buoyancy of the microsomes causes them to float up to an intermediate sucrose concentration, whereas both cytosolic proteins and aggregates remain at the bottom of the tube. Again, *in vitro* translated Shaker harvested largely with the membranes (in this case, the supernatant fraction) when translated in the presence (Fig 4.3B, lane 7) but not in the absence (Fig 4.3B, lane 3) of microsomes. This was also true for the β-lactamase control (Fig 4.3, lanes 1 & 5).

4.1.2. Integration of Shaker into the lipid bilayer

Having established that *in vitro*-translated/translocated Shaker targets efficiently to ER membranes, we wanted to determine whether the channel was stably integrated into the lipid bilayer or merely peripherally associated with it. Membrane integration is assayed by extraction with alkali (100 mM NaOH), as a result of which all but stably integrated proteins are stripped away from the membrane. The Shaker channel was not extractable from the bilayer with alkali and sedimented with the membranes, while a lumenal control protein (β-lactamase) was completely extracted (Fig 4.4A). This sedimentation is not due to aggregation of the channel, since it did not occur when Shaker was alkali-treated in the absence of microsomes (Fig 4.4B).

4.2. Sequence requirements for Shaker targeting

4.2.1. Truncated Shaker constructs (T-series)

To identify the minimum ER targeting information in the Shaker primary sequence, we generated a series of shortened constructs (the T-series) by introducing stop codons at various points in the coding region. The location of the stop codons relative to full-length channel is shown schematically (Fig. 4.5). *In vitro* translation of these constructs in the presence and absence of ER microsomes (Fig 4.6A) and competitor tripeptide (Fig 4.6B) resulted in bands of approximately the expected sizes (multiple bands for T2 are discussed below). Increasing signal intensity with increasing length can be explained by the fact that the methionines in Shaker are predominantly in the C-terminal half of the molecule.

T2 was seen to produce three bands upon *in vitro* translation in the absence of microsomes (Fig. 4.7A). The smallest band (*) is predicted to be unglycosylated T2. This is based on three observations. First, it is appropriately smaller (by ~3 Kd) than the unglycosylated T3. Second, it is appropriately smaller (by ~6 Kd) than the faint glycosylated T2 band (<>) that results upon addition of membranes and that is abolished by tripeptide treatment. Third, it was present in all T2 translations, unlike the slightly larger species (**), which was only sporadically seen (for example, it is almost absent in Fig 4.7B). The largest band (***) exactly co-migrates with that produced by translation of a construct of the same length, but lacking a stop codon (T2Δstop) (Fig 4.7B, compare lanes 1 & 3). The T2Δstop construct ends (with no subsequent nucleotides) at the penultimate codon of the T2 construct. The (***) species was therefore hypothesized to represent T2 that failed to release from its final tRNA and that remained spuriously

associated with the tRNA and/or the ribosome. Indeed, post-translational RNase treatment abolished the (***) band (Fig 4.7C, compare lanes 1 & 2), consistent with the idea that it represents protein bound to the terminal tRNA. Treatment with the aminoacyl-tRNA analogue puromycin partially released T2Δstop and T2 from the ribosome (Fig 4.7B). Since release by puromycin requires that the nascent chain is a substrate for the ribosome peptidyl transferase, this suggests that the (***) form of T2, while still attached to the tRNA, was partially no longer associated with a functional ribosome. This is not uncommon for truncated constructs lacking stop codons, in our experience. In an attempt to eliminate the (***) band we generated a T2 construct with multiple stop codons (T2MS), but this did not have the desired effect (Fig 4.7C, lane 3).

A glycosylated band is defined here as one that results upon addition of microsomes, and that is abolished in microsomes that have been treated with competitor tripeptide. All constructs except for the shortest (T2) were quite efficiently glycosylated (Fig. 4.6C), suggesting that they targeted to the ER membrane. This is confirmed by a flotation harvest, in which T3, T4 and T5 floated efficiently into the supernatant in the presence (Fig 4.8A, lower panel) but not in the absence (Fig 4.8A, upper panel) of microsomes. T2 however, remained predominantly in the (untargeted) pellet fraction even in the presence of microsomes (Fig 4.8A, lower panel, lane 1). As seen for full-length Shaker, the glycosylated forms of all the truncated proteins (T2 – T5) were recovered primarily in the membrane fraction (S), whereas the unglycosylated forms remained predominantly untargeted (P).

Quantification of the glycosylated fraction {G/(U+G)}(Fig 4.6C) and the targeted fraction {S/(S+P)}(Fig 4.8C) for each construct shows that, relative to the full-length

channel, the truncated constructs T3, T4 and T5 were efficiently targeted to the ER. T2, on the other hand, was inefficiently targeted as reported both by glycosylation and by fractionation with the membrane. Quantification of T2 membrane targeting was done either exclusive or inclusive of the putative tRNA-attached band. This was found to affect the reported targeted fraction to only a small degree, and did not change the overall trend relative to the other truncated constructs. RNase treatment prior to harvesting yielded no increase in the T2 membrane–targeted fraction (Figure 4.8B). Alkali extractions indicated that, once targeted, all constructs were stably integrated into the ER membrane (Fig. 4.9).

4.2.2. Is TM2 necessary for Shaker targeting ?

T2 is truncated in the loop between TM1 and TM2, while T3 is truncated at the very end of TM2 (Fig. 4.5). One possible explanation for the difference in targeting efficiency of T2 and T3 is that the additional sequence in T3 (part of extracellular loop 1 + TM2, amino acids 273-299) is important for this process. T2 is truncated 26 amino acids after TM1. Since the ribosome 'tunnel' is thought to enclose ~ 40 amino acids of a nascent polypeptide, an alternative explanation is that, in T2, TM1 is simply not far enough out of the ribosome to effect successful targeting. We tested this by assessing the targeting efficiency of two additional constructs (Fig 4.10A). T2.1 is truncated 40 amino acids after TM1, so that most of TM1 should have emerged from the ribosome. This construct includes only part of TM2 (the first 9 amino acids), and would consequently be predicted not to target efficiently if there is a specific requirement for TM2. T3ΔTM2 is approximately the same length as T3, but was created by fusing a random sequence from the Shaker C-terminus to the T2 construct. This should address the question of a specific

requirement for the last 5 amino acids of extracellular loop 1 and/or TM2 in targeting of Shaker to the ER.

4.2.3. Translation and targeting of T2.1 and T3ΔTM2

In vitro translation of these test constructs resulted in major bands of 38 - 40 kD (for T2.1) and ~ 42 kD (for T3Δ)(Fig. 4.10B). Since T2.1 is 14 amino acids shorter than T3, its migration is slightly slower than would be predicted based on size alone. We cannot explain this, beyond speculating that the presence of the second (half) TM domain affects migration in some non-linear fashion. T3Δ is expected to migrate slightly slower than T3, as is seen to be the case (Fig. 4.10B, compare lanes 3 & 5, or 4 & 6). The significant improvement in T3Δ signal, compared to T3, is likely due to two additional methionines in the added C-terminal sequence, rather than to improved translation efficiency.

Translation of T2.1 or T3Δ in the presence of microsomes resulted in glycosylation (Fig. 4.10B,D), which could be inhibited by treatment of the membranes with competitor tripeptide (Fig. 4.10C), thus suggesting that these constructs targeted more efficiently than T2. This was confirmed by a membrane floatation harvest. Both T2.1 and T3Δ were harvested with the membrane fraction when translated in the presence (Fig. 4.11A, lanes 5-10) but not in the absence (Fig.4.11A, lanes 1-4) of ER microsomes. Although the targeting of T2.1 and T3Δ was not quite at wild type levels, it was significantly improved over that of T2 (Fig. 4.11B). Further, the targeted T2.1 and T3ΔTM proteins were seen, by alkali extraction, to be stably integrated into the ER membrane (Fig. 4.11C).

We conclude that insufficient emergence of TM1 from the ribosome is most likely to be the reason for inefficient targeting of T2 to the ER. To re-iterate, this is based on two observations. First, the intermediate-length construct T2.1, in which TM1 is predicted to have fully emerged from the ribosome, targets much more efficiently than T2. Since T2.1 does not have a complete TM2, there is unlikely to be a specific requirement for this second transmembrane domain for targeting to the ER. Second, a construct of similar length as T3, but where all protein sequence downstream of amino acid 272 (i.e. the end of T2) has been replaced by random sequence, targets almost as efficiently as T3. Since the construct (T3Δ) does not have amino acids 273 – 299, which is the region that distinguishes T2 from T3, this suggests that these amino acids (i.e. 273 – 299; 5 aa of extracellular loop 1 + TM2) are not specifically important for the initial targeting (i.e. of TM1).

4.3. Expression of Shaker T2 and T3 in mammalian cells

Although T2 was targeted and glycosylated inefficiently with respect to full-length Shaker, both processes did occur at a level measurably above background. We expressed T2 and T3 in COS cells and assessed targeting to the ER in this system. Full-length channel is efficiently targeted in COS cells, as evidenced by the complete EndoglycosidaseH (EndoH) sensitivity of pulse-labeled immature (i.e. ER-localized) protein (Chapter 3). Cells transfected with HA-tagged T2 and T3 showed bands of 35-40 kD and 40–45 kD respectively (Fig. 4.12A) on an α-HA Western blot, similar in size to those produced by *in vitro* translation. In addition, T2 lysates showed a fuzzy, higher molecular weight band (#) (Fig. 4.12A, lane 2). EndoH digestion of immunoprecipitated

protein indicated that both T2 and T3 target quite efficiently to the ER in COS cells (Fig. 4.12B).

4.3.1. The EndoH-resistant fraction of T2 Shaker

The fact that the higher molecular weight form of T2 (#) was not affected by EndoH treatment could mean one of two things. First, its sugars could have matured to an EndoH resistant form, which would mean that the protein has trafficked to the Golgi. This is an unlikely scenario for a protein that is so drastically truncated relative to its native form, especially since the slightly longer T3 clearly does not traffic. Also, much less severe truncations of Shaker (175 aa versus the 384 aa removed in T2) serve to retain the channel in the ER (chapter 6). However, the topology that T2 assumes in the ER cannot be presumed to be the native one (for instance, it could be completely translocated into the lumen) and it is possible that, as such, it could have very different traffic characteristics from those of full-length Shaker. Second, the EndoH-resistant fraction may be unglycosylated, and the increased molecular weight may be due to aggregation or modification. Theoretically, this could occur as a result of inefficient targeting, followed by ubiquitination or some other cytosolic modification. Preliminary α-ubiquitin Western blots have been unsuccessful.

4.3.2. Immunolocalization of T2 and T3 Shaker in mammalian cells

We performed immunofluorescence staining on T2- and T3-transfected cells. Representative cells are shown (Fig. 4.13). In keeping with the biochemical data (*in vitro* and *in vivo*), T2 did indeed show aberrant targeting to the ER (Fig. 4.13A, upper panel). Some cells clearly did have T2 in the ER, as indicated by co-localization with the resident

ER protein calnexin (Fig. 4.13A, lower panel). A significant number of cells (~ 70%), however, additionally showed a diffuse staining that could be characteristic of either cytosolic or low-level cell surface distribution. In contrast, T3 co-localized almost perfectly with calnexin (> 95% of cells) (Fig. 4.13B). Untransfected cells were stained in parallel (Fig. 4.13C) to control for specificity and fluorescence bleed-through.

We conclude that targeting of T2 Shaker channel, truncated 26 amino acids after TM1, to the ER is significantly more efficient in cells than *in vitro*. We suggest that this emphasizes the pitfalls of relying exclusively on *in vitro* data to understand protein targeting and biogenesis. Nevertheless, some aspect of T2 biogenesis is likely to be compromised, relative to longer Shaker proteins.

4.3.3. Further experiments on EndoH-resistant T2 Shaker

First, PNGase treatment of Shaker T2 would show whether or not the high molecular weight form of T2 (#) is glycosylated. Depending on the outcome of this treatment, some of the following experiments would be more relevant than others. Second, pulse-chase experiments to compare the relative stability of the two constructs would indicate whether T2 is more quickly degraded than T3, and whether it is selectively the T2 high molecular weight material (#) that is unstable. Third, the effect of proteasome inhibitors on the ratio of ER-glycosylated T2 (o) to high molecular weight T2 (#) could indicate whether the proteasome is involved in the putative degradation process. Fourth, cell fractionation could determine whether the protein is membrane bound or soluble. Lastly, surface biotinylation could be used to determine whether there is measurable T2 on the plasma membrane.

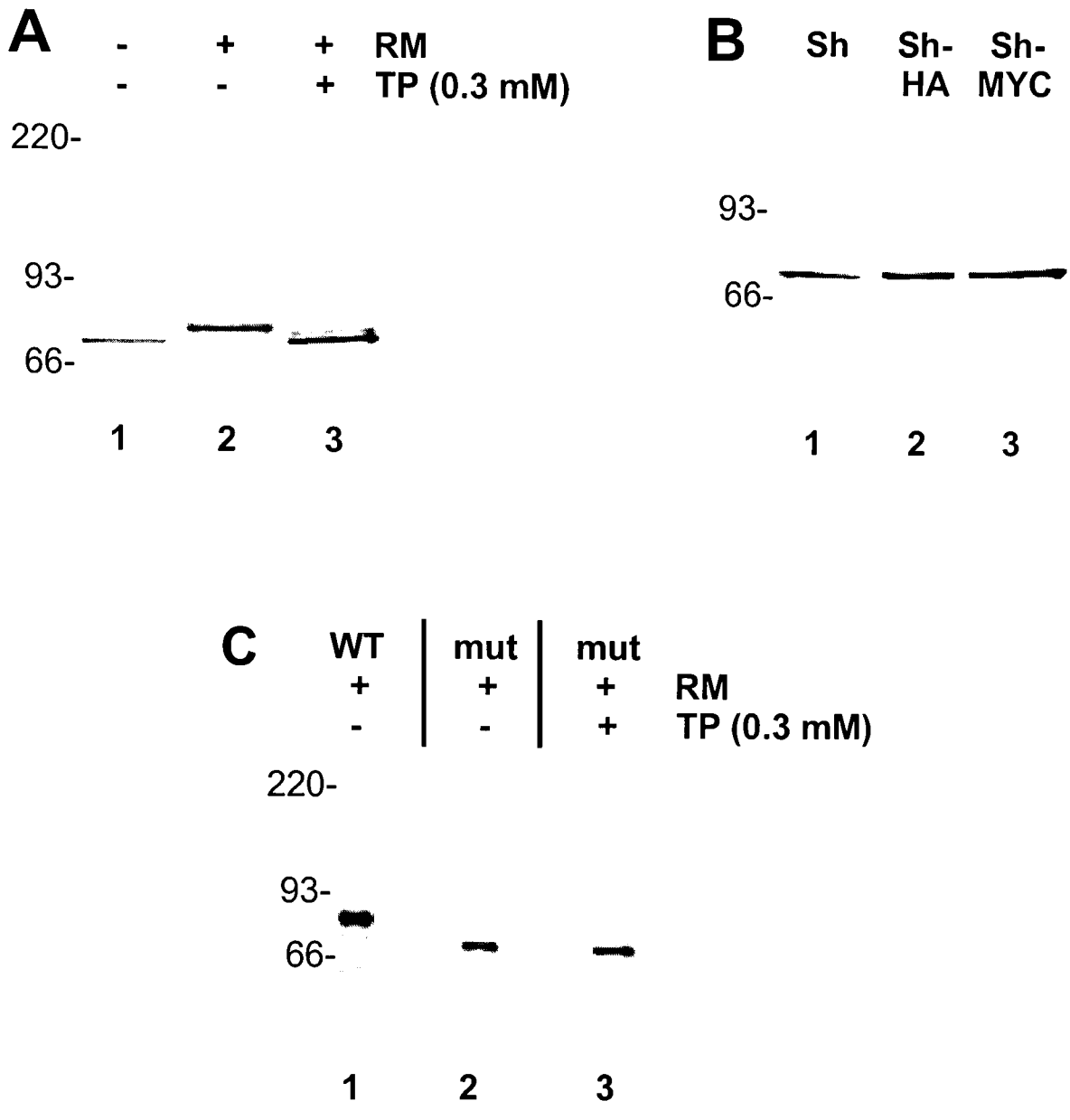

Figure 4.1 : Shaker channel translated in vitro. **(A)** Shaker was translated in RRL in the absence (1) or presence (2,3) of microsomes, with (3) or without (2)competitor tripeptide, separated by SDS-PAGE, and visualized by autoradiography. **(B)** Untagged or epitope-tagged Shaker was translated in the absence of microsomes and processed as above. **(C)** Wild type or N259Q+N263Q mutant Shaker was translated in RRL/microsomes -/+ competitor tripeptide and processed as above.

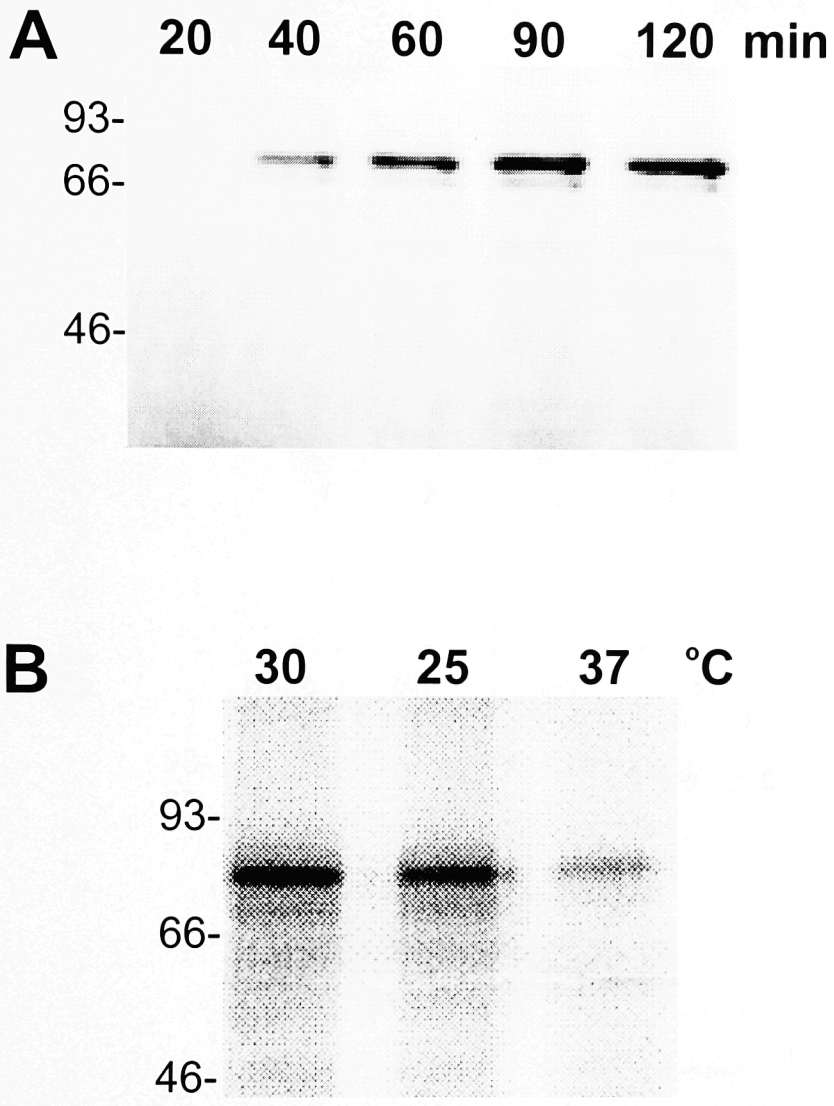

Figure 4.2 : Shaker translation conditions. (A) Shaker mRNA was translated in RRL/microsomes (30 °C) for various times, separated on SDS-PAGE (12%) and visualized by autoradiography. **(B)** Shaker mRNA was translated (90 min) at the indicated temperatures and processed as above.

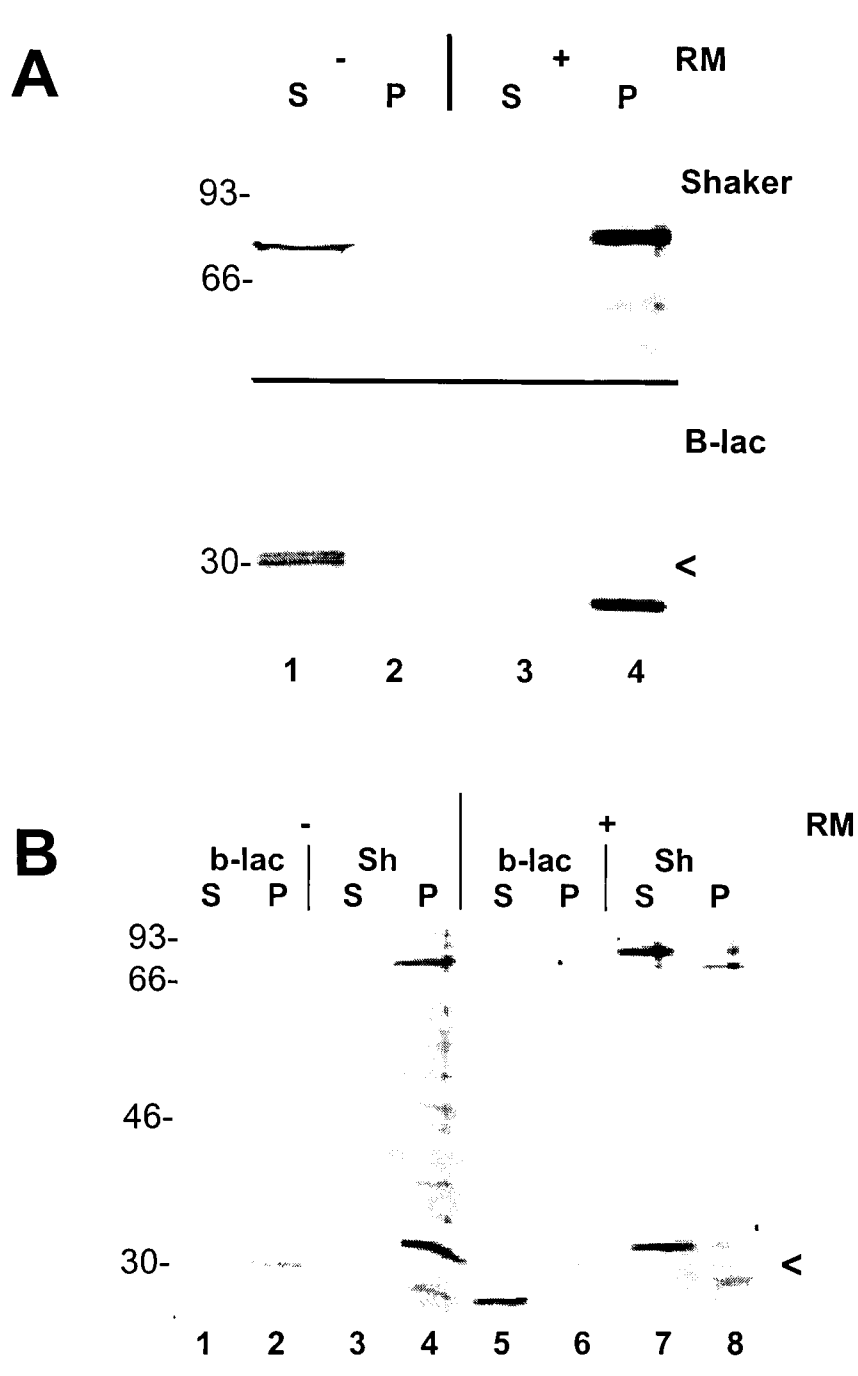

Figure 4.3 : Shaker targeting to ER microsomes. **(A)** Shaker (upper panel) or beta-lactamase (lower panel) was translated in RRL -/+ microsomes and sedimented through a 1.0M sucrose cushion. The untargeted material was in the supernatant (S) and the targeted material was in the pellet (P). **(B)** Translations as above were adjusted to 2.1M sucrose, layered at the bottom of a 0.25M/1.9M sucrose step gradient, and centrifuged. The untargeted material was in the pellet (P) and the targeted material was in the supernatant (S). Non-signal-cleaved beta-lactamase has been indicated in each case (<).

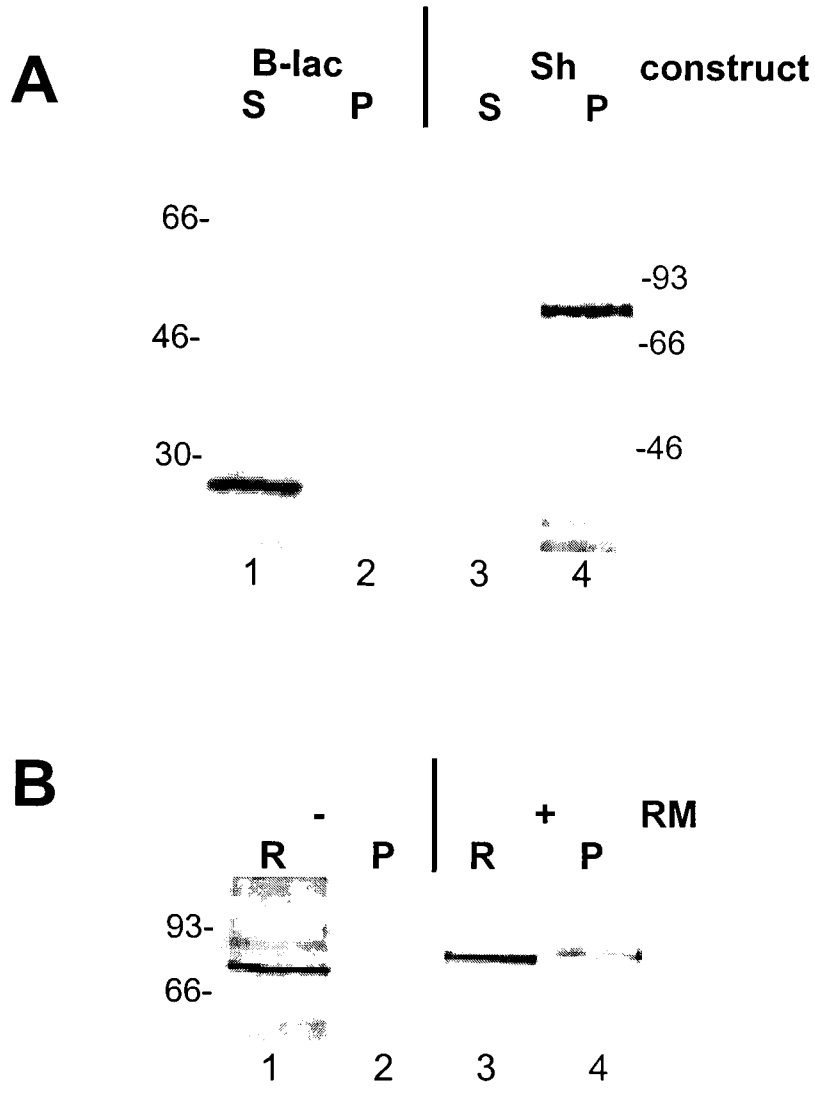

Figure 4.4 : Shaker integration into ER microsomes. **(A)** Shaker or beta-lactamase was translated in RRL/microsomes, the targeted material harvested by sedimentation, alkali-extracted (100 mM NaOH) and re-pelleted. The unextracted material was in the pellet (P) and the extracted material in the supernatant (S). **(B)** Shaker was translated with (lanes 3-4) or without (lanes 1-2) microsomes, and alkali extracted without a prior membrane harvest. Half the translation reaction was reserved (R) and is shown for comparison to the unextracted material (P), in each case.

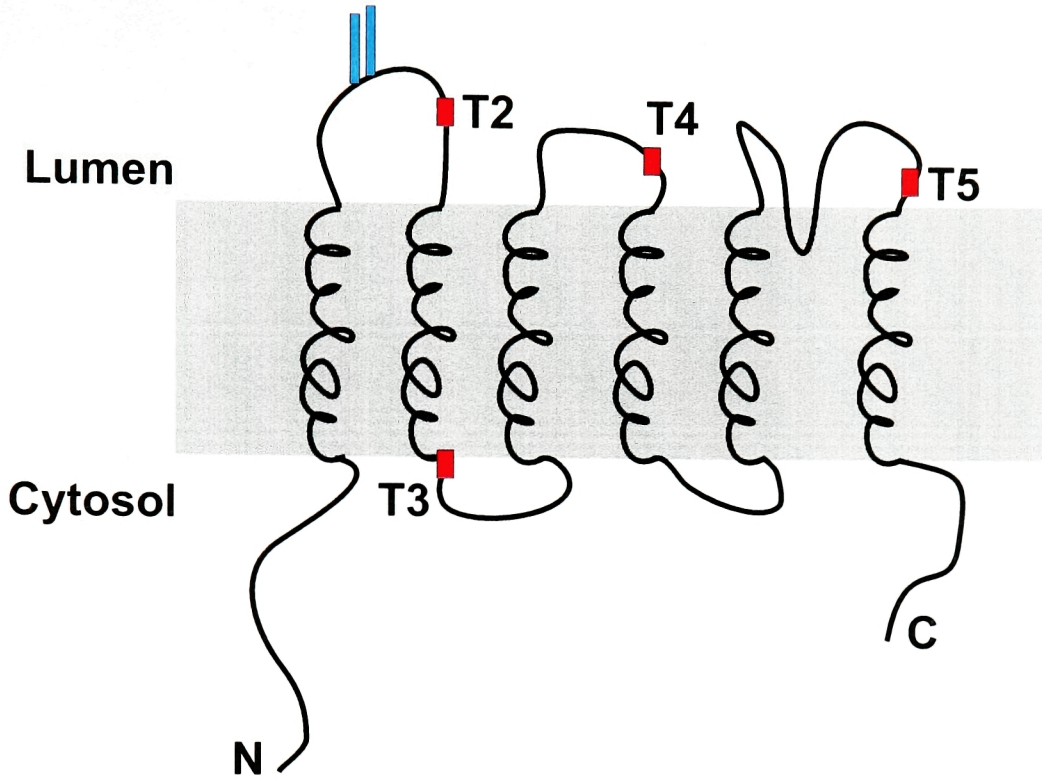

Construct	Amino acids	Position of stop
T2	272	Tm1 + 26
T2.1	286	Tm1 + 40
T3	299	Tm2 + 0
T3deltaTM	315	N.A.
T4	391	Tm4 - 4
T5	456	Tm6 - 0
Full length	656	Tm6 + 177

Figure 4.5 : Short constructs of the Shaker channel. The position of the stop codon is indicated as a red bar, in each case.

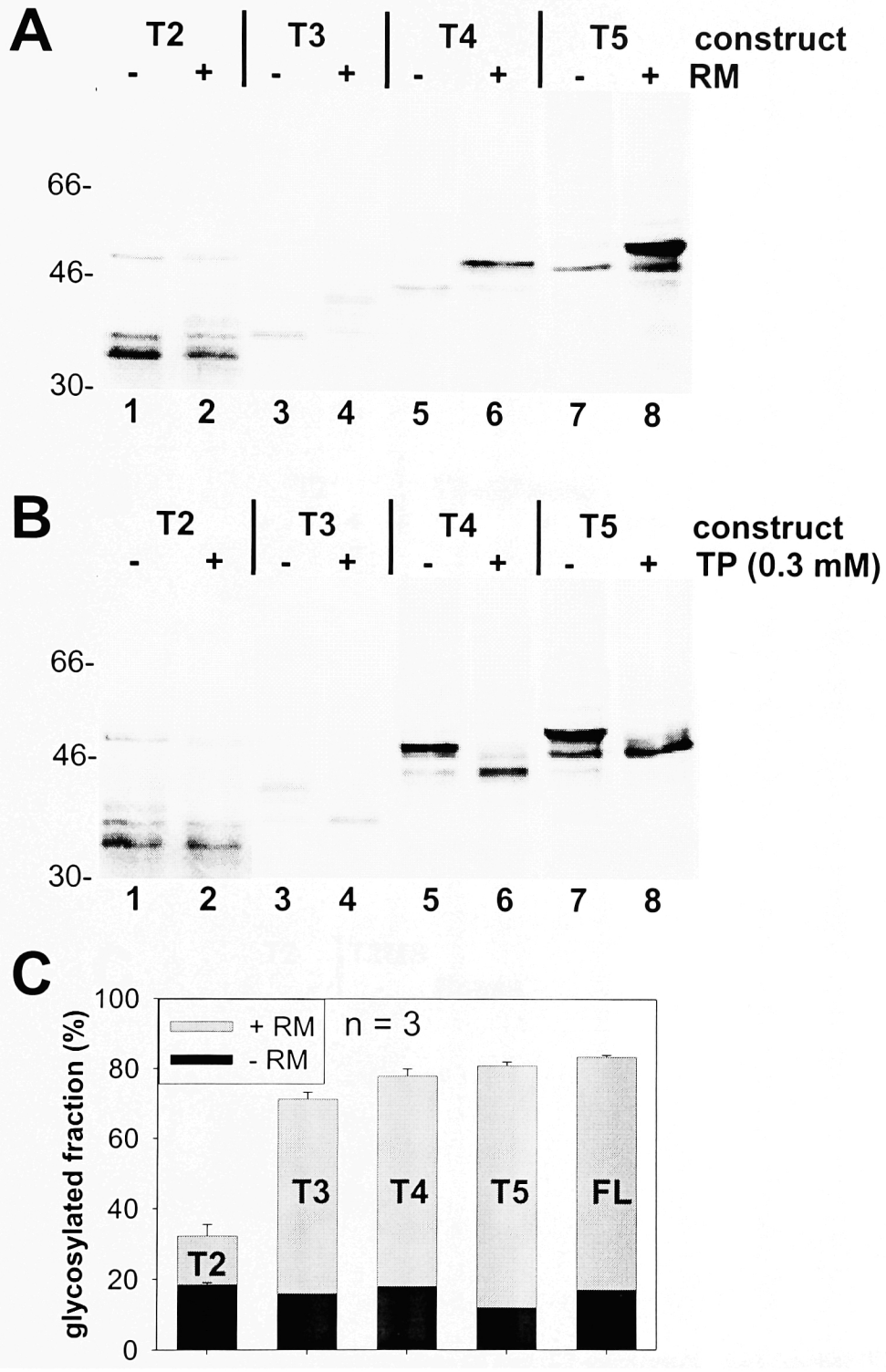

Figure 4.6 : Translation of Shaker short constructs. **(A)** Truncated Shaker was translated in RRL -/+ microsomes, separated by SDS-PAGE, and visualized by autoradiography. **(B)** Truncated Shaker was translated in RRL/microsomes -/+ competitor tripeptide and processed as above. **(C)** Band intensities on the gel were determined on a phosphorimager and the mean glycosylated fraction {G/(U+G)}*100 (n = 3) plotted for the indicated constructs. Data represents the mean +/- SEM.

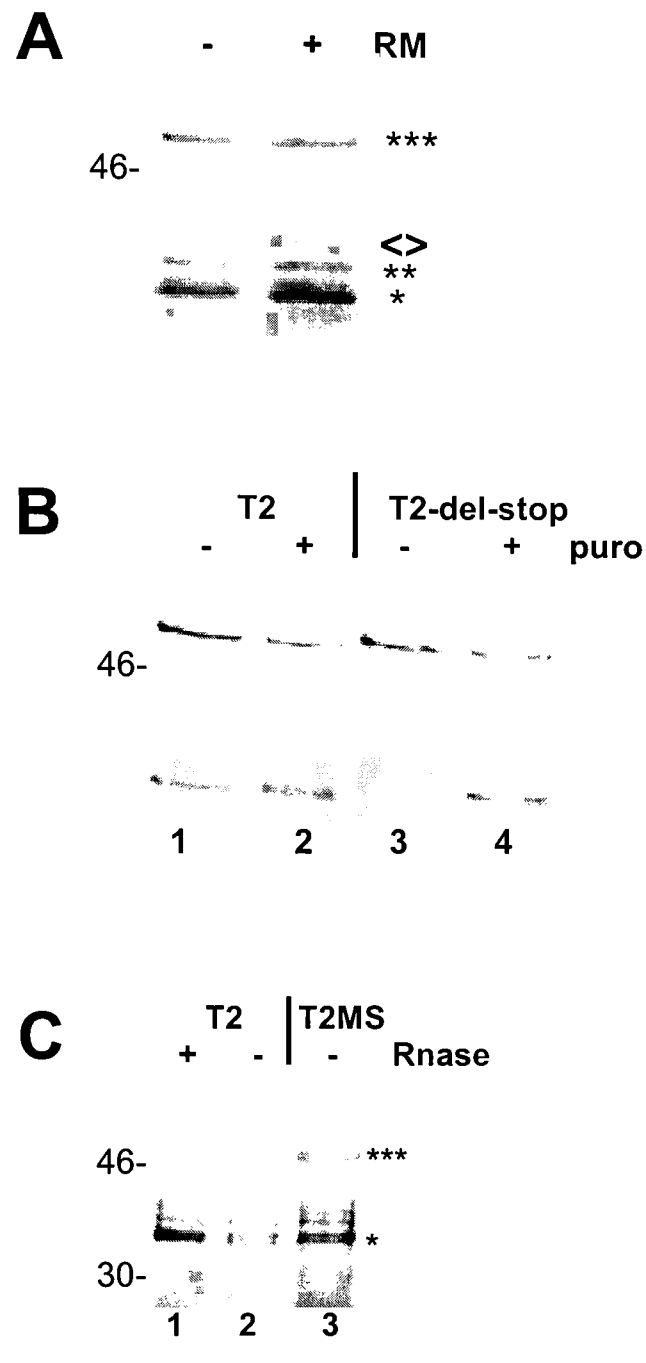

Figure 4.7 : Multiple bands upon translation of the T2 construct. **(A)** Shaker T2 was translated in RRL -/+ microsomes, separated by SDS-PAGE and visualized by autoradiography. **(B)** Shaker T2 mRNA with (lanes 1-2) or without (lanes 3-4) a stop codon was translated as above, treated with puromycin post-translationally, and then processed as above. **(C)** Shaker T2 mRNA with either a single stop codon or multiple stop codons was translated and processed as above. Where indicated, RNase was added post-translationally. The tRNA-attached (***), released-glycosylated (<>), released-unglycosylated (*) and unidentified (**) bands have been indicated.

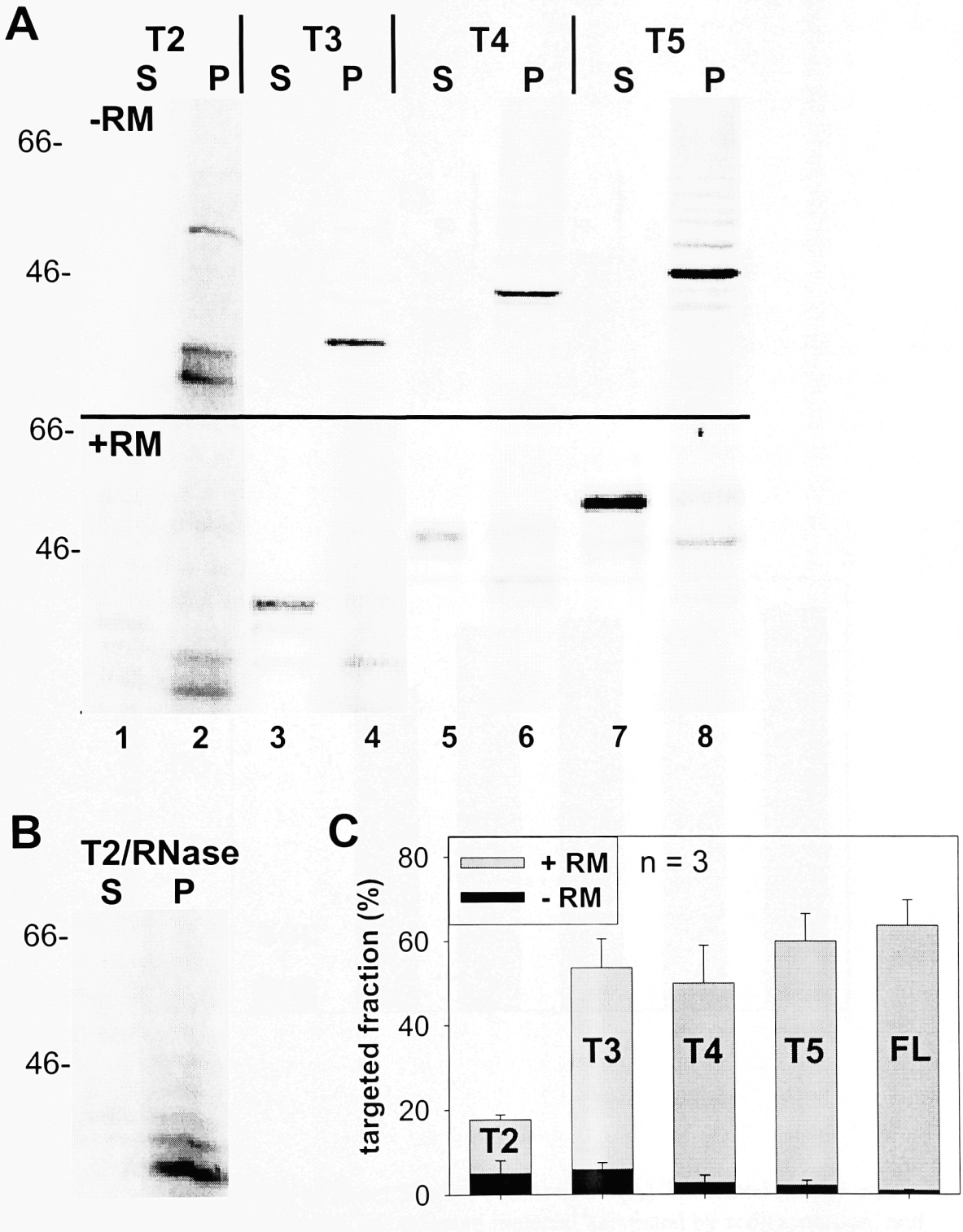

Figure 4.8 : Targeting of short Shaker constructs. **(A)** Truncated Shaker was translated in RRL without (upper panel) or with (lower panel) microsomes and the targeted material harvested by floatation. The targeted (S) and untargeted (P) fractions are shown. **(B)** Shaker T2 was translated and processed as above, except that the translation was treated with RNase prior to floatation. **(C)** Band intensities on the gel were determined on a phosphorimager and the targeted fraction {S/(S+P)}*100 was plotted. Data represents the mean +/- SEM (n=3).

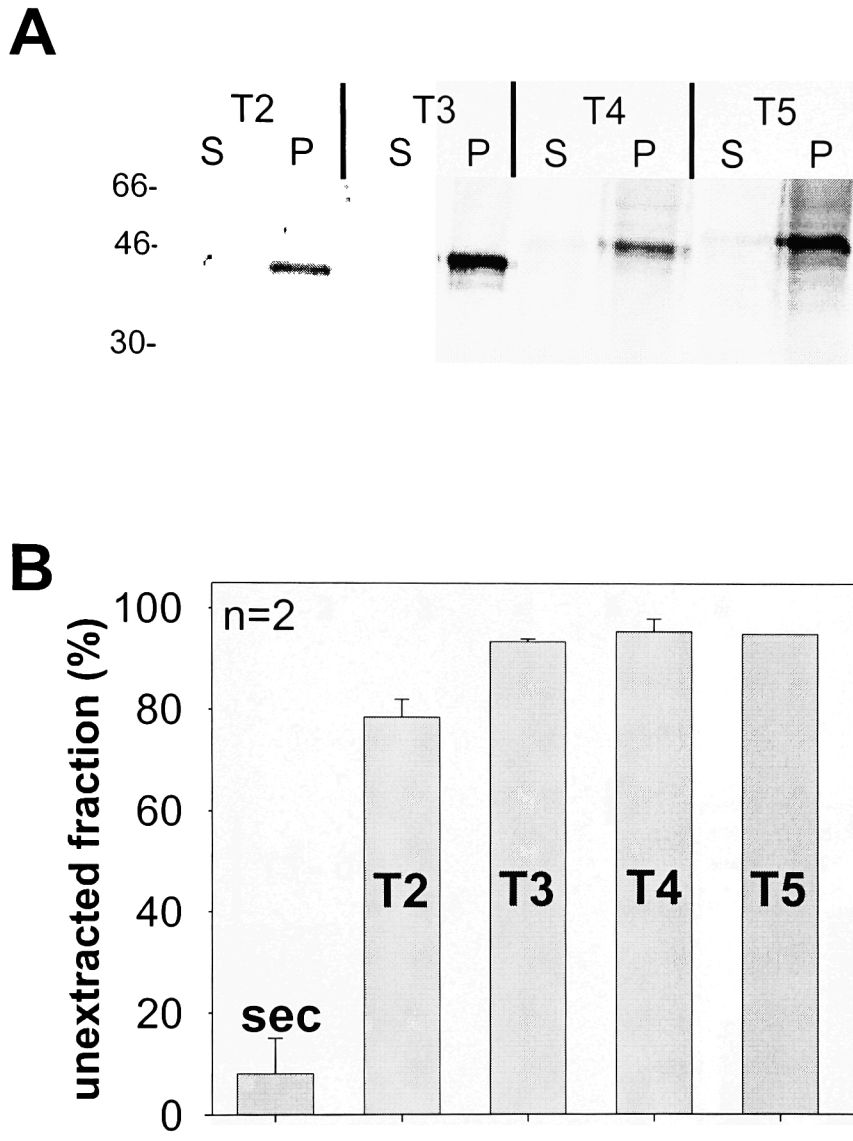

Figure 4.9 : Integration of short Shaker constructs. (A) Truncated Shaker was translated in RRL/microsomes, the targeted material harvested by sedimentation, and alkali-extracted (100 mM NaOH). The extracted (S) and unextracted (P) fractions are shown. **(B)** Band intensities were determined on a phosphorimager and the integrated fraction {P/(S+P)}*100 was plotted, for the indicated constructs. Data represents the mean +/-SEM (n = 2).

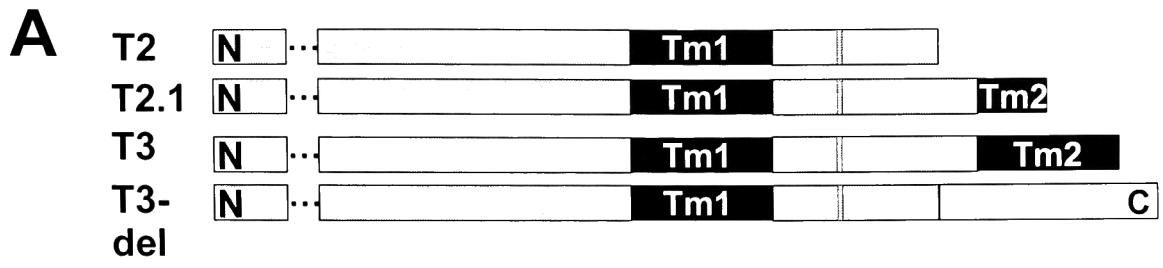

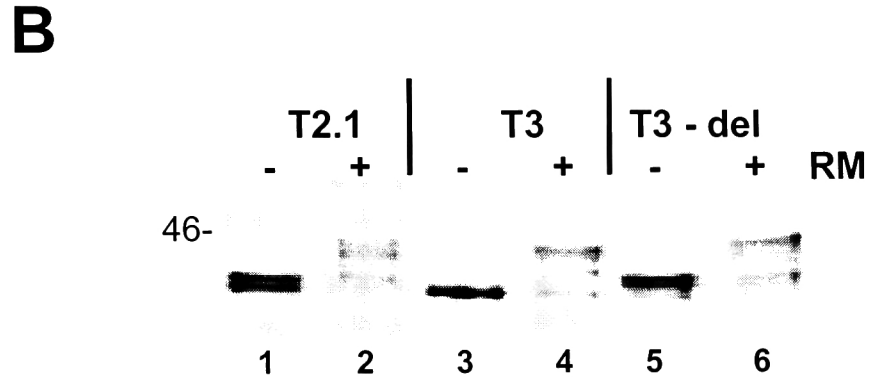

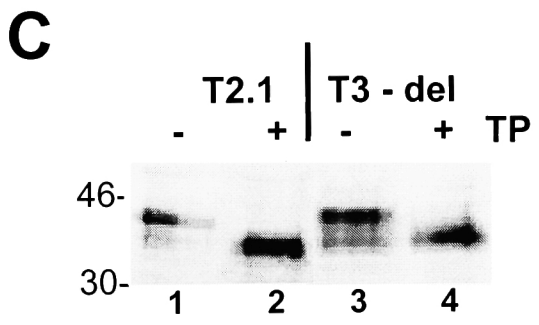

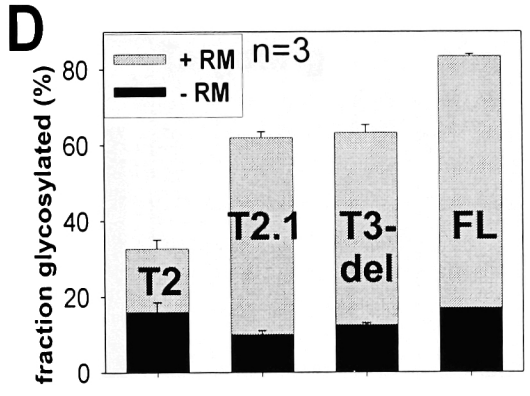

Figure 4.10 : Is TM1 sufficient for Shaker targeting ? **(A)** Design of the T2.1 and T3-del-TM2 constructs. **(B)** Truncated Shaker was translated in RRL -/+ microsomes, separated by SDS-PAGE and visualized by autoradiography. **(C)** Truncated Shaker was translated in RRL/microsomes -/+ competitor tripeptide and processed as above. **(D)** Band intensities were determined on a phosphorimager and the mean glycosylated fraction {G/(U+G)}*100 was plotted. Data represents the mean -/+ SEM (n=3).

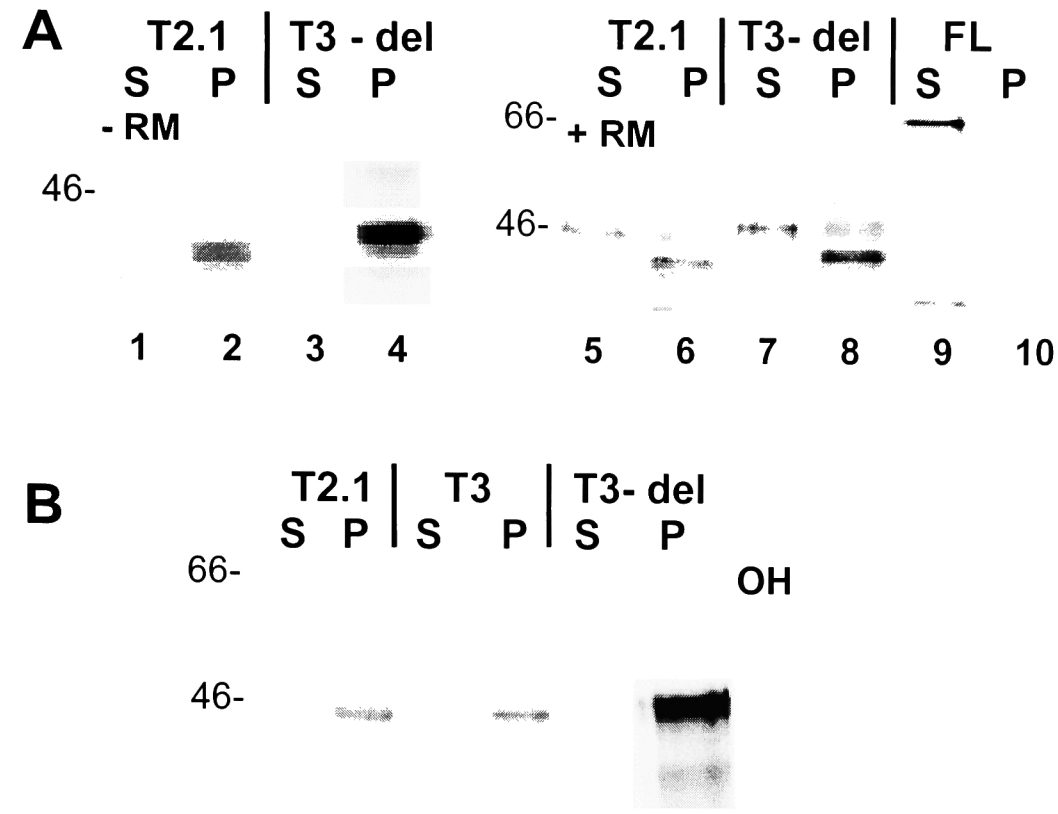

Figure 4.11 : Targeting and integration of T2.1 and T3-del-TM2. **(A)** Truncated Shaker was translated in RRL -/+ microsomes, and the targeted material harvested by membrane floatation. The targeted (S) and untargeted (P) fractions are shown. **(B)** Band intensities were determined on a phosphorimager and the targeted fraction {S/(S+P)}*100 was plotted. Data represents the mean +/-SEM (n = 3). **(C)** Translations as above were harvested by sedimentation and the targeted material was alkali-extracted (100 mM NaOH). The extracted (S) and unextracted (P) fractions are shown.

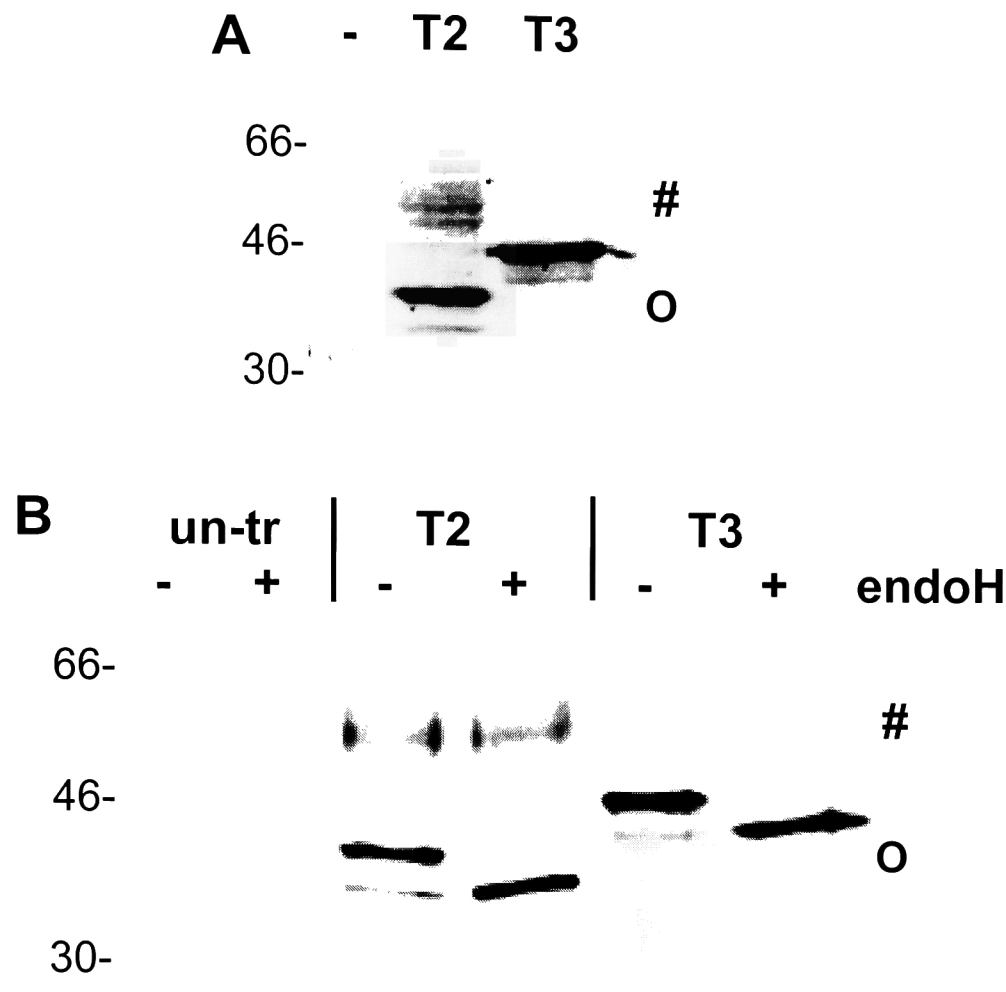

Figure 4.12 : Shaker short constructs expressed in COS-1 cells. COS cells transfected as indicated were lysed, and the lysates probed directly on an anti-HA Western blot **(A)** or subjected to anti-HA IP and endoH digestion prior to anti-HA Western blotting **(B).**

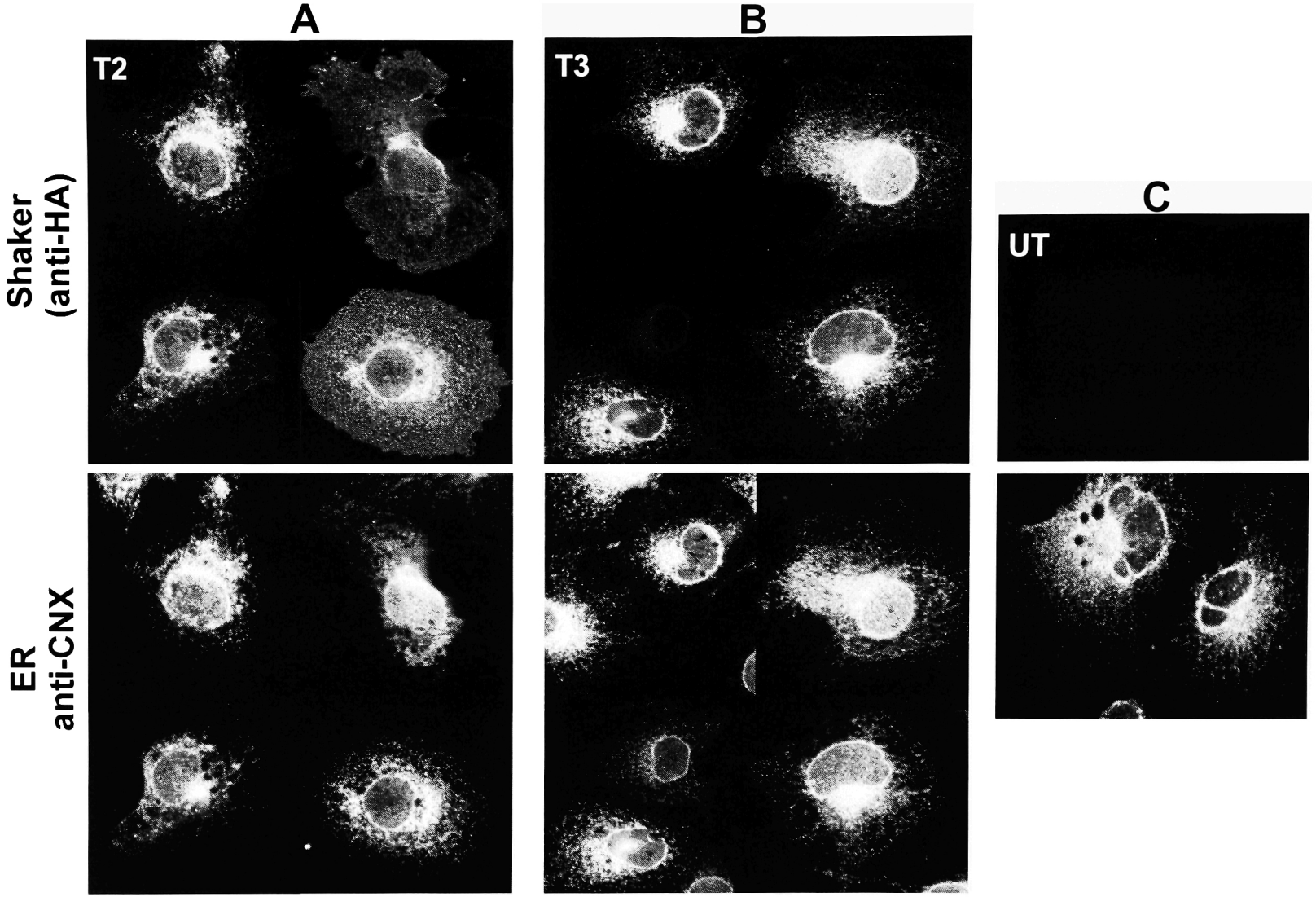

Figure 4.13 : Imaging of Shaker short constructs in transfected cells. T2-transfected **(A)**, T3-transfected **(B)**, or untransfected **(C)** COS-1 cells were fixed and stained for Shaker (anti-HA, upper panel) or for the ER (anti-CNX, lower panel). All panels are composites of more than one field.

5. BIOGENESIS OF THE SHAKER CHANNEL

Protein targeting to the endoplasmic reticulum (ER), translocation into the ER lumen, and integration into the ER membrane have been widely studied using established assays. A method that reports on folding/biogenesis of a particular membrane protein may arguably require a more 'tailor-made' approach. We are interested in the biogenesis of the tetrameric, multi-transmembrane (TM) domain Shaker channel. To this end, we attempted to develop a method that monitored Shaker folding in the ER, to apply this method to Shaker translated/translocated *in vitro*, and thus to begin to dissect out the ER factors that may be required for this process. Our attempt to develop a new assay for Shaker folding was unsuccessful. However, since Shaker biogenesis has been so sparingly examined, even established approaches can provide novel information. In this chapter, the following topics are presented.

1. Biogenesis (i.e. targeting, integration and assembly) of the Shaker channel in ER microsomes depleted of glycoproteins.
2. Biogenesis of unglycosylated Shaker channel.
3. Biogenesis of Shaker in ER microsomes depleted of lumenal proteins.
4. Shaker folding assay - attempts.

5.1. Assembly of *in vitro* translated Shaker

The methods used to assay Shaker targeting and integration were described previously (chapter 4). Assembly of the channel into homotetramers had not been monitored, for *in vitro* translated Shaker, prior to this work. We characterized the

migration of Shaker on sucrose density gradients. Whereas the small, secreted control protein β-lactamase (Fig. 5.1A, panel 1), and the monomeric membrane protein opsin (Fig. 5.1A, panel 2) migrated at the top of a 5 – 20 % sucrose gradient, Shaker migrated deeper into the gradient (Fig. 5.1A, panel 3), when solubilized in CHAPS. Relative signal intensities on the autoradiographs are shown below, normalized to peak signal, for each gradient (Fig. 5.1B). *In vitro* synthesized Shaker migrated indistinguishably, within experimental error, from channel expressed in mammalian cells (COS-1) (Fig. 5.1A, panel 4, Fig. 5.1C). Solubilization in Zwittergent, which is known to render the channel monomeric, shifted the Shaker peak to the top of the gradient (Fig. 5.1A, panel 5, Fig. 5.1C). Lastly, a comparison to size markers shows that the material in the light (i.e. Zwittergent) and heavy (i.e. CHAPS) peaks sediments roughly as predicted for monomeric and tetrameric forms of the channel. That Shaker migrates slightly smaller than theoretically expected was discussed previously (chapter 3). We conclude that in vitro-translated/translocated Shaker channel assembles into tetramers. Unless otherwise mentioned, all subsequent sedimentations were done on channel solubilized in CHAPS.

Two peripheral observations were made. First, the secreted protein preprolactin (ppl), perhaps the most commonly used reporter for *in vitro* translocation studies, was repeatedly seen to smear throughout a 5 – 20 % gradient, indicating aggregation (Fig. 5.2A). This has previously been reported (Haynes et al., 1997), and is presumably an aberration of the *in vitro* system. Second, different preparations of ER microsomes showed varying abilities to promote Shaker tetramerization. Shaker was translocated separately into two canine microsomal preparations indistinguishable in both targeting and integration efficiency (not shown). The channel was then sedimented on parallel

sucrose gradients. In one case, a normal tetramer peak was seen (Fig. 5.2B, RM1, upper panel); in the other, the channel was predominantly aggregated (Fig. 5.2B, RM2, lower panel). In all subsequent studies, care was taken to begin with tetramerization-competent microsomal preparations, and to always use the 'parent' preparation as a standard for comparison with subsequently modified membranes.

5.2. Shaker biogenesis in glycoprotein-depleted microsomes

5.2.1. Rationale for glycoprotein depletion

The three protein components of the mammalian translocon (sec 61α, β and γ) as well as the signal recognition peptide (SRP) receptor α and β subunits are thought to be required for the translocation and integration of all proteins. The translocon-associated membrane protein (TRAM) is a glycosylated ER protein that can be cross-linked to secretory and transmembrane nascent chains as they traverse the bilayer (Do et al., 1996). A functional significance of TRAM-translocon-nascent chain proximity, however, remains to be established. Lectin affinity chromatography may be used to deplete ER microsomes of glycoproteins, including TRAM, leaving behind the non-glycosylated core components of the translocation machinery (i.e. the sec 61 complex and the SRP receptor) (Hegde et al., 1998). We compared Shaker targeting, integration and assembly in 'parent' porcine microsomes (RM), concanavalin A-depleted microsomes (cRMs), mock-depleted microsomes (rRMs) and conA-depleted microsomes reconstituted with purified TRAM (cRM+). All membranes were prepared by R. Hegde (NIH).

5.2.2. A possible role for TRAM in Shaker biogenesis

The targeting efficiency of Shaker was significantly reduced in glycoprotein-depleted cRMs compared to untreated porcine RMs (Fig. 5.3A, B). However, the mock-depleted rRMs showed similarly low targeting levels and reconstitution of the cRMs with TRAM had no amelioratory effect. In contrast, the fraction of Shaker stably integrated into the bilayer was significantly reduced in cRMs, compared to untreated RMs ($P = 0.01$, Student's t-test), but not in mock depleted rRMs (Fig. 5.3 C, D). Three independent preparations of cRMs that had been reconstituted with TRAM were reproducibly seen to support Shaker integration at control levels. Possibly, TRAM plays a role in the efficient integration of Shaker, and perhaps of other membrane proteins, into the bilayer. A secretory control is also shown (Fig. 5.3C, lanes 9–10).

Lastly, assembly of Shaker prepared in different microsomes was compared by sucrose gradient centrifugation. Shaker translocated into the glycoprotein-depleted cRMs migrated aberrantly. However, sedimentation of Shaker prepared in control rRMs was equally perturbed, thus absolving TRAM in the effect. In either case, the channel showed no clear peak, but smeared through the denser part of the gradient (Fig. 5.4A).

Apart from their effect on Shaker assembly, the rRMs and the cRMs showed two obvious deficiencies, both of which are predictable consequences of solubilization and reconstitution. First, the membranes did not glycosylate, as is clearly seen with a control protein, preproαfactor (Fig. 5.4B). Translation in the presence of untreated RMs resulted in the appearance of a 30 kD glycosylated band (*) in the targeted fraction (Fig. 5.4B, lane 2), whereas rRMs (Fig. 5.4B, lane 6) or cRMs (Fig. 5.4B, lane 4) generated no glycosylated band in the targeted fraction. Second, the rRMs and cRMs would be

predicted to have lost much of their lumenal protein content through dilution upon solubilization. Indeed, Western blots against the ER lumenal chaperone protein disulfide isomerase (PDI, Fig. 5.4C, lower panel) showed that it is present at 5 to 10-fold lower levels than in untreated microsomes, when equivalent amounts of membrane were compared. As one might expect, the membrane protein calnexin (CNX, Fig. 5.4C, upper panel) was not significantly depleted in the rRMs and cRMs. It is plausible that either the failure to glycosylate or the loss of lumenal chaperones or both resulted in aberrant migration of Shaker on sucrose gradients. However, it is equally possible that a third factor (or even several factors) were perturbed in the solubilized microsomes and contributed to the effect on the channel. Nevertheless, we mimicked the two obvious deficiencies in rRMs and cRMs by independent methods, and examined the sedimentation of *in vitro*-translated Shaker under these conditions.

5.3. Biogenesis of unglycosylated Shaker channel

Glycosylation was blocked by treatment with a competitor tripeptide (Fig. 5.5A) or by using the N259Q+N263Q mutant channel (Fig. 5.5B), in which both glycosylated asparagines have been mutated to glutamine. Neither treatment had an effect on Shaker targeting (Fig. 5.5C). Further, the N259Q+N263Q mutant integrated efficiently compared to a secretory control (Fig. 5.5D), and at levels comparable to wild type. Neither tripeptide-treated channel (Fig. 5.6A) nor unglycosylated mutant channel (Fig. 5.6B) migrated differently from wild type on a sucrose gradient. For the N259Q+N263Q mutant channel, this was tested for channel prepared *in vitro* (Fig. 5.6B) as well as for pulse-labeled channel expressed in COS cells (Fig. 5.6C). In the case of tripeptide-treated Shaker (Fig. 5.6A), separate Shaker translations with or without tripeptide were

mixed post-solubilization, and then sedimented on the same gradient. The results were very similar if the material was sedimented separately. An experiment to control for post-solubilization subunit assembly is shown later in this chapter.

5.4. Shaker biogenesis in RM depleted for lumenal proteins

5.4.1. Preparation of depleted microsomes

A brief alkali treatment (pH 9.5) of rough microsomes (RM) has been shown to selectively remove ER lumenal proteins (Nicchitta and Blobel, 1993). Depletion may also be effected by treatment with the detergent saponin, followed by repeated washing (Bulleid and Freedman, 1990). Since saponin is reversible, this results in a re-sealing of the microsomal membrane around a significantly depleted lumen. We prepared depleted microsomes by both methods. Western blots against a lumenal marker (PDI) and a membrane marker (CNX) showed that lumenal protein levels were reduced to <5% of that in the starting material in saponin-extracted microsomes, while membrane proteins remained at similar levels (Fig. 5.7A). This was also true for alkali-extracted membranes. Curiously, porcine microsomes were reproducibly recalcitrant to alkaline "wash-out" (Fig. 5.7B, lanes 1-3), as a result of which we switched to canine membranes (Fig. 5.7B, lanes 4-6) for all subsequent experiments. Further satisfying evidence for lumenal protein depletion was the apparent loss of lumenal ER-glucosidase II activity, but not membrane-bound ER glucosidase I activity, in depleted microsomes. This was manifest in the size difference and castanospermine-induced gel shift of ppαf translocated into depleted microsomes, relative to control (not shown).

5.4.2. Shaker biogenesis in the absence of lumenal proteins

Shaker targeting was tested by membrane sedimentation and was found to be slightly reduced by both alkali washout (Fig. 5.8A, lanes 1-4; B) and saponin extraction (Fig. 5.8 A, lanes 5-8; B). Shaker integration was tested by hydroxide extraction and was found to be unaffected in both preparations of depleted microsomes (Fig. 5.8C, D). Initial assessments of Shaker assembly showed significant tendencies, in both depleted preparations, towards channel aggregation (Fig. 5.9). Some increase in high molecular weight material was also seen for opsin in depleted microsomes (Fig 5.10A), but this material was mostly the unglycosylated protein (<), which preferentially pellets in control membranes as well, and which was quite substantially increased in depleted membranes. The effects on Shaker sedimentation proved difficult to reproduce, in part because lumenal depletion increased the variability of the sedimentation. However, we could not completely rule out that increased variability was due to technical problems.

Co-sedimentation (i.e. sedimentation on the same gradient) of differentially epitope-tagged channels, followed by immunoprecipitation of the gradient fractions with different antibodies, significantly improved the reproducibility of our centrifugation experiments. We compared Sh-HA and Sh-MYC that had been translocated into different microsomes, solubilized in CHAPS, and then mixed prior to centrifugation on the same gradient. To control for hetero-oligomerization in the gradient, we attempted to co-immunoprecipitate Sh-HA and Sh-MYC from post-translationally mixed CHAPS lysates. The signal from *in vitro* translated protein on Western blots was quite low, and although no co-immunoprecipitation was seen above background, we were concerned that we were too close to the detection limit. Indeed, even co-translated channels were

seen to co-IP only marginally above background, if at all. Therefore, we compared co-IP of Sh-HA and Sh-MYC either co-expressed in COS cells, or expressed separately, solubilized in CHAPS, and then mixed post-lysis. Co-expressed Sh-HA and Sh-MYC channels showed significant co-IP (Fig. 5.10B, lane 6), while channels mixed post-lysis did not (Fig. 5.10B, lane 4).

The results of a co-sedimentation experiment, with three pair-wise combinations of Sh-MYC/ Sh-HA translocated into A) control/control, B) control/alkali washed-out, or C) control/saponin-extracted microsomes, are shown (Fig. 5.11A-C). There was no detectable signal on lanes 1 – 4, for all gradients; only lanes 5 – 16 have been shown on the gels. It is additionally informative to compare the three parallel control sedimentations (Sh-MYC, in this case)(Fig. 5.12A & C) with the three parallel "test" sedimentations (Sh-HA, in this case)(Fig. 5.12B & D). This has been shown for two independent experiments. The effects of lumenal depletion by either method on Shaker sedimentation are not dramatic. Nevertheless, the relatively good reproducibility of the control gradients makes possible a conservative interpretation of the data. Treatment with alkali or saponin results in greater variability in channel sedimentation, with the trend being towards species that sediment heavier than the tetramer peak. We were not able to reconstitute lumenal proteins to a high enough level to establish conclusively that the effect on Shaker is indeed causally related to the loss of lumenal chaperones in the depleted microsomes. Further, the aberrant sedimentation in depleted microsomes is far less drastic than in the original rRMs and cRMs, relative to control. Thus it is likely that loss of lumenal chaperones alone was not the cause of Shaker aggregation in the rRMs and cRMs.

5.5. Shaker folding assays – attempts

5.5.1. Oxidation of cytosolic cysteines

Oxidative inter-subunit crosslinking of cytosolic cysteines (C96 and C505) has been shown to occur for Shaker channel expressed in oocytes or tissue culture cells, upon treatment with oxidising agents such as iodine (Schulteis et al., 1996). Putative folding mutants of Shaker lose the ability to form these cross-links, suggesting that proximity of C96 and C505 on adjacent subunits may be useful as an experimentally tractable hallmark of channel folding. We attempted oxidative cross-linking of Shaker translated *in vitro*. Oxidation resulted in the formation of DTT-sensitive aggregates, which for the most part did not enter a non-reducing polyacrylamide gel (Fig. 5.13A). Similarly, attempts at using a homobifunctional cysteine-directed crosslinker (DSP) resulted in aggregated channel (not shown). Lastly, we manipulated the redox conditions of the translation reaction using various ratios of reduced and oxidized glutathione (GSH/GSSG), in an effort to promote disulfide bond formation without the addition of an exogenous cross linker (not shown). This was based on the observation that Shaker expressed in cells also forms disulfides between C96 and C505 if the cells are lysed in the absence of a reducing agent or a protecting group (such as a maleimide or acetamide). Although initial results were promising, disulfide bond formation proved too variable to be a useful folding assay in the *in vitro* system.

5.5.2. Native gel electrophoresis

This approach has been successfully used to examine the assembly of other oligomeric membrane proteins (Tu and Deutsch, 1999). Under most conditions, *in vitro*

translated Shaker channel was aggregated and did not enter the gel (Fig. 5.13B, lane 1). Under conditions in which it did not aggregate, the Shaker channel ran either as a monomer (Fig. 5.13B, lane 2) or as two bands (Fig. 5.13B, lane 3) on a 6 % native gel. In the latter case, the predominant band was also the ~75 kD monomer. The second band migrated at ~ 220 kD, and accounted for 10% of the total signal, at best. We examined translations done for varying lengths of time (1 – 21 hours), and solubilized under several conditions (4 - 42°C; 1 hour to overnight). We were unable to find conditions under which the 200 - 220 kD band was generated at higher levels, in the absence of channel aggregation.

5.5.3. Agitoxin binding

The peptide agitoxin binds with high affinity to the extracellular face of the Shaker pore, at a stoichiometry of one peptide molecule per Shaker tetramer. Single amino acid changes at the toxin-channel binding interface can disrupt this interaction. We reasoned that high affinity binding of agitoxin to the Shaker channel could be considered evidence for a folded channel pore. We asked whether or not the toxin binds to Shaker translated *in vitro* and translocated into ER microsomes. We prepared radiolabeled agitoxin by conjugation of ^{3}H-N-ethyl maleimide to D20C mutant agitoxin according to (Aggarwal and MacKinnon, 1996). This was previously shown to be compatible with toxin binding to the Shaker channel. Agitoxin D20C dimerizes via an inter-molecular disulfide bond at cysteine20. In addition, the toxin bears three native intra-molecular disulfide bonds. Labeling of cysteine20 requires reduction of the toxin, and depends upon the more rapid formation of the intra-molecular bonds, relative to the inter-molecular bond, upon removal of the reducing agent.

His6-tagged agitoxin2 D20C was expressed in bacteria as a fusion protein, and purified by nickel column chromatography, cation exchange FPLC and reversed-phase HPLC (Fig. 5.14A-C). The dimer had a characteristic retention time of ~75 minutes on RP-HPLC under the conditions used (Fig. 5.14C). The chromatogram shown (Fig. 5.14C) is the final purification step. Material in the indicated peak (AgTx dimer) was collected, concentrated and quantified. Reduction with DTT generated monomeric toxin, which shifted to a retention time of 45 minutes under the same HPLC conditions (Fig. 5.14D). Upon reaction with ^{3}H-N-ethyl maleimide, the peak was delayed by 1-2 minutes (Fig. 5.14E). In the absence of NEM, the toxin re-dimerized upon removal of the reducing agent, and the 75' peak reappeared (not shown). The identity of the toxin dimer and cold NEM-labeled monomer was confirmed by MALDI-TOF mass spectrometry (Rockefeller University Protein Resource Center). Agitoxin was tritiated at a specific activity that ranged from 10-25 Ci/mmole, for different preparations.

In a filter-binding assay, ^{3}H-agitoxin D20C gave no signal when bound to Shaker channel translated *in vitro* and translocated into ER microsomes (Fig. 5.15A). Shaker-HA was indeed translated, as verified by a Western blot on an aliquot of the material used for toxin binding (Fig. 5.15B). The toxin was active, since it bound specifically to a membrane preparation from bacteria expressing the bacterial KcsA channel. Since the agitoxin binding site of Shaker is topologically extracellular, and therefore in the lumen of ER microsomes, binding to *in vitro* translated channel was done in the presence of the detergent saponin. In a separate experiment, we verified that saponin treatment does not inhibit toxin binding to bacterial KcsA membranes (not shown). Binding assays on in vitro translated Shaker that had been solubilized in (one of) various detergents and

immobilized on beads via the C-terminal epitope tag were also negative (not shown). We cannot rule out that there was insufficient protein synthesized *in vitro* to generate a detectable signal. We were additionally interested in whether or not the toxin binds to immature Shaker channel (i.e. the ER form of the channel) in cells. In binding assays on intact and saponin-permeabilized cells, the signal was again at insufficient levels to justify interpretation (not shown). Possibly the expression system yielded inadequate levels of folded Shaker.

In an alternative approach, we prepared biotinylated agitoxin D20C. This was intended as an affinity precipitation reagent, in order to determine the fraction of *in vitro*-translated Shaker, or of immature cellular Shaker, which has a "folded" pore region. We labeled reduced D20C toxin with biotin-PEO-maleimide. This resulted in significant diminution of the monomer peak (45', fig. 5.16A) on RP-HPLC. Two new peaks appeared, with retention times of 53' and 54' (Fig. 5.16B). The two major earlier eluting peaks (at ~30') contain no peptide, and most likely represent excess labeling reagent. Material from peaks 53 and 54 was collected, run on a 20% Tricine gel, and either silver stained (Fig. 5.16C) or transferred to nitrocellulose and probed for biotin (Fig. 5.16D). Both peaks contained biotinylated material that migrated at the appropriate size for monomeric toxin. MALDI-TOF mass spectrometry indicated that both peaks contained material consistent with monomeric agitoxin labeled with a single biotin-PEO-maleimide. Lastly, preliminary two-electrode voltage clamp measurements on Shaker expressed in Xenopus oocytes indicated that both peaks contained material that reversibly blocked the channel (data not shown).

The nature of the difference between the material in peaks 53 and 54 is not clear. Due to the poor resolution in our current preparations, it is possible that there is cross-contamination between them, and that some or all of the above properties (i.e. a single biotin-PEO-maleimide, blocking activity) are characteristic of one, but not both, peaks. Specifically, peak 53 is reproducibly more abundant, and has probably contaminated peak 54. Clarifying this issue would require efforts to resolve the two peaks on HPLC for preparation of pure material. We did not pursue this line of work, because of time pressure. Affinity precipitation with biotinylated agitoxin may be a viable future avenue to study folding of the Shaker pore either *in vitro* or *in vivo*.

Attempts to conjugate fluorescent molecules (FITC, rhodamine, Alexa 488 and Alexa 594) to D20C agitoxin were unsuccessful. Efforts to use unlabeled agitoxin to compete with methanethiosulfonate reagent biotinylation of an engineered cysteine in the Shaker pore (T449C) were also unsuccessful.

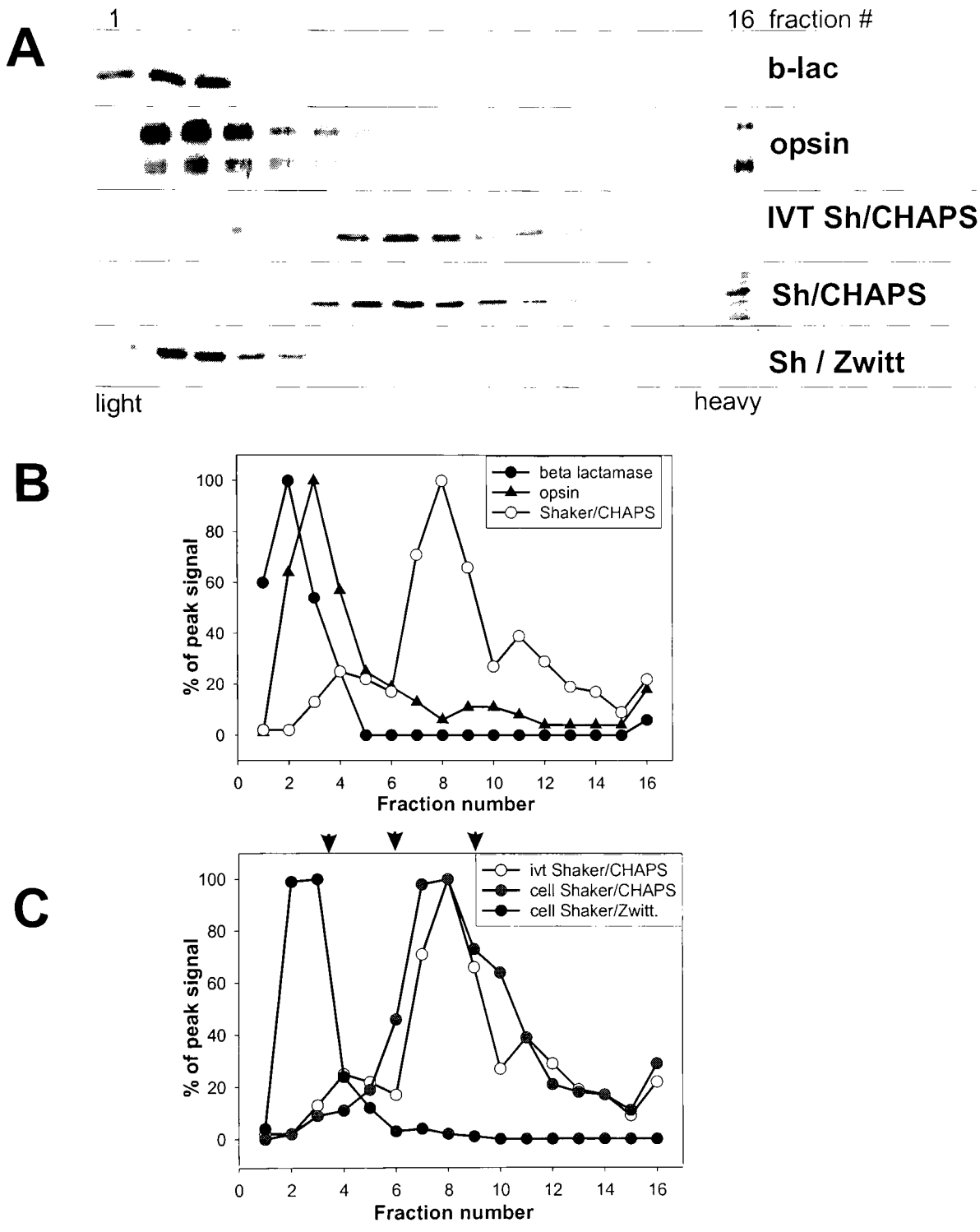

Figure 5.1 : Sucrose gradient centrifugation of Shaker. (A) β-lactamase, opsin or Shaker mRNA was translated in RRL/dog microsomes, harvested by sedimentation, solubilized and centrifuged on a 5 – 20 % continuous sucrose gradient. CHAPS or Zwittergent lysates of transfected and pulse-labeled COS cells were centrifuged as above. **(B) & (C)** The signal intensity in each fraction was determined on a phophorimager and plotted. For a given gradient, the signal in each fraction was normalized to the signal in the peak fraction (set as 100 %).

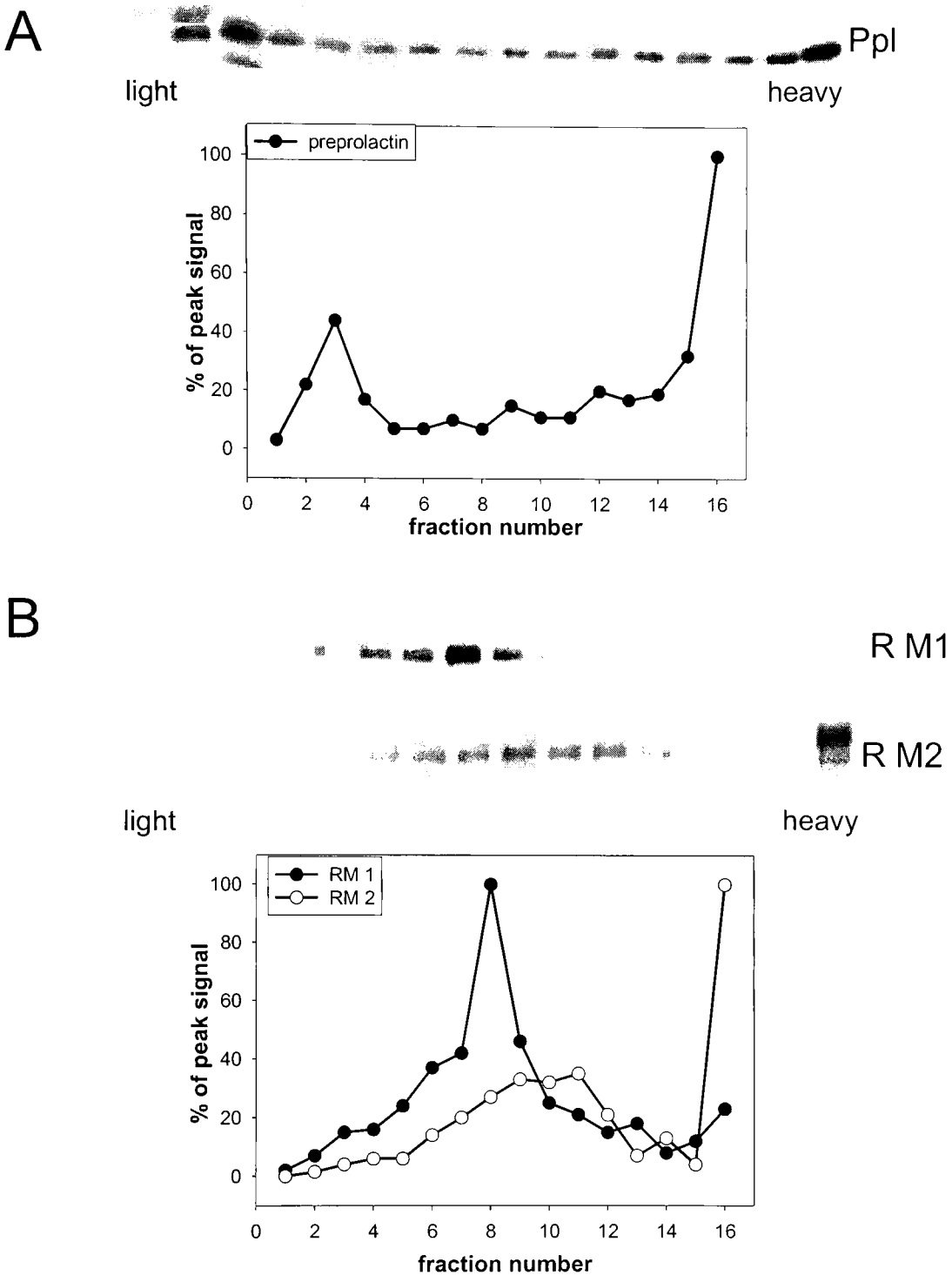

Figure 5.2 : Sucrose gradient centrifugation – peripheral observations. (A) Pre-prolactin mRNA was translated in RRL/dog microsomes, harvested by sedimentation, solubilized and centrifuged on a 5 – 20 % continuous sucrose gradient. The signal intensity in each fraction was determined on a phosphorimager and plotted. The signal in each fraction was normalized to the signal in the peak fraction (set as 100 %). **(B)** Shaker mRNA was translated in RRL, translocated into two different batches of dog microsomes and further processed as above.

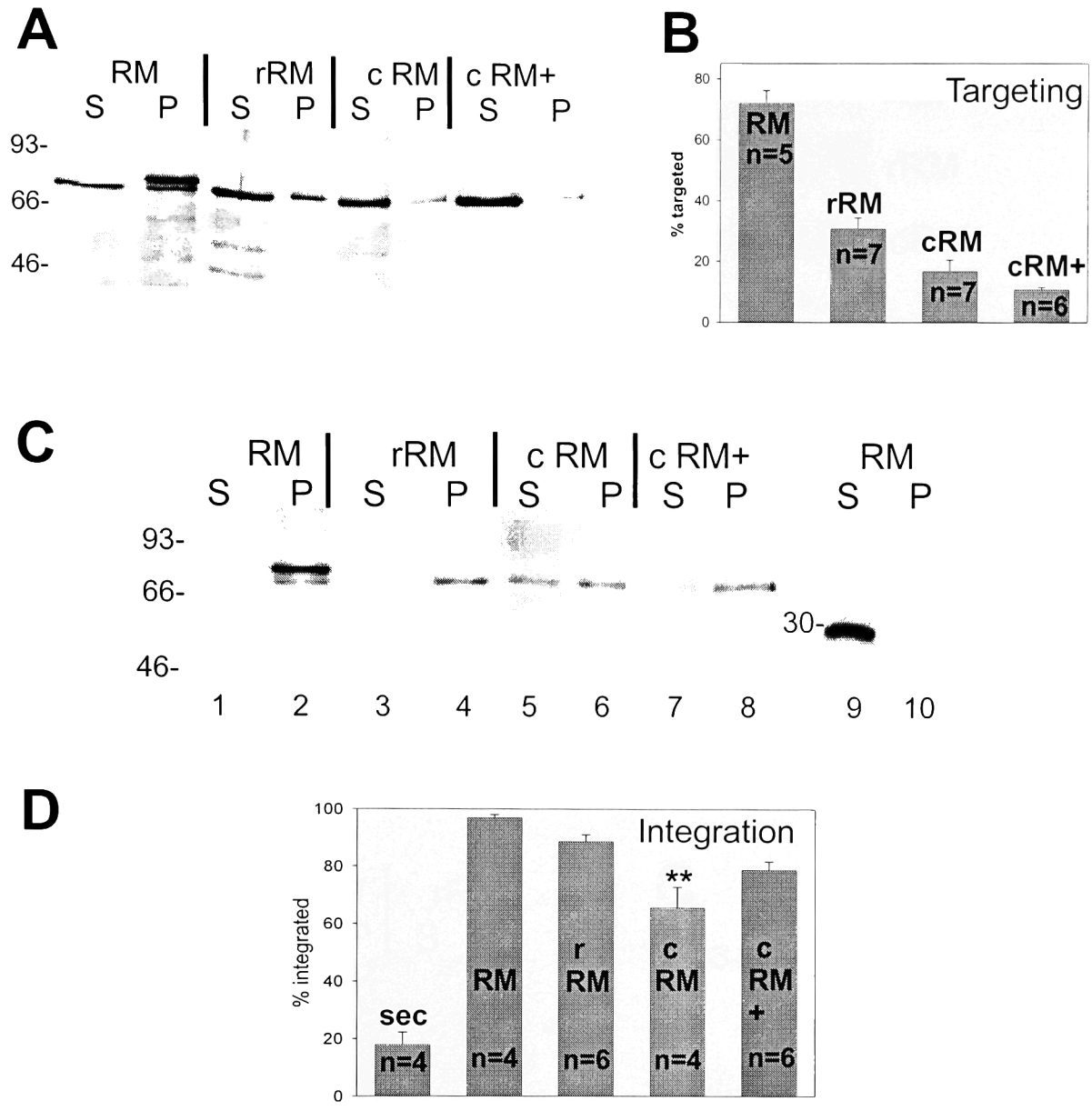

Figure 5.3 : Shaker targeting and integration in glycoprotein-depleted microsomes. **(A)** Shaker mRNA was translated in RRL with untreated microsomes (RM), glycoprotein-depleted microsomes (cRM), mock-depleted microsomes (rRM), or glycoprotein-depleted microsomes that had been reconstituted with TRAM (cRM+), and harvested by sedimentation. Targeted material is in the pellet (P) and untargeted material in the supernatant (S). **(B)** Signal intensities on the gel were determined on a phosphorimager and the mean targeted fraction {P/(S+P)} +/- SEM was plotted. **(C)** In vitro translations of Shaker or β-lactamase were harvested, alkali extracted (100 mM) and sedimented. Extracted material is in the supernatant (S) and unextracted material is in the pellet (P). **(D)** Signal intensities on the gel were determined on a phosphorimager and the mean integrated fraction {P/(S+P)} +/- SEM was plotted.

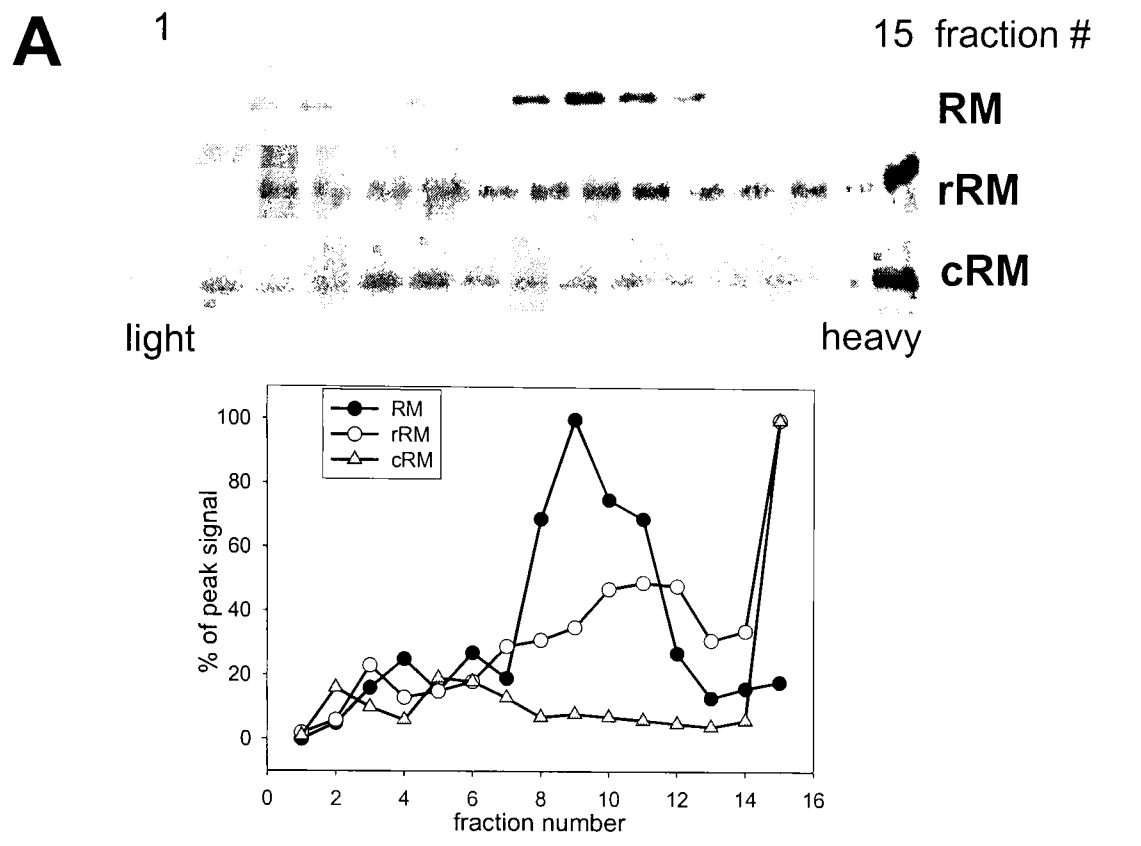

Figure 5.4 : Shaker assembly in reconstituted microsomes. **(A)** Shaker mRNA was translated in RRL with untreated microsomes (RM), glycoprotein-depleted microsomes (cRM) or mock-depleted microsomes (rRM). Targeted material was harvested by sedimentation, solubilized, and centrifuged on 5 – 20 % sucrose gradients. The signal intensity in each gradient fraction was plotted relative to peak intensity. **(B)** Preproα factor was translated in the presence of RM, rRM or cRM and harvested by sedimentation. Targeted material was in the pellet (P) and untargeted material was in the supernatant (S). The glycosylated band is indicated (*). **(C)** Equivalent amounts of RM, rRM and cRM were probed on an α-calnexin (CNX, upper panel) or an α-protein disulfide isomerase (PDI, lower panel) Western blot.

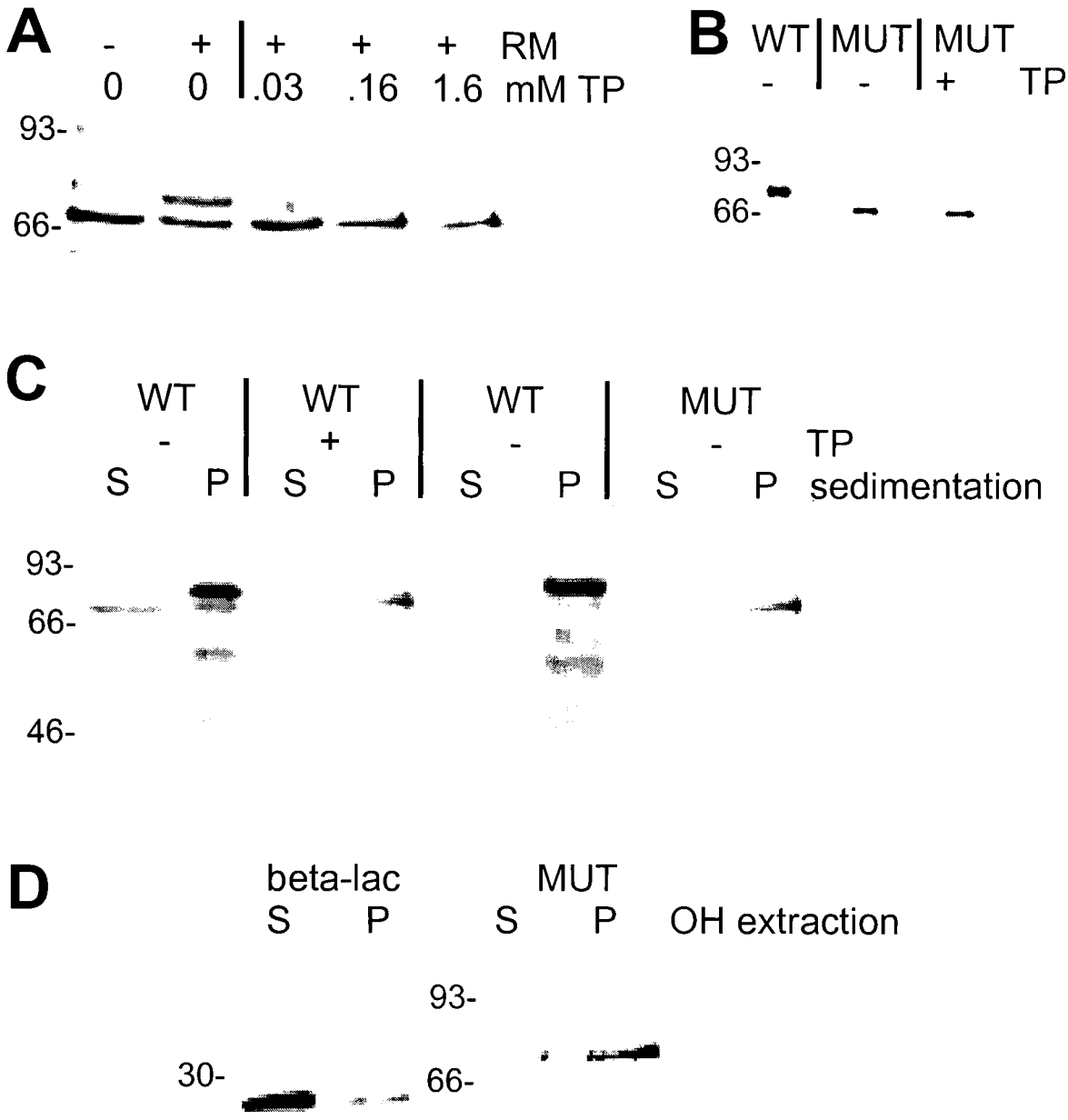

Figure 5.5 : Targeting and integration of unglycosylated Shaker. **(A)** Shaker was translated in RRL -/+ microsomes and with increasing concentrations of competitor tripeptide (TP). **(B)** WT or NQ mutant Shaker was translated in RRL/dog microsomes. Mutant Shaker translations were done -/+ competitor TP. **(C)** Translations were harvested by sedimentation. Untargeted material remained in the supernatant (S) and targeted material was recovered in the pellet (P). **(D)** The targeted fraction of mutant Shaker or β-lactamase was alkali extracted (100 mM NaOH) and sedimented. Unextracted material was in the pellet (P), extracted material was in the supernatant (S).

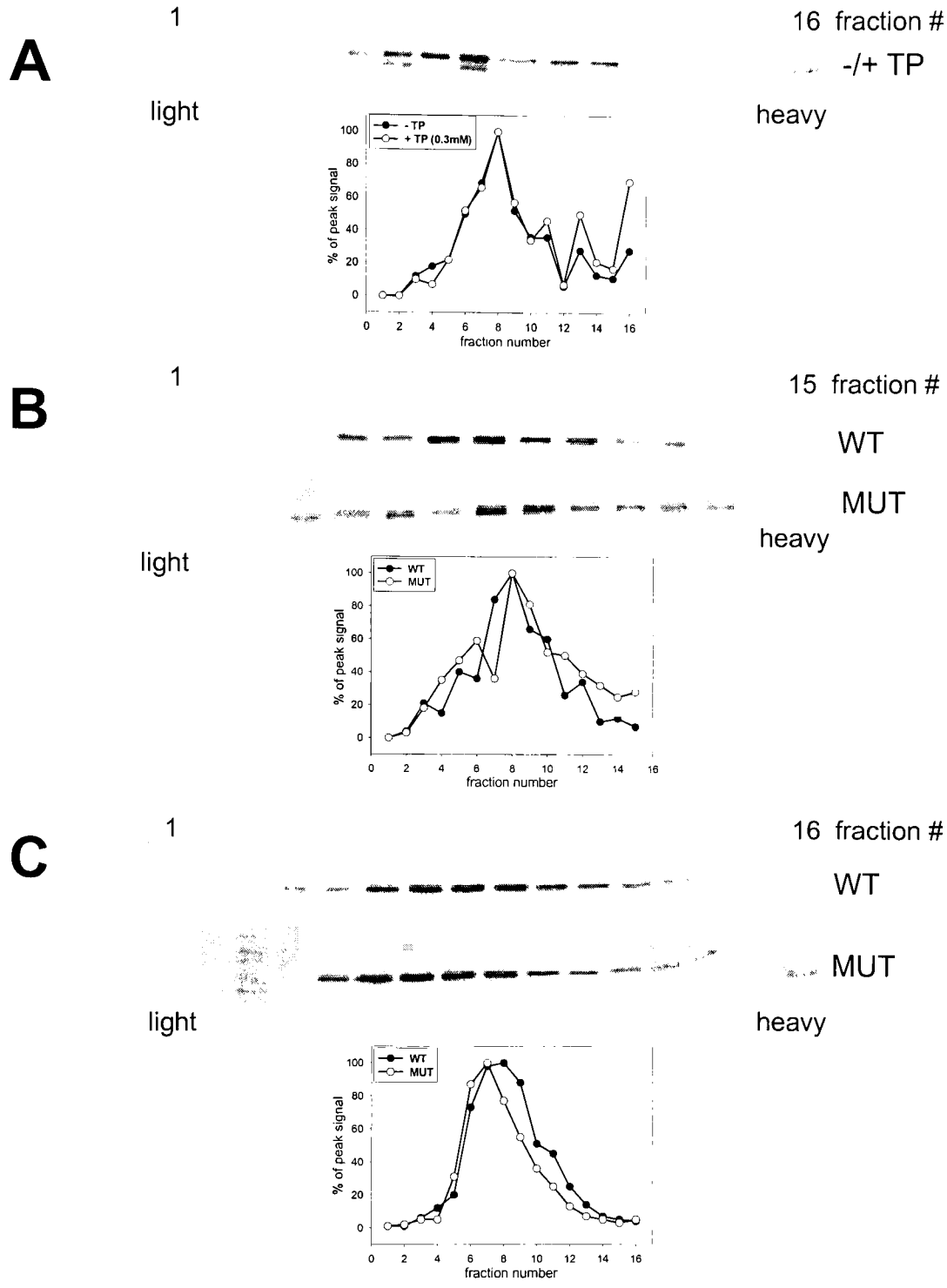

Figure 5.6 : Assembly of unglycosylated Shaker. (A) Shaker was translated in RRL and microsomes -/+ competitor tripeptide. Targeted material was harvested by sedimentation, solubilized, and centrifuged on a single 5 – 20% sucrose gradient. The signal intensity in each fraction was plotted relative to peak intensity. **(B)** WT or NQ mutant Shaker was translated in vitro and processed as above. **(C)** WT or mutant Shaker-transfected COS cells were pulse-labeled and then processed as above. Gradient fractions were subjected to α-HA IP and the data plotted as above.

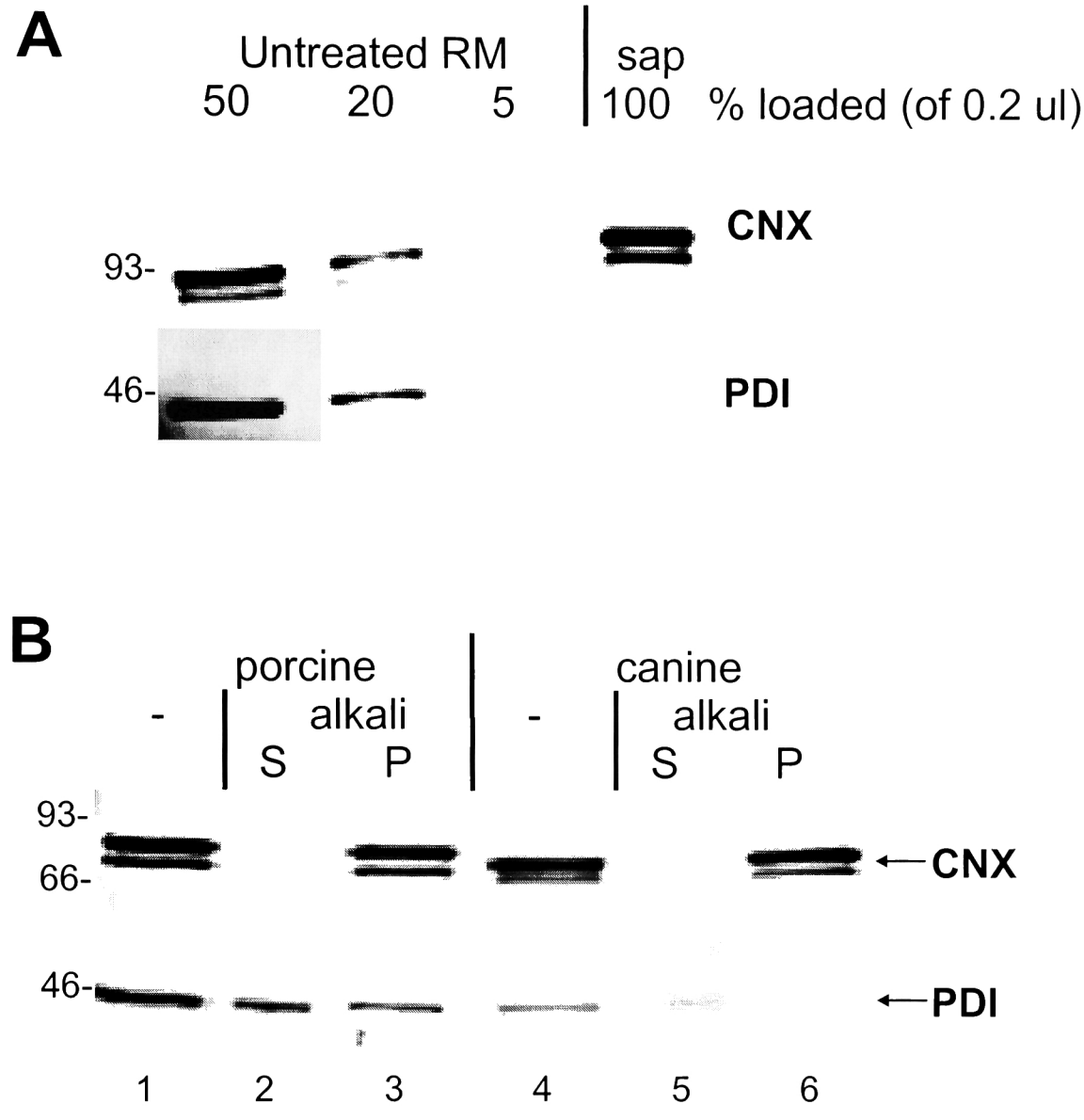

Figure 5.7 : Depletion of microsome lumenal proteins. (A) Saponin-treated microsomes were probed, in parallel with serial dilutions of untreated starting material, on α-protein disulfide isomerase (PDI, upper panel) or α-calnexin (CNX, lower panel) Western blots. **(B)** The supernatant (S) and pellet (P) fractions of alkali-extracted porcine (lanes1-3) or canine (lanes 4-6) microsomes were probed as above, in comparison to unextracted microsomes.

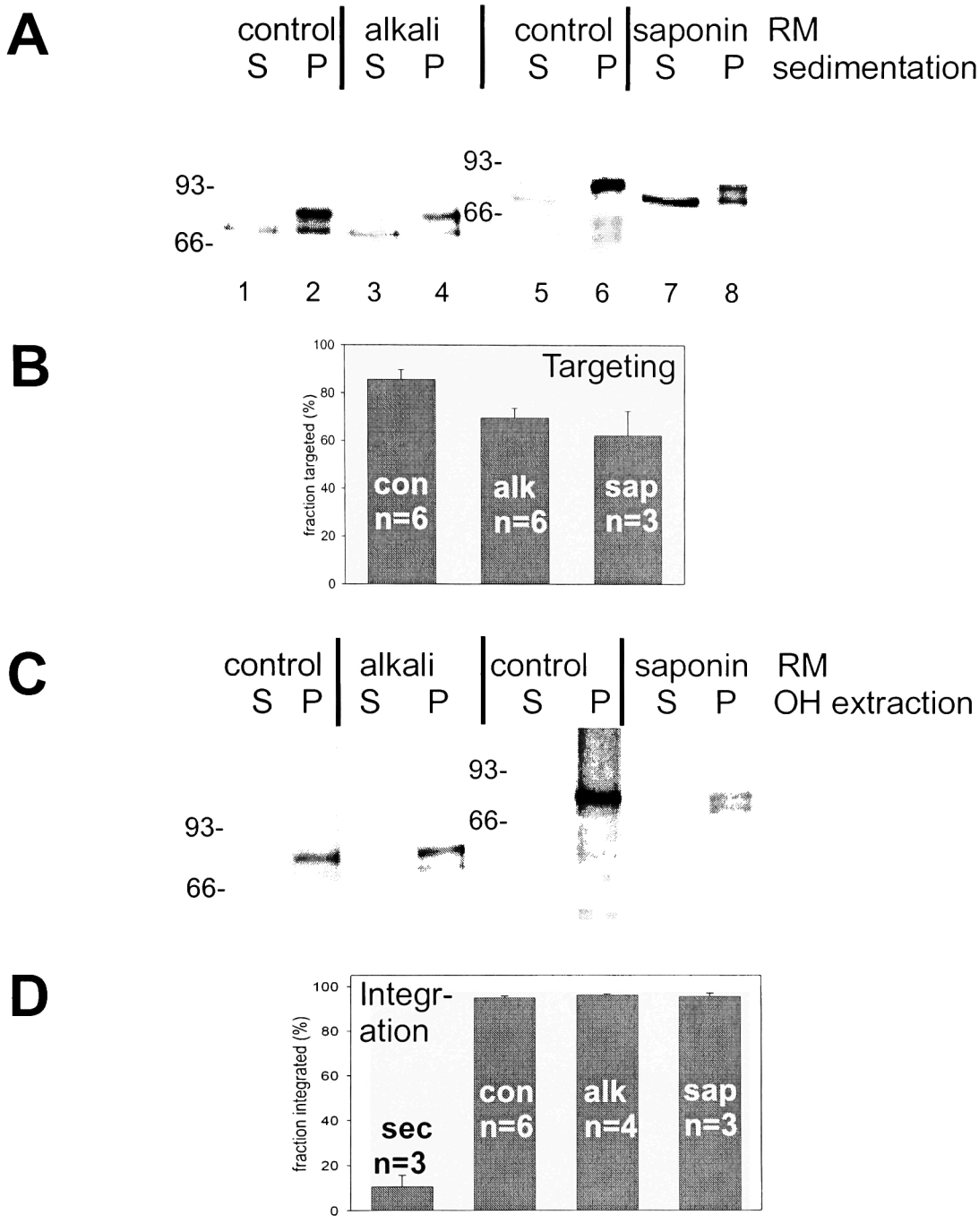

Figure 5.8 : Targeting and integration of Shaker in lumenally-depleted microsomes. Shaker was translated in RRL with untreated, alkali-extracted or saponin-treated microsomes. **(A)** Translations were harvested by sedimentation. Targeted material was in the pellet (P) and untargeted material in the supernatant (S) fractions. **(B)** Signal intensities on the gel were determined on a phosphorimager and the mean targeted fraction {P/(S+P)} +/- SEM was plotted. **(C)** Targeted material was extracted (100 mM NaOH) and sedimented. Extracted protein was in the supernatant (S) and unextracted material was in the pellet (P) fraction. **(D)** Signal intensities were determined as above and the mean integrated fraction {P/(S+P)} +/- SEM was plotted.

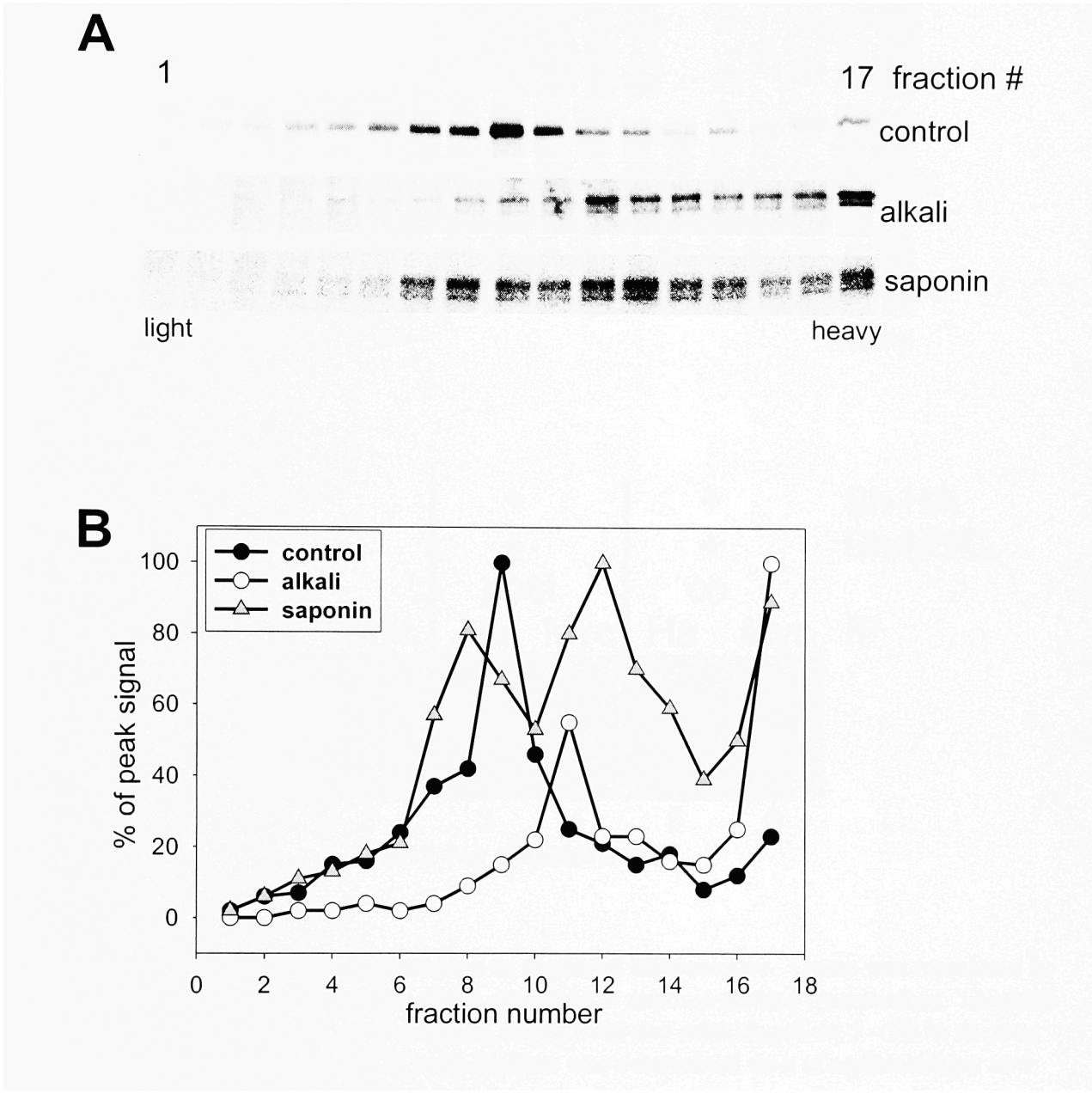

Figure 5.9 : Shaker assembly in depleted microsomes. (A) Shaker was translated in RRL in the presence of untreated, alkali-extracted or saponin-treated microsomes. Targeted material was harvested by sedimentation, solubilized and centrifuged on 5 – 20% sucrose gradients. **(B)** The signal intensity in each fraction was determined on a phosphorimager and plotted relative to peak intensity.

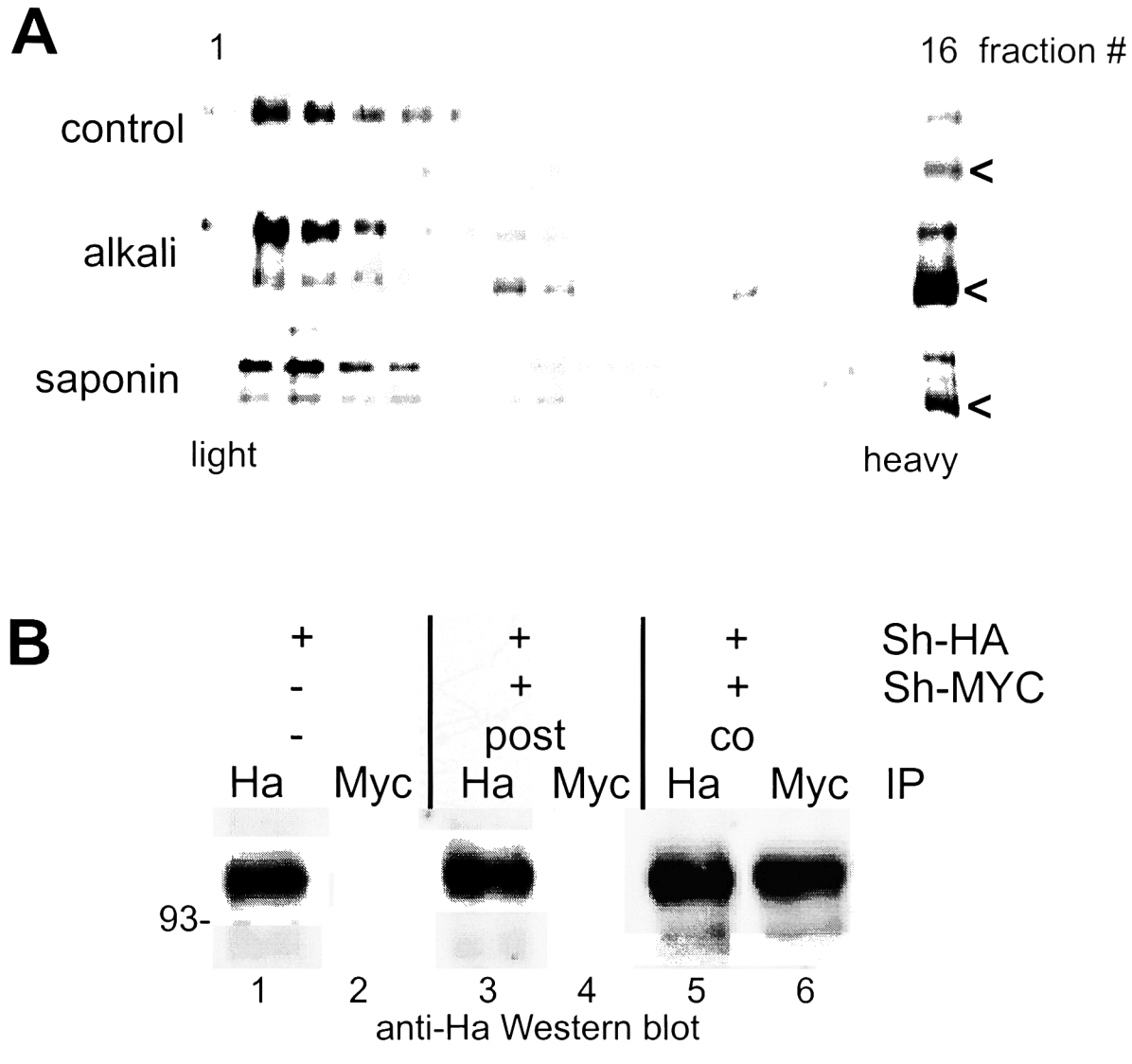

Figure 5.10 : (A) Opsin sedimentation in depleted microsomes. Opsin was translated in RRL in the presence of untreated, alkali-extracted or saponin-treated microsomes. Targeted material was harvested by sedimentation, solubilized and centrifuged on 5 – 20 % sucrose gradients. The signal intensity in each fraction was determined on a phosphorimager and plotted relative to peak intensity.
(B) Control for post-lysis assembly of Shaker subunits. Lysates of COS cells co-transfected (lanes 5-6) or separately transfected (lanes 3-4) with Sh-HA and Sh-MYC were subjected to α-HA or α-MYC IP and probed on an α-HA Western blot.

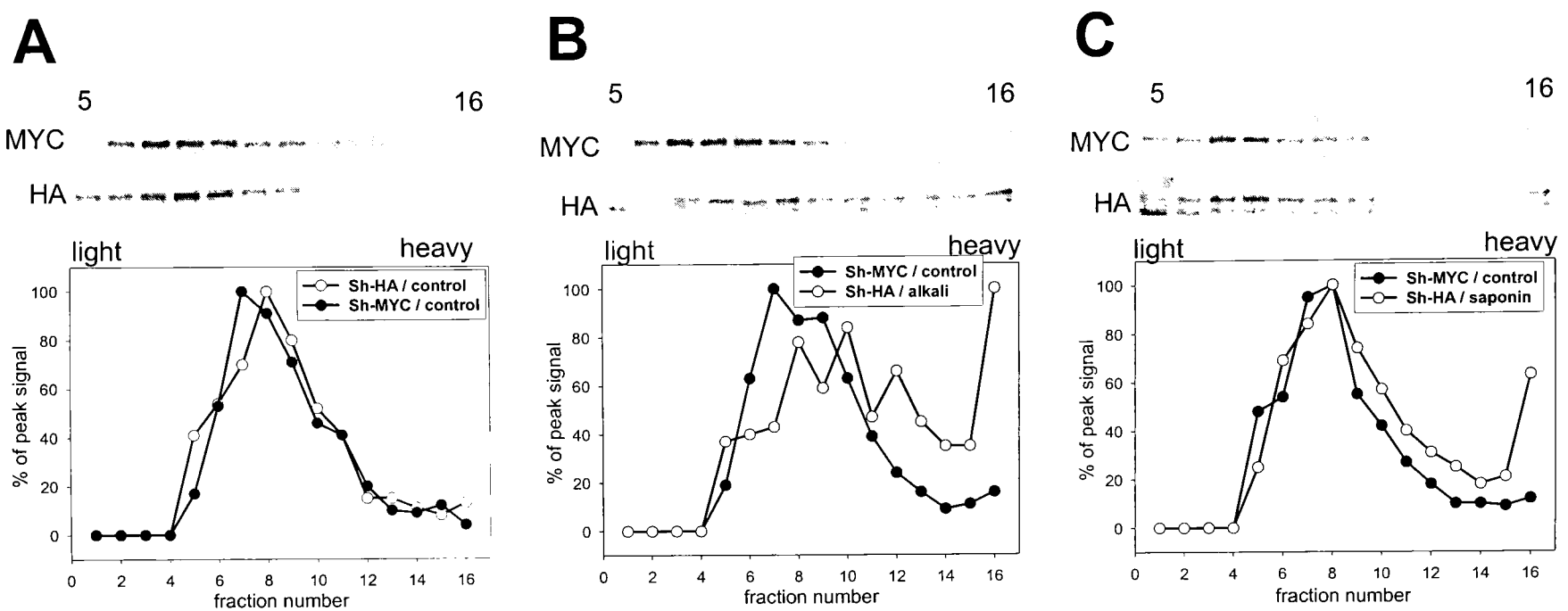

Figure 5.11 : Co-sedimentation of Shaker prepared in control and lumenally-depleted microsomes. Shaker-MYC /Shaker-HA were translated separately in RRL in the presence of **(A)** untreated/untreated, **(B)** untreated/alkai-extracted, or **(C)** untreated/saponin-treated microsomes, respectively. Targeted material was harvested by sedimentation and the lysates mixed post-solubilization and co-sedimented on 5 – 20 % sucrose gradients. Gradient fractions were split into two equal aliquots and subjected to either α-MYC or α-HA IP. The signal intensity in each fraction was determined on a phosphorimager and plotted relative to peak signal intensity.

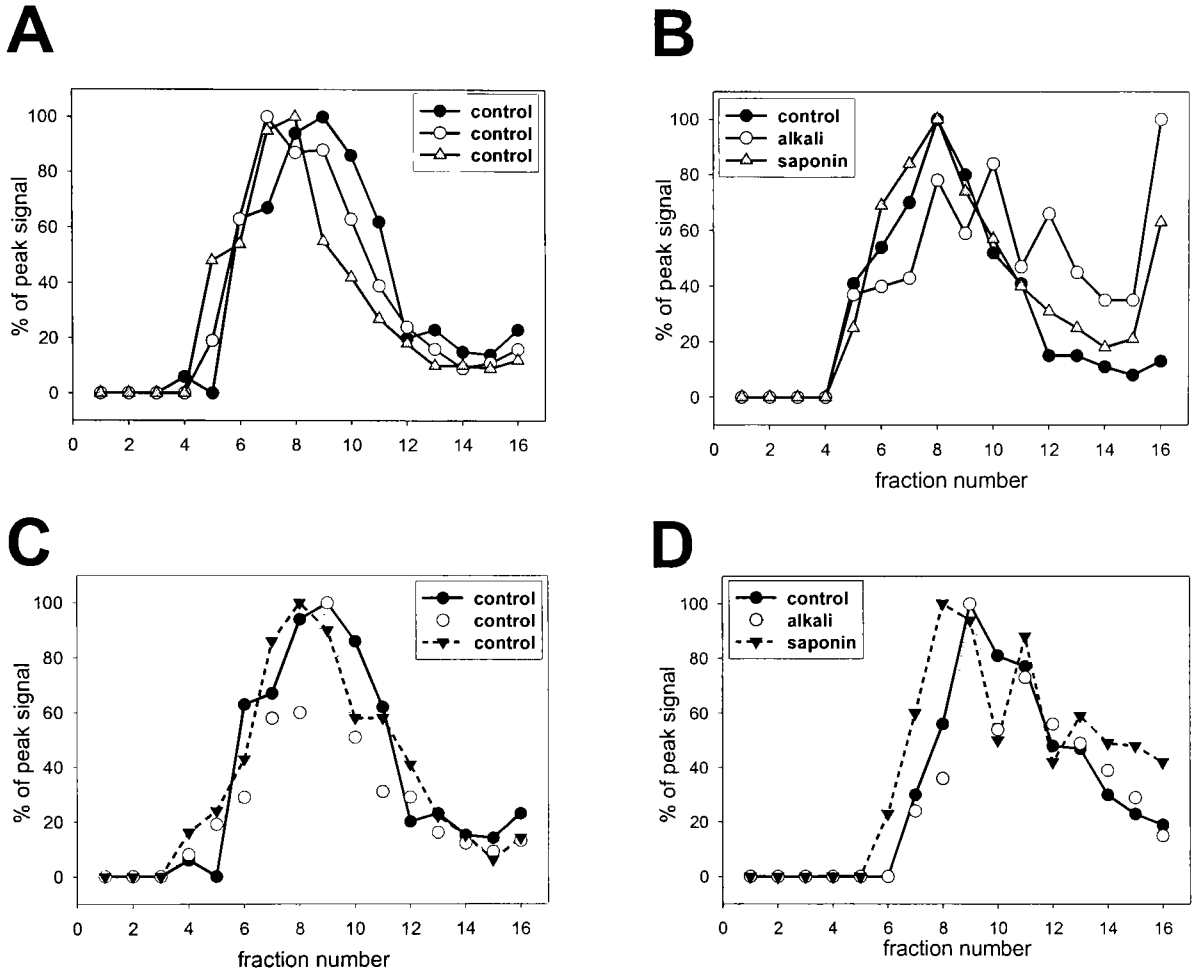

Figure 5.12 : Co-sedimentation of Shaker prepared in control and lumenally-depleted microsomes. Sh-MYC /Sh-HA were translated separately in RRL in the presence of either untreated/untreated, untreated/alkali-extracted, or untreated/saponin-treated microsomes, mixed together post-solubilization, and then co-sedimented on 5-20% sucrose gradients. The plots show two independent sets of three parallel sedimentations of Sh-MYC prepared in untreated microsomes **(A)** & **(C)** and two independent sets of three parallel sedimentations of Sh-HA prepared in untreated, alkali-extracted and saponin-extracted microsomes **(B)** & **(D).**

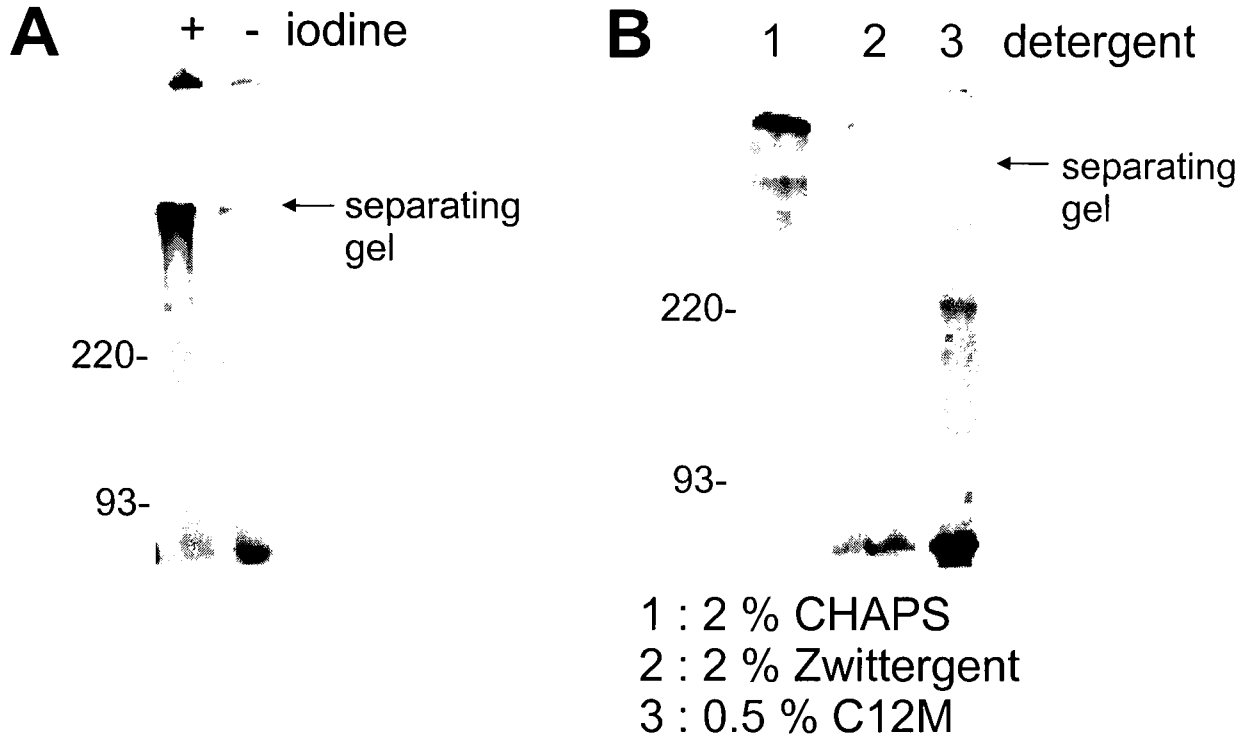

Figure 5.13 : Attempted Shaker assembly assays. Shaker was translated in RRL/ microsomes. Translations were either **(A)** post-translationally treated with 1 mM iodine and separated by non-reducing SDS-PAGE (6% gel), or **(B)** solubilized as indicated and separated by reducing, non-denaturing PAGE (6% gel).

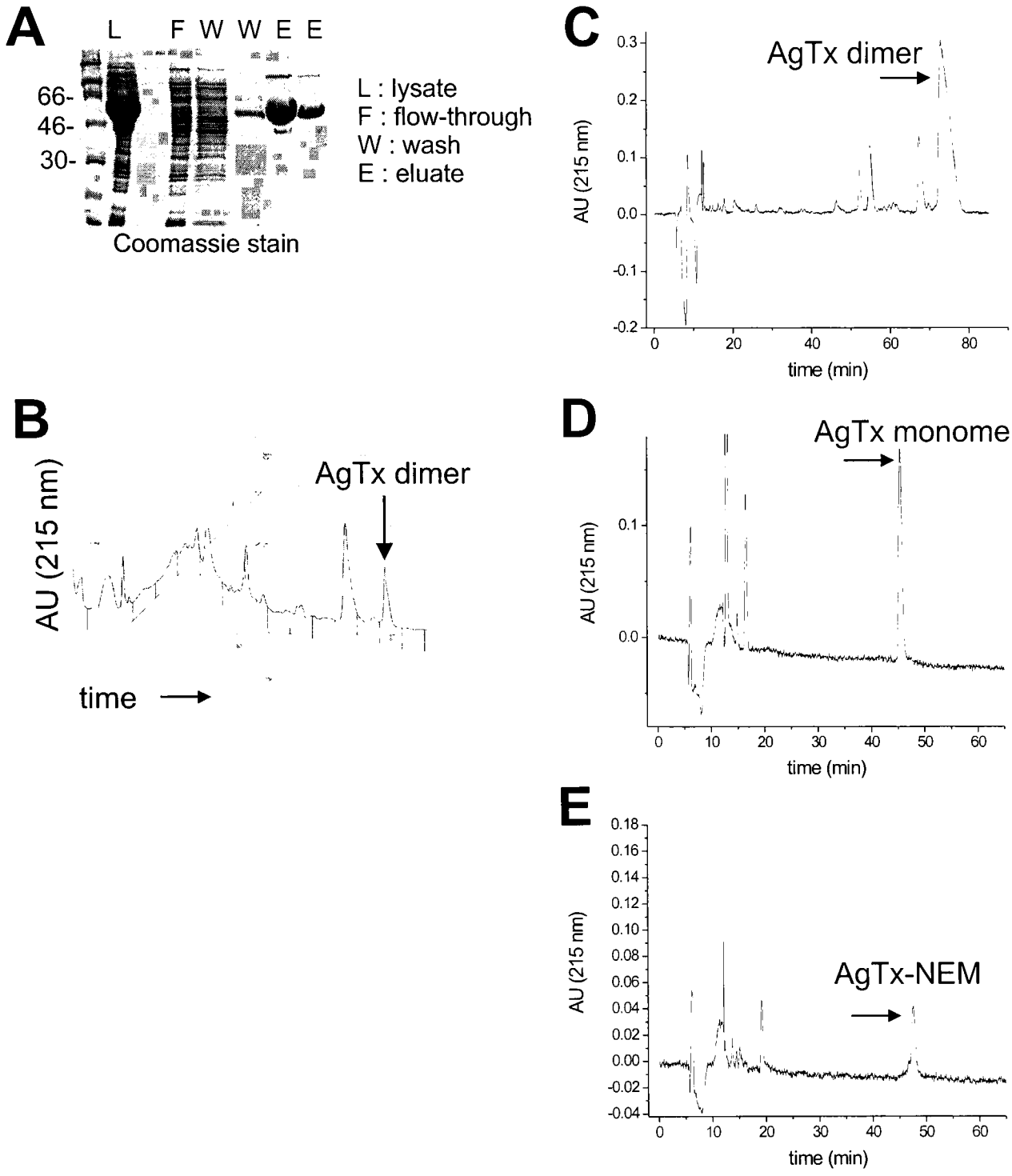

Figure 5.14 : Preparation of tritiated agitoxin D20C. **(A)** Agitoxin was expressed in bacteria as a His6-tagged fusion protein and purified by nickel-chelate affinity chromatography. **(B)** Trypsin digests of the fusion protein were separated on cation-exchange FPLC. **(C)** Disulfide-bonded agitoxin dimer eluted with ~75 min retention time on RP-HPLC. **(D)** Reduced dimer eluted with ~45 min retention time on RP-HPLC. **(E)** Reaction of monomer with ^{3}H-N-ethyl-maleimide generated tritiated toxin, which eluted slightly later than monomer (46-47 min) on RP-HPLC.

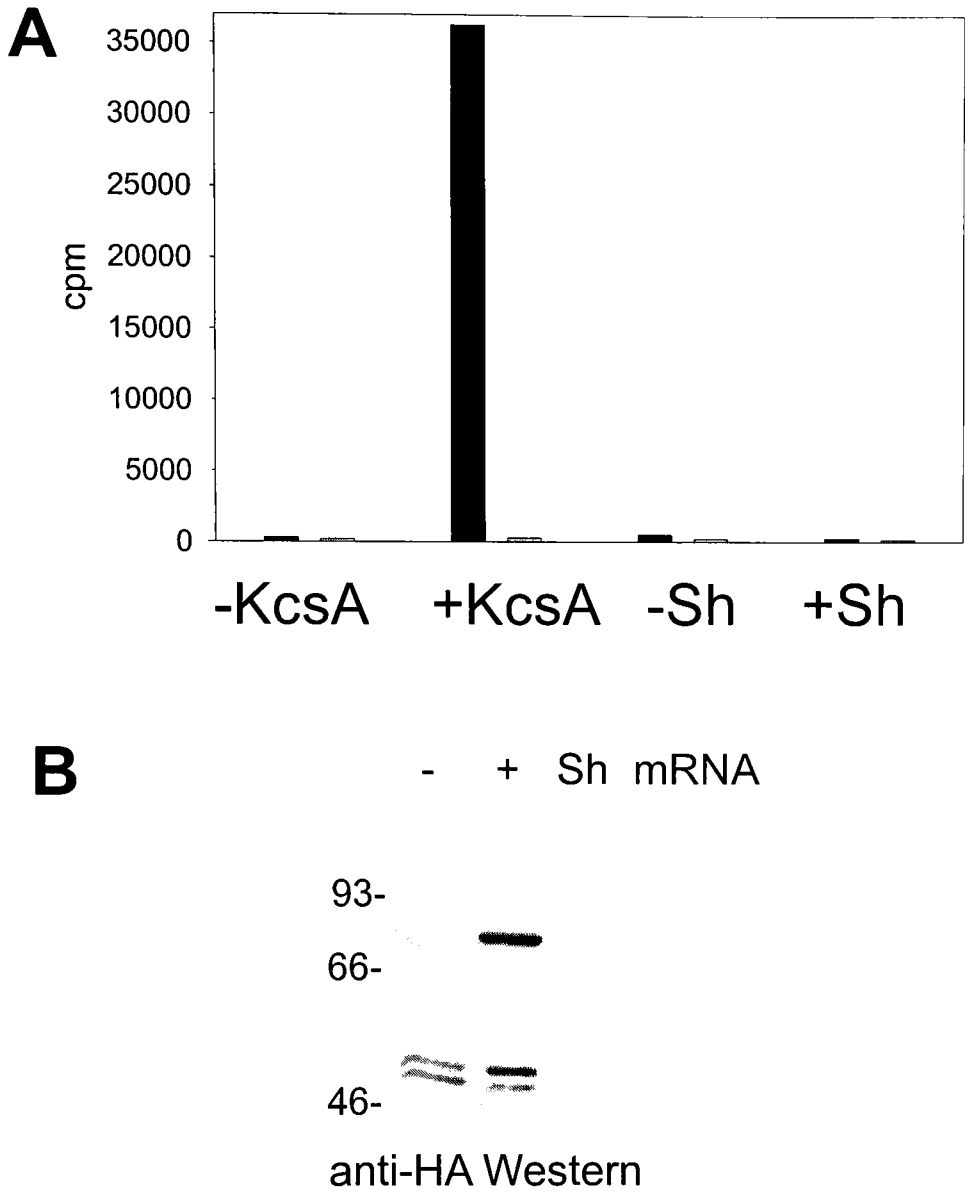

Figure 5.15 : Attempted binding of ^{3}H-AgTx to Shaker translated in vitro.
(A) Sh-HA was translated in RRL/microsomes without ^{35}S-methionine and targeted material was harvested by sedimentation. A control translation (- mRNA) was identically processed. ^{3}H-AgTx (24nM) -/+ excess cold toxin (2.4 μM) was incubated with targeted Shaker in the presence of 1% saponin, or with bacterial membranes -/+ the KcsA channel. Each reaction was bound to a filter, washed, dried and counted in a scintillation counter. Raw bound counts (cpm) have been plotted for each sample. **(B)** Aliquots of the in vitro translations were probed on an α-HA Western blot.

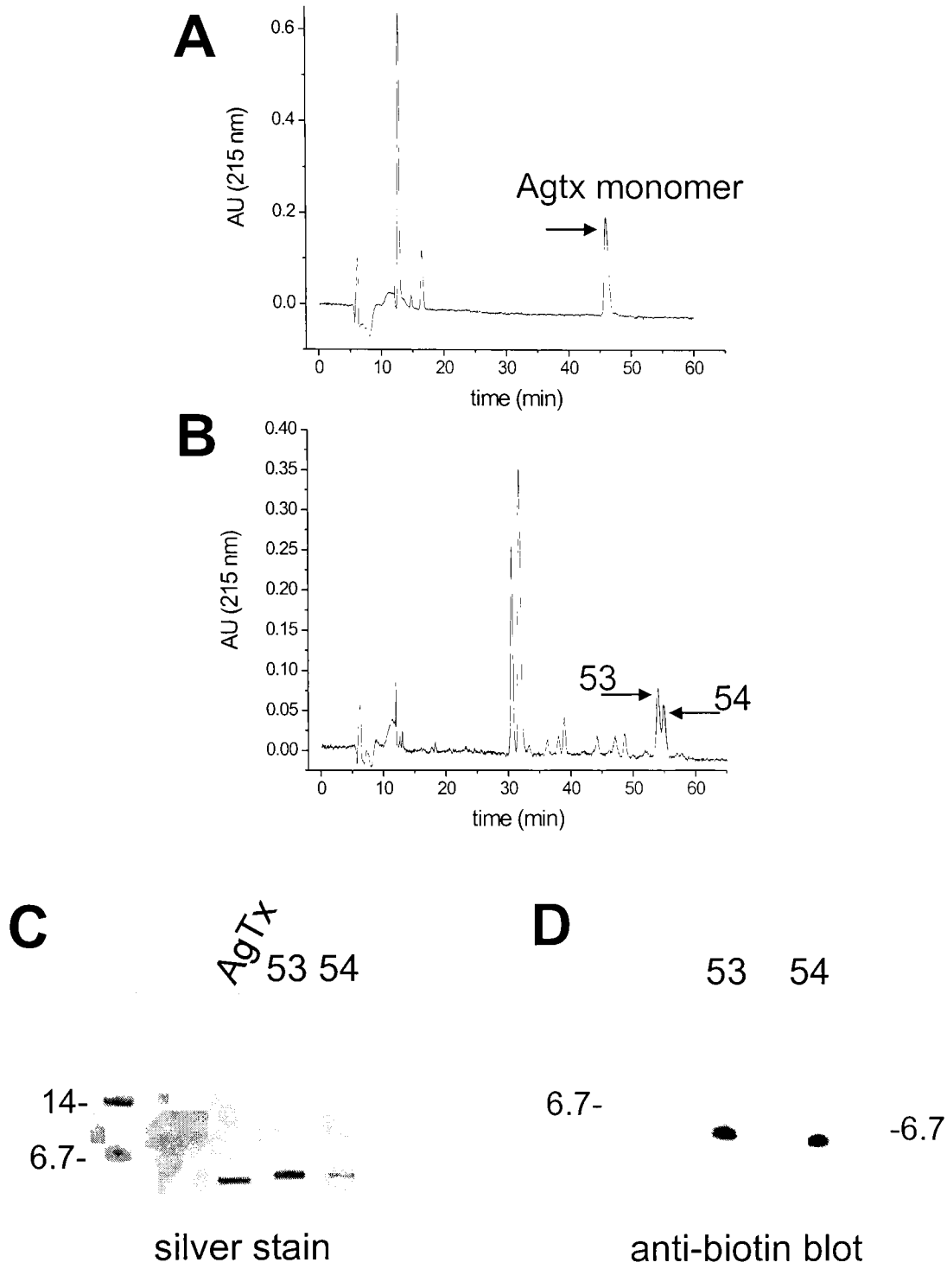

Figure 5.16 : Preparation of biotinylated agitoxin. **(A)** Reduced agitoxin dimer eluted with ~45 min retention time on RP-HPLC. **(B)** Agitoxin monomer was reacted with biotin-PEO-maleimide and the reaction separated on RP-HPLC. Material in the peaks at 53 and 54 minutes was collected and dried down. A fraction of this material was run on a 20% Tricine gel and silver stained, with reduced agitoxin for comparison **(C)**, or transferred to nitrocellulose and probed for biotin **(D)**.

6. ER-TO-GOLGI TRAFFIC OF THE SHAKER CHANNEL

The cytosolic carboxyl termini of several membrane proteins, including potassium channels, have been implicated in directing ER export . We generated C-terminal truncations (CTR) of the Shaker channel and monitored their ER-to-Golgi traffic as well as their steady-state distribution compared to full-length channel. The 177 amino acid Shaker carboxyl terminus tail contains two short stretches of residues that have been implicated in the export of other proteins from the ER. The diacidic DQE motif (aa 488-490), very close to transmembrane domain 6, is necessary for transport of the VSVG protein from ER to Golgi (Nishimura and Balch, 1997; Sevier et al., 2000). The VASSL motif (aa 564-568), about half way down the C-terminal tail, has been implicated in transport of the mammalian voltage-gated Kv1.1 channel (Levitan and Takimoto, 2000), although this sequence was recently reported not to be required for Shaker traffic (Khanna et al., 2001a).

6.1. Shaker truncated at the carboxyl terminus : CTR series

The constructs are shown schematically (Fig. 6.1A). The red bar indicates the position of the stop codon, in each case. The HA epitope tag was switched to the amino terminus of the protein, in order to avoid possible confounding effects of this extraneous sequence at the carboxyl terminus of truncated proteins. Full length channels with HA epitope tags at the N- and C-termini trafficked with very similar kinetics, as measured by pulse-chase and EndoH digestion in metabolically labeled cells (not shown). The CTR1 truncation has lost essentially the entire C-terminal tail, including the DXE and the VSSNL motifs. The CTR2 truncation retains DXE, but lacks VSSNL. The CTR3

truncation contains both DXE and VSSNL, but has lost the last third of the C-terminal tail. This membrane distal portion of the Shaker carboxyl terminus is characterized by long stretches of glutamine residues the function of which, if any, remains to be determined.

Western blots on the CTR constructs (Fig. 6.1B) indicated that the shortest (CTR1) is retained in the ER. Both CTR2 and CTR3, but not CTR1, showed the fuzzy, higher molecular weight band that is characteristic of the mature, Golgi-modified form of an N-glycosylated protein. In most cases, the smaller immature band was also seen. The CTR constructs migrated at the appropriate sizes, relative to the full-length channel. In immunoprecipitations from metabolically pulse-labeled cells, only the immature band was seen, in all cases (Fig. 6.1C).

6.2. ER-to-Golgi traffic of truncated Shaker constructs

Traffic of the CTR constructs was monitored by metabolic pulse labeling, followed by a chase of up to 2 hours and EndoH digestion. In keeping with the pattern seen at steady state, the CTR1 construct remained EndoH-sensitive after up to 2 hours of chase (Fig. 6.2A). This is also true after 3 hours of chase (not shown). Quantitative analysis of the longer constructs (Fig. 6.2B) is unfortunately complicated by the presence of the 93kD background band (labeled **, Fig. 6.2B, panel 1). This background protein was EndoH- sensitive and unstable, being virtually undetectable after 2 hours of chase (panel 1, Fig. 6.2B). We compared the EndoH-resistant fraction {R/(R+S)}*100 (where R is resistant and S is sensitive) of the CTR constructs at 2 hours of chase in several independent experiments. CTR3 (panel 3, Fig. 6.2B; 81 % +/- 4, n = 3) was indistinguishable from full length Shaker (panel 4, Fig. 6.2B; 83 % +/- 2, n =3).

However, CTR2 (panel 2, Fig. 6.2B; 62 % +/- 3, n = 3) trafficked more slowly, as is also evident from a visual inspection of the remaining EndoH sensitive fraction at 2 hours of chase, relative to that of CTR3 or full length Shaker.

6.3. Immunolocalization of Shaker truncated constructs

We examined the steady state distribution of the CTR truncations in transfected COS cells by immuofluorescence microscopy against the N-terminal HA tag. The full-length channel (Fig. 6.3) was present throughout the cell, presumably partly on the cell surface. Clear rim staining was seen in most cells. Co-staining of calnexin as a marker for the ER (Fig. 6.3A) and of GOS28 as a marker for the Golgi (Fig. 6.3B) have been shown. Although there is some spatial overlap between Shaker and the ER, the fluorescence patterns are clearly different. Likewise, full-length Shaker does not, for the most part, have the same fluorescence pattern as a Golgi marker, although in the cases where there is significant intracellular staining, co-localization with the Golgi is often seen (middle cell, Fig. 6.3B). This is not unexpected for a membrane protein that must transit through the secretory pathway. In stark contrast, the CTR1 protein is localized to the ER at steady state (Fig. 6.4).

The CTR2 truncation was quite variable in its sub-cellular distribution (Fig. 6.5). While CTR2 in some cells looked very similar to full length channel, ER localization was also seen, albeit to varying degrees. In some cases (e.g. cell 1, Fig. 6.5B, perinuclear stain), although the fluorescence was predominantly non-ER, some ER stain could be seen. In other cases (e.g. cell 5, Fig. 6.4B), what appears to be ER stain was predominant. This data is extremely qualitative, but it is not inconsistent with the inefficiency in ER export reported by pulse-chase of the CTR2 construct relative to full-

length channel (Fig. 6.2). Further, CTR2 frequently showed a juxtanuclear speckled pattern (e.g. cell 2, Fig 6.5A or cells 2, 3 &4, Fig. 6.5B). This pattern did not overlap with either the ER or the Golgi, but was often seen to "interlace" with the Golgi. Speculatively, the pattern is reminiscent of ER exit sites, but further experiments are needed to test this. As for full length Shaker channel, CTR3 fluorescence (Fig. 6.6) was for the most part distinct from the ER and the Golgi, although intracellular Shaker co-localizing with the Golgi was occasionally seen (e.g.. cell 3, Fig. 6.6B).

6.4. Further experiments on CTR1

Because of the unique nature of the ER as a "quality-controlled" folding compartment, the failure of a protein to traffic out of this organelle need not be the result of an export defect, *per se*. Misfolding can also result in retention in the ER, a situation for which there is extensive precedent. Further experiments were initially designed to elucidate the nature of the CTR1 defect since it was the most blatant, relative to full length Shaker. Specifically, we wished to distinguish between a problem in the folding versus the export of the truncated CTR1 channel. We co-expressed HA-tagged CTR1 with MYC-tagged full-length Shaker, and asked whether the latter, by virtue of assembly with CTR1, could "rescue" the export deficiency of CTR1 to any degree. Since the efficient assembly of the Shaker channel is promoted by amino-terminal domains, the truncated channel would be expected to assemble with full length.

Indeed, HA-CTR1 co-immunoprecipitated with co-expressed Sh-MYC (Fig. 6.7A, anti-HA blot, lane 5), but not with Sh-MYC that had been separately expressed and mixed with the CTR1 post-solubilization (Fig. 6.7A, lane 4). Full length Sh-HA was also co-immunoprecipitated with co-expressed Sh-MYC (lane 6), as was shown previously

(chapter 5). A comparison of CTR1 expressed either on its own (Fig. 6.7B, lanes 1 & 2) or co-expressed with full length Sh-MYC (Fig. 6.7B, lane 3) showed no evidence of enhanced ER export of the truncated construct. In other words, no additional putative mature band appeared upon co-expression of CTR1 with full length Shaker. On the other hand, an examination of full length Sh-MYC expressed either alone (Fig. 6.7C, lanes 1 & 2) or together with CTR1 (Fig. 6.7C, lane 3; also Fig. 6.7A, anti-MYC blot, lane 5) indicated that the mature (Golgi) fraction of the full-length protein may be reduced, upon co-expression with CTR1.

It is possible that the fraction of co-IP'd CTR1 (relative to total) is small, and that the fraction of any putative "rescued" mature CTR1 is smaller still and therefore below the detection limit. We imaged co-expressed CTR1 and Sh-MYC in order to assess, by a different method, whether the export phenotype of the full length or the truncated construct is dominant. The fluorescence pattern of the CTR1 channel has already been discussed, but is shown again in individually expressing COS cells that have been stained for both HA and MYC (Fig. 6.8A). The distribution of full-length Sh-MYC is very similar to that of the full-length HA-tagged channel (Fig. 6.8B). There was no evidence for rescue of CTR1 export by co-expression with full-length Shaker channel. In contrast, in every case of high CTR1 expression, full-length Sh-MYC was seen to redistribute to the ER, to some degree. There is still clearly non-ER (presumably surface)Sh-MYC channel in all cases, as evidenced by the fluorescent halo that surrounds the ER stain and extends to the edge of the cell, but a significant amount of full length channel is redistributed to the ER, to an extent never seen for Sh-MYC expressed alone.

Simply interpreted, the dominant effect of the CTR1 construct could mean one of two things. The truncated channel could be misfolded and consequently, as a result of heteromultimerization, could retain the full-length channel in the ER. Alternatively, there may indeed be a key ER export signal in the membrane proximal first third of the Shaker C-terminus, but this signal may be necessarily present on all four subunits of the tetramer in order to efficiently effect export. Nevertheless, our present data cannot rule out misfolding of the CTR1 construct. Since the defect of the CTR2 construct is subtler, productive co-expression experiments will require the re-establishment of a dependable quantitative trafficking assay.

6.5. Controls and future experiments

(i) Although co-IP of the CTR1 truncated construct with full length Shaker suggests that it assembles into tetramers, sucrose gradient centrifugation is needed to definitively determine this. Additionally, spurious aggregated forms of CTR1, if present, may be detected by this method.

(ii) Preliminary observations indicate that the CTR1 construct is not particularly unstable, relative to full length, arguing against a folding defect. Stability comparisons would need to be extended and quantified.

(iii) Analysis of ER-Golgi traffic of ΔDXE Shaker to specifically investigate the role of this sequence in the transport process.

(iv) Analysis of ER-Golgi traffic of ShakerΔregion1, where region1 is the membrane-proximal sequence that is present in CTR2 and absent in CTR1. If misfolding of CTR1 is merely due to the lack of any cytosolic sequence following TM6, then

the addition of the distal Shaker C-terminus (or of random sequence from any other protein) would be expected to restore export out of the ER.

(v) ER-Golgi traffic of full-length Shaker co-expressed with the cytosolic carboxy-terminal tail. Fragments of membrane proteins that contain ER export sequences have been shown to block ER export of the full-length forms of the same protein, presumably by competition with necessary cytosolic factors. The effect of a co-expressed C-terminal fragment on the traffic of Shaker itself, as well as of other secreted and membrane proteins, could be informative with regard to both the existence and the potential specificity of ER export sequences in the Shaker carboxyl terminus.

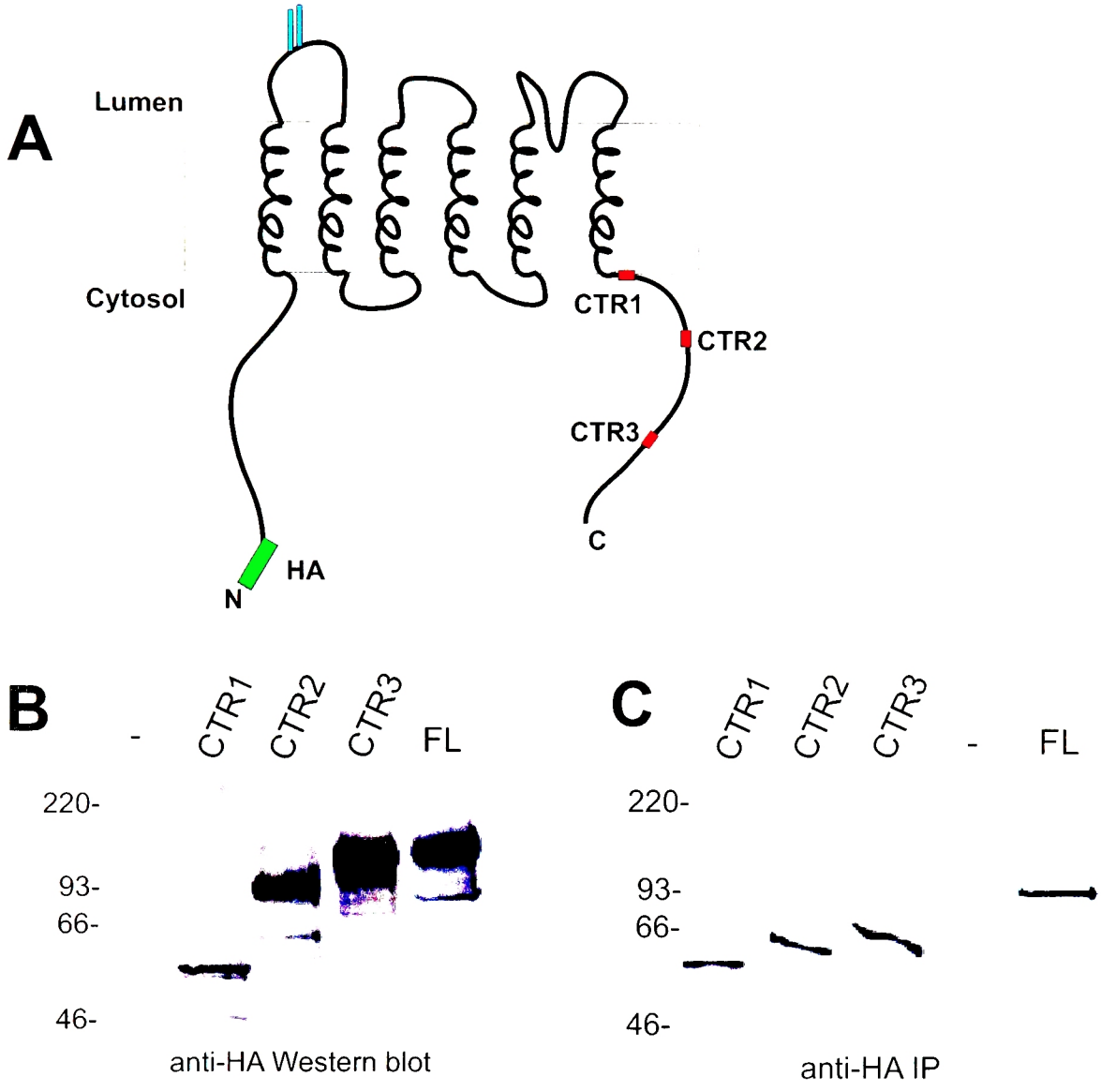

Figure 6.1 : Shaker C-terminal truncations (CTR) expressed in COS cells.
(A) Construct design. The red bars indicate the position of the stop codon for each truncation. **(B)** α-HA Western blot on CTR constructs expressed in COS cells. **(C)** α-HA IP on transfected COS cells pulse-labeled with ^{35}Scysteine+methionine.

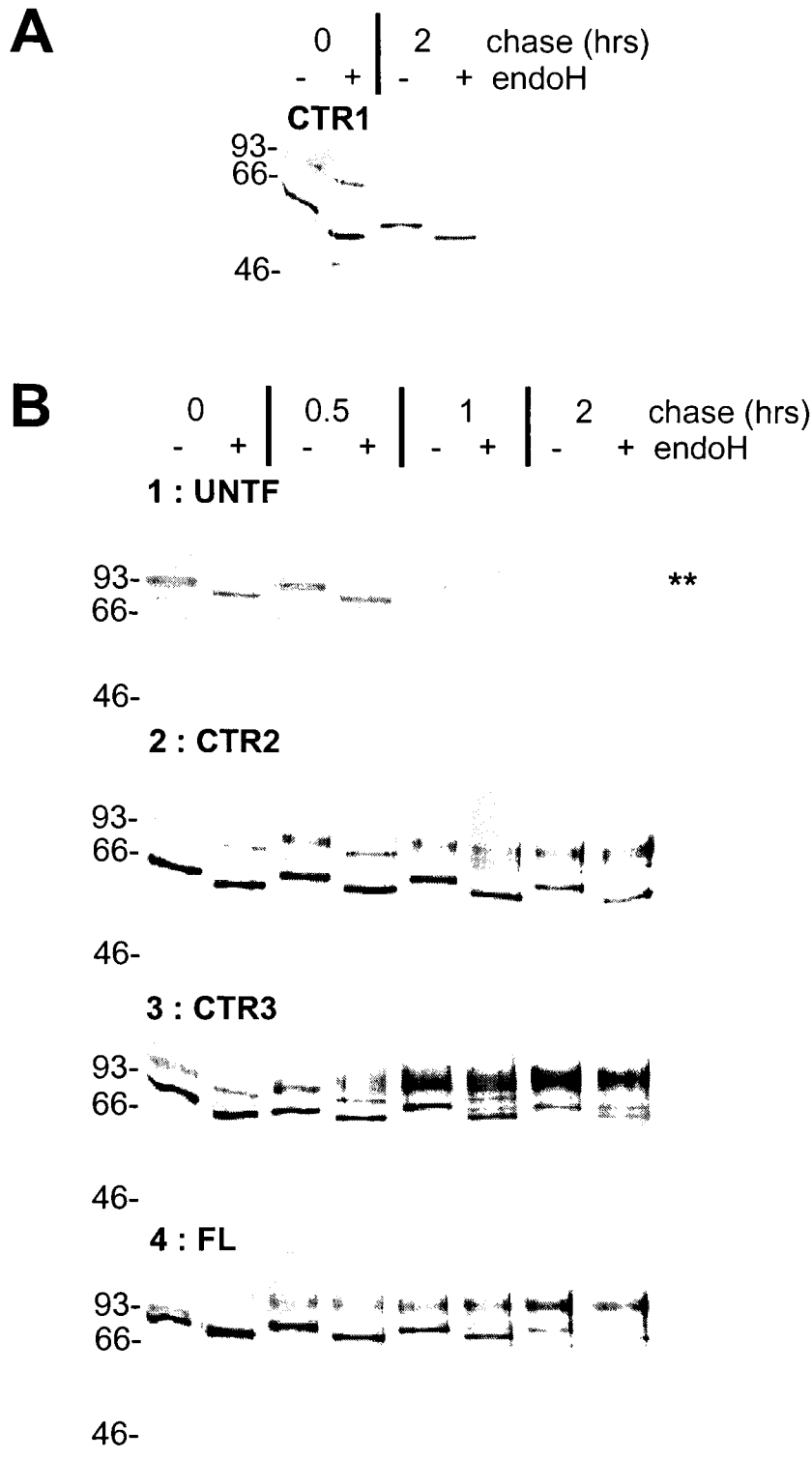

Figure 6.2 : ER-Golgi traffic of Shaker C-terminal truncations (CTR). **(A)** CTR1-transfected COS-1 cells were pulse-labeled, chased as indicated (0-2h), and the lysates subjected to α-HA IP and EndoH digestion. **(B)** Untransfected (panel 1) or CTR2-, CTR3- and full length Shaker-transfected COS cells (panels 2 – 4) were pulse-chased and processed as above. A background band at 93kD is indicated in panel 1 (**).

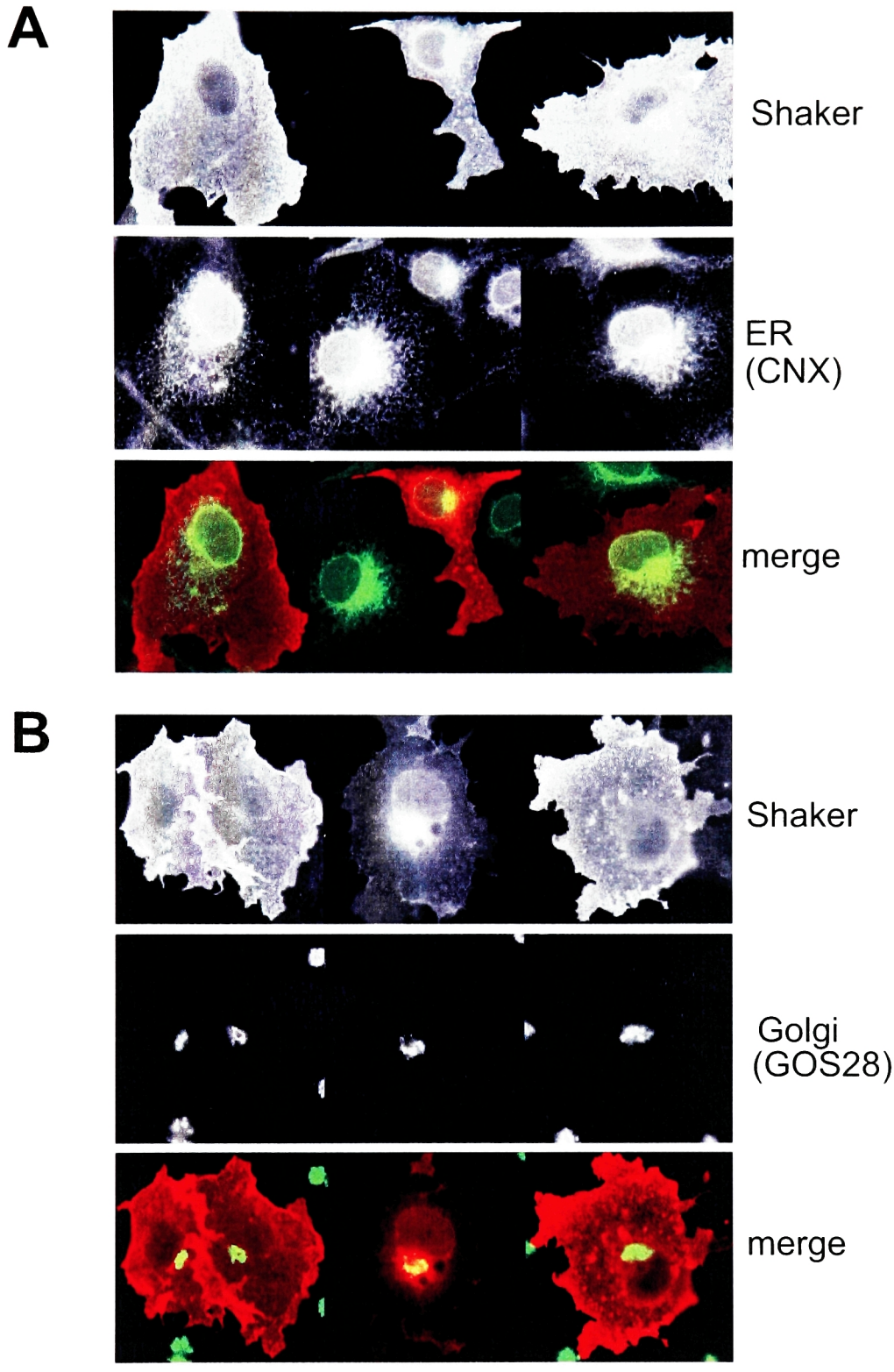

Figure 6.3 : Immunofluorescence microscopy on full-length Shaker. Shaker-transfected COS-1 cells were fixed and stained for Shaker (α-HA, red) and ER (α-CNX, green) **(A)** or Golgi (α-GOS28, green) **(B).** Fields including untransfected cells have been shown.

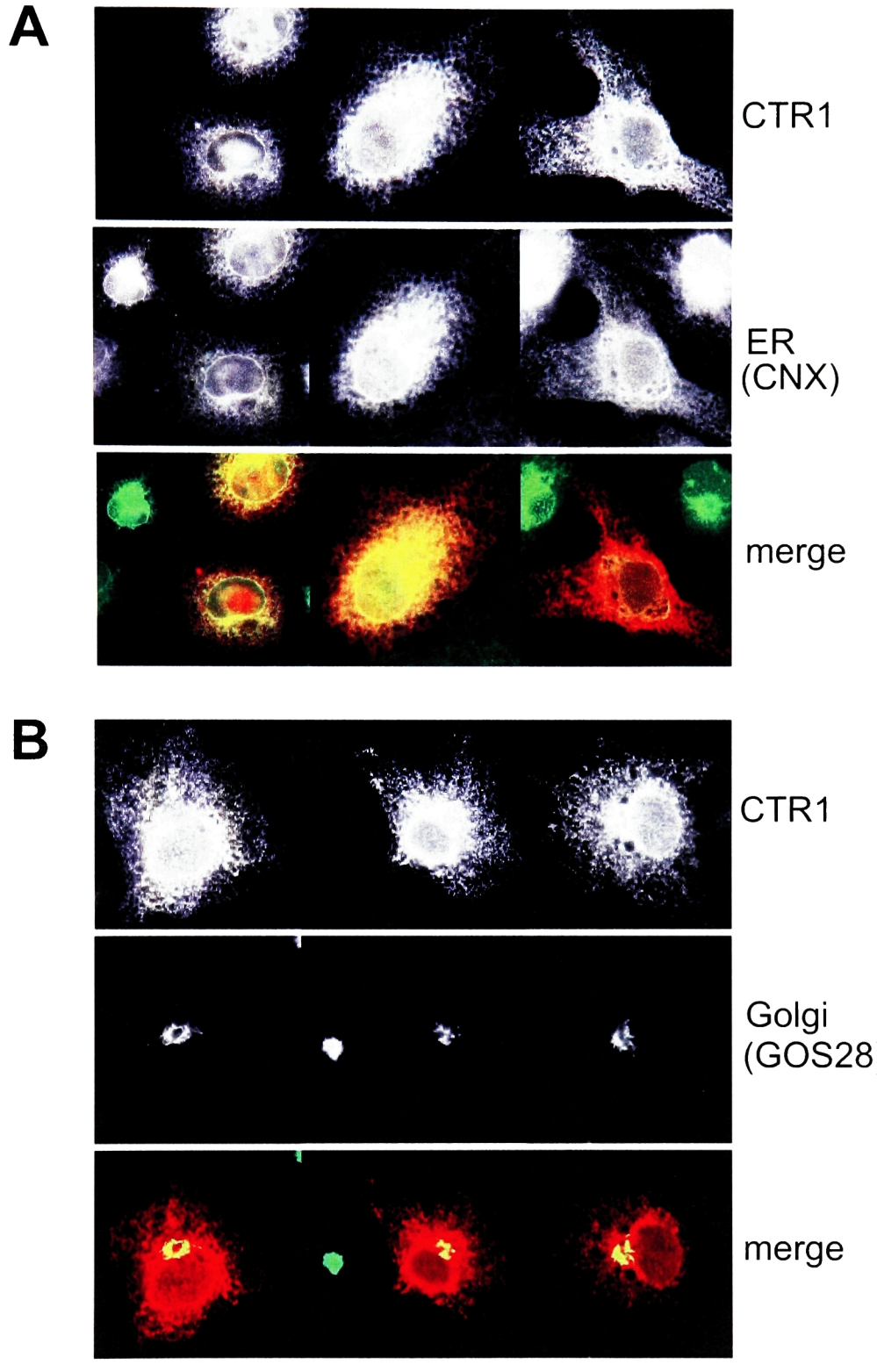

Figure 6.4 : Immunofluorescence microscopy on Shaker CTR1. CTR1-transfected COS-1 cells were fixed and stained for Shaker (α-HA, red) and ER (α-CNX, green) **(A)** or Golgi (α-GOS28, green) **(B).** Fields including untransfected cells have been shown. Yellow or orange color in the merge indicates co-localization.

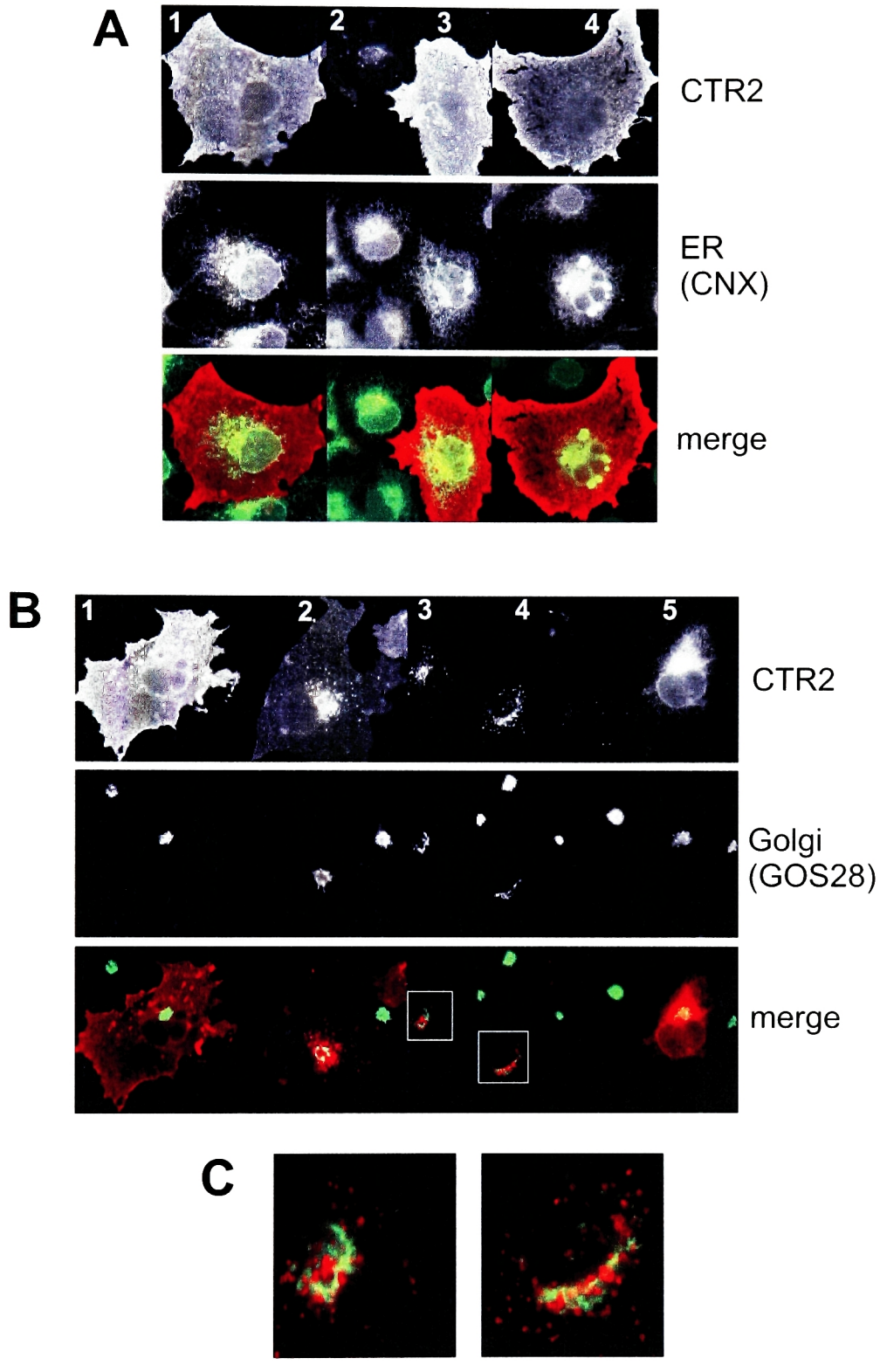

Figure 6.5 : Immunofluorescence microscopy on Shaker CTR2. CTR2-transfected COS-1 cells were fixed and stained for Shaker (α-HA, red) and ER (α-CNX, green) **(A)** or Golgi (α-GOS28, green) **(B).** Fields including untransfected cells have been shown. **(C)** Enlarged regions of cells 3 and 4 from (B).

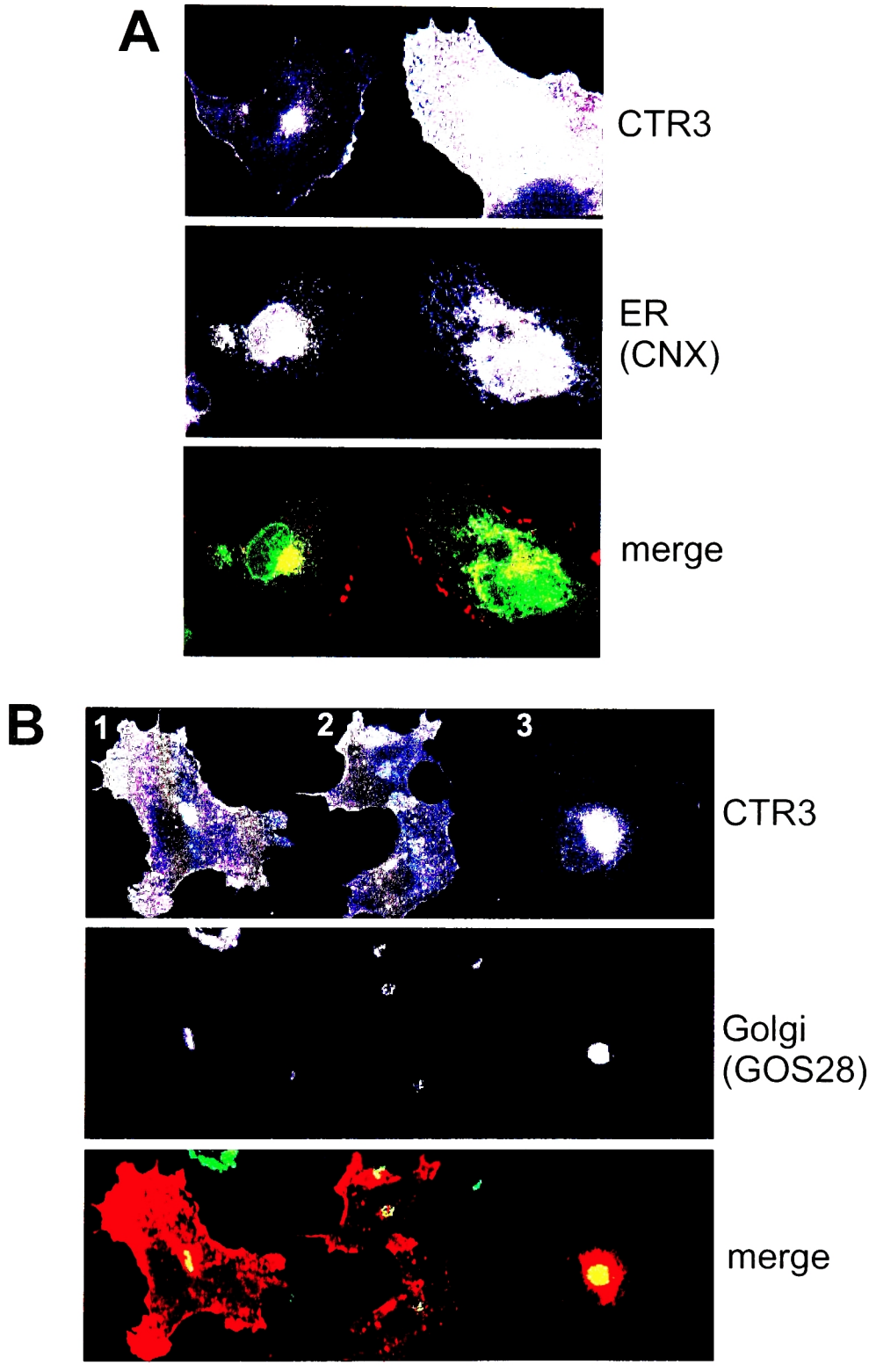

Figure 6.6 : Immunofluorescence microscopy on Shaker CTR3. CTR3-transfected COS-1 cells were fixed and stained for Shaker (α-HA, red) and ER (α-CNX, green) **(A)** or Golgi (α-GOS28, green) **(B).** Fields including untransfected cells have been shown.

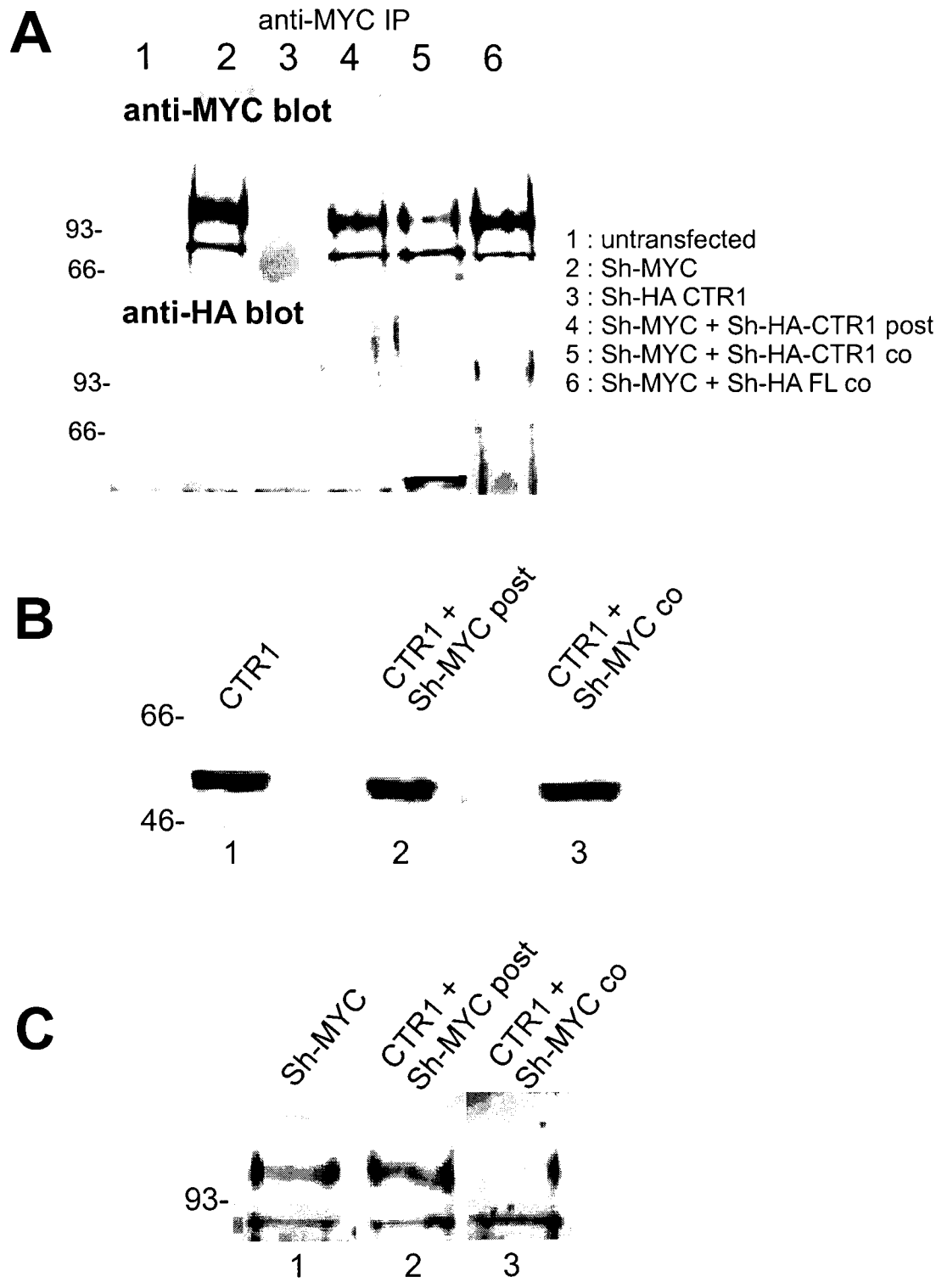

Figure 6.7 : Co-expression of CTR1 with full length Shaker. **(A)** Transfected COS-1 cells were lysed (2% CHAPS), the lysates subjected to α-MYC IP, and then probed either on α-MYC (upper panel) or α-HA (lower panel) Western blots. **(B)** & **(C)** Transfected COS-1 cells were lysed as above and equal fractions of the lysates probed on α-HA **(B)** or α-MYC **(C)** Western blots.

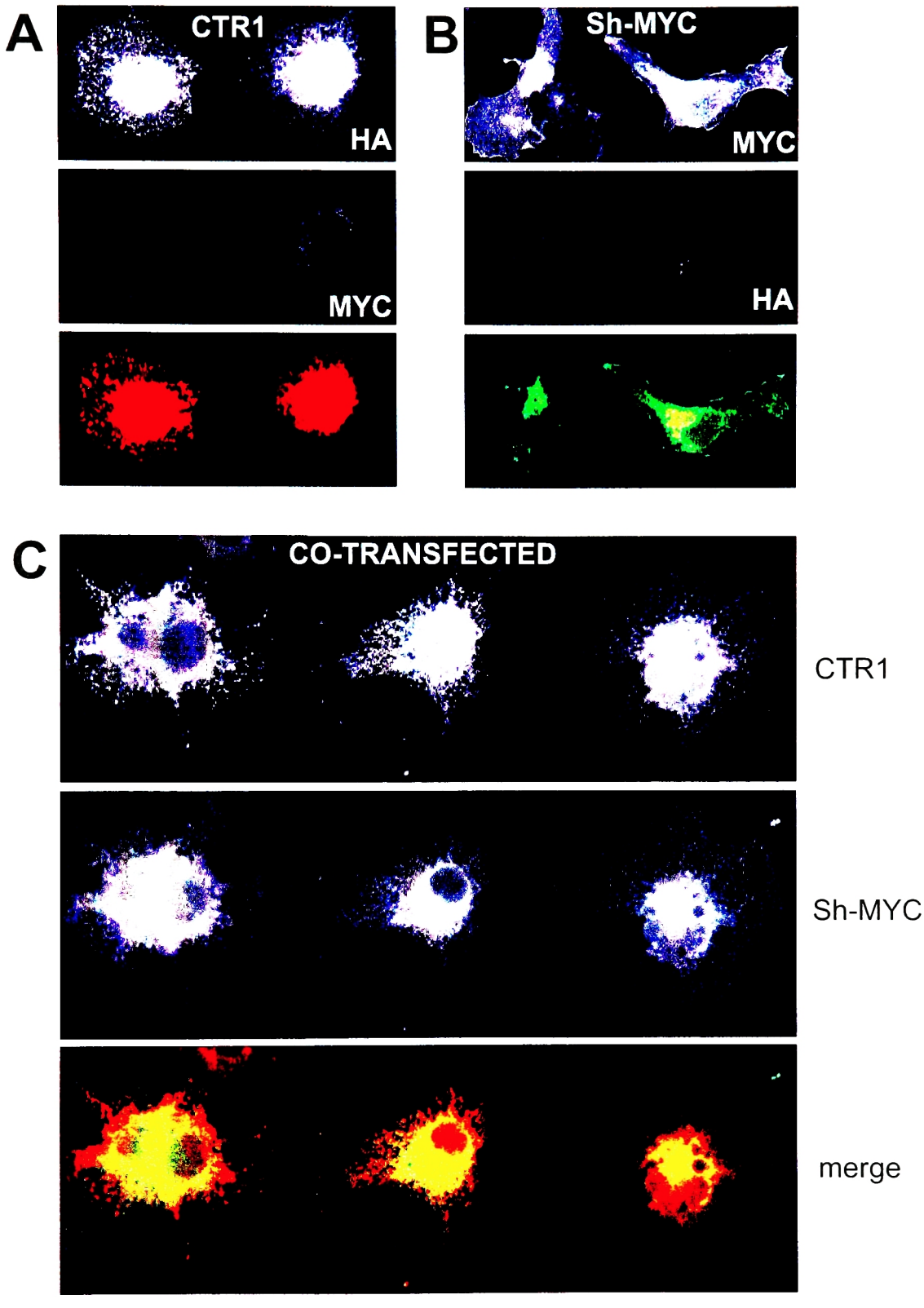

Figure 6.8 : Immunofluorescence microscopy on co-expressed CTR1 and full length Shaker. COS-1 cells expressing either **(A)** HA-CTR1 alone, **(B)** full length Sh-MYC alone, or **(C)** HA-CTR1 and Sh-MYC, were fixed and stained with α-HA (red) and α-MYC (green) antibodies.

7. DISCUSSION

In the work presented here, we have studied the process by which a voltage-gated potassium channel attains its final form, function and location in the cell. We have focused on certain aspects of this complex series of events, namely, targeting to the endoplasmic reticulum (ER), integration into the ER membrane, glycosylation and folding within the ER, and traffic out of the ER to the cell surface.

7.1. N-linked glycosylation in Shaker folding and traffic

7.1.1. Secretory delivery to the cell surface

Given the conserved nature of the N-linked glycosylation site(s) in the first extracellular loop of the voltage-gated potassium channels, it is surprising that all studies to date suggest only slight, if any, effects of partially or completely blocking the glycosylation process. To the extent it has been studied, this is true both for the effect of sugar groups on the biophysical properties of the mature channel, as well as on its intracellular folding and traffic. Glycans in mature proteins at the cell surface commonly affect adhesion properties, protein-protein interactions or serum stability. In addition, for an ion channel that responds to changes in membrane potential, the charged nature of many complex sugars could be expected to modulate gating. That Shaker-like channels without sialic acid show a depolarized shift in voltage-dependent activation is in keeping with this prediction (Thornhill et al., 1996). Since this has been studied only in heterologous cells, however, it is unclear to what extent it impacts physiology.

The same criticism holds true for our own and other work on Shaker channel traffic through the secretory pathway. We have studied the effects of glycosylation on traffic of the Shaker channel. The initial rate of delivery of unglycosylated N259Q+N263Q (NQ) mutant Shaker to the surface of COS cells is slowed, compared to that of wild type, but the fraction of either channel on the surface at steady state does not measurably differ. At least part of the retardation in mutant Shaker is due to slowed traffic early in the secretory pathway, possibly at the level of transport out of the endoplasmic reticulum. Aplysia Kv1 (sqKv1A) channels that had been rendered unglycosylated by mutation showed a similar retardation in initial arrival at the surface of Xenopus oocytes, whereas the steady state surface levels, determined electrophysiologically, were indistinguishable from wild type (Liu et al., 2001). Given the sequence similarity (Chandy and Gutman, 1995) of the Drosophila and Aplysia channels, the identical location of the glycosylation site, and the very similar consequences of mutating this site for traffic of either channel, it is reasonable to assume that the sqKv1A channel is also retarded in the ER-Golgi traffic step. It is worth noting that the experiment in oocytes was done at a lower temperature than in mammalian cells (20°C versus 37°C). If the basis for slower surface delivery of the squid and fly channels is indeed the same, then it appears that the putative folding defect of the unglycosylated channel is not completely rescued at lower temperature. This is consistent with the fact that we measured a difference between wild type and mutant Shaker traffic in the early secretory pathway at 20°C.

In contrast to our results, others have reported a 3 to 5-fold decrease in the surface fraction of unglycosylated Shaker relative to wild type in HEK293T cells (Khanna et al.,

2001b). Traffic kinetics were not measured in these experiments, but it is not implausible that slowed traffic of mutant Shaker affects its steady state surface level to a greater or lesser degree, depending on the cell type. Curiously, unglycosylated channel was also more rapidly degraded than wild type in HEK293T cells, in a lactacysin-sensitive and brefeldin A (BFA)-insensitive manner. This led to the interpretation that mutant degradation occurred in the cytosolic proteasome, directly from the ER. All other things being equal, increased degradation of the mutant from an intracellular location should result in lower total protein levels, compared to wild type, but a *higher* surface fraction, at steady state. They did not compare overall protein levels. Possibly, degradation in the prolonged (36 hr) presence of BFA is not a reliable indicator of the situation in actively trafficking cells. Selective degradation of surface unglycosylated channel or retarded delivery to the cell surface would be more consistent with the steady state surface levels reported in (Khanna et al., 2001b).

7.1.2. Endocytic retrieval from the cell surface

The surface level of a protein may depend upon the relative rates of several processes, including surface delivery via the secretory pathway, surface delivery via the recycling pathway, internalization from the cell surface and degradation. All other rates being equal, since WT and NQ channels are delivered to the cell surface at different initial rates, there should theoretically be a difference in the steady state surface fraction, in our experiments. Since the difference in initial surface delivery rate is not large, however (about two fold), it is possible that any difference at steady state is within the experimental variation. This (theoretical) difference in steady state levels would shrink further if the endocytic rate, of both channels, is slow in comparison to secretion.

Alternatively, similar surface levels of WT and NQ Shaker could be the result of a compensatory difference in endocytic or recycling rates. Although the oligosaccharide groups are topologically extracellular, there is substantial precedent for transmembrane lectin-mediated regulation of glycoprotein traffic in the cell. Specifically, interactions with transmembrane lectins have been suggested as a mechanism for targeting glycosylated proteins to the apical surface of polarized cells (Zafra and Gimenez, 2001; Scheiffele et al., 1995). Our attempts to compare WT and NQ mutant Shaker endocytic rates were unsuccessful.

7.1.3. Traffic in the early secretory pathway

We further dissected Shaker channel secretory traffic in mammalian cells. Using intranuclear microinjection and quantitative imaging, we compared the ER-Golgi traffic rates of wild type and mutant unglycosylated Shaker. We found that unglycosylated Shaker appeared more slowly in the Golgi than the wild type, at 20°C. We would predict that this difference contributes at least partially to the difference in surface delivery rate of the two channels, at 37°C. We cannot formally distinguish between an effect of glycosylation on retrograde (ERGIC-ER or *cis* Golgi-ER as compared to forward (ER-Golgi) secretory traffic. Based on the fact that first, retrograde traffic is coatomer-mediated and, second, coatomer does function in forward secretory traffic at 20°C, the prediction is that retrograde traffic also does occur at the lower temperature. In principle, if loss of glycosylation speeded up channel retrograde movement, this would also result in apparently slower traffic from ER to Golgi. However, the net effect would be the same, namely slower traffic through the secretory pathway to the cell surface.

Similarly, since our experiment only monitors Shaker co-localization with the Golgi, we cannot theoretically distinguish between effects of glycosylation on ER-ERGIC versus ERGIC-Golgi traffic. The ERGIC is a dynamic compartment at the functional interface of the ER and the Golgi, and is regarded by some as representing a maturation of ER-Golgi transport intermediates, rather than as a discrete organelle. The fact that proteins that cycle between ER, ERGIC and *cis*-Golgi can be blocked at the ER-ERGIC (Appenzeller et al., 1999; Pryde et al., 1998; Shima et al., 1998; Andersson et al., 1999), ERGIC-ER or ERGIC-Golgi (Lippincott-Schwartz et al., 1990; Klumperman et al., 1998; Palokangas et al., 1998) stages of this cycle suggests that the compartments are, in fact, distinct. At the ultrastructural level, the ERGIC is seen to form vesiculo-tubular clusters that are morphologically distinguishable from both the ER reticulum and Golgi cisternae (Aridor et al., 1995; Klumperman et al., 1998). At the level of light microscopy, however, the ERGIC may not be entirely distinguishable from the ER and the *cis*-Golgi (Hammond and Glick, 2000; Hauri et al., 2000). We have not examined the degree to which a protein in the ERGIC could contribute to our Golgi-localized fluorescence signal. Even if the ERGIC were 100% co-localized with the Golgi in our images, however, this would not invalidate the experiment. Rather, it would be suggestive of an effect of Shaker glycosylation at a pre-ERGIC stage of secretion. The fact that ER resident proteins did not significantly co-localize with the Golgi is far more central for our interpretation of the experiment, namely, that exit of the unglycosylated mutant Shaker channel from the ER occurs slower than than of wild type.

Lastly, it is possible that in addition to the effects on transport from the ER to the Golgi, there is a difference between mutant and wild type in terms of their Golgi-plasma

membrane transport rates. A similar imaging experiment to compare these rates, although theoretically feasible, becomes complicated by the fact that the two channels differ markedly in the extent to which traffic out of the ER occurs, even after 4-5 hours of traffic at 20°C. This makes quantitative interpretation of a "Golgi exit" experiment very difficult. Importantly, inhibition of Golgi glycosylation enzymes seems to have little effect on the transport of a number of proteins (Elbein, 1991; Stanley, 1984).

7.1.4. Possible explanations for retarded N259Q+N263Q traffic

The most obvious explanation for slowed ER-Golgi traffic of unglycosylated Shaker is that the absence of the carbohydrate moiety results in a reduced rate of channel folding, slower acquisition of an ER export-competent conformation, and consequently slower ER export. As already mentioned, this could be through a direct effect of the sugar groups on folding rate, as has been demonstrated *in vitro* on other proteins (Imperiali and O'Connor, 1999; Wormald and Dwek, 1999; Kern et al., 1993). Alternatively, but not necessarily exclusively, the effect of glycosylation could be indirect, via interaction with a chaperone, the obvious candidates being the lectin-like chaperones calnexin and calreticulin (CNX/CRT). Surface delivery of the WT channel is not significantly affected by the ER-glucosidase inhibitor castanospermine, which greatly reduces interaction of Shaker with calnexin. This does not, of course, rule out a role for the chaperone in Shaker biogenesis, but it does indicate that such a role, if any, is not rate limiting in the glycosylation-dependent effect that we report here. Alternatively, this could merely be yet another example of redundancy in ER chaperone function, as has been previously demonstrated (Zhang et al., 1997; Braakman and van Anken, 2000; Gaudin, 1997). We have not determined whether abolishing glycosylation leads to

increased association of mutant Shaker with the lumenal ATPase BiP, as has been shown for some other proteins (Molinari and Helenius, 2000). BiP levels are not increased in COS cells expressing NQ mutant Shaker, relative to WT, suggesting that the mutant channel does not induce a stress response (data not shown). This is consistent with the apparently rather mild effect of the NQ mutations on channel assembly, traffic and mature structure. Finally, it is possible that there are other glycosylation-dependent chaperones that promote either folding or export of the Shaker channel. We have not determined whether or not the putative "glycoprotein transport receptor" ERGIC 53 (Appenzeller et al., 1999) interacts with Shaker. It is certainly conceivable that it, or some other unidentified ER-Golgi transport factor, affects Shaker channel traffic out of the ER in a glycosylation dependent manner.

7.1.5. Does Shaker glycosylation matter ?

Since the activity of an excitable cell is determined by the type and number of ion channels on its cell surface, factors that affect one or other of these parameters could affect cell and organismal physiology. An authentic understanding of whether or not voltage-gated potassium channel glycosylation is important will require experiments in homologous systems. As it stands, we do not know (i) if the rate differences observed in tissue culture also exist in neurons and/or muscle, either of Drosophila or of mammals, (ii) if such rate differences, if any, have an effect on channel surface levels, and (iii) if the difference in surface levels, if any, has an effect on physiology. A transgenic Drosophila line expressing the unglycosylated channel could be extremely informative. Reduced channel surface levels in fly muscle would be predicted to result in a classical *Shaker* phenotype, with uncontrolled leg-twitching under ether anesthesia. Indeed, reduction in

channel surface levels contributes partially, if not completely, to the hyperexcitability of mutants at the hyperkinetic locus (Chouinard et al., 1995), and of some mutants (e.g. Sh^{E62}) at the Shaker locus (Jan et al., 1983).

7.2. Regulation of ion channel traffic

7.2.1. Regulation of channel levels at the plasma membrane

The cell surface levels of several pumps, transporters and channels are dynamically regulated by varying the rates of exocytosis/ endocytosis at the plasma membrane (Al Awqati, 1985; Rea and James, 1997). For instance, the levels of the H^+ATPase at the apical surface of bladder epithelial cells increase substantially in response to carbon dioxide, thus effecting increased trans-epithelial proton flux (Cannon et al., 1985). Likewise, insulin treatment causes net translocation of the glucose transporter GLUT4 from an intracellular location to the surface of the cell, as a result of increased exocytic and decreased endocytic rates (Jhun et al., 1992). Phosphorylation-based modulation of cell surface expression has been suggested for the gap junctions (Musil et al., 1990) and for CFTR (Weber et al., 1999; Weber et al., 2001), although differing conclusions have been reached in other studies of CFTR (Moyer et al., 1998).

7.2.2. Do ER export sequences regulate K^+ channel surface levels ?

In addition to, and most likely interfacing with, the effect of extracellular stimuli, regions within the polypeptide itself are often important for directing sub-cellular traffic. In the case of the potassium channels, the recent identification of ER export sequences in the C-termini of mammalian K_{IR} channels (Ma et al., 2002; Ma et al., 2001) has led to speculation that regulated ER exit may be a mechanism for adjusting channel surface

profiles. This could, broadly speaking, occur in one of two ways. First, accessibility of the export sequence to decoding factors (for instance, coat proteins or transport receptors) could be regulated, depending on the needs of the cell. Second, since heteromultimerization can occur between channel sub-family members with very different intrinsic tendencies to traffic out of the ER, changes in the relative levels of different monomers could vary the surface channel profile of the cell. Although heterologous co- expression of voltage-gated channels with inherently different surface expression levels (Kv1.1< Kv1.2< Kv1.4) was seen to produce heteromultimers with intermediate properties (Manganas and Trimmer, 2000), intrinsic cellular regulation of the surface repertoire in this manner has not been reported.

7.2.3. The Shaker carboxyl terminus in traffic out of the ER

Putative ER export sequences in the voltage-gated channels have not been extensively characterized. We carried out preliminary experiments on C-terminal truncations of Shaker (CTR), to begin to define regions of the cytosolic tail that may be required for ER export. Removal of the last 60 amino acids of Shaker (CTR3) had no deleterious effect on ER-Golgi traffic. If a further 50 amino acids were deleted (CTR2), pulse-chase experiments as well as immunostain indicated that traffic out of the ER occurred slower. Further experiments are required, including a more statistical comparison of the CTR2 and FL Shaker immunofluorescence pattern, before any definitive statement can be made. Nevertheless, in the event that there *is* an ER export signal in the central region of the Shaker C-terminal tail (aa 539-592), it is clearly not absolutely required, but rather, increases the rate of the ER export process. In contrast, Shaker that entirely lacks the C terminal tail (CTR1) is completely retained in the ER.

We cannot as yet distinguish between a folding defect or a transport defect of CTR1. This has been discussed in chapter 6, and will therefore not be repeated here.

7.3. Biogenesis of Shaker in the endoplasmic reticulum

7.3.1. Characterization of Shaker translated *in vitro*

In vitro translation of the Shaker channel had not been well characterized prior to this work. Shaker translated in rabbit reticulocyte lysate (RRL) targets efficiently to canine and porcine pancreatic microsomes, stably integrates into the bilayer and assembles into tetramers. The RRL/pancreatic microsome system reproduces the glycosylation-dependent interaction between Shaker and the chaperone calnexin seen in the ER of tissue culture cells. Efficient targeting and integration do not preclude aberrant assembly, since certain preparations of microsomes were seen to produce entirely aggregated, albeit targeted and integrated, channel.

The Shaker monomer is a 656 amino acid protein and migrates on SDS-PAGE with an apparent molecular weight of 70-75 kD. In translations of Shaker in reticulocyte lyate, there is consistently an additional prominent band at ~ 30 kD. The 30 kD band is recognized by antibodies to an HA epitope tag at the carboxyl terminus of the channel, indicating that it is a C-terminal fragment of the Shaker protein. Interestingly, this band is also seen on Western blots of Shaker transfected into COS, HeLa or HEK293T cells (not shown), and a similar C-terminal fragment has recently been reported for the mammalian Kv1.1 channel expressed in COS. The amino-terminal end of the 30K fragment is not known. Further it is not clear whether it is generated by internal initiation or by proteolytic cleavage, and if it is of any significance for Shaker physiology. *In vitro*,

the 30K band was targeted and integrated efficiently, but it was neither glycosylated nor tetramerized (not shown). Since the glycosylation sites are in the amino-terminal half of Shaker, this is again consistent with the 30K band being a carboxyl terminus fragment. Presumably, it contains at least one TM domain, by which it targets and integrates into the ER. Essentially, then, the 30K fragment must consist of at least TM6 (and possibly TM5) together with the (177 aa) cytosolic carboxyl terminus. Especially if it turns out that there is indeed ER export information in the Shaker cytosolic tail, it is tantalizing to speculate that this 30K fragment may be involved, in some currently non-obvious way, in the regulation of channel traffic out of the ER.

7.3.2. Targeting of Shaker to the endoplasmic reticulum

Using a series of truncated constructs, we showed that Shaker TM1 (transmembrane domain 1) is likely to be the earliest targeting information in the nascent Shaker polypeptide. Further, when TM1 has adequately emerged from the ribosome, it is also sufficient to effect this process. However, a major caveat to this interpretation is discussed in the next section. The T2 construct (23 amino acids after TM1) does not target to the ER whereas T2.1 (40 amino acids after TM1) does, as do all longer constructs. It is the added length of the nascent chain in T2.1, and not the specific sequence, that is most probably important, since replacement of all amino acids after T2 with random sequence produces a construct that is still able to target efficiently. Our observations are in keeping with previous studies on Kv1.1 channel targeting in vitro (Shen et al., 1993). In this case, too, TM1 was found to be minimally required for efficient ER targeting. In contrast, the lymphocyte Kv1.3 channel was shown to require TM1 and TM2 for efficient targeting to the ER (Tu et al., 2000). However, the

possibility that this reflected a requirement for sufficient polypeptide length after TM1, and not TM2 *per se*, was not addressed.

Although we have not precisely defined the minimum length of the TM1-TM2 loop that must be synthesized in order that TM1 emerges sufficiently from the ribosome, we have narrowed it down to between 23 and 40 amino acids after TM1. This is in keeping with current understanding of the ribosomal "tunnel", which estimates that 30 – 40 nascent chain amino acids are protected by the ribosomal subunits (Malkin and Rich, 1967; Blobel and Sabatini, 1970; Matlack and Walter, 1995), and are therefore not free to interact with cytosolic factors. In contrast, studies on the seven-TM domain membrane protein rhodopsin have shown that nascent chains truncated immediately after TM1 are still able to target to co-translationally added ER microsomes (S.M. Simon, unpublished experiments). This requires that opsin TM1, which by conventional wisdom is buried within the ribosomal tunnel, can direct targeting of the ribosome-nascent chain complex to the ER. There is no evidence for this in the case of Shaker. This may reflect the fact that opsin and Shaker are topologically different proteins. The Shaker N-terminus is cytosolic whereas the opsin N-terminus is translocated to the ER lumen. Possibly, the targeting program varies for these two proteins.

T2, but not T2.1 – T5, shows an aberrantly prolonged association with the tRNA. The partial puromycin insensitivity of this association indicates that it is (partially) not in the context of a functional ribosome. We cannot completely rule out that this prolonged tRNA association is causally linked to inefficient T2 targeting. The argument against this interpretation is that, in our analysis of T2 targeting, we have only taken into account the released (ie non-tRNA attached) form of the protein. In our experience with truncated

constructs lacking stop codons, a certain (unpredictable) fraction does show an increased propensity to remain tRNA-attached even after puromycin treatment, as seen for T2. If targeting of only the puromycin-releasable protein is assessed, there is typically no correlation with a targeting problem. However we do not really know when, in the course of our experiment, release of T2 from the tRNA occurred. In other words, it is possible that fully synthesized (272aa), ribosome-released T2 was never present during incubation with ER microsomes, but only as an aberrant, targeting-incompetent complex with the tRNA. In this scenario, the released protein that is seen on the gel (and quantified to assess targeting) could have been generated during post-translational processing of the sample. Experiments that assess targeting of puromycin-released constructs (T2-T5) lacking stop codons could be informative. Specifically, it would be interesting to know whether the existing trend in targeting efficiency persists for truncated constructs that have been specifically released by puromycin in the presence of ER microsomes.

In part as a consequence of this alternative interpretation of our data, we examined the ER targeting of the T2 and T3 constructs expressed in COS cells in order to validate (or invalidate) the *in vitro* data at the cellular level. Targeting of the T2 construct was much more efficient than seen *in vitro*. However, immunostain of transfected cells clearly showed diffusely localized (probably cytosolic) T2 in about 70% of cells, whereas T3 was tightly co-localized with the ER. This suggests that inefficient T2 targeting *in vitro* reflects to some degree, although not with precision, the situation in the cellular milieu.

7.3.3 Membrane integration of Shaker : a role for TRAM ?

The translocon associated membrane protein (TRAM) has remained functionally somewhat engimatic. As the name suggests, it associates with the translocon, and has been shown to cross-link to a number of protein nascent chains. In one case, cross-linking intensity to sec 61α (the translocon) and TRAM was seen to vary inversely for membrane protein nascent chains of different lengths, leading to the suggestion of a "hand-off" of the nascent protein from the translocon to TRAM (Do et al., 1996). While cross-linking does suggest proximity of the protein nascent chain to TRAM, a functional significance of this proximity remains to be established. TRAM has been implicated in translocational pausing of a secreted protein (Hegde et al., 1998) and in early steps of translocation for some signal sequences (Voigt et al., 1996).

In experiments designed to further investigate a possible role for this poorly understood protein in channel biogenesis, we examined the targeting, integration and tetramerization of Shaker in microsomes that had been depleted of glycoproteins. The rationale was that none of the proteins that comprise the "basal" translocation/integration machinery are glycosylated, whereas TRAM is. The specificity of the effect was tested by comparison with solubilized, mock-depleted microsomes and with depleted microsomes that were reconstituted with purified TRAM. Targeting of Shaker was reduced in the depleted microsomes. Further, the Shaker that was targeted proved to be incompletely integrated into the bilayer. Lastly, the Shaker that was integrated was seen largely in high molecular weight complexes, under non-denaturing conditions, suggesting that it was aberrantly assembled and/or folded. The effects on Shaker targeting and

assembly were not specific to TRAM. The efficient integration of Shaker into the membrane, however, significantly and specifically correlated with TRAM.

It is worth noting that, in our experience, integration of targeted membrane proteins is a difficult process to disrupt (although integration in the correct topology may be another issue entirely). Targeting is easily abrogated with many different perturbations (i.e. various treatments of ER microsomes, mutations or truncations of the substrate protein itself). However, all targeted membrane protein almost always integrates into an alkali-inextractable form. TRAM depletion is the only treatment that we have seen to affect Shaker integration *beyond* any effects it has on ER targeting.

Interestingly, TRAM has been reported to remain in prolonged proximity, as measured by cross-linking, to nascent chains of a membrane protein in which charged residues were introduced into the TM domain, and which was consequently impaired in its ability to stably integrate into the bilayer (Heinrich et al., 2000). TM4 of Shaker, which constitutes the channel voltage sensor, contains seven positively charged residues (Papazian et al., 1991; Jan and Jan, 1992; Liman et al., 1991). Charged voltage sensing TM domains are not only present in all voltage-sensitive ion channels (Catterall, 1988), as might be expected, but in the cyclic nucleotide-gated channels as well (Kaupp et al., 1989). Moreover, pore-lining TM domains of many ion channels, by virtue of the fact that they must face both a hydrophobic and an aqueous environment, tend to be amphipathic, rather than hydrophobic. It is interesting to speculate that there exists a specific ER machinery to assist in the integration of sub-optimal transmembrane domains such as these. A systematic examination of the integration of proteins of varying

hydrophobicity in the presence and absence of TRAM may prove informative, in this regard.

7.3.4. Folding of Shaker in the endoplasmic reticulum

We attempted to further dissect the misassembly (i.e. the aggregation on sucrose gradients) of the Shaker channel translocated into solubilized, reconstituted microsomes. Since these microsomal preparations were (i) glycosylation-deficient and (ii) significantly depleted for lumenal proteins, we examined whether either of these treatments (or a combination, not shown) also caused Shaker aggregation. Neither block of Shaker glycosylation nor depletion of microsome lumenal content could reproduce the extent of Shaker aggregation seen in solubilized microsome preparations, although a lack of ER lumenal chaperones was correlated with a slightly increased tendency of Shaker to aggregate.

Taken at face value, ER lumenal chaperones appear virtually dispensable for Shaker channel assembly. However, it has been shown that depletions of ER lumenal proteins (either by alkali extraction or by saponin treatment) require the presence of ATP for effective removal of the lumenal hsp70 homologue BiP (Hebert et al., 1998). Since we were trying to mimic preparation of the reconstituted membranes (i.e. the rRM and cRM), our depletions were done in the absence of ATP. We have not tested BiP levels of our alkali- and saponin-treated preparations, but the chaperone is likely to be measurably present. So, we cannot broadly rule out a role for all ER lumenal factors in channel assembly, based on these experiments. Depletion of protein disulfide isomerase (PDI) to less than 5% of normal levels, however, has minimal consequences for Shaker tetramerization.

7.3.5. Do ion channels conduct ions at intracellular organelles ?

Sucrose gradient centrifugation shows that Shaker channel prepared *in vitro* assembles into tetramers, in a manner indistinguishable from Shaker prepared in the cellular ER. However, it is not clear to what degree immature (ie ER-localized) channels are functional for the conduction of ions, and if so, whether conduction does indeed occur at this intracellular location en route to the plasma membrane. This aspect of Shaker cell biology is additionally interesting since it applies to ion channels in general. The presence of large numbers of promiscuously open ion channels in the limiting membranes of various intracellular organelles is likely to be an undesirable proposition for the cell. In the case of the voltage-gated potassium channels, since there is probably no potential difference across the ER membrane, the channels are likely to be in the inactivated state. The HVA voltage-gated calcium channels, however, would not inactivate rapidly at 0 mV (Hille, 1984). It is quite possible that unregulated activity of large numbers of calcium channels at the ER membrane would be deleterious to the cell. On the other hand, it is also possible that the extensive cellular machinery that has evolved to lower cytosolic calcium levels following signaling events is also capable of counteracting a basal "leak" of the ion from various organelles into the cytosol.

Speculation notwithstanding, very little is known about when in its biogenesis, an ion channel or a receptor typically attains its fully functional form. In principle, there are several ways in which the function of a receptor or channel could be restricted to the plasma membrane, such that deleterious intracellular effects are avoided. In the simplest model, the protein may not acquire function until it has reached the plasma membrane. The EGF receptor is thought to acquire the ability to bind EGF in the Golgi, although

there was no requirement shown for exit from the ER *per se* (Gamou et al., 1989). Similarly, the connexins have been reported to assemble into functional gap junctions only in the Golgi apparatus (Musil et al., 1990), although this view has been challenged by the fact that connexins translated *in vitro* and translocated into ER microsomes were seen to be functional channels when fused to a planar lipid bilayer (Falk et al., 1997). In an alternative model for the prevention of harmful intracellular activity, a channel or receptor could fold to a functional state in the ER, but remain inhibited. Such inhibition could be active, via interaction with a negative regulator, or passive, resulting from the absence of the appropriate stimulus (i.e. potential difference, in the case of a voltage-gated channel, or ligand, in the case of a receptor). Notably, the RAP chaperone/escort protein has been proposed as a negative regulator of ligand binding to members of the LDL receptor family, until traffic of the receptor past the medial Golgi has occurred (Bu et al., 1995; Moestrup and Gliemann, 1991; Herz et al., 1991; Biemesderfer et al., 1993; Bu and Schwartz, 1998).

Perhaps the best evidence for the fact that ion channels *can* attain their functional form in the ER comes from the reconstitution of *in vitro* translated/translocated Shaker and gap junctions into planar lipid bilayers (Rosenberg and East, 1992; Falk et al., 1997). However, the sensitivity of the electrophysiological approach (a single channel per microsome could theoretically be detected), precludes an assessment of the extent to which the functional pores were representative of the majority of channels. This caveat also applies to the report that ion channels with the properties of voltage-gated channels of the neuronal plasma membrane were identified in vesicles isolated from squid axoplasm (Wonderlin and French, 1991). We wished to examine whether or not ER-

localized Shaker binds the peptide toxin agitoxin, or in other words, whether the pore of the ER-localized channel has attained its characteristic extracellular fold. Unfortunately, our attempts to establish this assay, either in microsomes or in the cellular ER, did not reach fruition.

BIBLIOGRAPHY

Accili,E.A., Kiehn,J., Yang,Q., Wang,Z., Brown,A.M., and Wible,B.A. (1997). Separable Kvbeta subunit domains alter expression and gating of potassium channels. J Biol. Chem. *272*, 25824-25831.

Accili,E.A., Kuryshev,Y.A., Wible,B.A., and Brown,A.M. (1998). Separable effects of human Kvbeta1.2 N- and C-termini on inactivation and expression of human Kv1.4. J Physiol *512 (Pt 2)*, 325-336.

Adelman,J.P., Bond,C.T., Pessia,M., and Maylie,J. (1995). Episodic ataxia results from voltage-dependent potassium channels with altered functions. Neuron *15*, 1449-1454.

Aebi,M. and Hennet,T. (2001). Congenital disorders of glycosylation: genetic model systems lead the way. Trends Cell Biol. *11*, 136-141.

Aggarwal,S.K. and MacKinnon,R. (1996). Contribution of the S4 segment to gating charge in the Shaker K+ channel. Neuron *16*, 1169-1177.

Aiyar,J., Grissmer,S., and Chandy,K.G. (1993). Full-length and truncated Kv1.3 K+ channels are modulated by 5-HT1c receptor activation and independently by PKC. Am. J. Physiol *265*, C1571-C1578.

Akabas,M.H. and Karlin,A. (1995). Identification of acetylcholine receptor channel-lining residues in the M1 segment of the alpha-subunit. Biochemistry *34*, 12496-12500.

Al Awqati,Q. (1985). Rapid insertion and retrieval of pumps and channels into membranes by exocytosis and endocytosis. Soc. Gen. Physiol Ser. *39*, 149-157.

Albrecht,B., Woisetschlager,M., and Robertson,M.W. (2000). Export of the high affinity IgE receptor from the endoplasmic reticulum depends on a glycosylation-mediated quality control mechanism. J. Immunol. *165*, 5686-5694.

Aldrich,R.W. (1994). Potassium channels. New channel subunits are a turn-off. Curr. Biol. *4*, 839-840.

Anderson,D.J. and Blobel,G. (1981). In vitro synthesis, glycosylation, and membrane insertion of the four subunits of Torpedo acetylcholine receptor. Proc. Natl. Acad. Sci. U. S. A *78*, 5598-5602.

Andersson,H., Kappeler,F., and Hauri,H.P. (1999). Protein targeting to endoplasmic reticulum by dilysine signals involves direct retention in addition to retrieval. J Biol. Chem. *274*, 15080-15084.

Antonny,B., Madden,D., Hamamoto,S., Orci,L., and Schekman,R. (2001). Dynamics of the COPII coat with GTP and stable analogues. Nat. Cell Biol. *3*, 531-537.

Antonny,B. and Schekman,R. (2001). ER export: public transportation by the COPII coach. Curr. Opin. Cell Biol. *13*, 438-443.

Appenzeller,C., Andersson,H., Kappeler,F., and Hauri,H.P. (1999). The lectin ERGIC-53 is a cargo transport receptor for glycoproteins. Nat. Cell Biol. *1*, 330-334.

Aridor,M., Bannykh,S.I., Rowe,T., and Balch,W.E. (1995). Sequential coupling between COPII and COPI vesicle coats in endoplasmic reticulum to Golgi transport. J Cell Biol. *131*, 875-893.

Aridor,M., Fish,K.N., Bannykh,S., Weissman,J., Roberts,T.H., Lippincott-Schwartz,J., and Balch,W.E. (2001). The Sar1 GTPase coordinates biosynthetic cargo selection with endoplasmic reticulum export site assembly. J Cell Biol. *152*, 213-229.

Ashcroft,F.M., Ashcroft,S.J., and Harrison,D.E. (1988). Properties of single potassium channels modulated by glucose in rat pancreatic beta-cells. J Physiol *400*, 501-527.

Attardi,B., Takimoto,K., Gealy,R., Severns,C., and Levitan,E.S. (1993). Glucocorticoid induced up-regulation of a pituitary K+ channel mRNA in vitro and in vivo. Receptors. Channels *1*, 287-293.

Babenko,A.P., Aguilar-Bryan,L., and Bryan,J. (1998). A view of sur/KIR6.X, KATP channels. Annu. Rev. Physiol *60*, 667-687.

Babila,T., Moscucci,A., Wang,H., Weaver,F.E., and Koren,G. (1994). Assembly of mammalian voltage-gated potassium channels: evidence for an important role of the first transmembrane segment. Neuron *12*, 615-626.

Barhanin,J., Lesage,F., Guillemare,E., Fink,M., Lazdunski,M., and Romey,G. (1996). K(V)LQT1 and lsK (minK) proteins associate to form the I(Ks) cardiac potassium current. Nature *384*, 78-80.

Barlowe,C., Orci,L., Yeung,T., Hosobuchi,M., Hamamoto,S., Salama,N., Rexach,M.F., Ravazzola,M., Amherdt,M., and Schekman,R. (1994). COPII: a membrane coat formed by Sec proteins that drive vesicle budding from the endoplasmic reticulum. Cell *77*, 895-907.

Bass,J., Chiu,G., Argon,Y., and Steiner,D.F. (1998). Folding of insulin receptor monomers is facilitated by the molecular chaperones calnexin and calreticulin and impaired by rapid dimerization. J Cell Biol. *141*, 637-646.

Bennett,E., Urcan,M.S., Tinkle,S.S., Koszowski,A.G., and Levinson,S.R. (1997). Contribution of sialic acid to the voltage dependence of sodium channel gating. A possible electrostatic mechanism. J. Gen. Physiol *109*, 327-343.

Berkower,C., Taglicht,D., and Michaelis,S. (1996). Functional and physical interactions between partial molecules of STE6, a yeast ATP-binding cassette protein. J Biol. Chem. *271*, 22983-22989.

Bermak,J.C., Li,M., Bullock,C., and Zhou,Q.Y. (2001). Regulation of transport of the dopamine D1 receptor by a new membrane- associated ER protein. Nat. Cell Biol. *3*, 492-498.

Biemesderfer,D., Dekan,G., Aronson,P.S., and Farquhar,M.G. (1993). Biosynthesis of the gp330/44-kDa Heymann nephritis antigenic complex: assembly takes place in the ER. Am. J Physiol *264*, F1011-F1020.

Blobel,G. and Sabatini,D.D. (1970). Controlled proteolysis of nascent polypeptides in rat liver cell fractions. I. Location of the polypeptides within ribosomes. J Cell Biol. *45*, 130-145.

Bockenhauer,D. (2001). Ion channels in disease. Curr. Opin. Pediatr. *13*, 142-149.

Borel,A.C. and Simon,S.M. (1996). Biogenesis of polytopic membrane proteins: membrane segments assemble within translocation channels prior to membrane integration. Cell *85*, 379-389.

Braakman,I. and van Anken,E. (2000). Folding of viral envelope glycoproteins in the endoplasmic reticulum. Traffic. *1*, 533-539.

Breitwieser,G.E. (1996). Mechanisms of K+ channel regulation. J Membr. Biol. *152*, 1-11.

Bu,G., Geuze,H.J., Strous,G.J., and Schwartz,A.L. (1995). 39 kDa receptor-associated protein is an ER resident protein and molecular chaperone for LDL receptor-related protein. EMBO J *14*, 2269-2280.

Bu,G. and Schwartz,A.L. (1998). RAP, a novel type of ER chaperone. Trends Cell Biol. *8*, 272-276.

Bugg,T.D. and Brandish,P.E. (1994). From peptidoglycan to glycoproteins: common features of lipid-linked oligosaccharide biosynthesis. FEMS Microbiol. Lett. *119*, 255-262.

Bulleid,N.J. and Freedman,R.B. (1990). Cotranslational glycosylation of proteins in systems depleted of protein disulphide isomerase. EMBO J *9*, 3527-3532.

Butler,A., Wei,A.G., Baker,K., and Salkoff,L. (1989). A family of putative potassium channel genes in Drosophila. Science *243*, 943-947.

Cannon,C., van Adelsberg,J., Kelly,S., and Al Awqati,Q. (1985). Carbon-dioxide-induced exocytotic insertion of H+ pumps in turtle- bladder luminal membrane: role of cell pH and calcium. Nature *314*, 443-446.

Cannon,K.S. and Helenius,A. (1999). Trimming and readdition of glucose to N-linked oligosaccharides determines calnexin association of a substrate glycoprotein in living cells. J Biol. Chem. *274*, 7537-7544.

Catterall,W.A. (1988). Structure and function of voltage-sensitive ion channels. Science *242*, 50-61.

Chan,K.W., Csanady,L., Seto-Young,D., Nairn,A.C., and Gadsby,D.C. (2000). Severed molecules functionally define the boundaries of the cystic fibrosis transmembrane conductance regulator's NH(2)-terminal nucleotide binding domain. J Gen. Physiol *116*, 163-180.

Chandy,K.G. and Gutman,G.A. (1995). Ligand- and voltage-gated ion channels. In Handbook of Receptors and Channels, R.A.North, ed. CRC Press), pp. 1-71.

Chen,W. and Helenius,A. (2000). Role of ribosome and translocon complex during folding of influenza hemagglutinin in the endoplasmic reticulum of living cells. Mol. Biol. Cell *11*, 765-772.

Chouinard,S.W., Wilson,G.F., Schlimgen,A.K., and Ganetzky,B. (1995). A potassium channel beta subunit related to the aldo-keto reductase superfamily is encoded by the Drosophila hyperkinetic locus. Proc. Natl. Acad. Sci. U. S. A *92*, 6763-6767.

Christie,M.J., Adelman,J.P., Douglass,J., and North,R.A. (1989). Expression of a cloned rat brain potassium channel in Xenopus oocytes. Science *244*, 221-224.

Christie,M.J., North,R.A., Osborne,P.B., Douglass,J., and Adelman,J.P. (1990). Heteropolymeric potassium channels expressed in Xenopus oocytes from cloned subunits. Neuron *4*, 405-411.

Cole, K. S. Electric impedance of *Nitella* during activity. Curtis, H. J. J.Gen.Physiol 22, 37-64. 1938.
Ref Type: Generic

Cole,K.S. (1949). Dynamic electrical characteristics of the squid axon membrane. Arch. Sci. Physiol. *3*, 253-258.

Cole,K.S. (1968). Membranes, Ions and Impulses: A Chapter of Classical Biophysics. (Berkeley: University of California Press), p. -569.

Cole,K.S. and Curtis,H.J. (1939). Electrical impedance of the squid giant axon during activity. J. Gen. Physiol *22*, 649-670.

Cooper,E.C., Milroy,A., Jan,Y.N., Jan,L.Y., and Lowenstein,D.H. (1998). Presynaptic localization of Kv1.4-containing A-type potassium channels near excitatory synapses in the hippocampus. J Neurosci. *18*, 965-974.

Covarrubias,M., Wei,A.A., and Salkoff,L. (1991). Shaker, Shal, Shab, and Shaw express independent K+ current systems. Neuron *7*, 763-773.

Curtis,H.J. and Cole,K.S. (1940). Membrane action potentials from the squid giant axon. J. Cell. Comp. Physiol. *15*, 147-157.

Cushman,S.J., Nanao,M.H., Jahng,A.W., DeRubeis,D., Choe,S., and Pfaffinger,P.J. (2000). Voltage dependent activation of potassium channels is coupled to T1 domain structure. Nat. Struct. Biol. *7*, 403-407.

D'Alessio,C., Fernandez,F., Trombetta,E.S., and Parodi,A.J. (1999). Genetic evidence for the heterodimeric structure of glucosidase II. The effect of disrupting the subunit-encoding genes on glycoprotein folding. J. Biol. Chem. *274*, 25899-25905.

Davis,D.P., Rozell,T.G., Liu,X., and Segaloff,D.L. (1997). The six N-linked carbohydrates of the lutropin/choriogonadotropin receptor are not absolutely required for correct folding, cell surface expression, hormone binding, or signal transduction. Mol. Endocrinol. *11*, 550-562.

De Praeter,C.M., Gerwig,G.J., Bause,E., Nuytinck,L.K., Vliegenthart,J.F., Breuer,W., Kamerling,J.P., Espeel,M.F., Martin,J.J., De Paepe,A.M., Chan,N.W., Dacremont,G.A., and Van Coster,R.N. (2000). A novel disorder caused by defective biosynthesis of N-linked oligosaccharides due to glucosidase I deficiency. Am. J. Hum. Genet. *66*, 1744-1756.

Deal,K.K., Lovinger,D.M., and Tamkun,M.M. (1994). The brain Kv1.1 potassium channel: in vitro and in vivo studies on subunit assembly and posttranslational processing. J Neurosci. *14*, 1666-1676.

Dennis,J.W., Granovsky,M., and Warren,C.E. (1999). Protein glycosylation in development and disease. Bioessays *21*, 412-421.

Deutsch,C. (2002). Potassium channel ontogeny. Annu. Rev. Physiol *64*, 19-46.

Do,H., Falcone,D., Lin,J., Andrews,D.W., and Johnson,A.E. (1996). The cotranslational integration of membrane proteins into the phospholipid bilayer is a multistep process. Cell *85*, 369-378.

Dominguez,M., Dejgaard,K., Fullekrug,J., Dahan,S., Fazel,A., Paccaud,J.P., Thomas,D.Y., Bergeron,J.J., and Nilsson,T. (1998). gp25L/emp24/p24 protein family members of the cis-Golgi network bind both COP I and II coatomer. J. Cell Biol. *140*, 751-765.

Douglass,J., Osborne,P.B., Cai,Y.C., Wilkinson,M., Christie,M.J., and Adelman,J.P. (1990). Characterization and functional expression of a rat genomic DNA clone encoding a lymphocyte potassium channel. J Immunol. *144*, 4841-4850.

Doyle,D.A., Morais,C.J., Pfuetzner,R.A., Kuo,A., Gulbis,J.M., Cohen,S.L., Chait,B.T., and MacKinnon,R. (1998). The structure of the potassium channel: molecular basis of K+ conduction and selectivity. Science *280*, 69-77.

Dustin,M.L., Golan,D.E., Zhu,D.M., Miller,J.M., Meier,W., Davies,E.A., and van der Merwe,P.A. (1997). Low affinity interaction of human or rat T cell adhesion molecule CD2 with its ligand aligns adhering membranes to achieve high physiological affinity. J. Biol. Chem. *272*, 30889-30898.

Ehrenstein,G., Lecar,H., and Nossal,R. (1970). The nature of the negative resistance in bimolecular lipid membranes containing excitability-inducing material. J. Gen. Physiol *55*, 119-133.

El Husseini,A.E., Craven,S.E., Chetkovich,D.M., Firestein,B.L., Schnell,E., Aoki,C., and Bredt,D.S. (2000). Dual palmitoylation of PSD-95 mediates its vesiculotubular sorting, postsynaptic targeting, and ion channel clustering. J Cell Biol. *148*, 159-172.

Elbein,A.D. (1991). Glycosidase inhibitors: inhibitors of N-linked oligosaccharide processing. FASEB J. *5*, 3055-3063.

Ellgaard,L., Molinari,M., and Helenius,A. (1999). Setting the standards: quality control in the secretory pathway. Science *286*, 1882-1888.

Falk,M.M., Buehler,L.K., Kumar,N.M., and Gilula,N.B. (1997). Cell-free synthesis and assembly of connexins into functional gap junction membrane channels. EMBO J *16*, 2703-2716.

Fanchiotti,S., Fernandez,F., D'Alessio,C., and Parodi,A.J. (1998). The UDP-Glc:Glycoprotein glucosyltransferase is essential for Schizosaccharomyces pombe viability under conditions of extreme endoplasmic reticulum stress. J. Cell Biol. *143*, 625-635.

Fernandez,F.S., Trombetta,S.E., Hellman,U., and Parodi,A.J. (1994). Purification to homogeneity of UDP-glucose:glycoprotein glucosyltransferase from Schizosaccharomyces pombe and apparent absence of the enzyme fro Saccharomyces cerevisiae. J. Biol. Chem. *269*, 30701-30706.

Friedlander,M. and Blobel,G. (1985). Bovine opsin has more than one signal sequence. Nature *318*, 338-343.

Gamou,S., Shimagaki,M., Minoshima,S., Kobayashi,S., and Shimizu,N. (1989). Subcellular localization of the EGF receptor maturation process. Exp. Cell Res. *183*, 197-206.

Ganetzky,B. and Wu,C.F. (1983). Neurogenetic analysis of potassium currents in Drosophila: synergistic effects on neuromuscular transmission in double mutants. J. Neurogenet. *1*, 17-28.

Garratt,J.C., McEvoy,M.P., and Owen,D.G. (1996). Blockade of two voltage-dependent potassium channels, mKv1.1 and mKv1.2, by docosahexaenoic acid. Eur. J Pharmacol. *314*, 393-396.

Gaudin,Y. (1997). Folding of rabies virus glycoprotein: epitope acquisition and interaction with endoplasmic reticulum chaperones. J. Virol. *71*, 3742-3750.

Gehle,V.M., Walcott,E.C., Nishizaki,T., and Sumikawa,K. (1997). N-glycosylation at the conserved sites ensures the expression of properly folded functional ACh receptors. Brain Res. Mol. Brain Res. *45*, 219-229.

Gelman,M.S., Chang,W., Thomas,D.Y., Bergeron,J.J., and Prives,J.M. (1995). Role of the endoplasmic reticulum chaperone calnexin in subunit folding and assembly of nicotinic acetylcholine receptors. J Biol. Chem. *270*, 15085-15092.

Gelman,M.S., Kannegaard,E.S., and Kopito,R.R. (2002). A Principal Role for the Proteasome in Endoplasmic Reticulum-associated Degradation of Misfolded Intracellular Cystic Fibrosis Transmembrane Conductance Regulator. J. Biol. Chem. *277*, 11709-11714.

Ghosh,R.N., Gelman,D.L., and Maxfield,F.R. (1994). Quantification of low density lipoprotein and transferrin endocytic sorting HEp2 cells using confocal microscopy. J Cell Sci. *107 (Pt 8)*, 2177-2189.

Gilstring,C.F., Melin-Larsson,M., and Ljungdahl,P.O. (1999). Shr3p mediates specific COPII coatomer-cargo interactions required for the packaging of amino acid permeases into ER-derived transport vesicles. Mol. Biol. Cell *10*, 3549-3565.

Gorlich,D., Hartmann,E., Prehn,S., and Rapoport,T.A. (1992). A protein of the endoplasmic reticulum involved early in polypeptide translocation. Nature *357*, 47-52.

Gorlich,D. and Rapoport,T.A. (1993). Protein translocation into proteoliposomes reconstituted from purified components of the endoplasmic reticulum membrane. Cell *75*, 615-630.

Griffith,L.C. (2001). Potassium channels: the importance of transport signals. Curr. Biol. *11*, R226-R228.

Gruters,R.A., Neefjes,J.J., Tersmette,M., de Goede,R.E., Tulp,A., Huisman,H.G., Miedema,F., and Ploegh,H.L. (1987). Interference with HIV-induced syncytium formation and viral infectivity by inhibitors of trimming glucosidase. Nature *330*, 74-77.

Gulbis,J.M., Mann,S., and MacKinnon,R. (1999). Structure of a voltage-dependent K+ channel beta subunit. Cell *97*, 943-952.

Gulbis,J.M., Zhou,M., Mann,S., and MacKinnon,R. (2000). Structure of the cytoplasmic beta subunit-T1 assembly of voltage- dependent K+ channels. Science *289*, 123-127.

Gurantz,D., Ribera,A.B., and Spitzer,N.C. (1996). Temporal regulation of Shaker- and Shab-like potassium channel gene expression in single embryonic spinal neurons during K+ current development. J. Neurosci. *16*, 3287-3295.

Hagiwara,S. and Saito,N. (1959). Voltage-current relations in nerve cell membrane of *Onchidium verruculatum*. J. Gen. Physiol.

Hamill,O.P., Marty,A., Neher,E., Sakmann,B., and Sigworth,F.J. (1981). Improved patch-clamp techniques for high-resolution current recording from cells and cell-free membrane patches. Pflugers Arch. *391*, 85-100.

Hammond,A.T. and Glick,B.S. (2000). Dynamics of transitional endoplasmic reticulum sites in vertebrate cells. Mol. Biol. Cell *11*, 3013-3030.

Hammond,C., Braakman,I., and Helenius,A. (1994). Role of N-linked oligosaccharide recognition, glucose trimming, and calnexin in glycoprotein folding and quality control. Proc. Natl. Acad. Sci. U. S. A *91* , 913-917.

Hammond,C. and Helenius,A. (1994a). Folding of VSV G protein: sequential interaction with BiP and calnexin. Science *266*, 456-458.

Hammond,C. and Helenius,A. (1994b). Quality control in the secretory pathway: retention of a misfolded viral membrane glycoprotein involves cycling between the ER, intermediate compartment, and Golgi apparatus. J. Cell Biol. *126*, 41-52.

Hardie,R.C. (1991). Voltage-sensitive potassium channels in Drosophila photoreceptors. J. Neurosci. *11*, 3079-3095.

Hauri,H.P., Kappeler,F., Andersson,H., and Appenzeller,C. (2000). ERGIC-53 and traffic in the secretory pathway. J Cell Sci. *113 (Pt 4)*, 587-596.

Hawtin,S.R., Davies,A.R., Matthews,G., and Wheatley,M. (2001). Identification of the glycosylation sites utilized on the V1a vasopressin receptor and assessment of their role in receptor signalling and expression. Biochem. J. *357*, 73-81.

Hay,J.C., Klumperman,J., Oorschot,V., Steegmaier,M., Kuo,C.S., and Scheller,R.H. (1998). Localization, dynamics, and protein interactions reveal distinct roles for ER and Golgi SNAREs. J. Cell Biol. *141*, 1489-1502.

Haynes,R.L., Zheng,T., and Nicchitta,C.V. (1997). Structure and folding of nascent polypeptide chains during protein translocation in the endoplasmic reticulum. J Biol. Chem. *272*, 17126-17133.

Hebert,D.N., Foellmer,B., and Helenius,A. (1995). Glucose trimming and reglucosylation determine glycoprotein association with calnexin in the endoplasmic reticulum. Cell *81*, 425-433.

Hebert,D.N., Zhang,J.X., and Helenius,A. (1998). Protein folding and maturation in a cell-free system. Biochem. Cell Biol. *76*, 867-873.

Hegde,R.S., Voigt,S., Rapoport,T.A., and Lingappa,V.R. (1998). TRAM regulates the exposure of nascent secretory proteins to the cytosol during translocation into the endoplasmic reticulum. Cell *92*, 621-631.

Heginbotham,L., Lu,Z., Abramson,T., and MacKinnon,R. (1994). Mutations in the K+ channel signature sequence. Biophys. J. *66*, 1061-1067.

Heinemann,S., Rettig,J., Scott,V., Parcej,D.N., Lorra,C., Dolly,J., and Pongs,O. (1994). The inactivation behaviour of voltage-gated K-channels may be determined by association of alpha- and beta-subunits. J Physiol Paris *88*, 173-180.

Heinrich,S.U., Mothes,W., Brunner,J., and Rapoport,T.A. (2000). The Sec61p complex mediates the integration of a membrane protein by allowing lipid partitioning of the transmembrane domain. Cell *102*, 233-244.

Helenius,A. and Aebi,M. (2001). Intracellular functions of N-linked glycans. Science *291*, 2364-2369.

Herz,J., Goldstein,J.L., Strickland,D.K., Ho,Y.K., and Brown,M.S. (1991). 39-kDa protein modulates binding of ligands to low density lipoprotein receptor-related protein/alpha 2-macroglobulin receptor. J Biol. Chem. *266*, 21232-21238.

High,S., Andersen,S.S., Gorlich,D., Hartmann,E., Prehn,S., Rapoport,T.A., and Dobberstein,B. (1993). Sec61p is adjacent to nascent type I and type II signal-anchor proteins during their membrane insertion. J. Cell Biol. *121*, 743-750.

High,S., Gorlich,D., Wiedmann,M., Rapoport,T.A., and Dobberstein,B. (1991). The identification of proteins in the proximity of signal-anchor sequences during their targeting to and insertion into the membrane of the ER. J. Cell Biol. *113*, 35-44.

Hille-Rehfeld,A. (1995). Mannose 6-phosphate receptors in sorting and transport of lysosomal enzymes. Biochim. Biophys. Acta *1241*, 177-194.

Hille,B. (1967). The selective inhibition of delayed potassium currents in nerve by tetraethylammonium ion. J. Gen. Physiol *50*, 1287-1302.

Hille,B. (1975). Ionic selectivity, saturation, and block in sodium channels. A four- barrier model. J Gen. Physiol *66*, 535-560.

Hille,B. (1984). Ionic channels of excitable membranes. (Sunderland,MA: Sinauer Associates Inc.), pp. 1-427.

Ho,K., Nichols,C.G., Lederer,W.J., Lytton,J., Vassilev,P.M., Kanazirska,M.V., and Hebert,S.C. (1993). Cloning and expression of an inwardly rectifying ATP-regulated potassium channel. Nature *362*, 31-38.

Hodgkin,A.L. and Huxley,A.F. (1939). Action potentials recorded from inside a nerve fibre. Nature *144*, 710-711.

Hodgkin,A.L. and Huxley,A.F. (1952a). A quantitative description of membrane current and its application to conduction and excitation in nerve. J. Physiol. *117*, 500-544.

Hodgkin,A.L. and Huxley,A.F. (1952b). Currents carried by sodium and potassium ions through the membrane of the giant axon of Loligo. J. Physiol. *116*, 449-472.

Hodgkin,A.L. and Huxley,A.F (1952c). The components of membrane conductance in the giant axon of Loligo. J. Physiol. *116*, 473-496.

Hodgkin,A.L., Huxley,A.F., and Katz,B. (1949). Ionic currents underlying activity in the giant axon of the squid. Arch. Sci. Physiol. *3*, 129-150.

Hodgkin,A.L. and Katz,B. (1949). The effect of sodium ions on the electrical activity of the giant axon of the squid. J. Physiol. *108*, 37-77.

Hoshi,T., Zagotta,W.N., and Aldrich,R.W. (1990). Biophysical and molecular mechanisms of Shaker potassium channel inactivation. Science *250*, 533-538.

Hough,E., Beech,D.J., and Sivaprasadarao,A. (2000). Identification of molecular regions responsible for the membrane trafficking of Kir6.2. Pflugers Arch. *440*, 481-487.

Hurtley,S.M. and Helenius,A. (1989). Protein oligomerization in the endoplasmic reticulum. Annu. Rev. Cell Biol. *5*, 277-307.

Ikawa,M., Wada,I., Kominami,K., Watanabe,D., Toshimori,K., Nishimune,Y., and Okabe,M. (1997). The putative chaperone calmegin is required for sperm fertility. Nature *387*, 607-611.

Imoto,K., Busch,C., Sakmann,B., Mishina,M., Konno,T., Nakai,J., Bujo,H., Mori,Y., Fukuda,K., and Numa,S. (1988). Rings of negatively charged amino acids determine the acetylcholine receptor channel conductance. Nature *335*, 645-648.

Imperiali,B. and O'Connor,S.E. (1999). Effect of N-linked glycosylation on glycopeptide and glycoprotein structure. Curr. Opin. Chem. Biol. *3*, 643-649.

Isacoff,E.Y., Jan,Y.N., and Jan,L.Y. (1990). Evidence for the formation of heteromultimeric potassium channels in Xenopus oocytes. Nature *345*, 530-534.

Jakob,C.A., Burda,P., Roth,J., and Aebi,M. (1998). Degradation of misfolded endoplasmic reticulum glycoproteins in Saccharomyces cerevisiae is determined by a specific oligosaccharide structure. J Cell Biol. *142*, 1223-1233.

Jan,L.Y., Barbel,S., Timpe,L., Laffer,C., Salkoff,L., O'Farrell,P., and Jan,Y.N. (1983). Mutating a gene for a potassium channel by hybrid dysgenesis: an approach to the cloning of the Shaker locus in Drosophila. Cold Spring Harb. Symp. Quant. Biol. *48 Pt 1*, 233-245.

Jan,L.Y. and Jan,Y.N. (1992). Structural elements involved in specific K+ channel functions. Annu. Rev. Physiol *54*, 537-555.

Jan,Y.N., Jan,L.Y., and Dennis,M.J. (1977). Two mutations of synaptic transmission in Drosophila. Proc. R. Soc. Lond B Biol. Sci. *198*, 87-108.

Jhun,B.H., Rampal,A.L., Liu,H., Lachaal,M., and Jung,C.Y. (1992). Effects of insulin on steady state kinetics of GLUT4 subcellular distribution in rat adipocytes. Evidence of constitutive GLUT4 recycling. J Biol. Chem. *267*, 17710-17715.

Johnson,A.O., Subtil,A., Petrush,R., Kobylarz,K., Keller,S.R., and McGraw,T.E. (1998). Identification of an insulin-responsive, slow endocytic recycling mechanism in Chinese hamster ovary cells. J Biol. Chem. *273*, 17968-17977.

Jones,S.M. and Ribera,A.B. (1994). Overexpression of a potassium channel gene perturbs neural differentiation. J. Neurosci. *14*, 2789-2799.

Jurkat-Rott,K. and Lehmann-Horn,F. (2001). Human muscle voltage-gated ion channels and hereditary disease. Curr. Opin. Pharmacol. *1*, 280-287.

Kamb,A., Iverson,L.E., and Tanouye,M.A. (1987). Molecular characterization of Shaker, a Drosophila gene that encodes a potassium channel. Cell *50*, 405-413.

Kamb,A., Tseng-Crank,J., and Tanouye,M.A. (1988). Multiple products of the Drosophila Shaker gene may contribute to potassium channel diversity. Neuron *1*, 421-430.

Kaplan,W.D. and Trout,W.E., III (1969). The behavior of four neurological mutants of Drosophila. Genetics *61*, 399-409.

Kappeler,F., Klopfenstein,D.R., Foguet,M., Paccaud,J.P., and Hauri,H.P. (1997). The recycling of ERGIC-53 in the early secretory pathway. ERGIC-53 carries a cytosolic endoplasmic reticulum-exit determinant interacting with COPII. J Biol. Chem. *272*, 31801-31808.

Karlin,A. and Akabas,M.H. (1995). Toward a structural basis for the function of nicotinic acetylcholine receptors and their cousins. Neuron *15*, 1231-1244.

Katz,B. and Miledi,R. (1972). The statistical nature of the acetycholine potential and its molecular components. J. Physiol *224*, 665-699.

Kaupp,U.B., Niidome,T., Tanabe,T., Terada,S., Bonigk,W., Stuhmer,W., Cook,N.J., Kangawa,K., Matsuo,H., Hirose,T., and (1989). Primary structure and functional expression from complementary DNA of the rod photoreceptor cyclic GMP-gated channel. Nature *342*, 762-766.

Kaushal,S., Ridge,K.D., and Khorana,H.G. (1994). Structure and function in rhodopsin: the role of asparagine-linked glycosylation. Proc. Natl. Acad. Sci. U. S. A *91*, 4024-4028.

Kelleher,D.J., Kreibich,G., and Gilmore,R. (1992). Oligosaccharyltransferase activity is associated with a protein complex composed of ribophorins I and II and a 48 kd protein. Cell *69*, 55-65.

Kern,G., Kern,D., Jaenicke,R., and Seckler,R. (1993). Kinetics of folding and association of differently glycosylated variants of invertase from Saccharomyces cerevisiae. Protein Sci. *2*, 1862-1868.

Keynes,R.D. (1951). The ionic movements during nervous activity. J. Physiol. *114*, 119-150.

Khanna,R., Myers,M.P., Laine,M., Mock,A.F., Sandoval,B., and Papazian,D.M. (2001a). Putative cell surface targeting motif unnecessary for expression of functional Shaker channels. Biophys. J *80*, A218.

Khanna,R., Myers,M.P., Laine,M., and Papazian,D.M. (2001b). Glycosylation increases potassium channel stability and surface expression in mammalian cells. J. Biol. Chem. *276*, 34028-34034.

Kim,E., Niethammer,M., Rothschild,A., Jan,Y.N., and Sheng,M. (1995). Clustering of Shaker-type K+ channels by interaction with a family of membrane-associated guanylate kinases. Nature *378*, 85-88.

Kim,E. and Sheng,M. (1996). Differential K+ channel clustering activity of PSD-95 and SAP97, two related membrane-associated putative guanylate kinases. Neuropharmacology *35*, 993-1000.

Klumperman,J. (2000). Transport between ER and Golgi. Curr. Opin. Cell Biol. *12*, 445-449.

Klumperman,J., Schweizer,A., Clausen,H., Tang,B.L., Hong,W., Oorschot,V., and Hauri,H.P (1998). The recycling pathway of protein ERGIC-53 and dynamics of the ER-Golgi intermediate compartment. J Cell Sci. *111 (Pt 22)*, 3411-3425.

Knight,B.C. and High,S. (1998). Membrane integration of Sec61alpha: a core component of the endoplasmic reticulum translocation complex. Biochem. J *331 (Pt 1)*, 161-167.

Kobertz,W.R. and Miller,C. (1999). K+ channels lacking the 'tetramerization' domain: implications for pore structure. Nat. Struct. Biol. *6*, 1122-1125.

Kolb,V.A., Makeyev,E.V., and Spirin,A.S. (2000). Co-translational folding of an eukaryotic multidomain protein in a prokaryotic translation system. J. Biol. Chem. *275*, 16597-16601.

Kopito,R.R. (1997). ER quality control: the cytoplasmic connection. Cell *88*, 427-430.

Kornfeld,R. and Kornfeld,S. (1985). Assembly of asparagine-linked oligosaccharides. Annu. Rev. Biochem. *54*, 631-664.

Kreusch,A., Pfaffinger,P.J., Stevens,C.F., and Choe,S. (1998). Crystal structure of the tetramerization domain of the Shaker potassium channel. Nature *392*, 945-948.

Kundra,R. and Kornfeld,S. (1999). Asparagine-linked oligosaccharides protect Lamp-1 and Lamp-2 from intracellular proteolysis. J. Biol. Chem. *274*, 31039-31046.

Kunkel,T.A., Bebenek,K., and McClary,J. (1991). Efficient site-directed mutagenesis using uracil-containing DNA. Methods Enzymol. *204*, 125-139.

Lahey,T., Gorczyca,M., Jia,X.X., and Budnik,V. (1994). The Drosophila tumor suppressor gene dlg is required for normal synaptic bouton structure. Neuron *13*, 823-835.

Laird,V. and High,S. (1997). Discrete cross-linking products identified during membrane protein biosynthesis. J. Biol. Chem. *272*, 1983-1989.

Lechner,J. and Wieland,F. (1989). Structure and biosynthesis of prokaryotic glycoproteins. Annu. Rev. Biochem. *58*, 173-194.

Leonard,R.J., Labarca,C.G., Charnet,P., Davidson,N., and Lester,H.A. (1988). Evidence that the M2 membrane-spanning region lines the ion channel pore of the nicotinic receptor. Science *242*, 1578-1581.

Levitan,E.S., Hemmick,L.M., Birnberg,N.C., and Kaczmarek,L.K. (1991). Dexamethasone increases potassium channel messenger RNA and activity in clonal pituitary cells. Mol. Endocrinol. *5*, 1903-1908.

Levitan,E.S. and Takimoto,K. (1998). Dynamic regulation of K+ channel gene expression in differentiated cells. J. Neurobiol. *37*, 60-68.

Levitan,E.S. and Takimoto,K. (2000). Surface expression of Kv1 voltage-gated K+ channels is governed by a C- terminal motif. Trends Cardiovasc. Med. *10*, 317-320.

Li,D., Takimoto,K., and Levitan,E.S. (2000). Surface expression of Kv1 channels is governed by a C-terminal motif. J Biol. Chem. *275*, 11597-11602.

Liman,E.R., Hess,P., Weaver,F., and Koren,G. (1991). Voltage-sensing residues in the S4 region of a mammalian K+ channel. Nature *353*, 752-756.

Liman,E.R., Tytgat,J., and Hess,P. (1992). Subunit stoichiometry of a mammalian K+ channel determined by construction of multimeric cDNAs. Neuron *9*, 861-871.

Lingappa,V.R., Katz,F.N., Lodish,H.F., and Blobel,G. (1978). A signal sequence for the insertion of a transmembrane glycoprotein. Similarities to the signals of secretory proteins in primary structure and function. J. Biol. Chem. *253*, 8667-8670.

Lippincott-Schwartz,J., Donaldson,J.G., Schweizer,A., Berger,E.G., Hauri,H.P., Yuan,L.C., and Klausner,R.D. (1990). Microtubule-dependent retrograde transport of proteins into the ER in the presence of brefeldin A suggests an ER recycling pathway. Cell *60*, 821-836.

Liu,T.I., Lebaric,Z.N., Rosenthal,J.J., and Gilly,W.F. (2001). Natural substitutions at highly conserved T1-domain residues perturb processing and functional expression of squid Kv1 channels. J Neurophysiol. *85*, 61-71.

Liu,Y., Choudhury,P., Cabral,C.M., and Sifers,R.N. (1999). Oligosaccharide modification in the early secretory pathway directs the selection of a misfolded glycoprotein for degradation by the proteasome. J Biol. Chem. *274*, 5861-5867.

Lodish,H.F., Kong,N., Snider,M., and Strous,G.J. (1983). Hepatoma secretory proteins migrate from rough endoplasmic reticulum to Golgi at characteristic rates. Nature *304*, 80-83.

Lu,J., Robinson,J.M., Edwards,D., and Deutsch,C. (2001). T1-T1 interactions occur in ER membranes while nascent Kv peptides are still attached to ribosomes. Biochemistry *40*, 10934-10946.

Ma,D., Zerangue,N., Lin,Y.F., Collins,A., Yu,M., Jan,Y.N., and Jan,L.Y. (2001). Role of ER export signals in controlling surface potassium channel numbers. Science *291*, 316-319.

Ma,D., Zerangue,N., Raab-Graham,K., Fried,S.R., Jan,Y.N., and Jan,L.Y. (2002). Diverse trafficking patterns due to multiple traffic motifs in G protein-activated inwardly rectifying potassium channels from brain and heart. Neuron *33*, 715-729.

MacKinnon,R. (1991). Determination of the subunit stoichiometry of a voltage-activated potassium channel. Nature *350*, 232-235.

Makhina,E.N. and Nichols,C.G. (1998). Independent trafficking of KATP channel subunits to the plasma membrane. J Biol. Chem. *273*, 3369-3374.

Malkin,L.I. and Rich,A. (1967). Partial resistance of nascent polypeptide chains to proteolytic digestion due to ribosomal shielding. J Mol. Biol. *26*, 329-346.

Manganas,L.N., Akhtar,S., Antonucci,D.E., Campomanes,C.R., Dolly,J.O., and Trimmer,J.S. (2001). Episodic ataxia type-1 mutations in the Kv1.1 potassium channel display distinct folding and intracellular trafficking properties. J. Biol. Chem. *276*, 49427-49434.

Manganas,L.N. and Trimmer,J.S. (2000). Subunit composition determines Kv1 potassium channel surface expression. J Biol. Chem. *275*, 29685-29693.

Marmont,G. (1949). Studies on the axon membrane. I. A new method. J. Cell. Comp. Physiol. *34*, 351-382.

Martinez-Menarguez,J.A., Geuze,H.J., Slot,J.W., and Klumperman,J. (1999). Vesicular tubular clusters between the ER and Golgi mediate concentration of soluble secretory proteins by exclusion from COPI- coated vesicles. Cell *98*, 81-90.

Martoglio,B., Hofmann,M.W., Brunner,J., and Dobberstein,B. (1995). The protein-conducting channel in the membrane of the endoplasmic reticulum is open laterally toward the lipid bilayer. Cell *81*, 207-214.

Matlack,K.E., Mothes,W., and Rapoport,T.A. (1998). Protein translocation: tunnel vision. Cell *92*, 381-390.

Matlack,K.E. and Walter,P. (1995). The 70 carboxyl-terminal amino acids of nascent secretory proteins are protected from proteolysis by the ribosome and the protein translocation apparatus of the endoplasmic reticulum membrane. J Biol. Chem. *270*, 6170-6180.

Matsubara,H., Liman,E.R., Hess,P., and Koren,G. (1991). Pretranslational mechanisms determine the type of potassium channels expressed in the rat skeletal and cardiac muscles. J Biol. Chem. *266*, 13324-13328.

Matsuoka,K., Orci,L., Amherdt,M., Bednarek,S.Y., Hamamoto,S., Schekman,R., and Yeung,T. (1998). COPII-coated vesicle formation reconstituted with purified coat proteins and chemically defined liposomes. Cell *93*, 263-275.

Maue,R.A., Kraner,S.D., Goodman,R.H., and Mandel,G. (1990). Neuron-specific expression of the rat brain type II sodium channel gene is directed by upstream regulatory elements. Neuron *4*, 223-231.

McCune,J.M., Lingappa,V.R., Fu,S.M., Blobel,G., and Kunkel,H.G. (1980). Biogenesis of membrane-bound and secreted immunoglobulins. I. Two distinct translation products of human mu-chain, with identical N- termini and different C-termini. J. Exp. Med. *152*, 463-468.

Mesaeli,N., Nakamura,K., Zvaritch,E., Dickie,P., Dziak,E., Krause,K.H., Opas,M., MacLennan,D.H., and Michalak,M. (1999). Calreticulin is essential for cardiac development. J. Cell Biol. *144*, 857-868.

Miller,C. (2000). An overview of the potassium channel family. Genome Biol. *1*, REVIEWS0004.

Minor,D.L., Lin,Y.F., Mobley,B.C., Avelar,A., Jan,Y.N., Jan,L.Y., and Berger,J.M. (2000). The polar T1 interface is linked to conformational changes that open the voltage-gated potassium channel. Cell *102* , 657-670.

Moestrup,S.K. and Gliemann,J. (1991). Analysis of ligand recognition by the purified alpha 2-macroglobulin receptor (low density lipoprotein receptor-related protein). Evidence that high affinity of alpha 2-macroglobulin-proteinase complex is achieved by binding to adjacent receptors. J Biol. Chem. *266*, 14011-14017.

Molinari,M. and Helenius,A. (1999). Glycoproteins form mixed disulphides with oxidoreductases during folding in living cells. Nature *402*, 90-93.

Molinari,M. and Helenius,A. (2000). Chaperone selection during glycoprotein translocation into the endoplasmic reticulum. Science *288*, 331-333.

Moore,S.E. and Spiro,R.G. (1990). Demonstration that Golgi endo-alpha-D-mannosidase provides a glucosidase-independent pathway for the formation of complex N-linked oligosaccharides of glycoproteins. J Biol. Chem. *265*, 13104-13112.

Moore,S.E. and Spiro,R.G. (1992). Characterization of the endomannosidase pathway for the processing of N- linked oligosaccharides in glucosidase II-deficient and parent mouse lymphoma cells. J Biol. Chem. *267*, 8443-8451.

Mori,Y., Folco,E., and Koren,G. (1995). GH3 cell-specific expression of Kv1.5 gene. Regulation by a silencer containing a dinucleotide repetitive element. J. Biol. Chem. *270*, 27788-27796.

Mori,Y., Matsubara,H., Folco,E., Siegel,A., and Koren,G. (1993). The transcription of a mammalian voltage-gated potassium channel is regulated by cAMP in a cell-specific manner. J. Biol. Chem. *268*, 26482-26493.

Mothes,W., Heinrich,S.U., Graf,R., Nilsson,I., von Heijne,G., Brunner,J., and Rapoport,T.A. (1997). Molecular mechanism of membrane protein integration into the endoplasmic reticulum. Cell *89*, 523-533.

Moyer,B.D., Loffing,J., Schwiebert,E.M., Loffing-Cueni,D., Halpin,P.A., Karlson,K.H., Ismailov,I.I., Guggino,W.B., Langford,G.M., and Stanton,B.A. (1998). Membrane trafficking of

the cystic fibrosis gene product, cystic fibrosis transmembrane conductance regulator, tagged with green fluorescent protein in madin-darby canine kidney cells. J Biol. Chem. *273*, 21759-21768.

Mueller,P., Rudin,P.O., Tien,H.T., and Wescott,W.C. (1962). Reconstitution of cell membrane structure in vitro and its transformation into an excitable system. Nature *194*, 979-980.

Muniz,M., Morsomme,P., and Riezman,H. (2001). Protein sorting upon exit from the endoplasmic reticulum. Cell *104*, 313-320.

Musil,L.S., Cunningham,B.A., Edelman,G.M., and Goodenough,D.A. (1990). Differential phosphorylation of the gap junction protein connexin43 in junctional communication-competent and -deficient cell lines. J Cell Biol. *111*, 2077-2088.

Musil,L.S. and Goodenough,D.A. (1993). Multisubunit assembly of an integral plasma membrane channel protein, gap junction connexin43, occurs after exit from the ER. Cell *74*, 1065-1077.

Nagaya,N. and Papazian,D.M. (1997b). Potassium channel alpha and beta subunits assemble in the endoplasmic reticulum. J Biol. Chem. *272*, 3022-3027.

Nagaya,N. and Papazian,D.M. (1997a). Potassium channel alpha and beta subunits assemble in the endoplasmic reticulum. J. Biol. Chem. *272*, 3022-3027.

Nagaya,N., Schulteis,C.T., and Papazian,D.M. (1999). Calnexin associates with Shaker K+ channel protein but is not involved in quality control of subunit folding or assembly. Receptors. Channels *6*, 229-239.

Nakahira,K., Shi,G., Rhodes,K.J., and Trimmer,J.S. (1996). Selective interaction of voltage-gated K+ channel beta-subunits with alpha-subunits. J Biol. Chem. *271*, 7084-7089.

Narahashi,T., Haas,H.G., and Therrien,E.F. (1967). Saxitoxin and tetrodotoxin: Comparison of nerve blocking mechanism. Science *157*, 1441-1442.

Narahashi,T., Moore,J.W., and Scott,W.R. (1964). Tetrodotoxin blockage of sodium conductance increase in lobster giant axons. J. Gen. Physiol *47*, 965-974.

Neerman-Arbez,M., Johnson,K.M., Morris,M.A., McVey,J.H., Peyvandi,F., Nichols,W.C., Ginsburg,D., Rossier,C., Antonarakis,S.E., and Tuddenham,E.G. (1999). Molecular analysis of the ERGIC-53 gene in 35 families with combined factor V-factor VIII deficiency. Blood *93*, 2253-2260.

Neher,E. and Sakmann,B. (1976). Single-channel currents recorded from membrane of denervated frog muscle fibres. Nature *260*, 799-802.

Nicchitta,C.V. and Blobel,G. (1993). Lumenal proteins of the mammalian endoplasmic reticulum are required to complete protein translocation. Cell *73*, 989-998.

Nichols,W.C., Seligsohn,U., Zivelin,A., Terry,V.H., Hertel,C.E., Wheatley,M.A., Moussalli,M.J., Hauri,H.P., Ciavarella,N., Kaufman,R.J., and Ginsburg,D. (1998). Mutations in the ER-Golgi intermediate compartment protein ERGIC-53 cause combined deficiency of coagulation factors V and VIII. Cell *93*, 61-70.

Nichols,W.C., Terry,V.H., Wheatley,M.A., Yang,A., Zivelin,A., Ciavarella,N., Stefanile,C., Matsushita,T., Saito,H., de Bosch,N.B., Ruiz-Saez,A., Torres,A., Thompson,A.R., Feinstein,D.I., White,G.C., Negrier,C., Vinciguerra,C., Aktan,M., Kaufman,R.J., Ginsburg,D., and Seligsohn,U. (1999). ERGIC-53 gene structure and mutation analysis in 19 combined factors V and VIII deficiency families. Blood *93*, 2261-2266.

Nicola,A.V., Chen,W., and Helenius,A. (1999). Co-translational folding of an alphavirus capsid protein in the cytosol of living cells. Nat. Cell Biol. *1*, 341-345.

Nilsson,I.M. and von Heijne,G. (1993). Determination of the distance between the oligosaccharyltransferase active site and the endoplasmic reticulum membrane. J. Biol. Chem. *268*, 5798-5801.

Nishimura,N. and Balch,W.E. (1997). A di-acidic signal required for selective export from the endoplasmic reticulum. Science *277*, 556-558.

Noda,M., Takahashi,H., Tanabe,T., Toyosato,M., Kikyotani,S., Furutani,Y., Hirose,T., Takashima,H., Inayama,S., Miyata,T., and Numa,S. (1983). Structural homology of Torpedo californica acetylcholine receptor subunits. Nature *302*, 528-532.

Olden,K., Parent,J.B., and White.S.L. (1982). Carbohydrate moieties of glycoproteins. A re-evaluation of their function. Biochim. Biophys. Acta *650*, 209-232.

Oliver,J.D., Roderick,H.L., Llewellyn,D.H., and High,S. (1999). ERp57 functions as a subunit of specific complexes formed with the ER lectins calreticulin and calnexin. Mol. Biol. Cell *10*, 2573-2582.

Oliver,J.D., Van der Wal,F.J., Bulleid,N.J., and High,S. (1997). Interaction of the thiol-dependent reductase ERp57 with nascent glycoproteins. Science *275*, 86-88.

Orci,L., Ravazzola,M., Volchuk,A., Engel,T., Gmachl,M., Amherdt,M., Perrelet,A., Sollner,T.H., and Rothman,J.E. (2000). Anterograde flow of cargo across the golgi stack potentially mediated via bidirectional "percolating" COPI vesicles. Proc. Natl. Acad. Sci. U. S. A *97*, 10400-10405.

Palokangas,H., Ying,M., Vaananen,K., and Saraste,J. (1998). Retrograde transport from the pre-Golgi intermediate compartment and the Golgi complex is affected by the vacuolar H+-ATPase inhibitor bafilomycin A1. Mol. Biol. Cell *9*, 3561-3578.

Papazian,D.M., Schwarz,T.L., Tempel,B.L., Jan,Y.N., and Jan,L.Y. (1987). Cloning of genomic and complementary DNA from Shaker, a putative potassium channel gene from Drosophila. Science *237*, 749-753.

Papazian,D.M., Shao,X.M., Seoh,S.A., Mock,A.F., Huang,Y., and Wainstock,D.H. (1995). Electrostatic interactions of S4 voltage sensor in Shaker K+ channel. Neuron *14*, 1293-1301.

Papazian,D.M., Timpe,L.C., Jan,Y.N., and Jan,L.Y. (1991). Alteration of voltage-dependence of Shaker potassium channel by mutations in the S4 sequence. Nature *349*, 305-310.

Parlati,F., Dominguez,M., Bergeron,J.J., and Thomas,D.Y. (1995). Saccharomyces cerevisiae CNE1 encodes an endoplasmic reticulum (ER) membrane protein with sequence similarity to

calnexin and calreticulin and functions as a constituent of the ER quality control apparatus. J. Biol. Chem. *270*, 244-253.

Parodi,A.J. (1993). N-glycosylation in trypanosomatid protozoa. Glycobiology *3*, 193-199.

Parodi,A.J. (2000). Protein glucosylation and its role in protein folding. Annu. Rev. Biochem. *69*, 69-93.

Peng,R., Grabowski,R., De Antoni,A., and Gallwitz,D. (1999). Specific interaction of the yeast cis-Golgi syntaxin Sed5p and the coat protein complex II component Sec24p of endoplasmic reticulum-derived transport vesicles. Proc. Natl. Acad. Sci. U. S. A *96*, 3751-3756.

Perez-Garcia,M.T., Lopez-Lopez,J.R., and Gonzalez,C. (1999). Kvbeta1.2 subunit coexpression in HEK293 cells confers O2 sensitivity to kv4.2 but not to Shaker channels. J Gen. Physiol *113*, 897-907.

Pessia,M., Bond,C.T., Kavanaugh,M.P., and Adelman,J.P. (1995). Contributions of the C-terminal domain to gating properties of inward rectifier potassium channels. Neuron *14*, 1039-1045.

Peterson,J.R., Ora,A., Van,P.N., and Helenius,A. (1995). Transient, lectin-like association of calreticulin with folding intermediates of cellular and viral glycoproteins. Mol. Biol. Cell *6*, 1173-1184.

Pfaffinger,P.J. and DeRubeis,D. (1995). Shaker K+ channel T1 domain self-tetramerizes to a stable structure. J Biol. Chem. *270*, 28595-28600.

Plath,K., Mothes,W., Wilkinson,B.M., Stirling,C.J., and Rapoport,T.A. (1998). Signal sequence recognition in posttranslational protein transport across the yeast ER membrane. Cell *94*, 795-807.

Pongs,O., Kecskemethy,N., Muller,R., Krah-Jentgens,I., Baumann,A., Kiltz,H.H., Canal,I., Llamazares,S., and Ferrus,A. (1988). Shaker encodes a family of putative potassium channel proteins in the nervous system of Drosophila. EMBO J. *7*, 1087-1096.

Poo,M. and Cone,R.A. (1974). Lateral diffusion of rhodopsin in the photoreceptor membrane. Nature *247*, 438-441.

Pryde,J.G., Farmaki,T., and Lucocq,J.M. (1998). Okadaic acid induces selective arrest of protein transport in the rough endoplasmic reticulum and prevents export into COPII-coated structures. Mol. Cell Biol. *18*, 1125-1135.

Qu,B.H., Strickland,E., and Thomas,P.J. (1997). Cystic fibrosis: a disease of altered protein folding. J Bioenerg. Biomembr. *29*, 483-490.

Raftery,M.A., Hunkapiller,M.W., Strader,C.D., and Hood,L.E. (1980). Acetylcholine receptor: complex of homologous subunits. Science *208*, 1454-1456.

Ramanathan,V.K. and Hall,Z.W. (1999). Altered glycosylation sites of the delta subunit of the acetylcholine receptor (AChR) reduce alpha delta association and receptor assembly. J. Biol. Chem. *274*, 20513-20520.

Rasband,M.N., Trimmer,J.S., Schwarz,T.L., Levinson,S.R., Ellisman,M.H., Schachner,M., and Shrager,P. (1998). Potassium channel distribution, clustering, and function in remyelinating rat axons. J Neurosci. *18*, 36-47.

Rea,S. and James,D.E. (1997). Moving GLUT4: the biogenesis and trafficking of GLUT4 storage vesicles. Diabetes *46*, 1667-1677.

Recio-Pinto,E., Thornhill,W.B., Duch,D.S., Levinson,S.R., and Urban,B.W. (1990). Neuraminidase treatment modifies the function of electroplax sodium channels in planar lipid bilayers. Neuron *5*, 675-684.

Rettig,J., Heinemann,S.H., Wunder,F., Lorra,C., Parcej,D.N., Dolly,J.O., and Pongs,O. (1994). Inactivation properties of voltage-gated K+ channels altered by presence of beta-subunit. Nature *369*, 289-294.

Rhodes,K.J., Keilbaugh,S.A., Barrezueta,N.X., Lopez,K.L., and Trimmer,J.S. (1995). Association and colocalization of K+ channel alpha- and beta-subunit polypeptides in rat brain. J Neurosci. *15*, 5360-5371.

Rhodes,K.J., Monaghan,M.M., Barrezueta,N.X., Nawoschik,S., Bekele-Arcuri,Z., Matos,M.F., Nakahira,K., Schechter,L.E., and Trimmer,J.S. (1996). Voltage-gated K+ channel beta subunits: expression and distribution of Kv beta 1 and Kv beta 2 in adult rat brain. J Neurosci. *16*, 4846-4860.

Rhodes,K.J., Strassle,B.W., Monaghan,M.M., Bekele-Arcuri,Z., Matos,M.F., and Trimmer,J.S. (1997). Association and colocalization of the Kvbeta1 and Kvbeta2 beta-subunits with Kv1 alpha-subunits in mammalian brain K+ channel complexes. J Neurosci. *17*, 8246-8258.

Roberts,W.M., Stuhmer,W., Weiss,R.E., Stanfield,P.R., and Almers,W. (1986). Distribution and mobility of voltage-gated ion channels in skeletal muscle. Ann. N. Y. Acad. Sci. *479*, 377-384.

Rosenberg,R.L. and East,J.E. (1992). Cell-free expression of functional Shaker potassium channels. Nature *360*, 166-169.

Rudd,P.M., Elliott,T., Cresswell,P., Wilson,I.A., and Dwek,R.A. (2001). Glycosylation and the immune system. Science *291*, 2370-2376.

Ruppersberg,J.P., Schroter,K.H., Sakmann,B., Stocker,M., Sewing,S., and Pongs,O. (1990). Heteromultimeric channels formed by rat brain potassium-channel proteins. Nature *345*, 535-537.

Salkoff,L., Baker,K., Butler,A., Covarrubias,M., Pak,M.D., and Wei,A. (1992). An essential 'set' of K+ channels conserved in flies, mice and humans. Trends Neurosci. *15*, 161-166.

Salkoff,L. and Wyman,R. (1981a). Genetic modification of potassium channels in Drosophila Shaker mutants. Nature *293*, 228-230.

Salkoff,L. and Wyman,R. (1981b). Outward currents in developing Drosophila flight muscle. Science *212*, 461-463.

Salkoff,L.B. and Wyman,R.J. (1983). Ion currents in Drosophila flight muscles. J. Physiol *337*, 687-709.

Sanguinetti,M.C., Curran,M.E., Zou,A., Shen,J., Spector,P.S., Atkinson,D.L., and Keating,M.T. (1996). Coassembly of K(V)LQT1 and minK (IsK) proteins to form cardiac I(Ks) potassium channel. Nature *384*, 80-83.

Santacruz-Toloza,L., Huang,Y., John,S.A., and Papazian,D.M. (1994a). Glycosylation of shaker potassium channel protein in insect cell culture and in Xenopus oocytes. Biochemistry *33*, 5607-5613.

Santacruz-Toloza,L., Perozo,E., and Papazian,D.M. (1994b). Purification and reconstitution of functional Shaker K+ channels assayed with a light-driven voltage-control system. Biochemistry *33*, 1295-1299.

Saraste,J. and Svensson,K. (1991). Distribution of the intermediate elements operating in ER to Golgi transport. J Cell Sci. *100 (Pt 3)*, 415-430.

Schagger,H. and von Jagow,G. (1987). Tricine-sodium dodecyl sulfate-polyacrylamide gel electrophoresis for the separation of proteins in the range from 1 to 100 kDa. Anal. Biochem. *166*, 368-379.

Schechter,I., Burstein,Y., Zemell,R., Ziv,E., Kantor,F., and Papermaster,D.S. (1979). Messenger RNA of opsin from bovine retina: isolation and partial sequence of the in vitro translation product. Proc. Natl. Acad. Sci. U. S. A *76*, 2654-2658.

Scheiffele,P., Peranen,J., and Simons,K. (1995). N-glycans as apical sorting signals in epithelial cells. Nature *378*, 96-98.

Schekman,R. and Orci,L. (1996). Coat proteins and vesicle budding. Science *271*, 1526-1533.

Schrempf,H., Schmidt,O., Kummerlen,R., Hinnah,S., Muller,D., Betzler,M., Steinkamp,T., and Wagner,R. (1995). A prokaryotic potassium ion channel with two predicted transmembrane segments from Streptomyces lividans. EMBO J *14*, 5170-5178.

Schulteis,C.T., Nagaya,N., and Papazian,D.M. (1996). Intersubunit interaction between amino- and carboxyl-terminal cysteine residues in tetrameric shaker K+ channels. Biochemistry *35*, 12133-12140.

Schulteis,C.T., Nagaya,N., and Papazian,D.M. (1998). Subunit folding and assembly steps are interspersed during Shaker potassium channel biogenesis. J. Biol. Chem. *273*, 26210-26217.

Schwarz,T.L., Papazian,D.M., Carretto,R.C., Jan,Y.N., and Jan,L.Y. (1990). Immunological characterization of K+ channel components from the Shaker locus and differential distribution of splicing variants in Drosophila. Neuron *4*, 119-127.

Schwarz,T.L., Tempel,B.L., Papazian,D.M., Jan,Y.N., and Jan,L.Y. (1988). Multiple potassium-channel components are produced by alternative splicing at the Shaker locus in Drosophila. Nature *331*, 137-142.

Schweizer,A., Fransen,J.A., Matter,K., Kreis,T.E., Ginsel,L., and Hauri,H.P. (1990). Identification of an intermediate compartment involved in protein transport from endoplasmic reticulum to Golgi apparatus. Eur. J Cell Biol. *53*, 185-196.

Scott,V.E., Rettig,J., Parcej,D.N., Keen,J.N., Findlay,J.B., Pongs,O., and Dolly,J.O. (1994). Primary structure of a beta subunit of alpha-dendrotoxin-sensitive K+ channels from bovine brain. Proc. Natl. Acad. Sci. U. S. A *91*, 1637-1641.

Sesso,A., De Faria,F.P., Iwamura,E.S., and Correa,H. (1994). A three-dimensional reconstruction study of the rough ER-Golgi interface in serial thin sections of the pancreatic acinar cell of the rat. J. Cell Sci. *107 (Pt 3)*, 517-528.

Sevier,C.S., Weisz,O.A., Davis,M., and Machamer,C.E. (2000). Efficient export of the vesicular stomatitis virus G protein from the endoplasmic reticulum requires a signal in the cytoplasmic tail that includes both tyrosine-based and di-acidic motifs. Mol. Biol. Cell *11*, 13-22.

Sharma,N., Crane,A., Clement,J.P., Gonzalez,G., Babenko,A.P., Bryan,J., and Aguilar-Bryan,L. (1999). The C terminus of SUR1 is required for trafficking of KATP channels. J. Biol. Chem. *274*, 20628-20632.

Shen,N.V., Chen,X., Boyer,M.M., and Pfaffinger,P.J. (1993). Deletion analysis of K+ channel assembly. Neuron *11*, 67-76.

Shen,N.V. and Pfaffinger,P.J. (1995). Molecular recognition and assembly sequences involved in the subfamily- specific assembly of voltage-gated K+ channel subunit proteins. Neuron *14*, 625-633.

Sheng,M., Liao,Y.J., Jan,Y.N., and Jan,L.Y. (1993). Presynaptic A-current based on heteromultimeric K+ channels detected in vivo. Nature *365*, 72-75.

Sheng,Z., Skach,W., Santarelli,V., and Deutsch,C. (1997). Evidence for interaction between transmembrane segments in assembly of Kv1.3. Biochemistry *36*, 15501-15513.

Shi,G., Nakahira,K., Hammond,S., Rhodes,K.J., Schechter,L.E., and Trimmer,J.S. (1996). Beta subunits promote K+ channel surface expression through effects early in biosynthesis. Neuron *16*, 843-852.

Shi,G. and Trimmer,J.S. (1999). Differential asparagine-linked glycosylation of voltage-gated K+ channels in mammalian brain and in transfected cells. J Membr. Biol. *168*, 265-273.

Shih,T.M. and Goldin,A.L. (1997). Topology of the Shaker potassium channel probed with hydrophilic epitope insertions. J. Cell Biol. *136*, 1037-1045.

Shima,D.T., Cabrera-Poch,N., Pepperkok,R., and Warren,G. (1998). An ordered inheritance strategy for the Golgi apparatus: visualization of mitotic disassembly reveals a role for the mitotic spindle. J Cell Biol. *141*, 955-966.

Silberstein,S. and Gilmore,R. (1996). Biochemistry, molecular biology, and genetics of the oligosaccharyltransferase. FASEB J. *10*, 849-858.

Snyder,P.M., Price,M.P., McDonald,F.J., Adams,C.M., Volk,K.A., Zeiher,B.G., Stokes,J.B., and Welsh,M.J. (1995). Mechanism by which Liddle's syndrome mutations increase activity of a human epithelial Na+ channel. Cell *83*, 969-978.

Solc,C.K., Zagotta,W.N., and Aldrich,R.W. (1987). Single-channel and genetic analyses reveal two distinct A-type potassium channels in Drosophila. Science *236*, 1094-1098.

Sommer,T. and Jentsch,S. (1993). A protein translocation defect linked to ubiquitin conjugation at the endoplasmic reticulum. Nature *365*, 176-179.

Sousa,M. and Parodi,A.J. (1995). The molecular basis for the recognition of misfolded glycoproteins by the UDP-Glc:glycoprotein glucosyltransferase. EMBO J. *14*, 4196-4203.

Springer,S. and Schekman,R. (1998). Nucleation of COPII vesicular coat complex by endoplasmic reticulum to Golgi vesicle SNAREs. Science *281*, 698-700.

Stanley,P. (1984). Glycosylation mutants of animal cells. Annu. Rev. Genet. *18*, 525-552.

Stern,M. and Ganetzky,B. (1989). Altered synaptic transmission in Drosophila hyperkinetic mutants. J Neurogenet. *5*, 215-228.

Stevens,C.F. (1972). Inferences about membrane properties from electrical noise measurements. Biophys. J. *12*, 1028-1047.

Stirling,C.J., Rothblatt,J., Hosobuchi,M., Deshaies,R., and Schekman,R. (1992). Protein translocation mutants defective in the insertion of integral membrane proteins into the endoplasmic reticulum. Mol. Biol. Cell *3*, 129-142.

Strang,C., Cushman,S.J., DeRubeis,D., Peterson,D., and Pfaffinger,P.J. (2001). A central role for the T1 domain in voltage-gated potassium channel formation and function. J Biol. Chem. *276*, 28493-28502.

Stuhmer,W., Ruppersberg,J.P., Schroter,K.H., Sakmann,B., Stocker,M., Giese,K.P., Perschke,A., Baumann,A., and Pongs,O. (1989). Molecular basis of functional diversity of voltage-gated potassium channels in mammalian brain. EMBO J. *8*, 3235-3244.

Su,K., Stoller,T., Rocco,J., Zemsky,J., and Green,R. (1993). Pre-Golgi degradation of yeast prepro-alpha-factor expressed in a mammalian cell. Influence of cell type-specific oligosaccharide processing on intracellular fate. J Biol. Chem. *268*, 14301-14309.

Takimoto,K., Fomina,A.F., Gealy,R., Trimmer,J.S., and Levitan,E.S. (1993). Dexamethasone rapidly induces Kv1.5 K+ channel gene transcription and expression in clonal pituitary cells. Neuron *11*, 359-369.

Tang,C.Y., Schulteis,C.T., Jimenez,R.M., and Papazian,D.M. (1998). Shaker and ether-a-go-go K+ channel subunits fail to coassemble in Xenopus oocytes. Biophys. J *75*, 1263-1270.

Tanouye,M.A. and Ferrus,A. (1985). Action potentials in normal and Shaker mutant Drosophila. J. Neurogenet. *2*, 253-271.

Tanouye,M.A., Kamb,C.A., Iverson,L.E., and Salkoff,L. (1986). Genetics and molecular biology of ionic channels in Drosophila. Annu. Rev. Neurosci. *9*, 255-276.

Tasaki,I. and Hagiwara,S. (1957). Demonstration of two stable potential states in the squid giant axon under tetraethylammonium chloride. J. Gen. Physiol *40*, 859-885.

Tatu,U. and Helenius,A. (1999). Interaction of newly synthesized apolipoprotein B with calnexin and calreticulin requires glucose trimming in the endoplasmic reticulum. Biosci. Rep. *19*, 189-196.

Tejedor,F.J., Bokhari,A., Rogero,O., Gorczyca,M., Zhang,J., Kim,E., Sheng,M., and Budnik,V. (1997). Essential role for dlg in synaptic clustering of Shaker K+ channels in vivo. J Neurosci. *17*, 152-159.

Tempel,B.L., Jan,Y.N., and Jan,L.Y. (1988). Cloning of a probable potassium channel gene from mouse brain. Nature *332*, 837-839.

Tempel,B.L., Papazian,D.M., Schwarz,T.L., Jan,Y.N., and Jan,L.Y. (1987). Sequence of a probable potassium channel component encoded at Shaker locus of Drosophila. Science *237*, 770-775.

Thornhill,W.B., Wu,M.B., Jiang,X., Wu,X., Morgan,P.T., and Margiotta,J.F (1996). Expression of Kv1.1 delayed rectifier potassium channels in Lec mutant Chinese hamster ovary cell lines reveals a role for sialidation in channel function. J Biol. Chem. *271*, 19093-19098.

Tiffany,A.M., Manganas,L.N., Kim,E., Hsueh,Y.P., Sheng,M., and Trimmer,J.S. (2000). PSD-95 and SAP97 exhibit distinct mechanisms for regulating K(+) channel surface expression and clustering. J Cell Biol. *148*, 147-158.

Tifft,C.J., Proia,R.L., and Camerini-Otero,R.D. (1992). The folding and cell surface expression of CD4 requires glycosylation. J. Biol. Chem. *267*, 3268-3273.

Tinker,A., Jan,Y.N., and Jan,L.Y. (1996). Regions responsible for the assembly of inwardly rectifying potassium channels. Cell *87*, 857-868.

Tiwari-Woodruff,S.K., Schulteis,C.T., Mock,A.F., and Papazian,D.M. (1997). Electrostatic interactions between transmembrane segments mediate folding of Shaker K+ channel subunits. Biophys. J. *72*, 1489-1500.

Trimmer,J.S. (1998). Regulation of ion channel expression by cytoplasmic subunits. Curr. Opin. Neurobiol. *8*, 370-374.

Trimmer,J.S., Cooperman,S.S., Tomiko,S.A., Zhou,J.Y., Crean,S.M., Boyle,M.B., Kallen,R.G., Sheng,Z.H., Barchi,R.L., Sigworth,F.J., and (1989). Primary structure and functional expression of a mammalian skeletal muscle sodium channel. Neuron *3*, 33-49.

Trombetta,E.S. and Helenius,A. (2000). Conformational requirements for glycoprotein reglucosylation in the endoplasmic reticulum. J. Cell Biol. *148*, 1123-1129.

Trout,W.E. and Kaplan,W.D. (1973). Genetic manipulation of motor output in shaker mutants of Drosophila. J. Neurobiol. *4*, 495-512.

Tu,L. and Deutsch,C. (1999). Evidence for dimerization of dimers in K+ channel assembly. Biophys. J *76*, 2004-2017.

Tu,L., Santarelli,V., and Deutsch,C. (1995). Truncated K+ channel DNA sequences specifically suppress lymphocyte K+ channel gene expression. Biophys. J *68*, 147-156.

Tu,L., Santarelli,V., Sheng,Z., Skach,W., Pain,D., and Deutsch,C. (1996). Voltage-gated K+ channels contain multiple intersubunit association sites. J Biol. Chem. *271*, 18904-18911.

Tu,L., Wang,J., Helm,A., Skach,W.R., and Deutsch,C. (2000). Transmembrane biogenesis of Kv1.3. Biochemistry *39*, 824-836.

Unwin,N. (1989). The structure of ion channels in membranes of excitable cells. Neuron *3*, 665-676.

van Dalen,A., van der,L.M., Driessen,A.J., Killian,J.A., and de Kruijff,B. (2002). Components required for membrane assembly of newly synthesized K+ channel KcsA. FEBS Lett. *511*, 51-58.

van Leeuwen,J.E. and Kearse,K.P. (1996). Calnexin associates exclusively with individual CD3 delta and T cell antigen receptor (TCR) alpha proteins containing incompletely trimmed glycans that are not assembled into multisubunit TCR complexes. J Biol. Chem. *271*, 9660-9665.

VanDongen,A.M., Codina,J., Olate,J., Mattera,R., Joho,R., Birnbaumer,L., and Brown,A.M. (1988). Newly identified brain potassium channels gated by the guanine nucleotide binding protein Go. Science *242*, 1433-1437.

Varki,A. (2001). Loss of N-glycolylneuraminic acid in humans: Mechanisms, consequences, and implications for hominid evolution. Am. J Phys. Anthropol. *Suppl 33*, 54-69.

Vassilakos,A., Cohen-Doyle,M.F., Peterson,P.A., Jackson,M.R., and Williams,D.B. (1996). The molecular chaperone calnexin facilitates folding and assembly of class I histocompatibility molecules. EMBO J *15* , 1495-1506.

Voigt, S., Jungnickel, B., Hartmann E., and T. Rapoport. (1996). Signal sequence-dependent function of the TRAM protein during early phases of protein transport across the ER membrane. J Cell Biol. *134*, 25-35.

Wada,I., Imai,S., Kai,M., Sakane,F., and Kanoh,H. (1995). Chaperone function of calreticulin when expressed in the endoplasmic reticulum as the membrane-anchored and soluble forms. J. Biol. Chem. *270*, 20298-20304.

Waechter,C.J., Schmidt,J.W., and Catterall,W.A. (1983). Glycosylation is required for maintenance of functional sodium channels in neuroblastoma cells. J Biol. Chem. *258*, 5117-5123.

Walter,J., Urban,J., Volkwein,C., and Sommer,T. (2001). Sec61p-independent degradation of the tail-anchored ER membrane protein Ubc6p. EMBO J *20*, 3124-3131.

Walter,P. and Johnson,A.E. (1994). Signal sequence recognition and protein targeting to the endoplasmic reticulum membrane. Annu. Rev. Cell Biol. *10*, 87-119.

Wang,H., Kunkel,D.D., Martin,T.M., Schwartzkroin,P.A., and Tempel,B.L. (1993). Heteromultimeric K+ channels in terminal and juxtaparanodal regions of neurons. Nature *365*, 75-79.

Wang,J.W. and Wu,C.F. (1996). In vivo functional role of the Drosophila hyperkinetic beta subunit in gating and inactivation of Shaker K+ channels. Biophys. J *71*, 3167-3176.

Ware,F.E., Vassilakos,A., Peterson,P.A., Jackson,M.R., Lehrman,M.A., and Williams,D.B. (1995). The molecular chaperone calnexin binds Glc1Man9GlcNAc2 oligosaccharide as an initial step in recognizing unfolded glycoproteins. J Biol. Chem. *270*, 4697-4704.

Warren,G. and Mellman,I. (1999). Bulk flow redux? Cell *98*, 125-127.

Weber,W.M., Cuppens,H., Cassiman,J.J., Clauss,W., and Van Driessche,W. (1999). Capacitance measurements reveal different pathways for the activation of CFTR. Pflugers Arch. *438*, 561-569.

Weber,W.M., Segal,A., Simaels,J., Vankeerberghen,A., Cassiman,J.J., and Van Driessche,W. (2001). Functional integrity of the vesicle transporting machinery is required for complete activation of cFTR expressed in xenopus laevis oocytes. Pflugers Arch. *441*, 850-859.

Wei,A., Covarrubias,M., Butler,A., Baker,K., Pak,M., and Salkoff,L. (1990). K+ current diversity is produced by an extended gene family conserved in Drosophila and mouse. Science *248*, 599-603.

Weill,C.L., McNamee,M.G., and Karlin,A. (1974). Affinity-labeling of purified acetylcholine receptor from Torpedo californica. Biochem. Biophys. Res. Commun. *61*, 997-1003.

Weiss,R.E., Roberts,W.M., Stuhmer,W., and Almers,W. (1986). Mobility of voltage-dependent ion channels and lectin receptors in the sarcolemma of frog skeletal muscle. J Gen. Physiol *87*, 955-983.

Wells,L., Vosseller,K., and Hart,G.W. (2001). Glycosylation of nucleocytoplasmic proteins: signal transduction and O- GlcNAc. Science *291*, 2376-2378.

Wible,B.A., Yang,Q., Kuryshev,Y.A., Accili,E.A., and Brown,A.M. (1998). Cloning and expression of a novel K+ channel regulatory protein, KChAP. J Biol. Chem. *273*, 11745-11751.

Wieland,F.T., Gleason,M.L., Serafini,T.A., and Rothman,J.E. (1987). The rate of bulk flow from the endoplasmic reticulum to the cell surface. Cell *50*, 289-300.

Wiertz,E.J., Tortorella,D., Bogyo,M., Yu,J., Mothes,W., Jones,T.R., Rapoport,T.A., and Ploegh,H.L. (1996). Sec61-mediated transfer of a membrane protein from the endoplasmic reticulum to the proteasome for destruction. Nature *384*, 432-438.

Wiggins,C.A. and Munro,S. (1998). Activity of the yeast MNN1 alpha-1,3-mannosyltransferase requires a motif conserved in many other families of glycosyltransferases. Proc. Natl. Acad. Sci. U. S. A *95*, 7945-7950.

Wilkinson,B.M., Tyson,J.R., Reid,P.J., and Stirling,C.J. (2000). Distinct domains within yeast Sec61p involved in post-translational translocation and protein dislocation. J Biol. Chem. *275*, 521-529.

Wonderlin,W.F. and French,R.J. (1991). Ion channels in transit: voltage-gated Na and K channels in axoplasmic organelles of the squid Loligo pealei. Proc. Natl. Acad. Sci. U. S. A *88*, 4391-4395.

Wong,B.S. and Binstock,L. (1980). Inhibition of potassium conductance with external tetraethylammonium ion in Myxicola giant axons. Biophys. J. *32*, 1037-1042.

Woods,D.F. and Bryant,P.J. (1991). The discs-large tumor suppressor gene of Drosophila encodes a guanylate kinase homolog localized at septate junctions. Cell *66*, 451-464.

Wormald,M.R. and Dwek,R.A. (1999). Glycoproteins: glycan presentation and protein-fold stability. Structure. Fold. Des *7*, R155-R160.

Wu,C.F., Ganetzky,B., Haugland,F.N., and Liu,A.X. (1983). Potassium currents in Drosophila: different components affected by mutations of two genes. Science *220*, 1076-1078.

Wu,C.F. and Haugland,F.N. (1985). Voltage clamp analysis of membrane currents in larval muscle fibers of Drosophila: alteration of potassium currents in Shaker mutants. J. Neurosci. *5*, 2626-2640.

Wymore,R.S., Negulescu,D., Kinoshita,K., Kalman,K., Aiyar,J., Gutman,G.A., and Chandy,K.G. (1996). Characterization of the transcription unit of mouse Kv1.4, a voltage- gated potassium channel gene. J. Biol. Chem. *271*, 15629-15634.

Yang,E.K., Alvira,M.R., Levitan,E.S., and Takimoto,K. (2001). Kvbeta subunits increase expression of Kv4.3 channels by interacting with their C termini. J Biol. Chem. *276*, 4839-4844.

Yu,H., Kaung,G., Kobayashi,S., and Kopito,R.R. (1997). Cytosolic degradation of T-cell receptor alpha chains by the proteasome. J Biol. Chem. *272*, 20800-20804.

Zafra,F. and Gimenez,C. (2001). Molecular determinants involved in the asymmetrical distribution of glycine transporters in polarized cells. Biochem. Soc. Trans. *29*, 746-750.

Zagotta,W.N., Hoshi,T., and Aldrich,R.W (1990). Restoration of inactivation in mutants of Shaker potassium channels by a peptide derived from ShB. Science *250*, 568-571.

Zerangue,N., Schwappach,B., Jan,Y.N., and Jan,L.Y. (1999). A new ER trafficking signal regulates the subunit stoichiometry of plasma membrane K(ATP) channels. Neuron *22*, 537-548.

Zhang,J.X., Braakman,I., Matlack,K.E., and Helenius,A. (1997). Quality control in the secretory pathway: the role of calreticulin, calnexin and BiP in the retention of glycoproteins with C-terminal truncations. Mol. Biol. Cell *8*, 1943-1954.

Zhou,Z., Gong,Q., Epstein,M.L., and January,C.T. (1998). HERG channel dysfunction in human long QT syndrome. Intracellular transport and functional defects. J Biol. Chem. *273*, 21061-21066.

Zhu,J., Watanabe,I., Gomez,B., and Thornhill,W.B. (2001). Determinants involved in Kv1 potassium channel folding in the endoplasmic reticulum, glycosylation in the Golgi, and cell surface expression. J Biol. Chem. *276*, 39419-39427.